DOE/METC-91/6120
(DE91002085)

Proceedings of the Third Annual Fuel Cells Contractors Review Meeting

Editor
W.J. Huber

June 1991

Sponsored by
U.S. Department of Energy
Office of Fossil Energy
Morgantown Energy Technology Center
Morgantown, West Virginia

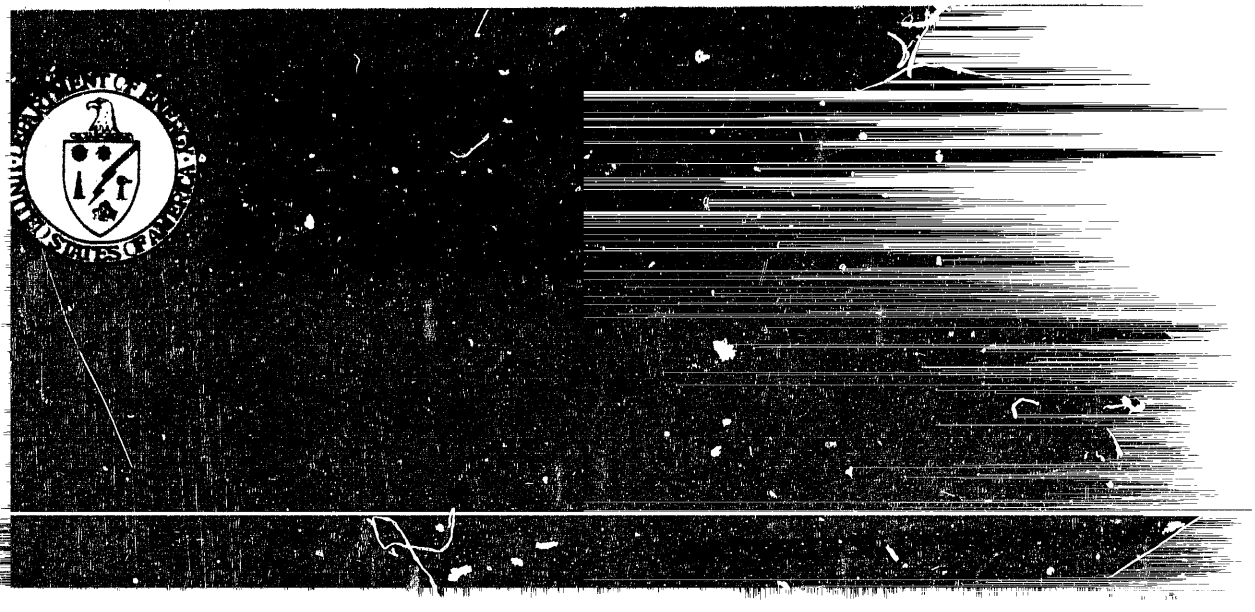

DISCLAIMER

DOE/METC--91/6120

DE91 002085

Proceedings of the Third Annual Fuel Cells Contractors Review Meeting

Editor
W.J. Huber

Sponsored by
U.S. Department of Energy
Office of Fossil Energy
Morgantown Energy Technology Center
P.O. Box 880
Morgantown, West Virginia 26507-0880

Held at
Morgantown Energy Technology Center
Morgantown, West Virginia

June 5-6, 1991

Foreword

The Third Annual Fuel Cells Contractors Review Meeting was held June 5-6, 1991, at the Morgantown Energy Technology Center in Morgantown, West Virginia. This meeting was sponsored and hosted by the Morgantown Energy Technology Center of the U.S. Department of Energy.

The overall objective of this program is to develop the essential technology for private sector commercialization of the various fuel cell electrical generation systems. These systems promise high fuel to electricity efficiencies (40 to 60 percent), distinct possibilities for cogeneration applications, modularity of design, possibilities of urban siting, and environmentally benign emissions.

The purpose of this meeting was to provide the research and development (R&D) participants in the DOE/Fossil Energy-sponsored Fuel Cells Program with the opportunity to present key results of their research and to establish closer business contacts. Major emphasis was on phosphoric acid, molten carbonate, and solid oxide technology efforts. Research results of the coal gasification and gas stream cleanup R&D activities pertinent to the Fuel Cells Program were also highlighted. Two hundred seventeen attendees from industry, utilities, academia, and Government participated in this 2-day meeting. Twenty-three papers were given in three formal sessions:

- Molten Carbonate Fuel Cells R&D (9 papers)
- Solid Oxide Fuel Cells (8 papers)
- Phosphoric Acid Fuel Cells R&D (6 papers)

In addition to the papers and presentations, these proceedings also include comments on the Fuel Cells Program from the viewpoint of

- DOE/METC Fuel Cell Overview by Rita A. Bajura,
- DOE/METC Perspective by Manville J. Mayfield,
- Electric Power Research Institute by Daniel M. Rastler,
- Natural Gas by Hugh D. Guthrie, and
- Transportation Applications by Pandit G. Patil.

We gratefully acknowledge the cooperation of the non-DOE funding agencies in offering their comments and support as well as encouraging the contractors to discuss the R&D being funded by their respective agencies.

The papers printed in these proceedings have been reproduced from camera-ready manuscripts provided by the authors. They have been neither refereed nor extensively edited.

William J. Huber
Conference Chairman
Fuel Cells Branch

Table of Contents

Table of Contents
(Continued)

Table of Contents
(continued)

DOE/METC Fuel Cell Overview

R. A. Bajura
Morgantown Energy Technology Center

Good morning. Welcome to DOE's Third Annual Fuel Cell Contractors Review Meeting. This is the first time we have held a contractors review meeting in our new conference center. We ask your indulgence and patience as we break in new equipment and new logistical procedures at this meeting.

During this past year, a number of events have occurred which have implications for the fuel cell community.

- President Bush issued the National Energy Strategy (NES).
- Congress passed the amendments to the Clean Air Act (CAA).
- DOE issued the Round 4 solicitation for its Clean Coal Technology (CCT) Program.
- The National Academy of Science recommended immediate action to control greenhouse gases.

There were also a number of changes at the Morgantown Energy Technology Center (METC).

- We initiated a Total Quality Management (TQM) Program.
- We started using another transfer technology tool -- cooperative research and development agreements (CRADAs).
- Implementation procedures for the National Environmental Policy Act (NEPA) were revised.

In my talk today, I will share with you my view of how these pieces fit together and impact the fuel cell community.

The National Energy Strategy (NES) and the Amendments to the Clean Air Act

The NES is a comprehensive blueprint for planning America's energy future. A major theme of the NES is the need for high efficiency, environmentally superior power generations systems, a theme I am sure the fuel cell community noted.

The NES also predicted that U.S. power generation capacity will need to grow significantly to meet the needs of a growing economy. We have "eaten up" the comfortable reserve margin we enjoyed for the past 15 years. Even with demand-side management programs, by 2010 we will need 200,000 MW of additional capacity. The implication for the fuel cell community is that there is a major U.S. market for power generation equipment.

The NES also addressed the mix of fuels that will be used for power generation. The NES goal is an efficient market where all fuels -- and all technologies -- can compete fairly. Figure 1 is taken from the NES and shows the energy input in quads to electric generation. Coal and natural gas will continue to play major roles in power generation. Hugh Guthrie, the Director of METC's Extraction Project Management Division, will discuss gas availability in a later paper in this meeting.

The NES predicts that coal consumption will grow by almost 50 percent over the next 20 years. This projected growth is not surprising. Coal, our most abundant domestic fuel, represents more than 90 percent of all known U.S. fossil energy resources. Coal will last for 250 years at the current production rate.

Energy Input to Electricity Generation
National Energy Strategy Scenario

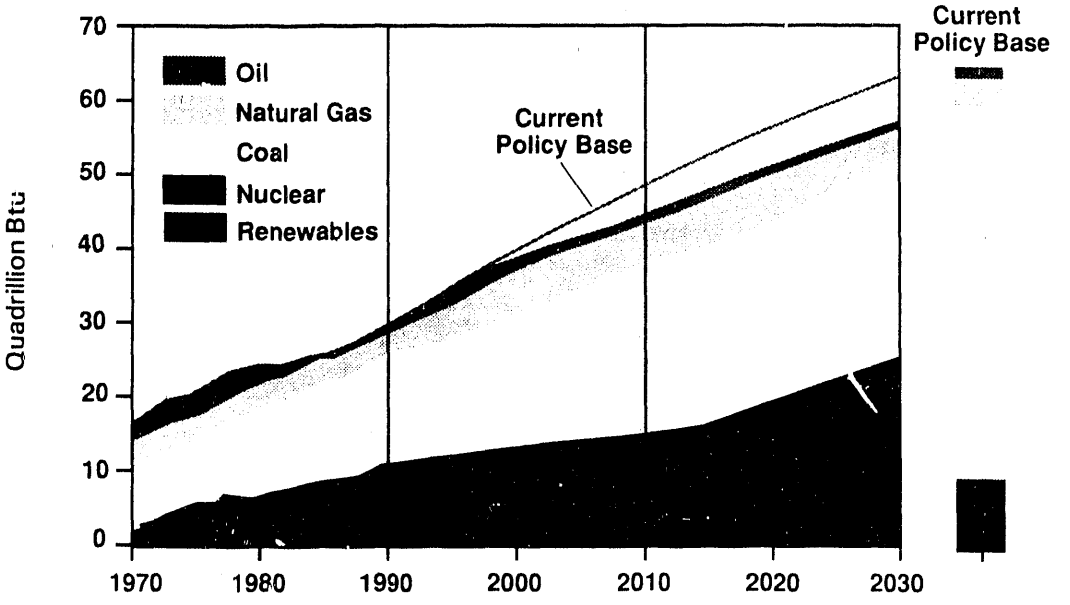

M91001488

The NES made it clear, however, that if we are going to benefit from our enormous, low-cost coal reserves, we need to develop coal technologies that are environmentally clean, have high conversion efficiencies, and are cost effective. These advanced technologies need to be ready for commercialization in the year 2000 and beyond when a surge of orders for new, base-load power plants is anticipated. In the interim, natural gas will fill much of the void, particularly for peaking and intermediate service. What is the message for the fuel cell community? If coal gasification/fuel cells are to be a viable market option for the post-2000 surge of new orders, we need to continue to accelerate development of this technology.

The CAA amendments assumed that clean coal technologies will be ready for commercial deployment in the year 2000. This new legislation capped SO_2 emissions at roughly 1985 levels. Given the projected growth in power demand, this cap is a dilemma unless clean coal technologies with their inherently low SO_2 emissions are available.

Clean Coal Technology (CCT) Program

DOE's CCT Program is a cooperative effort between the Federal Government and industry to demonstrate commercial-scale, clean coal technologies. The Government pays up to 50 percent of the project cost with the industrial participants paying the remainder. This Program was initiated in 1986. Since then, four of the five planned "Rounds" of CCT solicitations have been issued. As a result of the first three rounds, 34 demonstration projects are underway and one more is in final contract negotiations. The total cost of these projects is nearly $3.4 billion. Last month, 31 companies submitted 33 proposals for Round 4 of the CCT Program. These proposals are currently being evaluated. The Round 5 solicitation for the CCT Program should be issued in the spring of 1992.

The CCT question of greatest interest to the fuel cell community is one that I do not have an answer to. The question is how mature does a technology have to be to be considered for inclusion in the CCT Program? To put things in perspective, Round 1 focused on advanced technologies. Rounds 2 and 3 were driven by the acid rain agreement between the U.S. and Canada. The focus was on nearer term technologies. The focus of Round 4 was on advanced technologies for use in the post-2000 time frame. CCT-4 proposals included six integrated gasification combined-cycle (IGCC) projects and three advanced pressurized fluidized-bed combustion (PFBC) projects. Ground rules for Round 5 have not been established but logic suggests that post-2000 technologies will also be targeted.

I encourage you to consider CCT-5 as a possible opportunity for gasification/fuel cell demonstration projects -- it may be the last opportunity. Also recognize that the competing high efficiency technologies -- IGCC and advanced PFBC -- will be demonstrated in the 1990s. Thus your competition for the large, base-loaded utility market should be ready for the post-2000 window of opportunity.

Global Warming

Global warming is another key environmental issue -- a widely debated issue. Groups are taking a range of positions:

- The National Academy of Science considers global warming a serious threat and recommends taking action now to reduce the production of greenhouses gases.

- Two California utilities announced plans to reduce CO_2 emissions by 10 percent over the next decade, primarily through conservation.

- The Information Council on the Environment (ICE), a coalition of 24 power companies, initiated an advertising campaign with the theme "How much are you willing to pay to solve a problem that may not exist?"

The fuel cell community could respond to global warming in several different ways. One approach is to advocate high efficiency systems -- a approach which makes sense in its own right. The benefits of high efficiency include:

- Direct reduction in CO_2 emissions.

- A major cumulative effect on the energy infrastructure. High efficiency systems reduce the number of fuel production facilities and power plants needed.

- Increased U.S. industrial competitiveness through lower electric costs.

Alternatively, the fuel cell community could lobby for drastic measures to reduce CO_2 emissions -- for example, a carbon tax on fuels -- but recognize that advocating drastic measures for an issue that may not be real could be counterproductive. Until an alternative to coal-based power generation is practically available, a carbon tax would severely weaken the financial health of the electric industry. Without customers, fuel cells are unlikely to be commercialized -- jeopardizing a technology that could provide a rational approach to reduce CO_2 emissions.

Technology Transfer

METC has traditionally been a strong advocate of technology transfer. We have used several approaches:

- We conduct much of our R&D program using cost-shared cooperative agreements with industrial organizations. Through these agreements, we put technology into the hands of organizations capable of commercializing it -- your hands.

- We hold contractors review meetings, such as this one, which give potential users of the technology a snapshot of the technology status.

This past year, we started to use another transfer technology tool, CRADAs. Congress created the framework for CRADAs in various bills starting with the Stevenson-Wydler Act of 1980. Congress wanted to enhance U.S. industrial competitiveness by luring innovative technologies out of Government laboratories and into the commercial sector.

CRADAs are agreements between one or more Government laboratories and one or more industrial partners. Both Government-owned, Government-operated laboratories (such as METC) and Government-owned, contractor-operated laboratories (primarily national laboratories) can enter into CRADAs. The Government and/or industrial partner may provide personnel, facilities, or equipment. However, no Federal money can be transferred to the industrial partner.

Flexibility is a major advantage of CRADAs. They are not burdened with the "boilerplate" associated with contracts or cooperative agreements. Rights to intellectual party and potential royalties are negotiable. Data can be protected up to 5 years. The Government laboratory as well as individual Government researchers may receive monetary benefits.

At METC, we have been actively pursuing CRADA opportunities. In January 1991, we issued an announcement in the Commerce Business Daily indicating our interest in CRADAs. METC's director was recently delegated the authority to negotiate CRADAs. We are about to sign a CRADA with Allegheny Power Systems (APS) who will host the construction of an advanced fixed-bed gasification pilot plant at one of their existing sites.

I invite you to consider CRADA opportunities with our in-house R&D groups. Although METC does no hands-on R&D on fuel cells, CRADA opportunities exist in the areas of coal gasification, gas stream cleanup, and systems integration.

I also invite you to brainstorm with us and among yourselves on potential CRADA opportunities involving multiple industrial partners. Under the CRADA umbrella, R&D partnerships are possible that could be of interest to:

- Several DOE-funded U.S. fuel cell developers, or
- Individual developers and their component suppliers.

CRADA topics could be as diverse as solving critical technical issues or developing improved manufacturing processes.

Total Quality Management

The Government is encouraging Federal agencies to adopt total quality management or TQM. In October 1990, we initiated a TQM program at METC. Many of you are familiar with TQM, since you have used it as a quality control tool in establishing your prototype fuel cell manufacturing facilities. For those of you not familiar with it, TQM is a management system designed to meet customer requirements by doing the right thing right the first time.

Because of TQM, I hope that you will recognize two major changes in the way METC interacts with you -- our contractors. The first change is improved responsiveness to your needs. As part of our internal discussions on TQM, we attempted to answer the question, "who are our customers -- who are we trying to serve?" We concluded that our contractors are one of our major customers. Without you we can never achieve our mission -- which is to catalyze the private sector to commercialize advanced fossil energy technologies.

The procurement process is one area in which we're trying to better meet your needs -- recognizing that many of the constraints in the procurement process are imposed external to METC. A METC TQM team recently assessed our procurement process. The charter of this TQM team was limited -- identify and eliminate internally imposed barriers that slow down the procurement process. This was a small step. But we hope that it will be the first of many incremental changes that will improve our responsiveness to your needs. We solicit your suggestions on areas where we need to improve.

The second change that you will see as a result of TQM is an emphasis on product management. Products are defined as advanced fossil energy systems. We set up eight different product management teams. Two of the eight teams involve fuel cells: coal gasification/molten carbonate fuel cells and coal gasification/solid oxide fuel cells. For each of the eight METC products, we're identifying technical barriers and challenges, market opportunities and threats, and R&D needs. Initially these teams will be internal to METC. In the future, I anticipate that METC contractors will be involved through systems studies and other mechanisms. I also anticipate that there will be close interaction with the Electric Power Research Institute and with the Gas Research Institute, particularly on the fuel cell teams. We encourage you to share with us your views on what the real issues associated with these products are. We need your input to develop a rational strategic plan for our products that will help us guide the R&D program.

Environmental Initiative

In June 1989, Admiral Watkins, the Secretary of Energy, announced a 10-point environmental initiative designed to restore DOE's credibility in Environmental Health and Safety (EH&S). As your are aware, DOE's credibility was very low in 1989 following the disclosure of major EH&S problems at Rocky Flats and other DOE nuclear production facilities.

In 1990, as a result of the 10-point initiative, DOE established new policies for implementing the National Environmental Policy Act or NEPA. NEPA is a 1970 law designed to ensure that the government consider environmental consequences as part of the decision-making process. DOE's changes in NEPA policy have made us change the way we implement and manage contracts: For example:

- We are asking for more environmental information in proposal solicitation. The environmental implications of the proposed contract are factored into the procurement evaluation process.

- The first task in many contracts involves submitting additional environmental information to DOE so we can complete our NEPA assessment.

- A decision point is included in contracts point signaling the end of our NEPA review. Until the NEPA process is complete, the contractor can take no actions that

  - Have an adverse environmental impact; or

  - Limit the choice of reasonable alternatives.

- Current DOE policy requires us to prepare Environmental Assessments or Environmental Impact Statements for nearly all R&D contracts involving any experimental activity. Public reviews of these documents are mandatory.

It is important that the schedule and cost implications of NEPA compliance be factored into project planning. Clearly, DOE policy is to take environmental issues seriously -- even if it disrupts schedules. I think that you, as proponents of an environmentally superior technology, want us to take environmental issues seriously too.

Conclusion

In closing, Senator Byrd participated in the dedication ceremony for this building last Friday. Two and a half years ago, the Senator also participated in the ground breaking for this building. At that time, he paraphrased a poem titled "Earth is Enough" by Edwin Markham. Senator Byrd's quote, which is inscribed on the plaque next to the main entrance of this building, reads:

"Men and women of extraordinary skill...
Building America's energy future...
We, men of earth, have here, the stuff of paradise..."

I doubt if Mr. Markham had fuel cells in mind when he wrote his poem but fuel cells with their high efficiency, environmentally superiority may be the stuff of paradise. I wish you a good conference.

DOE/METC Perspective

M.J. Mayfield
Morgantown Energy Technology Center

Good morning, I would also like to welcome each of you to the Third Annual Fuel Cell Contractors Review Meeting. This is an excellent opportunity for communication and technology transfer between the research community, our contractors who are developing fuel cell systems, and potential utility and industrial users. As many of you are aware, we are seeing increased interest in fuel cells as the remaining technical issues get resolved and fuel cells move toward commercialization.

The planned presentations over the next two days are broader than just the DOE program. DOE, EPRI and GRI have joint agreements for coordination and cooperation between our respective organizations. We meet regularly for joint reviews. We have asked our contractors to present results from their overall programs regardless of the funding agency. Following my remarks, you will be hearing similar presentations from representatives from EPRI and GRI. We welcome their cooperation and participation in this meeting.

The overall objective of the DOE Fossil Energy program is to establish the technology basis for cost-effective fuel cell power generation which can be commercialized in the 1990s. Our primary activities are:

- The development of PAFC, MCFC and SOFC systems.
- Applied research to support the fuel cell systems under development.
- And to assist private sector commercialization of fuel cells.

As I did last year, it would probably be helpful for me to list the key elements in our program strategy:

- Aid the development to a point that commercial production is initiated.
- Emphasize MCFC and SOFC recognizing that PAFC are near commercialization.
- Focus on coal-derived fuel with natural gas as a back-up or interim fuel.
- Fund research needed to resolve major technical issues.
- Recognize the market potential for on-site natural gas systems.
- Work cooperatively with EPRI and GRI on program development and funding.

Each of the major U.S. funding agencies because of their constituency has a somewhat different focus for their fuel cell programs.

- DOE/FE is primarily interested in coal-fueled large size plants with natural gas as a back-up fuel.
- GRI concentrates on on-site energy systems using natural gas for cogeneration applications.
- EPRI supported by the electric utility industry is interested in environmentally benign power plants fueled with coal-gas, natural gas and possibly liquid fuels.

Shown below is a breakdown of U.S. public agency fuel cell funding for 1991. The total represents a significant increase over 1990 funding and reflects increasing costs as we move to larger size systems and demonstrations.

U.S. Fuel Cell Public Agency Funding
1991 ($000)

Organization	Technology	Budget
DOE*		
Fossil Energy	PAFC, MCFC, SOFC	42.9
Conservation	PAFC, Polymer, SOFC	10.9
EPRI	PAFC, MCFC, SOFC	4.0
GRI	PAFC, MCFC, SOFC	5.8
	TOTAL	63.6

* By Fiscal Year

I would also point out that funding worldwide has increased even faster than in the U.S. This reflects rising interest in Japan and Europe where higher fuel prices make fuel cells even more attractive. The estimated total is considered conservative and may be significantly larger than the numbers shown.

Worldwide Fuel Cell Funding

- Major private sector funding (U.S. and worldwide)
  - Technology
  - Market development
  - User tests and demonstration
- Worldwide fuel cell funding estimated at $200 to $250 million/year

The DOE Fossil Energy program funding for FY 1990 and FY 1991 by fuel cell type is shown on the following chart.

DOE/FE Fuel Cell Program Funding
($000)

Program Activity	FY 1990 Funding	FY 1991 Funding
Phosphoric Acid	8,291	8,853
Molten Carbonate	16,777	18,423
Solid Oxide	11,473	14,170
Advanced Research	1,458	1,444
TOTAL	37,999	42,890

There are several overall program needs that I would like to call to your attention. Certainly, some of these are already being implemented, but to bring a technology such as fuel cells to commercialization these and other needs will have to be met.

Overall Program Needs

- Continued funding of cell, stack and system development to support field verifications, and prototype demonstrations
- Increased private sector funding of manufacturing process development, system definition and application
- Establishment of joint ventures and teaming relationships for demonstrations and commercialization activities
- Market acceptance based on performance, reliability, cost and customer benefits
- Competitive suppliers of fuel cells to ensure product improvements, service and cost reduction

Turning to PAFC, there are several points regarding the status of this technology that I would like to make.

PAFC Status

- Decreased DOE funding as technology nears commercialization
- IFC Program -- Commercializing stacks for utility and on-site applications
  - Supplied stacks for 11 MW facility at Tokyo Electric
  - Over 60 orders for 200 kW, on-site power plants. New manufacturing facility constructed
- Westinghouse Program -- 375 kW module for industrial cogeneration application

Since PAFC are closest to being commercial, technical issues center around cost and operational performance.

Major Technical Issues -- PAFC

- Stack
  - Verification of long-term stack operation (up to 40,000 hours)
  - Stack fabrication cost
- System
  - Verification of long-term operation

A lot is happening relating to the development of MCFC. This chart highlights some of the major activities.

MCFC Status

- 3-year contracts awarded to 3 developers for 100-300 kW stacks
  - Energy Research Corporation
  - MC-Power Corporation
  - International Fuel Cells
- Solicitation for demonstration of full-size MCFC stacks
  - Report to Congress for FY 92 budget
- Progress towards commercialization
  - Construction of pilot manufacturing facilities
  - Licensing/marketing agreements in U.S., Japan and Europe
  - Establishment of U.S. utility commercialization groups

In contrast to PAFC there are a number of major technical issues that need further work under the MCFC program. Recently there have been breakthroughs, particularly in the area of electrolyte migration, but these still need to be demonstrated in full-size stacks. Some of the issues are listed on this chart.

Major Technical Issues -- MCFC

- Stack
  - Electrolyte migration
  - Cell stability/corrosion
  - Full area and height scale-up
- System
  - Reformer integration
  - System control strategy
  - Cycling and transient effects
  - System optimization

I would next like to present some points on the status of the SOFC program. As with MCFC, significant progress is being made developing SOFC. These are listed on the chart below:

SOFC Status

- Tubular SOFCs "gaining" on MCFCs
- DOE/FE Program supporting two concepts
  - Tubular -- Westinghouse
  - Monolithic -- Allied-Signal/AiResearch
- Tubular concept by far the most mature
  - Recent major performance and cell scale-up progress
  - 20 kW operational, 100 kW in same time frame as MCFC units
  - 5-year Cooperative Agreement leading to commercialization
- Monolithic concept offers high power densities
  - Currently only at bench-scale stage of development

SOFC have their own distinctive set of technical issues. While sizeable activities are underway on all of these, resolution of these is required prior to large-scale demonstration.

Major Technical Issues -- SOFC

- Stack -- Near-Term Focus
  - Cell fabrication techniques and cost
  - Scale-up of cell length and stack size
  - Stack performance, stability and life
- System -- Long-Term Focus
  - Reformer integration
  - Control strategy
  - Cycling and transient effects
  - System optimization

From our work on MCFC systems studies, there are several overall results that may be of interest to this audience. These are shown on the following chart.

Systems Study Results

- Fuel cells are candidates for integration with coal gasification/hot gas cleanup
- Duel fuel (coal and gas) capability is a benefit
  - Increases availability
  - Facilitates financing of demonstration projects
- Integrated gasifier/MCFC efficiencies > 50% are possible
- Oxygen-blown entrained-flow gasifiers with cold gas cleanup are not the optimum approach
- With "high methane producing" gasifiers, IG/MCFC efficiencies ~60% are possible

In summary, I would like to emphasize several points. Over the last year or so, our research progress and manufacturing scale-up has really begun to pay off. Solutions to many of the technical issues have been found. Facilities to manufacture demonstration stacks and systems are either in place or will be so over the next few months. Sizeable numbers of demonstration units are in the planning and negotiation stages. With their key advantages of efficiency and environmental performance, the time is right for all three types of fuel cells to come into their own. We all need to work diligently to make this happen for our own individual organizations and commercial success in our country. I look forward to a productive meeting.

9105311w.1bb

EPRI Fuel Cell Program Perspective

Daniel M. Rastler

ABSTRACT

EPRI's Fuel Cell Program is focused on the development and commercialization of molten carbonate fuel cell dispersed generators. These small multi-megawatt class units are believed to be a necessary prerequisite to achieving the manufacturing capability and scale-up to sizes needed for integration with coal gasifiers. Our efforts in MCFC technology include development and scale-up, pilot plant testing and confirming long term endurance of MCFC stacks for utility plant applications. An important effort underway is the endurance testing of a 20 kw to 100 kw MCFC stack on an actual coal derived gas. With the emergence of MCFC hardware from the laboratory to pilot and full scale demonstration, carbonate fuel cell vendors in the U.S. have begun to initiate commercialization initiatives and utility alliance groups.

Phosphoric acid fuel cells are becoming a commercial reality; there is a high potential for deployment of 50 kw to 11,000 kw size units in Japan and the Pacific rim countries. Early demonstration results from these units are very positive. EPRI has formed international agreements with utilities to monitor PAFC demonstration projects in Japan and Italy. Access to data and operational experiences from these projects will enable EPRI to provide information and guidance to utilities considering the purchase/deployment of PAFC systems. Commercialization in the U.S. is focused on small 200 kw class units for on-site commercial co-generation applications. Sales of multi-megawatt class units will depend on price and terms as well as vendor commitments to commercialization.

In the area of solid oxide fuel cells, EPRI is supporting research needed to determine technical feasibility of SOFC configurations and to define plant systems for utility market applications. We have recently collaborated with the Japan's New Energy and Industrial Technology Development Organization and five Japanese utilities to evaluate large (20 MW to 300 MW) plants utilizing a tubular SOFC configuration. We are investigating new and lower cost SOFC manufacturing concepts, as well as thin film SOFC designs. Field test units of 25 kw and 100 kw scale hardware are planned in the next several years to provide an indication of technical viability.

The utility market is responding favorably to deploying new technology in the 1990's. Increasing competition, uncertainties of load growth, increasing environmental concerns for improved air quality, and the need to up-grade and improve systems which distribute and deliver electricity to the end-user, may be issues potentially solvable by distributed fuel cells.

Utility expenditures, for example, in T & D upgrades over the next five years will be a staggering $ 62 billion throughout the nine NERC regions -- as sum that is 20% larger than utility's generation construction expenditures.

Distributed power supply systems (fuel cells, photo voltaics, and battery storage) can be used to defer, strengthen and improve the delivery of electricity to customers.

EPRI initiated a study last year to develop a methodology to assist utilities in evaluating the costs and benefits of distributed generation. Preliminary results from one utility case study demonstrate that distributed generation, can provide significant benefits.

Utility interest in fuel cells the past year has increased substantially; this is illustrated by the very positive response to several vendor commercialization initiatives. A model " framework " for introducing MCFC dispersed generator is being seriously implemented by 25 utilities, representing investor owned, public, and rural cooperative systems. Many utilities are waiting on the side lines for a " product offering " by fuel cell vendors.

As we look at the emerging market in the U.S., we can not ignore developments and alliances world wide. Just as industry is moving toward a global economy, EPRI is also moving more and more toward a global/ international R & D consortium. It is certain that market conditions off-shore, particularly in Japan and Europe, will determine the destiny and characteristics of fuel cell generating systems in the U.S..

Many of our contractors have formed alliances with world class utility equipment manufactures. Understanding of their business strategies and the market potentials abroad, is essential to developing our domestic strategy in R&D as well as commercialization.

Therefore, there is a window open for market opportunity in the 1990's as utilities will need to deploy new power generation systems; they are also looking for technological solutions to issues involving the environment, urban growth, improving service to customers, and managing the vast expenditures in T &D. The requirements of this market, however, must not be underestimated. Competitive cost, high reliability/availability, low operating & maintenance costs and compactness in size and modularity must be demonstrated and achieved. The combined collaboration and sharing of risks between manufactures , government, and utilities will be essential for fuel cells to make it through the window of the 1990's.

EPRI's Fuel Cell Program Strategy

Phosphoric Acid (PAFC)

- Monitor power plant demonstrations underway world-wide
- Provide information to utilities considering purchase in early 1990's

Molten Carbonate (MCFC)

- Develop Internal Reforming MCFC as interim product and as prerequisite to sizes needed for integration with coal gasifiers
- Evaluate MCFC on Coal-gas
- Utilize cell / stack components from larger DOE-funded efforts

Solid Oxide (SOFC)

- Support research needed to determine SOFC feasibility

Define and Identify Applications & Requirements
Assist Member Utilities in Evaluating Market Entry Units

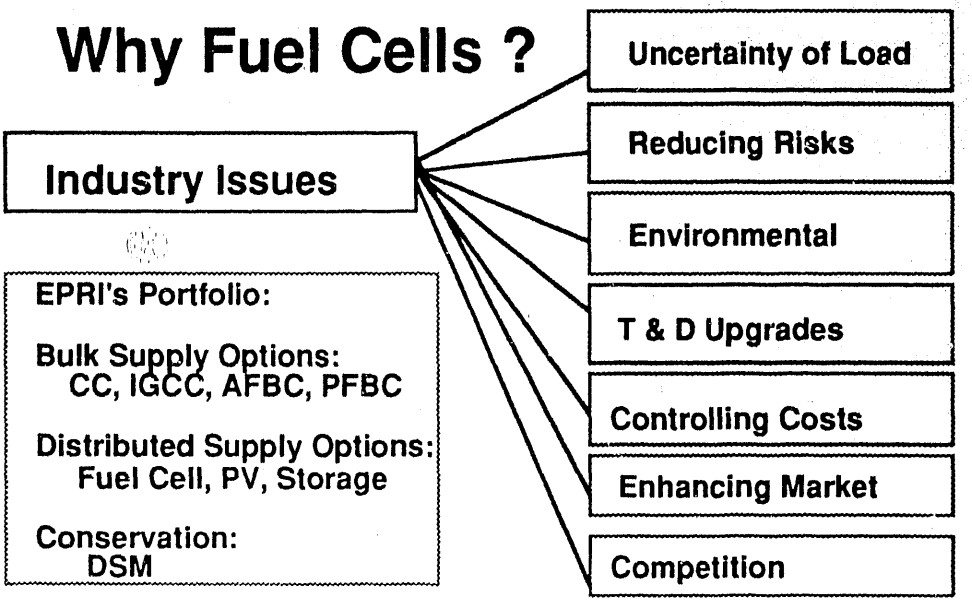

Applications For Distributed Generation

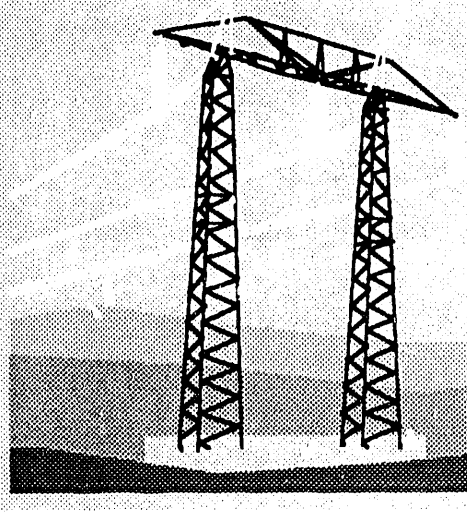

Sites:
- Industrial / Commercial
- Substation
- Subtransmission

Benefits:
- Defer Upgrades
- Loss Savings
- Reliability & Value of Service
- Strategic

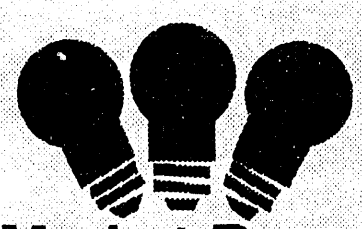

Utility Market Requirements

Competitive Cost

Reliability

Availability

Modularity and Compactness

EPRI

Frame Work For Commercialization

Necessary Elements:

- The Right Product to meet a Need, Issue, Constraint
- Product Timing
- Business & Commercialization Plan
- Pricing, Risks, Incentives
- Vendor Commitment
- Sharing of Risks

EPRI

Worldwide Fuel Cell Alliances

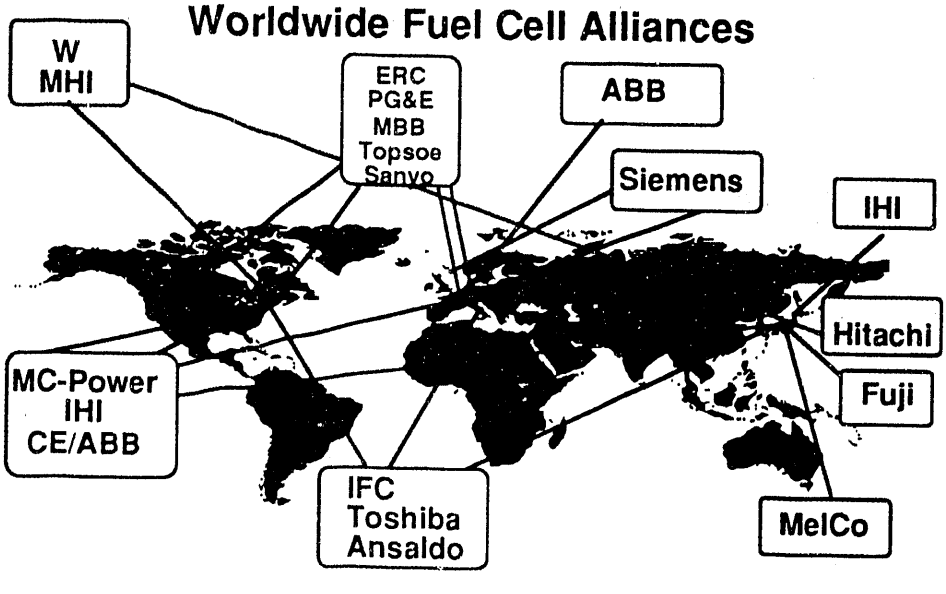

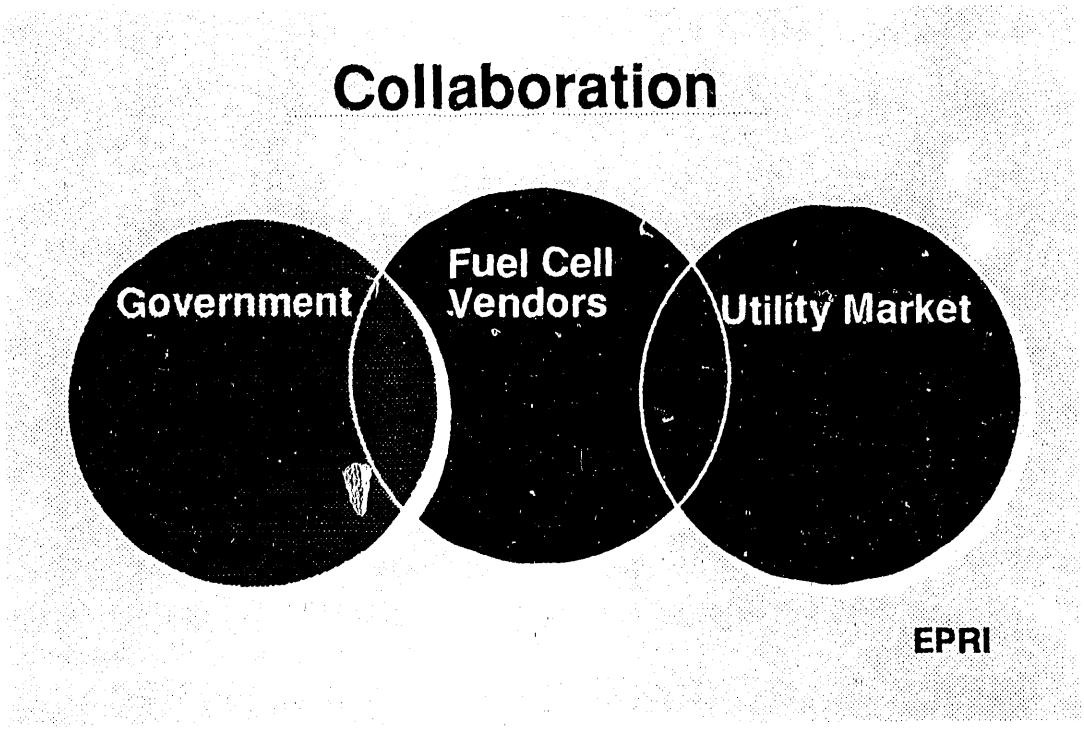
Collaboration
Government
Fuel Cell Vendors
Utility Market
EPRI

A Perspective On Natural Gas
General Outlook And Its Potential For Fuel Cells

Hugh D. Guthrie
Morgantown Energy Technology Center

Extraction research at METC involves Unconventional Gas, Enhanced Oil Recovery (CO_2 Flooding), Oil Shales, and Tar Sands. Research has also included Underground Coal Gasification and Arctic Research (Figure 1). Recently, the Unconventional Gas Research has been broadened to include Conventional Gas Research and has been retitled Natural Gas Research and Development. The discussion today will focus on natural gas.

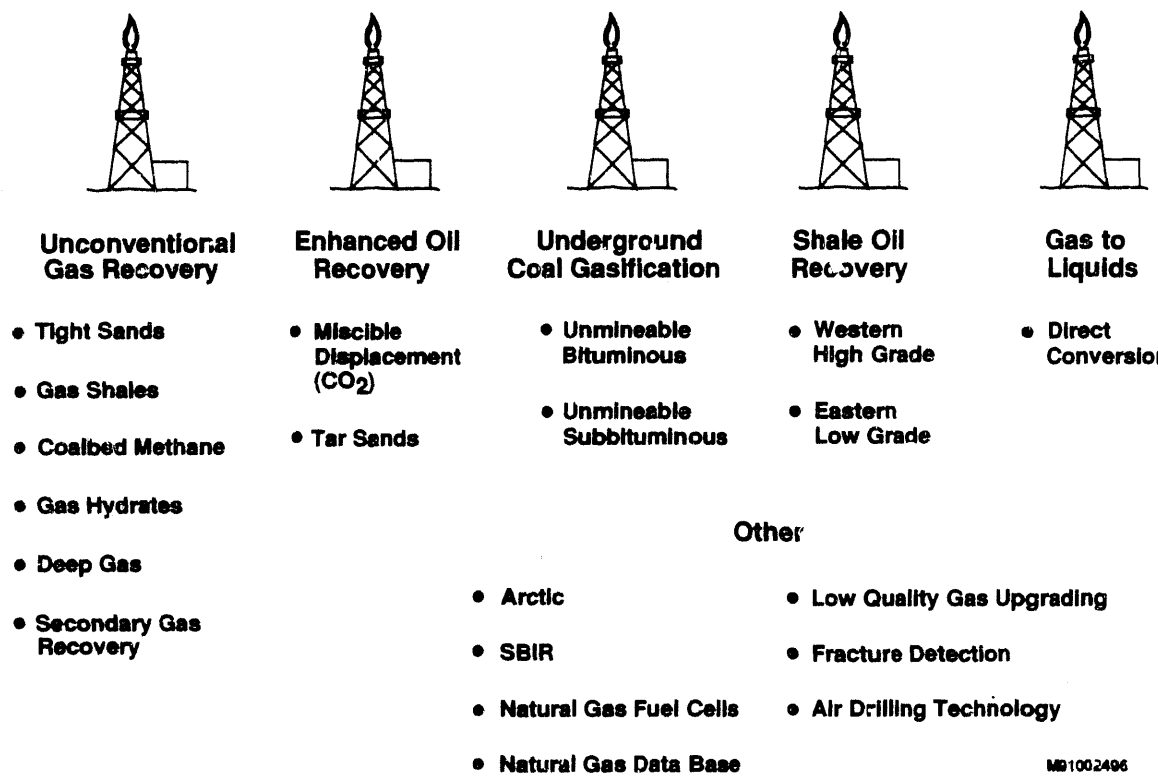

Figure 1. Extraction Programs

The work being supported in the Natural Gas Research and Development Program is in the areas of Tight Formations (sands, shales, coalbeds), Secondary Gas Recovery (by-passed formations, etc.), Deep Sedimentary Basins, Deep Source Gas, and Gas Hydrates. Portions of this research work require the development of a Natural Gas Data Base, as well as

crosscutting technology for horizontal drilling, fracture systems evaluation, and underground storage. Utilization research currently includes conversion of natural gas to liquid fuels or higher value hydrocarbons and natural gas fuel cells.

Natural gas is the fuel of choice for initial use with fuel cell systems. It is widely available and easily reformed, and with a minimum of contaminants, it is readily cleaned up to the purity required. Fuel cells, in converting the chemical energy in natural gas directly into electrical energy without going through typical combustion processes, maximize the benefits from this widely distributed and higher quality fuel.

U.S. proved reserves of natural gas are greater on a BTU equivalent basis than those for crude oil. U.S. production of natural gas exceeds that for crude oil on an equivalent energy basis, and energy production from gas wells exceeds that from oil wells. These differences are not great; the relative production of oil and gas and respective reserves are probably best viewed as about equal. However, it is generally agreed that the potential future production of natural gas will be increasingly greater than that for crude oil. Trends for crude oil and natural gas reserves from 1970 through 1990 indicate that world crude oil reserves have generally leveled out since 1977, while natural world gas reserves have shown a continued increase (Figure 2). This increase is expected to continue into the 21st century. This growth in natural gas reserves reflects the growing world-wide infrastructure for natural gas utilization.

A generally used rule-of-thumb for the wellhead price ratio of natural gas per mcf to that for crude oil per barrel is 1:10; whereas, the BTU equivalent ratio is about 1:6. Currently, that ratio is about 1:16. The ratio can be expected to move toward a value greater than 1:10, but less than 1:6. Market forces strongly influence that ratio; however, higher transportation costs for natural gas to end users is an important factor. Future use of natural gas in fuel cell applications can have potential economic advantage by locating such applications where local supply sources can minimize transportation cost and thus make natural gas use more attractive than the wellhead price ratio itself would indicate.

As the role of natural gas in the U.S. energy picture increases, the need to enhance natural gas supply will also steadily increase. Meeting the challenge will require the development of improved technical tools and innovative marketing approaches identifying the resource, defining the reservoirs, producing the resource, bringing the resource to market, and providing new economic applications for the resource. Areas of technology development are reservoir characterization technology (diagnostics), drilling technology, production technology, and utilization/application technology, which includes instrumentation, stimulation, completion, storage, and transportation technology, and the development of end use markets for gas technology.

The focus for development of utilization technology is primarily in four categories: storage of natural gas in subsurface reservoirs, transportation networks for the delivery of gas to appropriate markets, conversion of natural gas to higher value products, and use of natural gas as substitutes for other fuels. While current technology exists for these categories,

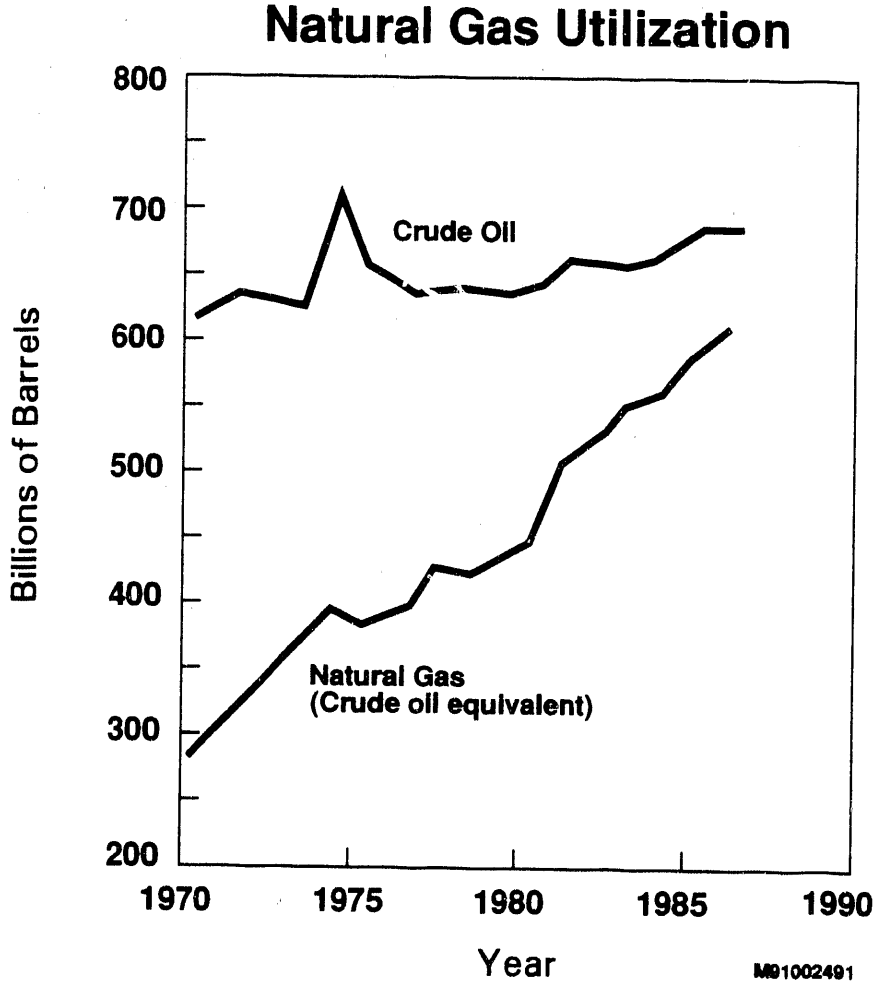

Figure 2. Total World Reserves

economics play a significant role in the marketplace and advances in technology could result in significant economic savings.

Fuel cells provide a number of important advantages in the use of natural gas. They are produced in modular units ranging from about 50kW to several hundred kW per stack. This allows applications in small commercial or industrial facilities or in the multi-megawatt utility size power plants. The advanced fuel cell types currently under development provide high temperature reject heat, which is ideal for dispersed cogeneration and highly efficient on-site use of the total available energy.

Technology development and appropriate cooperation of government and industry will be important in maintaining and improving the economic supply of natural gas. A particularly attractive aspect of fuel cell use can be level year-round demand or summer peak season

demand. In current use patterns, peak winter gas demand can be nearly twice that for the gas demand in summer months.

Another highly attractive feature of fuel cells involves their environmental performance. They can be sited in urban locations. They are quiet with no moving parts except for pumps and blowers. Their atmospheric emissions are far below that of conventional combustion processes.

As noted earlier, natural gas availability continues to increase on a world-wide basis. In this developing period, usage within the crude oil exporting nations can often have significant price advantage for natural gas uses. This could become an attractive marketing opportunity for fuel cells and at the same time represent minimum environmental impact for those developing nations.

Natural gas and coal, though long considered competitors for utility and commercial uses, can logically be viewed as parallel development paths. Locations which are advantageous for both interim supply of natural gas and longer term location of coal gasification facilities thus represent an important consideration in the development of fuel cells demonstration facilities and early commercial installations.

DOE Fuel Cell Program For Transportation Applications

Dr. Pandit G. Patil
Electric and Hybrid Propulsion Division
Conservation and Renewable Energy
U. S. Department of Energy
Washington, D. C. 20585
(202) 586-8055

INTRODUCTION

Fuel cells offer promise as a potential replacement of the internal combustion engine in transportation applications. Fuel cells operate more efficiently than internal combustion engines, and are capable of running on nonpetroleum fuels. Fuel cells could also have a major impact on improving the nation's air quality in urban areas by fuel cells virtually eliminating particulates, NOx, and sulfur oxide emissions, and by significantly reducing hydrocarbons and CO. Fuel cells can be applied in all areas of ground transportation which now utilize internal combustion or diesel engines. This includes passenger cars, vans, trucks, buses, and trains.

DOE FUEL CELL R&D ACTIVITIES

The DOE fuel cell program for transportation includes work on phosphoric acid fuel cell (PAFC), proton-exchange-membrane (PEM), and solid oxide fuel cell (SOFC) technologies and advanced fuel reformers. These programs are described in the following paragraphs.

Fuel Cell/Battery Powered Bus System Program

The Fuel Cell/Battery Powered Bus System Program was initiated in FY 1987. The objective of this program, co-sponsored by DOE, DOT/UMTA, and the California South Coast Air Quality Management District (SCAQMD) are to demonstrate the feasibility of a methanol-fueled phosphoric-acid fuel cell/battery propulsion system in a small urban bus to provide an alternative to diesel-powered buses.

The urban transit bus was selected as the entry point for application of fuel cells for transportation because operation in urban areas will accentuate environmental benefits; the transit route structure is relatively fixed and permits evaluation under controlled conditions; the transit industry has an infrastructure in place to support operation and evaluation of the fuel cell/battery bus; the long service life of transit buses allows amortization of higher acquisition cost over a reasonable time period; and the bus size permits accommodation of the first-generation fuel cell designs.

Phase I, now complete, included the conceptual design of the bus system, and the design, fabrication and laboratory evaluation of a half-size fuel cell/battery brassboard system. The brassboard systems met or exceeded design specifications. No fundamental design problems were uncovered, and the systems successfully demonstrated the ability to handle rapid load changes encountered in typical bus operation. An economic analysis was also performed, and

the results indicate that a methanol-fueled fuel-cell-powered bus can have a life-cycle cost competitive with a comparable diesel bus. Although the initial capital cost of the fuel cell bus will be somewhat higher than its diesel equivalent, the lower fuel and operating costs of the fuel cell bus compensate for this difference. DOE is proceeding with Phase II, in which three test-bed buses utilizing a PAFC/battery power source will be built.

Proton Exchange Membrane (PEM) Fuel Cell

For cars and vans, the program is directed at proton-exchange-membrane (PEM) fuel cells for mid-term introduction, and solid oxide fuel cells (SOFC) for long-term application and greater capability. PEM fuel cells can achieve the power density required for cars and vans, but much additional R&D is required towards cost reduction, performance optimization, and engineering scale-up.

DOE awarded a two-year contract in September 1990 to the Allison Gas Turbine Division of General Motors Corporation, selected through a competitive procurement to carry out the Phase I R&D. Allison plans to use Ballard Power Systems, Dow Chemical Company, Los Alamos National Laboratory, and General Motors Research Laboratories as subcontractors. The technical work under this 30% cost-shared contract includes the conceptual design of a PEM-based propulsion system, R&D on limiting components to advance the technology to meet transportation needs, and integration and testing of a complete 10-kW PEM fuel cell system. The expected outcome of this effort is a demonstration of the feasibility of PEM fuel cells for transportation, thereby laying the groundwork for a future engineering scale-up.

Fuel Reformers

Advanced reformer technology will be developed to improve the competitiveness of PAFC and PEM fuel cell powered vehicles by reducing system size and cost, reducing start-up times, and increasing transient response capability. Fuel flexibility will be attained with the capability of reforming methanol, ethanol, natural gas, or other hydrocarbons and through the direct use of hydrogen. An RFP for advanced reformer development will be issued during FY91.

Solid Oxide Fuel Cell (SOFC)

A study to evaluate the feasibility of SOFC for transportation applications will be conducted in the later part of FY 1991. The advantages of the SOFC advantages over other fuel cells include high fuel efficiency, high power density, and low cost materials, and it has fewer system components, not requiring an external reformer or auxiliary system for power peaking.

SUMMARY

The U.S. National Energy Strategy has identified the development of fuel cell propulsion technology as a means to promote greater energy security. The results the phosphoric acid fuel cell bus program thus far are very promising and represent a major step forward in the application of fuel cells in transportation. Advanced fuel cells such as the PEM and the SOFC could provide viable propulsion systems for cars, trucks, buses, or locomotives using nonpetroleum-based fuels and having dramatically reduced emissions.

Session 1

Molten Carbonate Fuel Cells

Full-Height Fuel-Flexible Carbonate Fuel Cell Stack Development

Contract Number:	DE-AC21-90MC27168
Contractor:	Energy Research Corporation 3 Great Pasture Road Danbury, CT 06813
Contract Project Manager:	Mohammad Farooque
Principal Investigators:	R. Bernard, J. Doyon, L. Paetsch, P. Patel, A. Skok, and C. Yuh
METC Project Manager:	Thomas J. George
Period of Performance:	September 21, 1990 to November 21, 1993

SCHEDULE AND MILESTONES

A simplified schedule and the major milestones of this cost-shared program are shown in Figure 1.

OBJECTIVE

ERC's carbonate fuel cell development efforts are focused on commercialization of the MW-Class natural gas units in the near-term and 100MW-Class dual-fuel units later. To achieve this, ERC plans to demonstrate 2MW power plants in the 1993-1996 time frame and commercialize thereafter. The present program is designed to bring the carbonate fuel cell technology from the engineering research stage to the demonstration stage in an approximately three-year period.

BACKGROUND

The carbonate fuel cell system is well-recognized as a potentially very highly efficient and environmentally superior power generator, both for pipeline natural gas and coal-gas fuels. ERC is committed to bringing this unique technology to the marketplace by the latter part of the 1990's.

Energy Research Corporation started developing this unique technology in 1976 under an ERDA (Energy Research and Development Administration) sponsored program which was the very first program for carbonate fuel cell development sponsored by a U.S. Government agency.

The carbonate fuel cell developmental activities in the early years (1976-1980)[1] at ERC concentrated on cell active component development and single-cell testing. The stack development activities were initiated in the early eighties and from the beginning ERC focused on the development of dual-fuel stacks. This stack design has incorporated the unique internal reforming feature which allows utilization of the hydrocarbon fuel directly in the fuel cell without requiring any external reforming or associated heat exchange equipment. Significant advances have been made at ERC in this direct fuel cell stack approach under the sponsorship of DOE, EPRI, GRI, PG&E, and ERC [1-4]. The cell technology has been scaled from a fraction of a

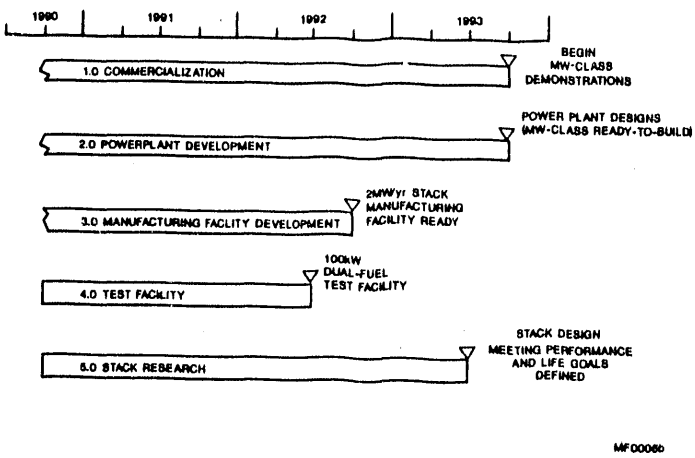

Figure 1. Overall Schedule and Major Milestones:

A Five-Task, Thirty-Eight Month Program With Five Specific Objectives is in Place

square foot to 4 ft^2. Prior to the start of this program, twenty-one multicell stacks were operated with up to 60 cells and capacities ranging from 1 to 8 kW. Stack operations on simulated coal-gas and natural gas were demonstrated. Lifetimes of over 5,000 hours were also achieved. In addition, a 7kW stack was successfully shipped and restarted at a utility site operating on natural gas and feeding electricity into the utility grid.

These successes provided a sound basis for the current program efforts which are designed to take the next steps towards commercialization of ERC's unique technology: (a) stack scale-up to full-height; (b) stack demonstration in an integrated system; (c) component durability demonstration, and (d) attainment of performance consistent with system commercialization goals. An aggressive stack development program is being pursued for attaining these goals. The recent accomplishments in this area are discussed in this paper.

ERC's commercialization and power plant development efforts to date have been focused on two electric utility markets: (a) the natural gas fueled generator in the 2-10 MW size range, and (b) the natural gas/coal-fueled 100-400 MW power plants. ERC believes that the former is a necessary precursor to the success of the latter. With this in mind, ERC has launched concerted commercialization activities for its natural gas fueled MW-Class generator. ERC plans demonstrations of 2MW power plants in the 1993-1996 time frame, and commercialization thereafter.

ERC's current program efforts are designed to conduct stack and power plant development, and to pursue commercialization activities in parallel to fulfill this plan.

PROJECT DESCRIPTION

The specific program objectives identified to bring the carbonate fuel cell technology to the demonstration stage are:

- Define the requirements for market responsive power plants and prepare a commercialization strategy for natural gas-fueled MW-Class dispersed and natural coal/gas-fueled 100MW-Class baseload carbonate fuel cell power plants.

- Demonstrate readiness of the full-size, dual-fuel stack (100kW-Class) and balance-of-plant systems for power plant demonstration(s).

- Develop a manufacturing facility for ERC's dual-fuel full-height stacks.

- Provide test facilities to support testing of full-size stacks at pipeline natural gas and simulated coal-gas system conditions.

- Demonstrate attainment of carbonate fuel cell stack performance and life goals for commercial entry.

A five-task program, where each task is dedicated to the realization of one of the specific program objectives, was started in September of 1990 (as shown in Figure 1). In this program, parallel activities for market development, system development, stack manufacturing, balance-of-plant development, and stack development are being pursued aggressively.

RESULTS/ACCOMPLISHMENTS

The overall approach and the status of the commercialization plan is discussed in Dr. Baker's paper presented at this conference. The progress in stack development is reported in this paper.

Since 1990, eight short stacks including a 54-cell, $4ft^2$ stack (20kW) were tested. The immediate stack research focus is on scale-up to full-height (100kW) and demonstration of integrated system operation. Also, in parallel, activities to improve cell performance and component durability are being pursued. Progress made in these areas is discussed next.

Scale-Up

ERC's carbonate fuel cell scale-up activities are directed towards preparing the stack for the 2MW power plant demonstration(s) planned for 1993-1996. The immediate activities in this area are concentrated on demonstration of the full-height stack design and integration with system equipment. ERC's full-height stack has a nominal 100kW per stack rating and is the repeat unit in a power plant stack module. Each stack module may carry up to ten stacks.

To date ERC has tested a total of 24 stacks with cell areas ranging from a fraction of a square foot to 4 ft^2, and number of cells ranging from 5 to 60. ERC has not experienced any performance penalty in either cell area scale-up or in height scale-up (Figure 2). Scale-up of active cell components from $4ft^2$ to $6ft^2$ size has already been verified. At ERC's 2MW/yr manufacturing facility, $6ft^2$ stacks will be produced. Testing of a $6ft^2$ area stack is planned in the third quarter of this year.

The largest stack tested to date at ERC is a quarter-height 20kW (54-cell) $4ft^2$ area cell stack. This stack was tested under EPRI/PG&E programs. Photographs of this stack in the test facility are shown in Figure 3. This stack was tested for repeat and non-repeat hardware design evaluation at ERC. The individual cell performances at 140 mA/cm^2 for simplified MW-Class system conditions (methane; 75% fuel utilization; 75% CO_2 utilization) are reported in Figure 4. Good cell-to-cell performance uniformity is evident. This test successfully verified ERC's dual-fuel stack design. The testing of this stack at ERC has been voluntarily terminated after 400 hours and has been transported to PG&E's San Ramon, CA site for 100kW power plant system equipment low power verification testing.

The successful testing of the quarter-height stack has provided a strong basis for the next stepping stone in stack height scale-up i.e., a $4ft^2$ cell area, full-height stack test. ERC has planned a full-height $4ft^2$ area stack test in the latter part of 1991. The design basis of

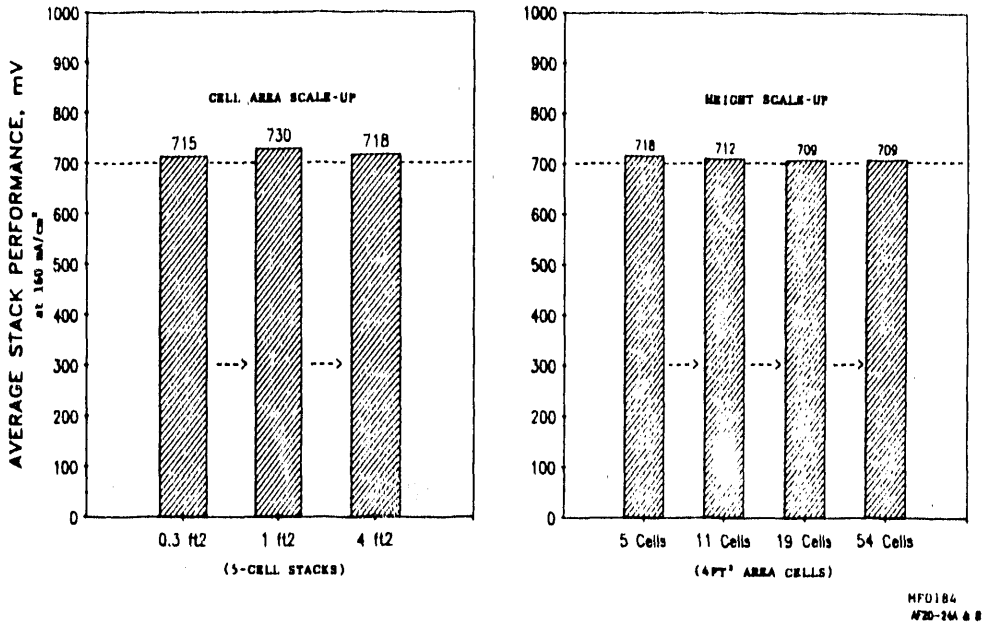

Figure 2. Effect of Scale-Up on Stack Performance:

No Effect on Performance from Either Cell Area or Height Scale-Ups

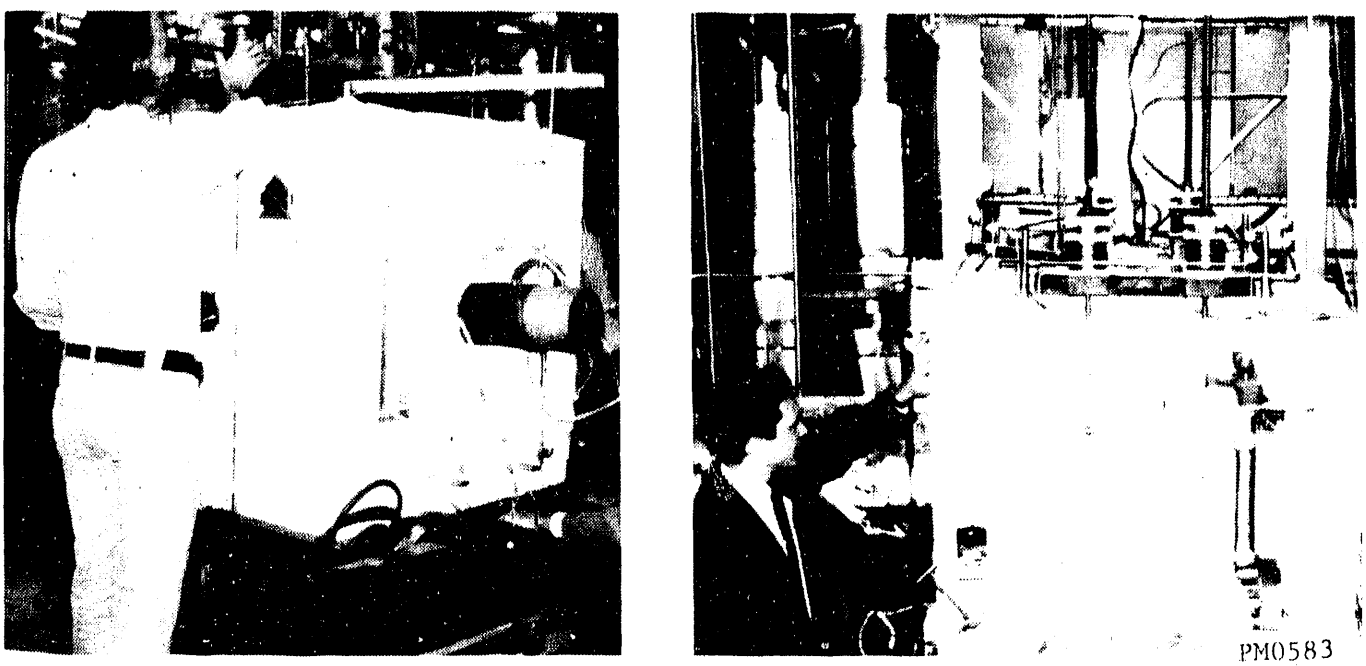

A) Stack Being Moved to the Test Facility

B) 20kW Stack on Test

Figure 3. Photographs of the 20kW Stack:

Successful Testing of the 20kW Stack Provides a Solid Basis for the Next-Step: Full-Height Tests

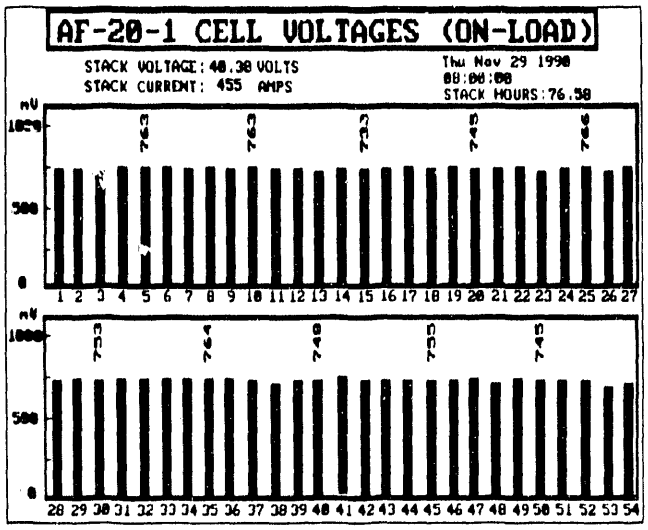

Figure 4. Individual Cell Performances of the 20kW Stack:

Good Performance Uniformity Qualifies ERC's Dual-Fuel Stack Design

this stack is shown in Table 1. An exploded view of the stack is shown in Figure 5. The cell repeat components and non-repeat stack components such as the end plates and compression hardware employed in this stack have been proven in numerous stack tests including the 20kW stack. The manifold and the dielectric separator designs are derived from the 20kW stack experience. The fabrication of this stack is 75% completed at this time. This stack will be truck-transported to the PG&E test site, integrated with the 100kW power plant equipment, and tested this fall. An additional 100kW-Class stack test (made with 6ft^2 area cells) is planned for 1992.

Table 1. Full-Height Stack Features:

Manufacture of this Stack is 75% Complete

CELL SIZE:	2' X 2' (4 ft^2 Nominal)
NO. OF CELL:	234
NO. OF RU:	39
NO. OF CELL/RU:	6
TYPE:	DUAL-FUEL
MANIFOLD:	EXTERNAL
TOTAL STACK HEIGHT:	11 ft
STACK NOMINAL POWER:	75 kW DC

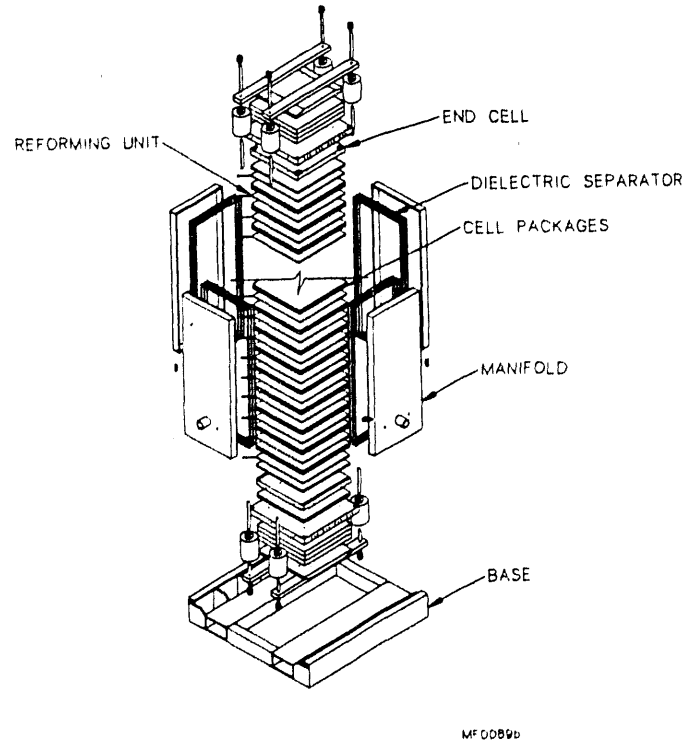

Figure 5. An Exploded View of the 4ft^2 Cell Area Full-Height Stack:

The Design Included here has been Proven in Shorter Stacks

Components Durability and Life Projection

The research objectives in this area are to: (a) resolve endurance issues and (b) demonstrate endurance projectable to 40,000-hour life.

ERC has recently conducted a thorough materials analysis of the components of a stack which was operated for 5,000 hours. The corrosion of the cathode side sheet metal hardware at various locations were measured. The corrosion penetrations for 40,000 hours operation projected from the 5,000 hour data are shown in Figure 6. The results suggest that the expected corrosion is <~3 mils, which is acceptable. No degradation of the Ni-protected anode side hardware was noticed. Metallographs of the Ni-protected hardware showed no significant penetration of Fe in the Ni layer; this was also verified by EDAX analysis.

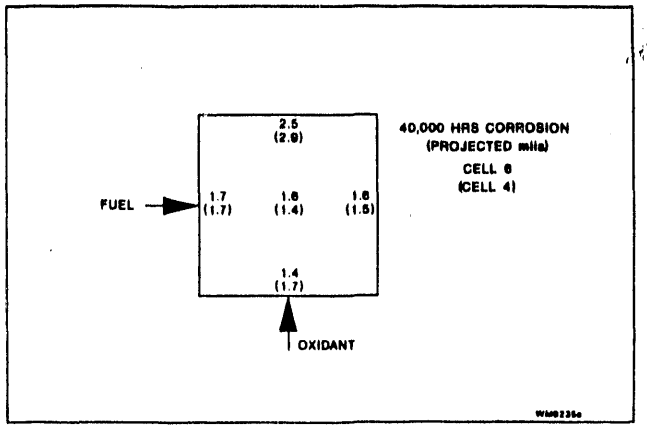

Figure 6. Cathode Side Sheet Metal Corrosion Projection Based on 5,000 Hour Stack Data:

Useful Life of 40,000 Hours is Assured

The matrix ceramic support material has also been analyzed for possible particle growth and phase change. Scanning Electron Microscope studies did not indicate any growth of the lithium-aluminate particles.

ERC has developed a unique carbonate fuel cell gasket design to alleviate the difficulties posed by electrolyte redistribution from the positive end of the stack to the negative end. The performance of this gasket has been evaluated in four recent stacks. One of these stacks is a five-cell, 0.3ft^2 area cell stack and provides approximately 15 times accelerated testing with respect to electrolyte redistribution compared to the same size 6ft^2 size stack planned for commercialization. This accelerated test has completed 6,000 hours of operation to date and is indicating no evidence of electrolyte redistribution, characterized in terms of end cell performance loss and resistance increase. The positive and negative end cells are very stable. The observed positive end cell resistance increase rate of this stack is compared in Figure 7 with two 10 times larger area stacks which employed the baseline gasket design. The results clearly show that the use of the advanced gasket has significantly reduced the electrolyte movement from the positive end cell.

ERC has developed a unified electrolyte loss model to predict the useful life from an electrolyte management vantage point. This model takes into account all forms of loss including the electrolyte redistribution. The useful life of the positive end cells of different stack designs predicted by this model is compared in Figure 8. The results show that the model predicts a life of only 6,800 hours for the positive end cell of the accelerated test discussed earlier. Note that this stack has already completed 6,000 hours and has shown no effect on positive end cell performance or

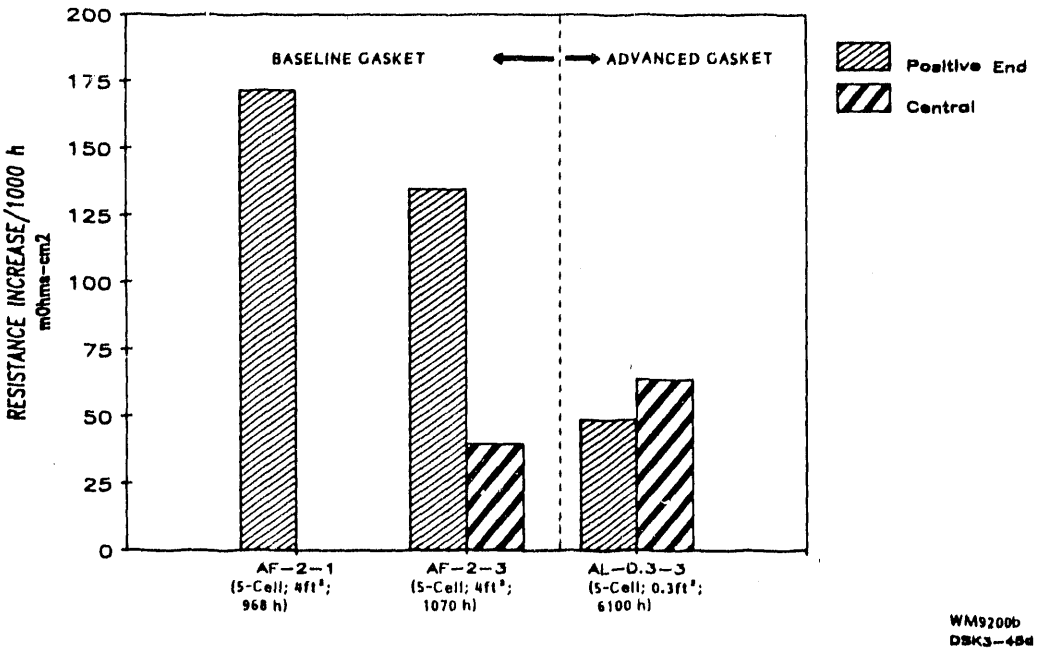

Figure 7. Comparison of Resistance in Positive End Cells:

Use of Advanced Gasket has Provided Significant Reduction in Electrolyte Loss from Positive End Cell

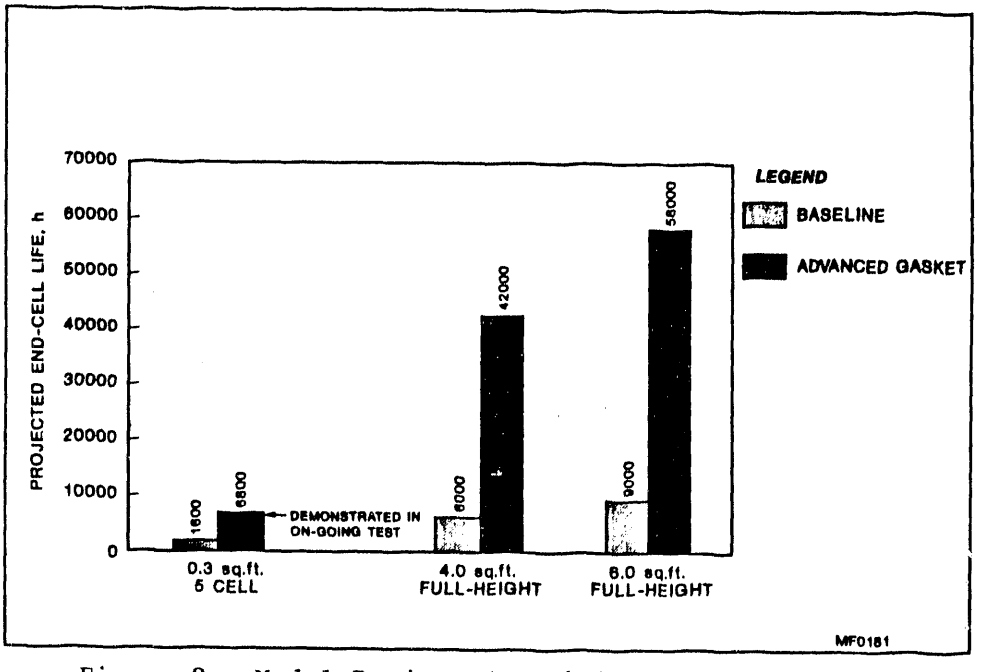

Figure 8. Model Projected Positive End-Cell Life:

40,000-Hour Life can be Projected (With Advanced Gasket) for the Full-Height Stack

resistance. The results clearly show that a 40,000-hour life can be easily predicted for ERC's 6ft^2 full-height stack.

Thermal cycleability is also an important issue. ERC has been successful in thermal cycling stacks down to room temperature without impacting the performance. Also, the manifold and matrix gas sealing efficiencies were unaffected by the thermal cycling.

In addition to the accelerated stack test discussed earlier, ERC is conducting an endurance test of a 2kW (five-cell, 4ft^2) stack under the EPRI program. This test has completed 6,000 hours and is continuing. The power and cell voltage lifegraphs are shown in Figure 9. As can be seen, very stable performance has been observed.

The performance decay observed in ERC stack tests has been mainly due to cell resistance increase. The average stack voltage and the resistance loss-free performance of the 0.3ft^2 stack being tested at the accelerated condition is illustrated in Figure 10. The results show that on the IR-free basis, the stack showed no performance loss in 6,000 hours. However, the net performance loss (including IR) is parabolic with time and projects to <~70 mV over the 40,000 hour life. This corresponds to an increase in heat rate of about 600BTU/kWh.

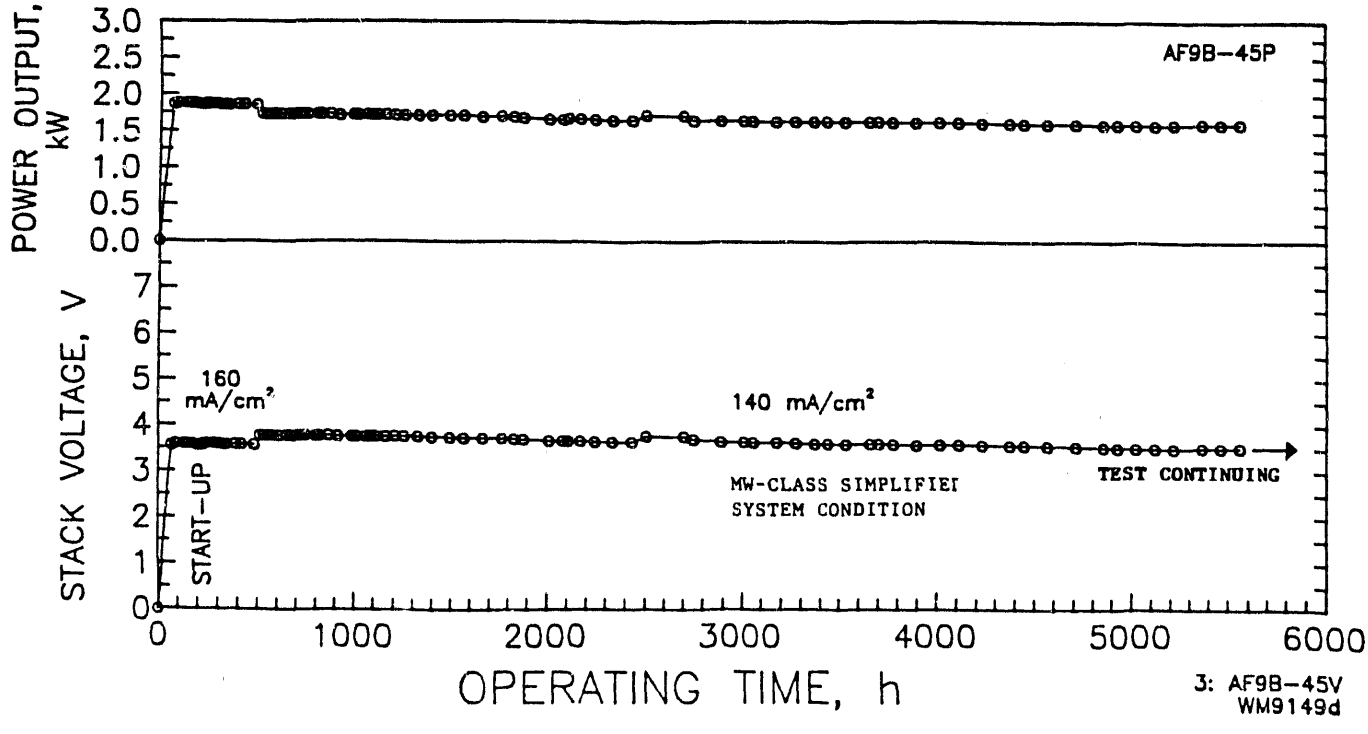

Figure 9. Endurance Testing of a 2kW Stack (5-Cell, 4ft^2):

Stable Performance Demonstrated

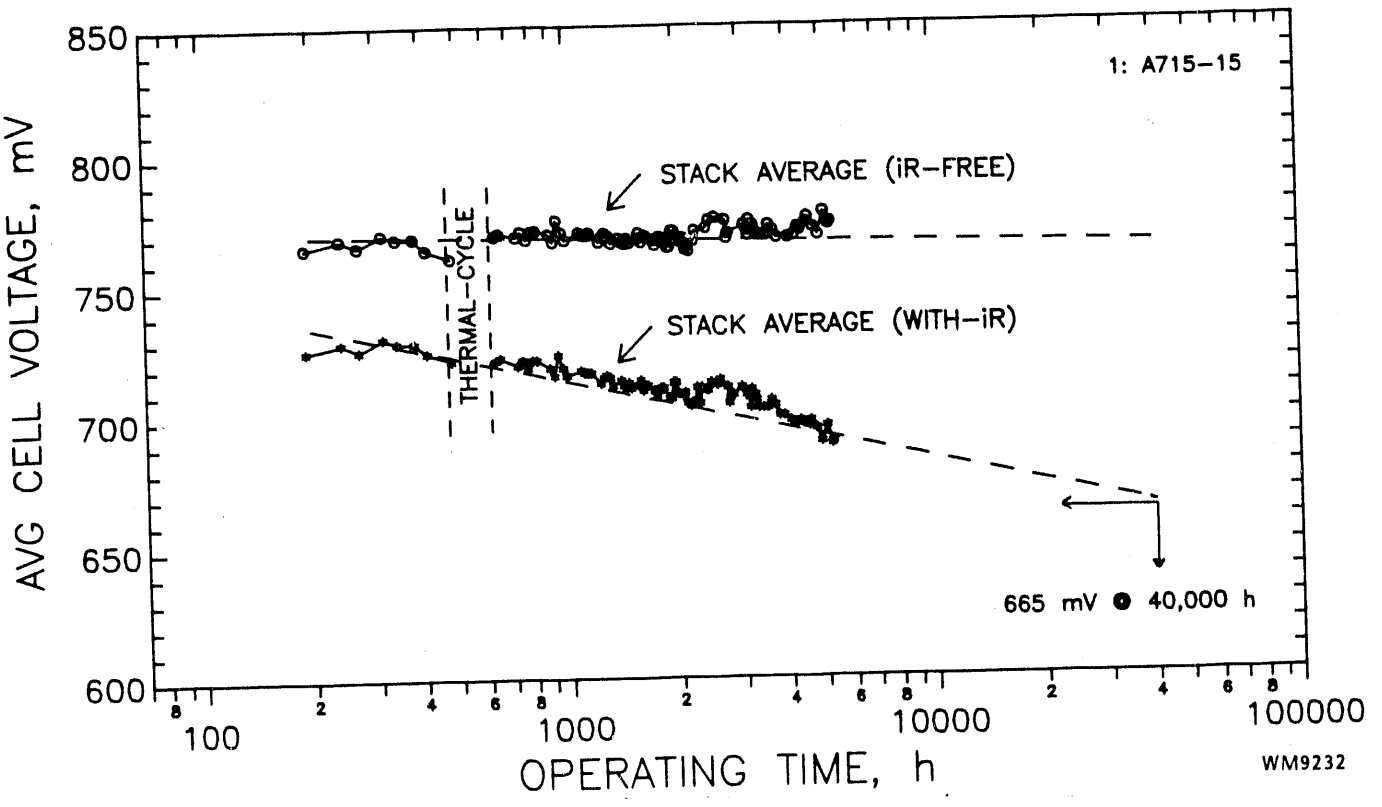

Figure 10. Performance Projection to 40,000 Hours (7"x7", 5-Cell Stack; 160 mA/cm^2 Operation at the MW-Class Integrated System Condition):

A Performance Decay of <70 mV in 40,000 Hours is Projected

Transportation

ERC plans to transport a full-height stack to PG&E's San Ramon, CA test site for system integrated testing during the latter part of 1991.

The shipping crate design, incorporating required environment and vibration controls, is ready and all logistics for handling and shipping have been settled. In fact, all the steps involved have been verified twice using subscale stacks.

A 7kW stack was successfully shipped in 1990 by truck and plane to a utility test site in Europe after operation at ERC. This stack was operated by the customer for ~3,500 hours on pipeline gas, feeding electricity into the utility grid.

More recently, ERC has shipped a 20kW stack to the PG&E site. A photograph of the stack on the truck bed enroute to San Ramon, CA is shown in Figure 11. An oversized full-height stack shipping crate was used here to expose and resolve issues associated with the transportation of a full-height stack. The shipping crate height is 11 ft. The maximum allowable clearance for the United States road transportation requiring no special permit and routing is 13.5 ft. Therefore, a double-drop low-bed truck has been used for the transportation of the stack. The 20kW shipping test provided a "dry run" for shipping of the full-height 100kW stack planned for later this year. In the transportation of a preconditioned stack, control of humidity, impact, and vibration ("G" force) is very important. ERC's shipping crate design limits impact and vibration loads to a maximum of 3 "G's"

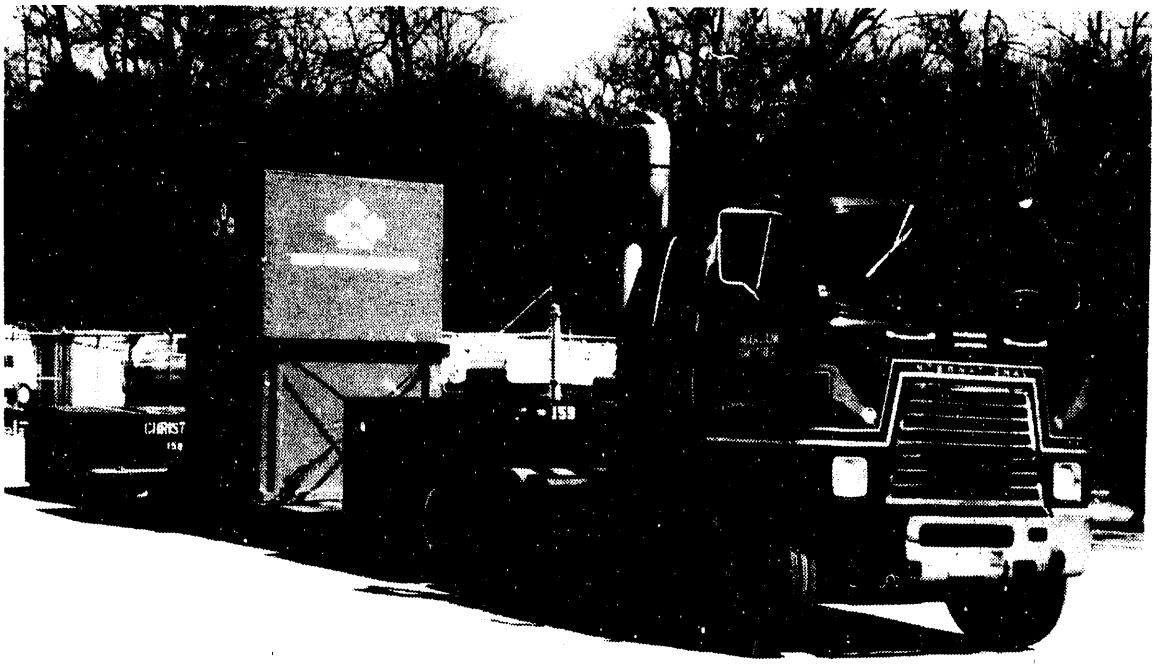

MFP0017

Figure 11. Photograph of a Stack on Low-Bed Truck Enroute to San Ramon, CA:

This Test Provided a "Dry-Run" for the Full-Height Stack Transportation During the Fall of 1991

and controls relative humidity. In the 20kW transportation experiment, the stack relative humidity and the "G" force in all three directions were recorded. The "G" force as well as the humidity in the stack enclosure were maintained within the desired range, although, as expected, both the humidity and "G" force variations were registered outside the stack. These experiences provide a sound basis for the transportation structure design for the full-height stack.

ERC has thus demonstrated significant progress in stack height scale-up and resolving issues relevant to attainment of a long useful life for the carbonate fuel cell.

FUTURE PLANS

The plan for the immediate future includes:

1. Manufacture and system integrated testing of a 234-cell, 4ft^2 area stack.

2. Manufacture and testing of 6ft^2 area 2 and 8kW subscale stacks at simulated system conditions.

3. Manufacture and testing of a 20kW 6ft^2 area stack on a gasifier slip stream.

REFERENCES

[1] B. Baker, et al., "Development of Molten Carbonate Fuel Cell Technology," Interim Technical Progress Report (March 1976 to January 1980), ERDA-DOE Contract Nos. E(043)1196, EY-76-AC03-1196, DE-AC03-76ET11304.

[2] A. Pigeaud, "Development of Molten Carbonate Fuel Cell Technology," Final Report for the Period of February to December 1980, Contract No. DE-AC03-76ET11304.

[3] L. Paetsch, et al., "Development of Molten Carbonate Fuel Cell Components," EPRI AP-5789, Research Project 1085-3, Final Report, July 1988.

[4] L. Paetsch, et al., "Molten Carbonate Fuel Cell Development," DOE Contract No. DE-AC03-76ET11304, Final Report, April 1987.

Simulated Coal Gas MCFC Power Plant System Verification

CONTRACT INFORMATION

Contract Number DOE Contract No. DE-AC21-90MC27394

Contractor
M-C Power Corporation
8040 South Madison Street
Burr Ridge, IL 60521
(708) 986-8040

Contractor Project Manager E.H. Cámara

Principal Investigators
Thomas G. Benjamin, M-C Power
Elias H. Cámara, M-C Power
Rene M. Laurens, M-C Power
Leonard G. Marianowski, Institute of Gas Technology
Michael W. Snow, ABB C-E

METC Project Manager Dr. Mark C. Williams

Period of Performance September 14, 1990 to September 14, 1993

Schedule and Milestones

FY 91-92 Program Schedule

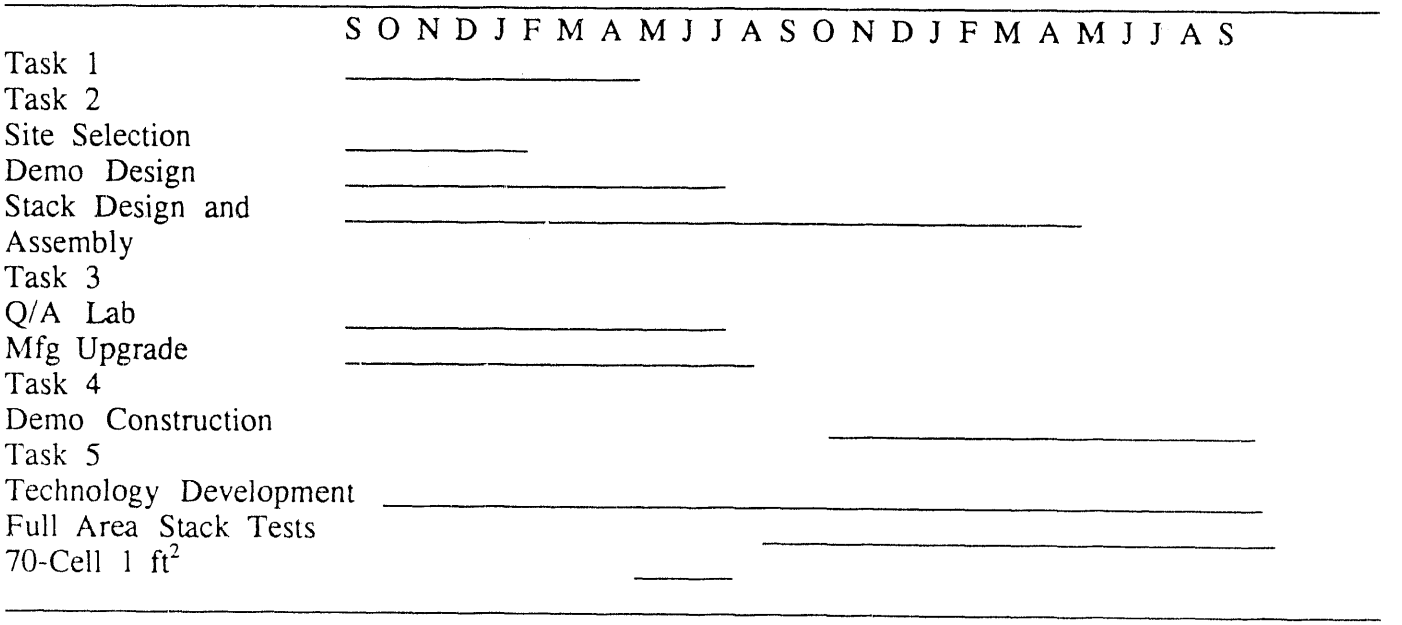

OBJECTIVES

The overall program objective is the demonstration of a full-scale, full-height IMHEX® molten carbonate fuel cell stack in a 250 kW integrated dual-fuel power plant system on natural gas and simulated coal gas. Issues impeding development of manufacturing and testing facilities will be addressed in support of MCFC stack research and power plant development. Issues will be identified and resolved in engineering, manufacturing, assembling, cost, performance, and endurance of the stack repeat and non-repeat components.

BACKGROUND

The program is being executed by M-C Power (MCP) and two major subcontractors. M-C Power's role in the team is to scale up the IMHEX® stack technology and to fabricate commercial scale stacks and to demonstrate progress in full-area stacks. ABB C-E (ABB) is responsible for power plant design and commercialization, design and construction of the balance of plant for the 250 kW power plant system demonstration, and operation of the power plant. The Institute of Gas Technology (IGT) is addressing active area component technology development and demonstration of advances in subscale 1 ft^2 stack tests.

In addition to the DOE support and the cost sharing of MCP, IGT, and ABB, cost sharing is being provided by the Electric Power Research Institute (EPRI), Southern California Gas Company (SoCalGas), the South Coast Air Quality Management District (SCAQMD), and Union Oil of California (UNOCAL). The power plant system demonstration will be sited at UNOCAL's Science and Technology Center in Brea, California. Separate but highly integrated programs are also being funded by the Gas Research Institute (GRI), San Diego Gas & Electric (SDG&E), and the State of Illinois.

PROJECT DESCRIPTION

The tasks of the program are:

Task 1. Commercialization
Task 2. Power Plant Development
Task 3. Manufacturing Facilities Development
Task 4. Testing Facility Development
Task 5. Stack Research

Technology developments are aimed at reducing cost and improving life and performance through development of alternative anode materials, stabilized cathodes, and strengthened components. Subscale (1 ft^2) stack testing under this program includes two stacks of nominally 10 cells operating for about 1,000 hours each and one stack of about 5,000 hours to demonstrate and qualify advanced active components. Operation of a 70-cell 1 ft^2 at MCP began in April 1991 with primary funding from EPRI.

Full-area stack testing comprises two stacks of 20 kW and one of 50 kW in addition to the 250 kW power plant system verification at UNOCAL. A 10 kW stack will be operated in the fall of 1991 under the sponsorship of the Gas Research Institute (GRI). The separator plates for the 10 kW stack have been stamped and welding and aluminizing trials are

underway. Design activities for the 250 kW demonstration are beginning for the balance of plant and the stack. The natural gas version of the 250 kW power plant is being developed with GRI support.

STATUS

Technology Development

IGT has successfully tested numerous laboratory single cells to screen and evaluate advanced components, formulations, and fabrication processes. Several advancements are ready for scale up: low-cost copper-based anodes (EPRI cost sharing), stabilized and strengthened cathodes, and clean binders.

A 3 cm^2 single cell with a copper-based anode has been operating for nearly 3,800 hours at stable, state-of-the-art performance. The cell was subjected to an involuntary thermal cycle at 3,024 hours when a temperature controller failure caused the temperature to drop to 100°C. The cell was restarted and has shown no deleterious effect caused by the involuntary thermal cycle. Two other 3 cm^2 cells with low-cost Cu-based anodes have been operating stably at state-of-the-art performance for more than 1,900 hours.

Identification of a tape casting binder system with clean removal characteristics has been successful. Scale up to 18" wide tapes is in progress.

Mitigation of nickel dissolution has been demonstrated in single cells. Stabilization reduces nickel deposits in the matrix by about 50%.

Stack Testing

Stack MCP-1 (1 ft^2, 20 cells) was operated for about 1,350 hours with major funding from GRI. The stack performance increased continuously throughout the test until termination, when two cells experienced rapid decay which was found to be caused by carbon deposition. No evidence of electrolyte migration was observed. Post-test analysis of the stack is in progress.

Stack MCP-2 (1 ft^2, 70 cells) is currently operating. Performance is still increasing after more than 450 hours of operation and power output of 8.1 kW at 160 mA/cm^2 has been demonstrated. The planned duration of this stack is 1,000 hours.

Stack MCP-3 (10 ft^2, 10 cells) operation is planned for August 1991 with primary funding from GRI. Separator plates have been stamped and welding and aluminizing trials have recently been performed. Full area electrode tape casting has begun and initial sintering trials were successful.

Systems

ABB has modified two conceptual coal-gas fired MCFC systems designs developed under Contract No. DE-AC21-88MC25026 to improve performance and reduce cost. Efficiencies have been improved by 1 - 4 percentage points and TAG I costs reduced by 0.5 to 3 mills/kW. Further analysis at the TAG II level will be performed after product definition and market analysis work is completed.

Demonstration

A nominal 250 kW IMHEX® demonstration is planned for January 1993 at UNOCAL's Science and Technology Center in Brea, California. The stack and systems designs have been initiated and permitting activities have begun.

FUTURE WORK

During the next 12 months, the following stacks will be tested:

- 1 subscale (1 ft^2) performance stack at IGT with advanced components (DOE) and 1 endurance stack (SDG&E)
- 10 kW full-area (GRI)
- 20 kW full-area (DOE)
- 20 kW test in a systems simulator (GRI)

The design of the 250 kW balance of plant will be completed and construction will begin. Design of the stack will be completed.

IFC MCFC Stack Research Status

1. CONTRACT INFORMATION:

Contract Number: DE-AC21-91MC27393

Contractor: International Fuel Cells Corporation (IFC)
P.O. Box 739
195 Governors Highway
South Windsor, CT 06074
(203) 727-2215

Contractor Program Manager: Walter H. Johnson

Principal Investigator: Carl A. Reiser

METC Project Manager: Mark C. Williams

Period Of Performance: December 18, 1990 to March 18, 1994

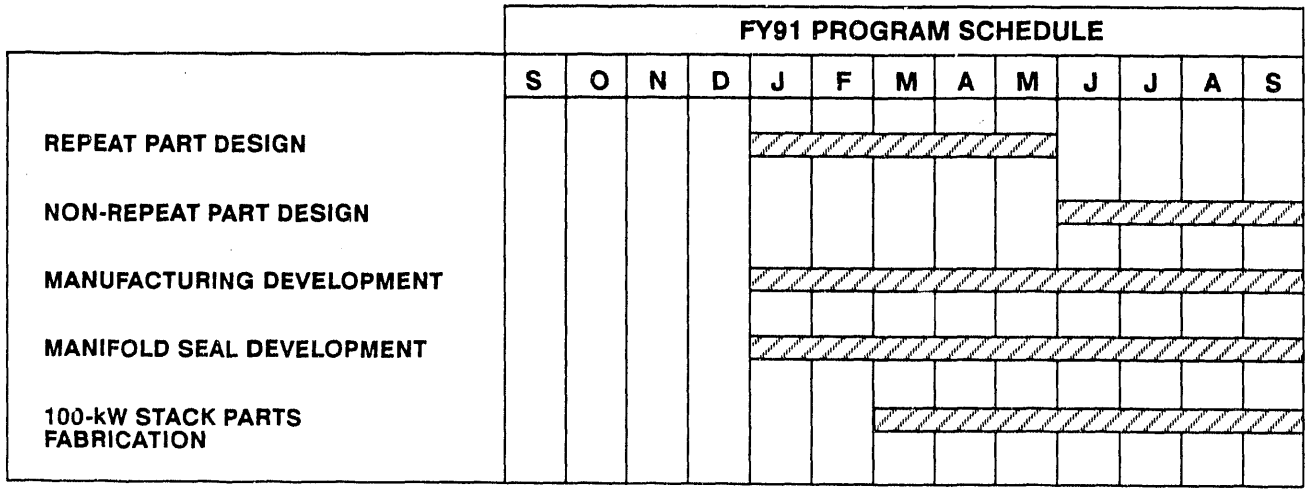

2. OBJECTIVES

The Department of Energy's Fossil Energy Program is supporting the development of molten carbonate fuel cells (MCFC) to help achieve its goal of accelerating the introduction of new clean coal technologies to utilize the nation's coal reserves as fuel to produce electricity. The MCFC power plants must be capable of dual-fuel (coal-derived fuel and natural gas) operation and generate electricity in a competitive, highly efficient, and environmentally benign manner.

IFC's objectives are aligned with those of the Fossil Energy Program. A 100-MW MCFC power plant conceptual design which meets the objectives has been completed. The heart of the design is IFC's Integrated Stack Unit (ISU), which includes the MCFC stack, a sensible (waste) heat reformer, and the stack ancillary equipment, all housed in a vessel. The ISU is a factory-constructed and factory-checked unit which uses coal gas or natural gas as fuel input and produces dc power, heat, and completely reacted exhaust products as outputs. The ISU has simple mechanical, fluid, and electrical interfaces which permit it to be incorporated into a power plant by any utility or A&E, without special knowledge or skills. All the equipment unique to the molten carbonate fuel cell is incorporated within the ISU.

The rating of the ISU is expected to be 1 MW or greater. Since the ISU can be a building block element for natural-gas-fueled plants or coal-gas plants, it is readily adaptable to phased construction. In this concept, small blocks of natural gas capacity are installed at a site initially. Additional blocks are added as needed. When sufficient fuel cell capacity is available, the power plant can be converted to coal operation by the addition of a coal gasification plant.

The primary objective of this DOE program is to demonstrate operation of a full-area, 100-kW MCFC stack for 3000 hours. This demonstration utilizes a pressurized 8-ft^2 stack of 140 cells capable of integration with the required ancillary components. The stack will operate without modification on both a variety of simulated coal gases and simulated natural gas. This 100-kW integrated stack is a first step to full-scale (1 MW or greater) ISU operation.

3. BACKGROUND

IFC has identified as its commercial MCFC product a 1-MW Integrated Stack Unit (ISU) shown in Figure 1. This self-contained 1-MW dc power generating device is the fundamental building block for a range of power plants operating on coal, natural gas, and other fuels. The ISU operates at pressure and incorporates a sensible (waste) heat reformer. These features provide high efficiency on all fuel gases, and permit a common cell stack design (common cell components, flow fields, etc.) for all applications and fuel gases. The design is compatible with processed gas from all gasifiers.

System studies have been conducted for a wide range of utility power station sizes and fuel sources. These studies show that use of a common ISU results in power plants for these applications that have nearly the same performance and cost characteristics as power plants incorporating ISU designs optimized separately for each application. This single-product focus is a key element to IFC's commercialization strategy. It provides for a single development and demonstration path for multiple applications, thus reducing overall program financial risk.

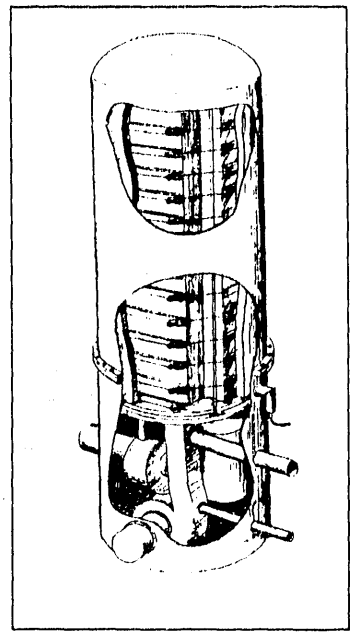

HP-267-01
911206

Figure 1. IFC's Product is 1-MW Integrated Stack Unit

Based on current projections of fuels and applications, IFC envisions power plant opportunities in the size range between 10 and 100 MW operating on natural gas or in multiples of 100 MW operating on processed gas from coal gasifiers. Examples of power plants incorporating the common ISU are shown in Figure 2. These power plants share the common characteristics of fuel flexibility, high efficiency, and negligible emissions, and offer excellent opportunities for cogeneration. Application studies show that the MCFC power plant has the best opportunity for competitive economics at these ratings. These characteristics make them suitable in both rural and urban areas, most especially in non-attainment areas with strict limits on emissions.

Between the present and the time frame beyond 2000, when MCFC plants are expected to become commercially available, fuel type (coal gas, natural gas, coal bed methane, landfill gas and other bio-waste gases) and power plant design (rating, siting, all-electric or cogeneration) preferences will change. IFC's commercialization strategy provides the flexibility of a product capable of integration into power plants to satisfy this changing market.

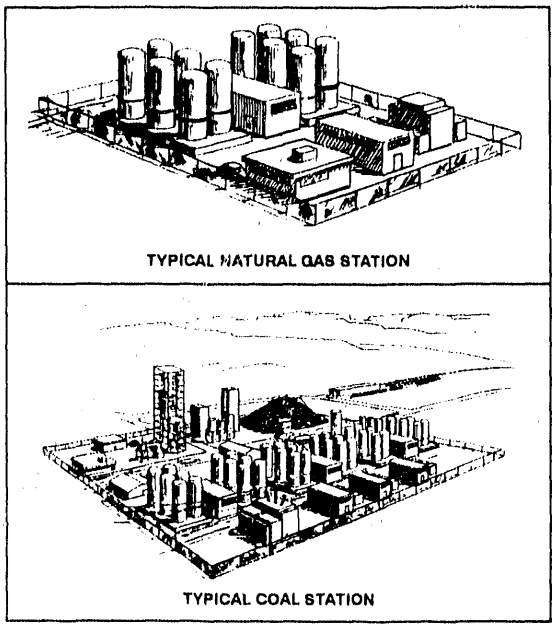

Figure 2. ISU is Fundamental Building Block for Range of Future Power Plants HP-267-02 911206

The ISU is a fundamental repeating element in a larger commercial power station. The simple interfaces enable a constructor to install a power station using multiple ISU's with commercial process equipment (balance-of-plant). The ISU is to be sold to competent (but not specially trained) engineer/constructor firms that assemble electric generating stations for independent power producers or electric utilities.

A flow schematic of the ISU is shown in Figure 3 below. The MCFC stack is represented by the block at the center of the schematic. All components specific to MCFC technology are within the ISU envelope. Cold fuel gas is supplied through the ISU pressure vessel to the anode recirculation loop. A sensible heat reformer in the anode recirculation loop utilizes the cell stack waste heat the same as an internal reformer but has the advantage of being outside the stack where it is accessible for service and does not complicate the stack design. The sensible heat reformer ensures the ISU operates at high efficiency regardless of the heating value of the incoming fuel. This allows a single ISU design to operate on various fuel sources such as natural gas or coal gas. Different ISU designs are ***not*** required for different fuels. Thus, development is limited to a single configuration.

Cold air is introduced into the cathode recirculation loop where a catalytic burner is utilized to ensure proper thermal operation at all power settings. This includes heat for start-up and standby operation. The exhaust from the ISU is at a pressure and temperature suitable for cogeneration or as a heat source for a bottoming cycle.

The recirculation loops provide several advantages over once-through fuel and/or air systems. First, they enable the stack waste heat to be removed by the introduction of both cold fuel and air without the use of any heat exchangers. Elimination of heat exchangers has the advantages of simplifying the system, increasing the reliability, and reducing the cost. A second advantage to the recirculation loops is that they permit multi-fuel operation with a single piece of equipment that is not changed for different fuel inputs and which can operate at high utilizations with different fuels having different heating values. A third advantage of the recirculation loops is that this unit is able to operate on natural gas fuel without water recovery or makeup site water required. This can be a distinct advantage in applications where water is a premium commodity.

As shown in Figure 3 and Figure 4, all components operating at elevated temperatures are located inside the vessel. Such close coupling ensures high-efficiency operation by greatly re-

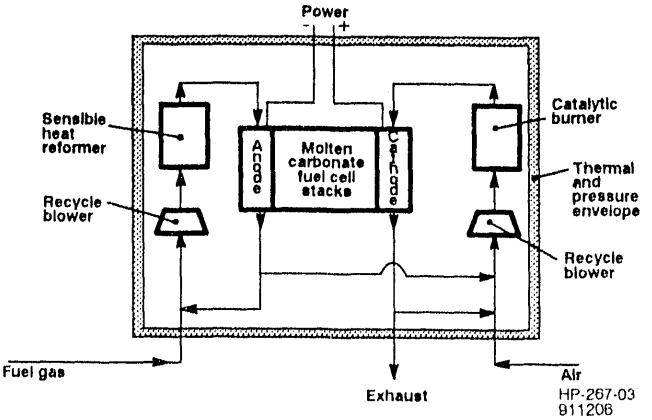

Figure 3. MCFC Integrated Stack Unit Schematic

ducing the extent of high temperature, pressurized piping, which in turn reduces the heat loss and cost significantly.

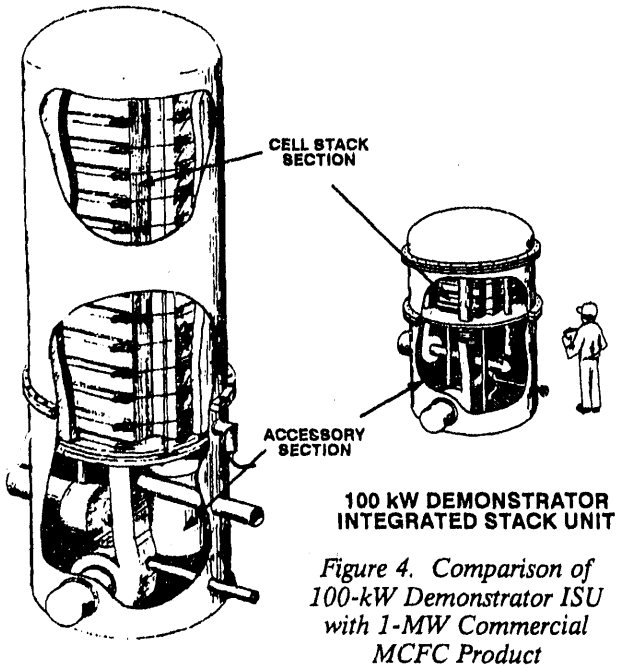

Figure 4. Comparison of 100-kW Demonstrator ISU with 1-MW Commercial MCFC Product

Another advantage to the ISU concept is that only passive controls are required to operate the equipment shown. The ISU is factory assembled and factory checked prior to shipment. Transport is by common carrier to the site where the ISU is installed with no further on-site construction required.

4. PROJECT DESCRIPTION

To validate the commercial product concept at the earliest possible time, IFC proposes to build and test a 100-kW ISU, using a full-area, full-height MCFC building block stack and subscale accessories. The 100-kilowatt ISU functionally simulates the commercial product, using the same control modes and operating conditions.

Figure 4 shows the planned 100-kW ISU in comparison with the commercial product. The 100-kW ISU design incorporates the same control characteristics and balance-of-plant interfaces as expected in commercial service. It operates at 50 psia and 1200°F, the same conditions used in the commercial ISU.

As shown in Table 1, the MCFC cell and the 100-kW stack building block for the 100-kW ISU are identical to those in the commercial ISU. The accessory components are arranged as shown in the process schematic for the commercial ISU (Figure 3). They utilize the same design concepts and operate at exactly the same thermodynamic and process flow conditions as those in the commercial unit. IFC has all of the necessary design data to scale the ISU accessory designs to the 1-MW size. The 1-MW ISU accessory components are commercially available today.

TABLE 1. COMPARISON OF DEMONSTRATOR WITH COMMERCIAL PRODUCT

COMPONENT	DESIGN CONCEPT	OPERATING CONDITIONS	SCALE
CELL/STACK SECTION			
• MCFC CELL	SAME	SAME	SAME
• STACK* BUILDING BLOCK	SAME	SAME	SAME
ACCESSORY SECTION			
• VESSEL AND PIPING	SAME	SAME	SMALLER**
• ANODE RECYCLE BLOWER	SAME	SAME	SMALLER**
• CATALYTIC BURNER	SAME	SAME	SMALLER**
• SENSIBLE HEAT REFORMER	SAME	SAME	SMALLER** (SAME REFORM CATALYST)
• CATHODE RECYCLE BLOWER	SAME	SAME	SMALLER**

* DEMONSTRATOR WILL CONTAIN ONE 100-KW STACK BUILDING BLOCK. THE COMMERCIAL PRODUCT WILL CONTAIN MULTIPLES OF THIS SAME BUILDING BLOCK

** COMPONENT WILL BE DOWNSIZED FOR REDUCED FLOW REQUIREMENTS

The stack building block is constructed of 140, 8-ft^2 molten carbonate cells. Each cell operates at 0.68 volts and 150 amps per square foot, or 102 watts per square foot. The cell stack configuration incorporates an advanced manifold seal to inhibit electrolyte migration which affects

end-cell life. The stack building block uses external reactant gas manifolds which are required for acceptable gas distribution in large-area tall stacks. The commercial 1-MW ISU contains multiples of this same stack building block.

Preliminary packaging studies of the 100-kW ISU indicate the components can be arranged within a pressure vessel 8 ft in diameter and 13 ft high. Accessory components are arranged in the lower section. Interface penetrations are through the vessel wall.

Over the last three years, IFC developed a new thin cell design and verified its operation in a short stack, as discussed below. Work beyond the short stack verification includes development of an improved manifold seal for the tall 100-kW stack and completion of two manufacturing development tasks needed for the 100-kW stack. These tasks are the development of an improved electrode tape casting slurry and development of an improved electrode debinding process. These activities have been started and results are discussed below.

RESULTS

The two significant accomplishments in the last year were the fabrication, assembly and verification test of a 25-kW molten carbonate stack and the development of a new manifold seal configuration. This stack shown in Figure 5 was comprised of 20, 8-sq.- ft. cells of the new IFC thin cell design. The stack was tested for over 2200 hours. The new manifold seal solved the electrolyte migration problem. The new seal configuration retards electrolyte migration well beyond 40,000 hours and still retains good gas sealing qualities.

This stack test met its objectives of verifying the fabricability and the operation of the new cell design, which incorporates many desirable features. First, the design incorporates thinner parts for the purpose of reducing the raw material content in the stack. IFC's approach to the commercial design is to fit the most square feet of active cell area per pound of raw material into the largest pressure vessel that is transportable

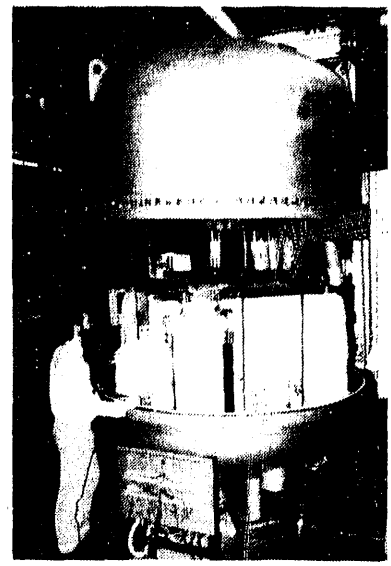

PUBS 6316

Figure 5. IFC 25-kW Molten Carbonate Stack

by common carrier. The reduced material design accomplished a significant step towards that goal. In addition to material reduction, other materials were changed to more economical grades. This reduced amount of material now is considered at a level which can be projected to competitive cell stack and power plant costs.

The cell configuration was simplified in order to make the parts more manufacturable and adaptable to continuous low cost processing techniques. The specific goal was to design a configuration that could be manufactured with existing processes and existing equipment in a continuous and automatic fashion. The simple design is made possible by the external manifolds which IFC has used as its baseline for some time. External manifolds allow a simple and symmetrical cell design which can be projected to a low added value. In addition, external manifolds allow larger manifold cross sections with a minimum amount of material to obtain low pressure loss through the manifold. This feature results in uniform gas distribution, a significant issue for large-area tall stacks.

In addition to the external manifold, the design contains a waste heat or sensible heat reformer which is external to the cell and stack, but is placed in very close proximity to the stack inside the vessel. By keeping the reform catalyst outside the stack, stack construction is greatly sim-

plified. Just as important, the reformer can be treated as a unique component and not be constrained by geometric and operating conditions within the cell and be vulnerable to contamination from other cell components, especially the electrolyte. An additional advantage to the sensible heat reformer is that it can be placed inside the vessel, but accessible enough that any maintenance required, such as change-out of the catalyst, is easily accomplished without having to remove the stack.

A third feature of the new cell design is the incorporation of low pressure drop flow fields in the current collectors for both reactant gases. These low pressure drop flow fields in turn permit recirculation systems to be designed into the ISU system. Reactant recirculation simplifies stack cooling without the need for heat exchangers. It also permits multi-fuel capability and high reactant utilization.

During the 2200 hour test no decay was observed in the center cells of the stack. Figure 6 shows a performance history of the center cells at different power levels over the life of the test.

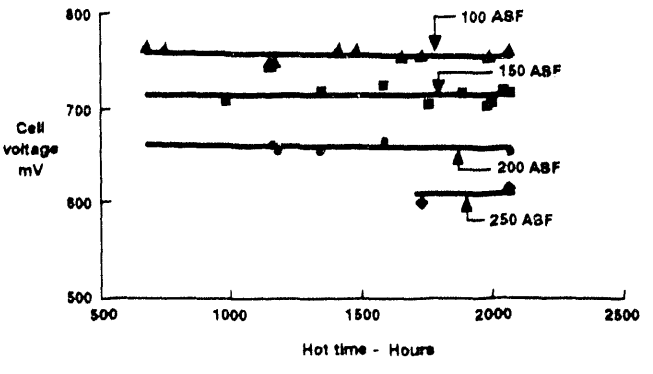

Figure 6. Average Voltage - Center Cells vs Hot Time

The performance is very stable, which is typical of previous experience. All the center cells were of the new cell design. However, the top grouping and bottom grouping of cells were assembled with additional reservoir capacity in order to accommodate electrolyte transfer from the bottom cells to the top cells through the manifold seals. These additional reservoirs were being tested to verify the capability of accommodating that electrolyte should a parallel development effort to reduce electrolyte transfer to the manifold seal not be 100% successful. Because of this extra reservoir capacity, these cells could not be expected to perform as well as the center cells. A criterion of no more than 50 mV penalty was set for the average performance of these top and bottom cells. The data in Figure 7 show the center cell performance at 150 ASF taken from Figure 6 compared to the average performance of the top and bottom cells at 150 ASF. The average loss is just about 50 mV. However, the performance was still changing at the end of the test. It was concluded that electrolyte management must be improved (1) to eliminate the special end cells and (2) to reduce or eliminate the cell-to-cell transfer of electrolyte through the manifold seal.

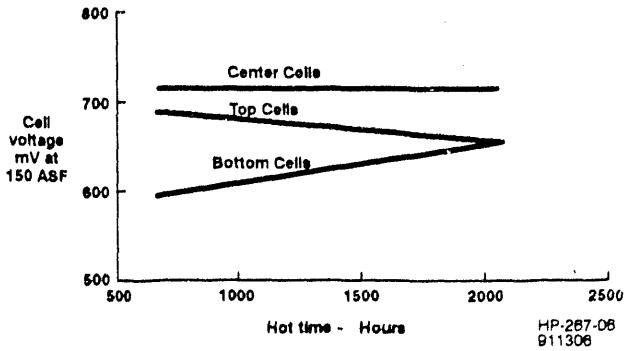

Figure 7. Average Voltage vs Hot Time

Manifold seal development was conducted in parallel with the 20-cell stack test with the goals of reducing the cell-to-cell electrolyte transfer rate consistent with a 40,000 hour operating life and at the same time meeting the manifold sealing requirements. Included in the objective was elimination of the special end cells.

In order to evaluate manifold seal candidates it was necessary to develop a tool which both simulated the conditions in a real stack as closely as possible and at the same time provided the ability to measure electrolyte transfer as the test proceeded. Shown in Figure 8 is a sketch of the electrolyte transfer test rig which was designed,

built, and used to conduct 21 tests leading to the development of the improved seal which meets all of the objectives. The rig consists of elec-

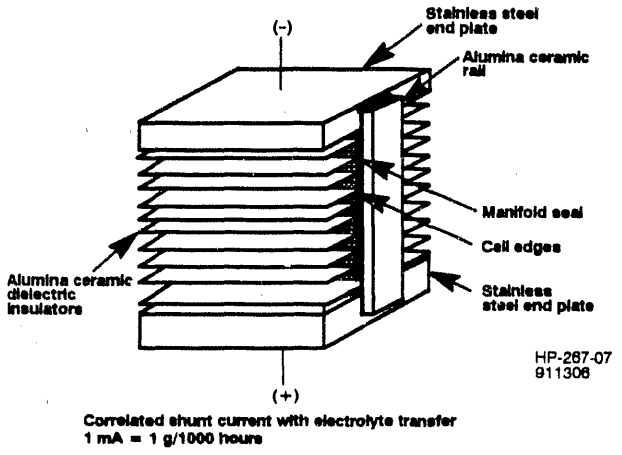

Figure 8. Electrolyte Transfer Test Rig

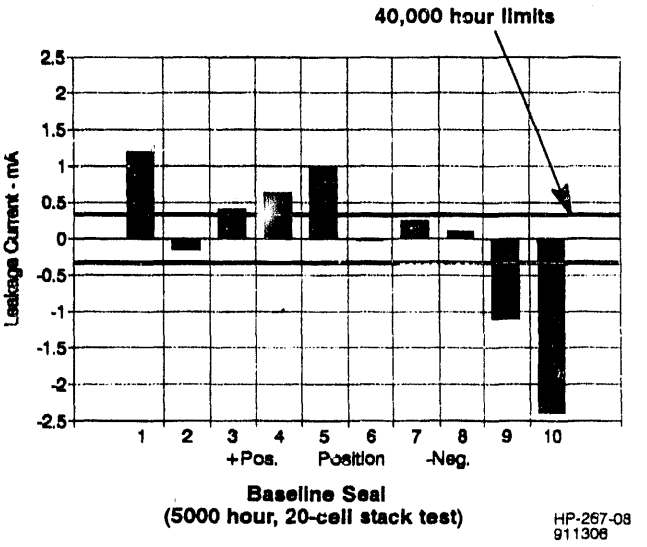

Figure 9. Leakage Current Measured with Baseline Manifold Seal

trodes, matrices and separators for 10 "cells" which are stacked to simulate the sealing surface of a real stack. Each cell was electrically isolated with alumina separators in order to provide the ability to impress a voltage individually on each cell and also to measure the current flowing through the electrolyte transfer paths from each cell into and through the manifold seal. The idea was to correlate these shunt currents with electrolyte transfer in order to provide a measure of the electrolyte transfer which could be obtained in real time. This correlation was obtained; the relation is 1 milliamp is equivalent to 1 gram of electrolyte transfer per 1000 hours. This was verified in initial tests with the gravimetric analysis of the electrolyte distribution.

The first several rig tests were devoted to correlating the rig data with actual stack data obtained previously. The baseline seal which was utilized on a 5000-hour, 20-cell stack test was run in the test rig. The data is shown in Figure 9. This data correlated with the stack data very well and confirmed that this test rig was capable of duplicating results in a real stack. Shown on Figure 9 also are the 40,000 hour limits which reflect the maximum amount of allowable electrolyte transfer expressed in leakage current. As you can see, the baseline seal exceeded this which made it unacceptable for long term applications.

The next 17 tests were devoted to evaluating new seal configurations aimed at reduced electrolyte transfer. In Figure 10 data for the selected improved seal are shown. Electrolyte transfer is almost negligible and well below the 40,000-hour limits. This means that there is a significant degree of margin available to provide a safety factor as the seal is scaled and run in full size stacks. Additional verification tests such as the sealability of this new manifold seal configuration are now being initiated. However, preliminary sealing tests have indicated that this seal will perform very well in containing leakage. The electrolyte transfer problem previously associated with the external manifold seal has been resolved and is no longer an issue.

Two additional tasks in the area of manufacturing development were also conducted. They addressed development of a more stable electrode tape casting slurry system, and developing a continuous electrode tape debinding process.

In fabricating the 8-ft^2 parts for the 25-kW stack mentioned earlier, a limited shelf life of the electrode tape casting slurry was identified. If the limited shelf life were exceeded, then slurries would agglomerate and/or the tapes would crack. Although enough acceptable tapes for this stack were made, the process was hindered by the limited life of the slurries (sometimes just a few hours). Consequently, a different solvent-

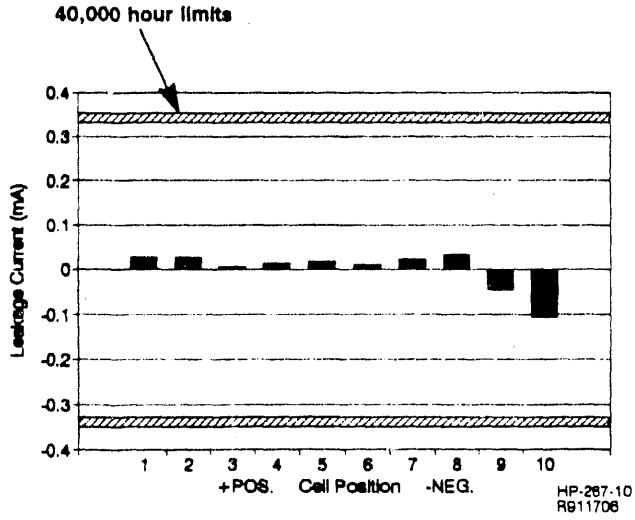

Figure 10. Leakage Current Measured with Improved Manifold Seal

base binder system was developed and tested in several tape casting runs. The shelf life has been extended significantly. Agglomeration in the slurries and cracking in the tape has been eliminated. This new solvent-base binder system is compatible with continuous tape casting and will be used to make electrodes for future stacks.

The second manufacturing development task was to develop a continuous electrode tape debinding process. The need became apparent when electrodes for the 8-sq.-ft. cells in the previous stack were processed through heat treatment after tape casting. The problem was manifested in two ways, the first being incomplete burnout which caused low yield of good parts, and the second being undesirable variations in good parts. Figure 11 shows how these variations are evident in comparing the electrode width after debinding and presintering in relation to their position in the retort. This variation is far greater than is acceptable and confirms that using a batch debinding and heat treating process is not acceptable for large area parts as it had been for small area parts. The solution was to develop a continuous electrode tape debinding process, shown in Figure 12. The process utilizes a continuous belt running through the heat treating oven. Each part goes through the oven at the same speed and is subjected to the same temperature and atmospheric conditions.

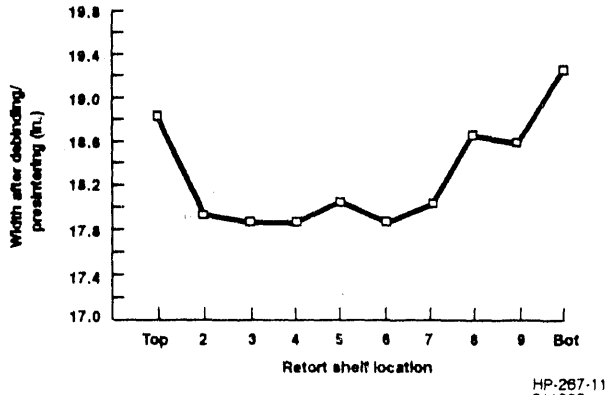

Figure 11. Electrode Tape Debinding

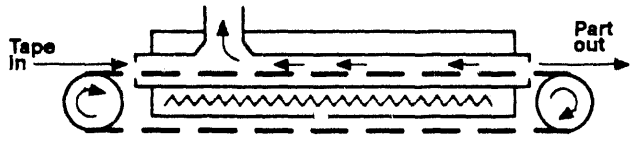

Figure 12. Electrode Tape Debinding Continuous Debinding Process

This process was reproduced in small scale and operated many times to develop the proper conditions to get good quality parts. The process is now being scaled to a large oven (shown in Figure 13) which will handle the 8-sq.-ft parts for

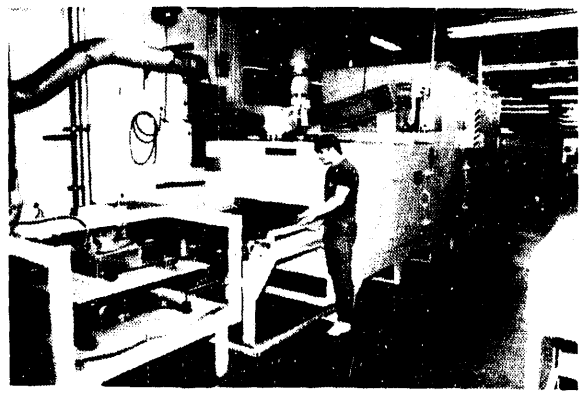

Figure 13. PAFC Oven to be Used for Continuous Debinding of Electrode Tapes

the planned 100-kW stack. The oven is in IFC's phosphoric acid fuel cell production facilities. It meets all the requirements for the MCFC heat treating process. The oven will be used to process both types of parts interchangeably. This oven illustrates how IFC will utilize manufacturing technology developed for PAFC produc-

tion in future MCFC parts fabrication. The most adaptable processes are automated handling and transfer of large, fragile parts and automated inspection and quality control techniques.

In addition, IFC has also acquired through a partner, the use of the 1.2–meter wide tape casting machine shown in Figure 14. In the photograph a full–width MCFC matrix tape of is shown emerging from the machine. The drying oven and casting head are being upgraded to produce matrices for the 100-kW stack.

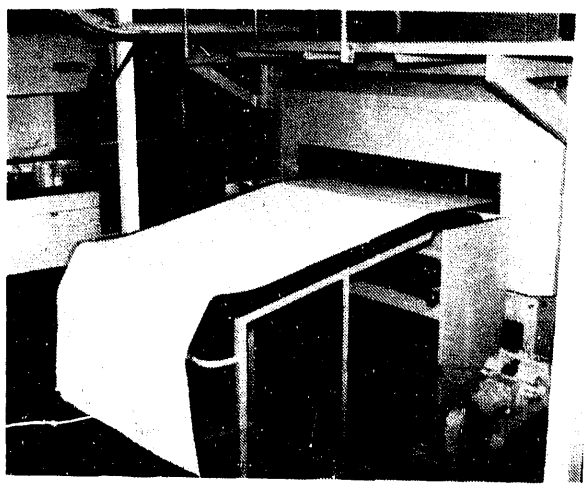

WCN14602

Figure 14. 1.2 Meter-Wide Matrix Tape Casting

FUTURE WORK

Figure 15 shows IFC's ISU product concept and its associated features and advantages. This is the goal and focus of IFC's future work in MCFC development. More specifically, work under this DOE contract effort over the next two years will be directed at verifying that concept in a 100-kW test of a 140-cell stack of full area, 8-sq. ft. cells of the new design. Following a successful stack test, the 100-kW stack will be incorporated in an ISU with all the ancillaries scaled for 100-kW operation in order to verify the entire ISU concept at the 100-kW level.

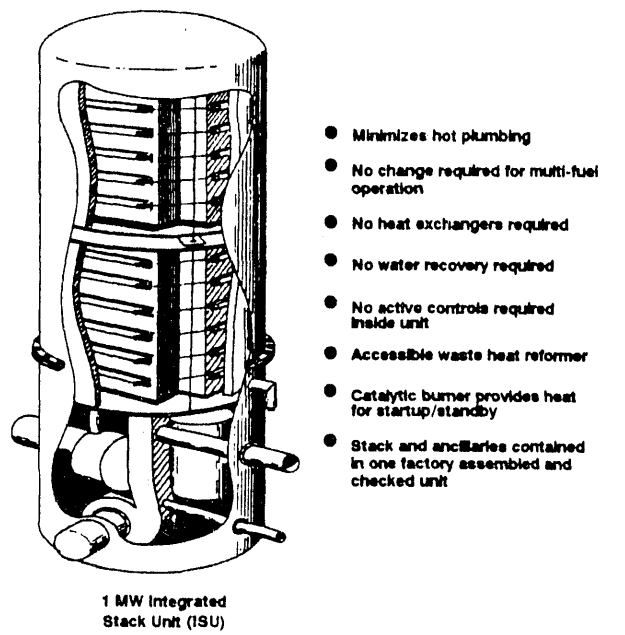

Figure 15. Integrated Stack Unit Features

ANL's Development of Conductive Ceramic Components for MCFC

CONTRACT INFORMATION

Contract Number	49943
Contractor	Argonne National Laboratory 9700 South Cass Avenue Argonne, IL 60439 (708) 972-4038
Contractor Project Manager	Kevin M. Myles
Principal Investigators	G. H. Kucera
Co-Investigator:	A. P. Brown
METC Project Manager	William J. Huber
Period of Performance	October 1, 1982 to Open

Schedule and Milestones

FY91 Program Schedule

	S	O	N	D	J	F	M	A	M	J	J	A	S
Anode Performance	----------												
Cathode Performance	----------												
Through-plane Conductivity of $LiFeO_2$ with Single Dopant				----------									

OBJECTIVES

The emphasis of this project is to develop new, conductive ceramic materials and to produce structures from these materials for use as the components in the molten carbonate fuel cell (MCFC). The components under study include the cathode, anode, and interconnect, each of which is at a different stage of development. The cathode work focuses on

assessing the viability of $LiFeO_2$ as a replacement for the state-of-the-art NiO; this assessment relies on cell testing, with the performance data serving as the bases for component improvement. The anode studies seek to develop the required conductivity in a stable compound that exhibits little sensitivity to the range of anode oxygen partial pressures; this can be achieved through doping. The interconnect work emphasizes determining the effect of fuel and oxidant on conductivity, material properties, and structural integrity.

BACKGROUND INFORMATION

The development of ceramic components at Argonne National Laboratory (ANL) has followed a general approach, which emphasizes the experimental determination of stable compounds, conductivity enhancement through doping of stable compounds, fabrication of appropriate structures, and in-cell testing. In an earlier effort at ANL, a fairly extensive list of materials stable under cathode and/or anode conditions was produced in an experimental effort. This list provides the basis for initial material selection in the development of MCFC components.

After selection of a stable material, meeting the cell requirements of the component is emphasized. For each of the three components under development at ANL, the conductivity of candidate materials was improved through doping. For cathode use doping was necessary, and for anode use it appeared desirable. The probability for conductivity enhancement was high because the parent material was chosen to contain a cation capable of existing in more than one valence state. At least two orders of magnitude improvement in conductivity were achieved with cathode-prepared $LiFeO_2$ and Li_2MnO_3.

The progression from conductive material to component requires that fabrication processes be developed to produce the desired structure. In our electrode work, state-of-the-art (SOA) NiO structures served as the initial guide. Using a fabrication process based on small-diameter polycrystalline ceramic fibers, porous ceramic bodies were produced from a variety of oxide-based materials.[1] In general, the materials and structures produced were stable in an oxidizing environment. These techniques have also been adapted to certain anode materials, e.g., $LiFeO_2$ and MnO.

Cell testing with diagnostic half-cells and 25 cm^2 full cells remains the basis for evaluating the components under study. The results of systematic tests give insight into electrode mechanisms. The in-cell performance serves as a guide to component improvement.

PROJECT DESCRIPTION

This project consists of three major tasks: the evaluation of $LiFeO_2$ cathode performance, the evaluation/improvement of anode material conductivity and structure fabrication, and the study of separator materials. While each component has different cell requirements, the techniques and understanding gained from earlier cathode work provide a strong foundation for the individual component development.

Both full cells (25 cm^2) and diagnostic half-cells are operated to evaluate the $LiFeO_2$ cathode performance. Previous data from both the full and half-cell tests suggest that the cathodes are generally kinetically limited,[2] and that the performance would benefit from increased surface area. The surface area of current cathode structure has been increased by decreasing the porosity and by using starting

materials with higher surface area. Studies with these improved structures focus on increasing performance and determining reaction kinetics. The current work includes an assessment of the influence of temperature, electrode thickness, electrolyte composition, and oxygen and carbon dioxide partial pressures on cathode overpotential.

Anode development emphasizes the strong influence of oxygen partial pressure on the stoichiometry of candidate materials and, hence, on conductivity. Our earlier studies on undoped $LiFeO_2$ showed that in the fuel environment, where the oxygen partial pressure is about 10^{-23} atm, Fe will remain in an oxidized state.[3] These studies also showed that the Fe^{2+}/Fe^{3+} ratio is sensitive to even small changes (e.g., 0.9×10^{-23} vs 4×10^{-23} atm) in oxygen partial pressure. The current studies focus on the use of dopants to minimize the changes in conductivity resulting from changes in oxygen partial pressure in an operating cell. Electrode fabrication procedures, adapted from earlier-developed cathode fabrication techniques, were demonstrated for undoped iron- and manganese-based materials. Recent efforts center on doped anode materials.

Ceramic separator/interconnect development requires the fabrication of a thin, dense sheet free from defects that would allow gas crossover. Traditional sintering aids, such as a reactive liquid, may have adverse effects on cell performance and/or may cause solubility and stability problems. The first approach taken is to examine the effectiveness of dopants as sintering aids. The initial selection of separator materials has as its foundation the materials previously identified as being stable in the anode and cathode environments. The relative diffusivity of oxygen and hydrogen in sintered pellets is examined by following the change in conductivity as a function of cover gas composition; the accompanying change in stoichiometry is determined by X-ray diffraction analysis. The through-plane conductivity of the separator in the presence of fuel and oxidant is also under study.

RESULTS AND ACCOMPLISHMENTS

Electrode Development

$LiFeO_2$ Cathodes. Previous work on assessing the performance and reaction kinetics of doped $LiFeO_2$ cathodes in full cells and half-cells suggested that performance was dominated by low active area.[3] Electrode surface area (hence, active area) has been increased by decreasing the pore volume from 80% to about 65% and by using small particle starting material. The performance of a high-surface-area electrode approached that of SOA NiO, particularly at current densities up to 100 mA/cm^2. However, the performance of this cathode decreased with time; post-test analysis by scanning electron microscopy showed that particle growth had occurred and reduced surface area. Further increases in surface area will be possible only through electrode densification.

Analysis of the polarization curves for these high-surface-area cathodes reveals the presence of two independent, simultaneous-reaction mechanisms. There is a fast reaction that under normal operating conditions becomes diffusion limited at current densities below about 100 mA cm^{-2}. There is also a much slower reaction that follows the Tafel Equation[4] and determines the shape of the polarization curves at the higher current densities.

To gain more insight into the $LiFeO_2$ electrode reactions and to find those conditions

that promote the fast mechanism, half-cells have been run to study the influence of temperature, oxygen partial pressure, carbon dioxide partial pressure, electrode thickness, and electrolyte composition on the cathode performance. A brief summary follows.

Increasing the temperature has a big effect on the performance of Co-doped $LiFeO_2$ cathodes as shown by the series of polarization curves in Fig. 1. At 160 mA/cm^2, these data show that cathode overpotentials are reduced by about 250 mV on going from 650 to 700 °C. Also, the steeply rising portions of the lower-temperature polarization curves correspond to the diffusion limit of the fast mechanism (their deviation from a true vertical is because of there being two additive sources of polarization). As can be seen in Fig. 1, increasing the temperature causes a significant shift in the diffusion limit to higher current densities, which is the reason for the large gains in performance.

Figure 2 shows the effect of varying the $p(O_2)$ on the cathode performance at 650 °C. The curves in this figure closely resemble those in Fig. 1, clearly indicating that increasing the $p(O_2)$ is also very beneficial for improving cell performance. Varying the $p(CO_2)$ from 10% to 60% has less effect on the cathode performance as shown in Fig. 3. At 5% CO_2, however, the diffusion limit of the fast reaction is increased significantly.

Changing the electrode thickness between 0.015 and 0.030 cm and varying the lithium content of the electrolyte between 50 and 70% Li_2CO_3 have only a relatively small influence on the cathode performance; overpotential differences were less than about 100 mV between the best and worst cases. The fast reaction is promoted by cathodes at least as thick as 0.030 cm and by a high lithium content electrolyte.

Based on the above results, an alternative oxidant mixture was formulated that is expected to improve cathode performance; the new mixture is 95% air/5% CO_2 (i.e., about 20% O_2/5% CO_2). The comparison of polarization curves in Fig. 4 shows that when this new oxidant is coupled with a 25 °C increase in temperature, a Co-doped $LiFeO_2$ cathode in the half-cell will perform comparably to a SOA NiO cathode.

$LiFeO_2$ and MnO Anodes. In the iron- and manganese-based anode materials, the oxygen partial pressure and temperature determine their stoichiometry and, therefore, the conductivity of the electrode. In an operating cell, where changes in oxygen partial pressure are expected, changes in the number of electronic charge carriers are likely to have an adverse effect. Doping can minimize this effect by keeping the charge carriers/conductivity nearly constant.

Undoped, anode-prepared $LiFeO_2$ is a good conductor. It has a conductivity at 650 °C of 3 $(ohm\text{-}cm)^{-1}$ and is an n-type conductor with electron hopping between Fe^{2+} and Fe^{3+} as the conduction mechanism. By doping with a cation, 4+ or greater, the n-type character can be maintained irrespective of the resultant defect mechanism, i.e., substitution on an Fe or Li site or interstitial incorporation. Doping with a 2+ cation can result in either an n- or p-type conductor, depending on the substitution site. At this time, it is not possible to determine the advantages or disadvantages of either conductor type.

Anode-prepared $LiFeO_2$ has been doped with Mn^{2+} and Nb^{5+}. The conductivity at 650 °C was still about 3 $(ohm\text{-}cm)^{-1}$, but each dopant caused a lattice parameter change in the $LiFeO_2$, thus indicating some dopant incorporation.

Undoped, anode-prepared MnO has a conductivity at 650°C of 0.06 $(ohm\text{-}cm)^{-1}$. The conductivity appears to be the result of in situ lithiation. For simple substitution of Li^{1+} on a Mn^{2+} site, a p-type conductor would be formed; interstitial incorporation would result in an n-type conductor.

Both Nb and Mg were selected as potential dopants for MnO. Niobium doping resulted in a decrease in conductivity to 0.03 $(ohm\text{-}cm)^{-1}$; Mg doping, on the other hand, increased the conductivity to 0.2 $(ohm\text{-}cm)^{-1}$.

To determine the effect of dopants on electrode behavior, several batches of undoped and doped MnO have been synthesized in preparation for fabrication of a 25 cm^2 electrode. The fabrication process has already been demonstrated on smaller structures.

Ceramic Interconnect Development

The emphasis to date in this area of the program has been assessing the changes that are likely to occur in a ceramic interconnect as hydrogen and oxygen diffuse into the component. These changes include stoichiometry, crystalline form, and conductivity.

Iron- and manganese-based compounds were selected for initial study from the list of materials that were previously determined to be stable in the anode and cathode environments. The changes in anode-prepared Nb- and Mg-doped MnO and Mn-doped $LiFeO_2$ as a result of exposure to oxidant gas at 650°C have been examined. The conductivity of Nb- and Mg-doped manganese-based material increased to 5 $(ohm\text{-}cm)^{-1}$ from 0.06 and 0.2 $(ohm\text{-}cm)^{-1}$, respectively. The MnO also oxidized to Mn_2O_3. Despite a change of about 12% in volume, the specimen did not show any signs of deterioration. The Mn-doped $LiFeO_2$ under similar conditions showed a decrease in conductivity, going from 3 to about 0.03 $(ohm\text{-}cm)^{-1}$. The $LiFeO_2$ crystalline form remains the same in both anode and cathode gas, but undergoes a 3% change in crystal volume. This structure also showed no signs of deterioration.

Because the materials under consideration for this application are unusual, little exists in the literature concerning not only their physical properties, but their use as refractory materials. Our initial approach to fabricating a thin, dense body is to investigate the use of stable materials, e.g., Li_3NbO_4, MgO, Li_2TiO_3, as additives to prevent or slow down boundary migration to a point at which it is possible to eliminate pores. In other studies with Li_2MnO_3, we were able to produce a small specimen that was 99% dense using Li_3NbO_4.

FUTURE WORK

The results of the $LiFeO_2$ cathode cell studies will be the basis for evaluating the fundamental electrode processes and for predicting the requirements for alternative MCFC cathodes. The understanding gained through these studies will guide the development of Li_2MnO_3 cathodes.

The effect of dopants on the in-cell performance of iron- and manganese-based anodes will be evaluated. Cell testing will continue to be the guide for electrode improvement.

Work will continue on the development of a more corrosion-resistant separator. The degree of gas penetration in the separator and the resulting changes in composition and conductivity will continue as a primary issue.

The compatibility of the separator with adjacent cell components will be assessed.

Cell testing and development of cells consisting of the materials and structures developed in the preceding studies will form the basis for producing a cell with all new ceramic components.

ACKNOWLEDGMENT

This work was supported by the U.S. Department of Energy under contract No. W-31-109-Eng-38.

REFERENCES

1. G. H. Kucera, J. L. Smith, and A. P. Brown, "Fabrication of Porous Ceramic Electrode Structures," Proceedings of the Symposium on Fuel Cells, The Electrochemical Soc. Inc., Vol. 89-14, pp. 137-146, 1989.

2. A. P. Brown, J. L. Smith, and G. H. Kucera, "Characterization of New Cathode Materials for Molten Carbonate Fuel Cells," Proceedings of the Symposium on Fuel Cells, The Electrochemical Soc. Inc., Vol. 89-14, pp. 160-167, 1989.

3. J. L. Smith, G. H. Kucera, and A. P. Brown, Molten Carbonate Fuel Cell Research, Proceedings of the 2nd Annual Fuel Cells Contractors Review Meeting, W. J. Huber, ed., p. 51-60, 1990.

4. Electrochemistry: Theoretical Foundations, J. Goodisman, John Wiley and Sons, NY, 1987.

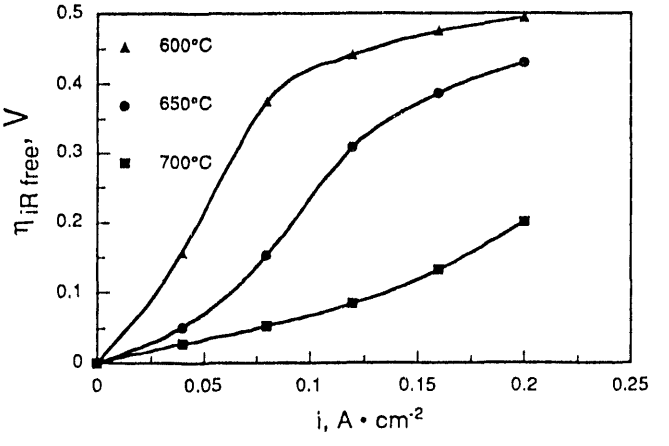

Fig. 1. Cathode overpotential as a function of current density and temperature.

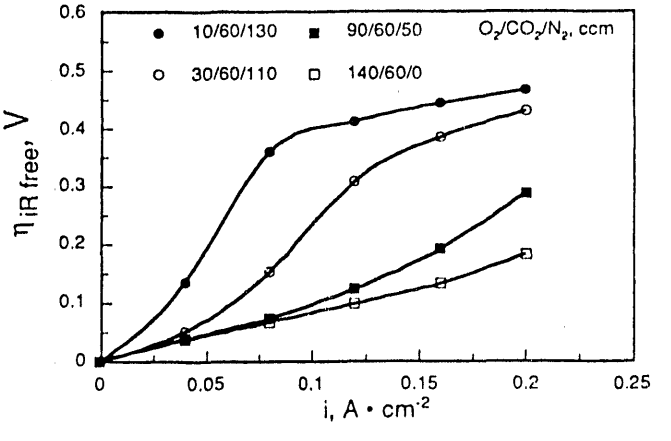

Fig. 2. Cathode overpotential as a function of current density and oxygen partial pressure.

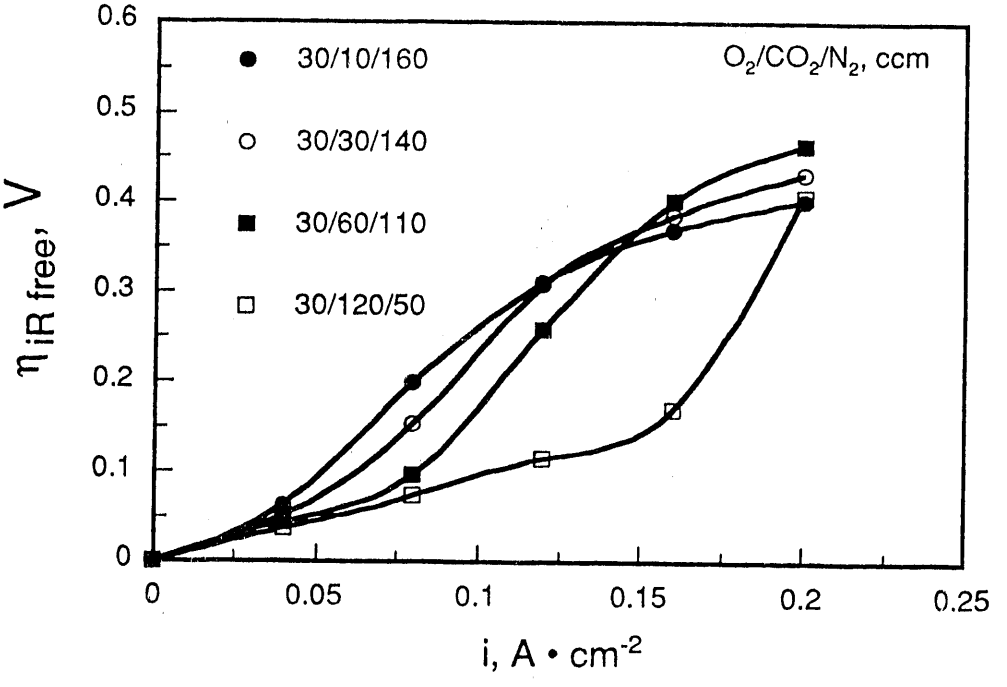

Fig. 3. Cathode overpotential as a function of current density and carbon dioxide partial pressure.

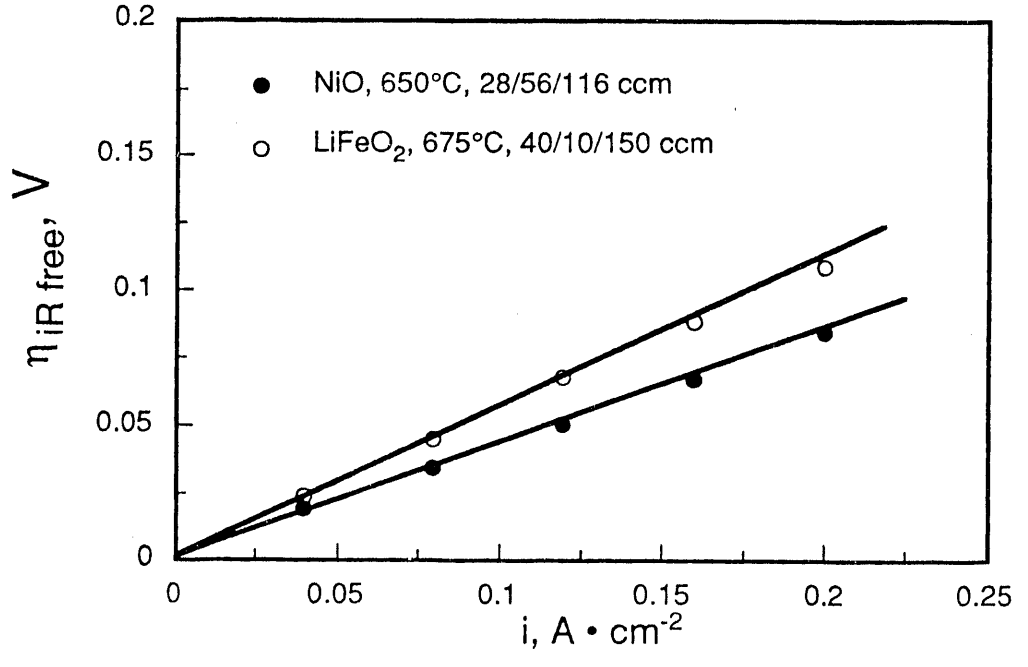

Fig. 4. Cathode overpotential as a function of current density operated with optimized conditions.

Effects of Coal-Derived Trace Species on the Performance of Carbonate Fuel Cells

CONTRACT INFORMATION

Contract Number	DE-AC21-88MC25009
Contractor	ENERGY RESEARCH CORPORATION 3 Great Pasture Road Danbury, CT 06813 (203) 792-1460
Contractor Project Manager	George Steinfeld
Principal Investigator	Ed Pigeaud
METC Project Manager	Mark C. Williams
Period of Performance	August 22, 1988 to Sept. 30, 1991

Schedule and Milestone

FY1991 Program Schedule

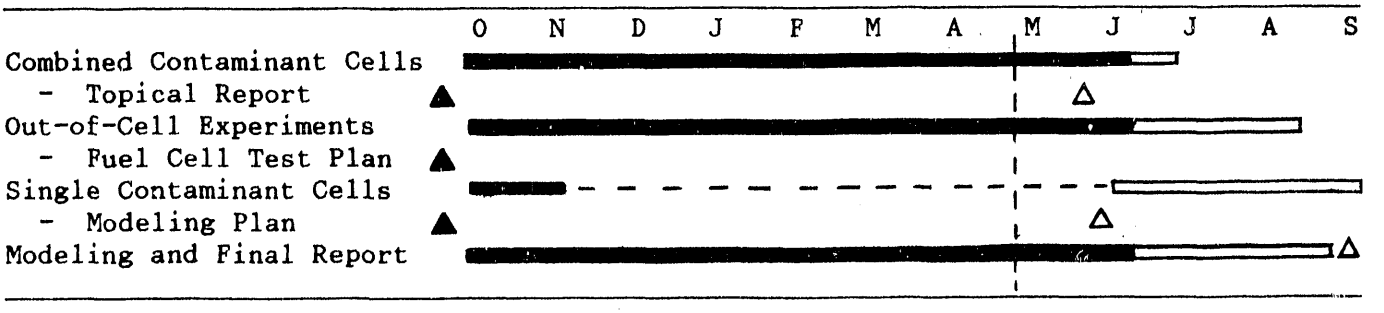

OBJECTIVES

The overall objective of this contaminant program at ERC has been to study and model the impact of coal-derived contaminants on the Carbonate Fuel Cell to facilitate prediction for future cleanup. The goals were to: 1) analyze all known thermochemical equilibria between trace species and the interactions with active fuel cell components on the anode side; 2) confirm such results by out-of-cell and 300-cm^2 bench-scale fuel cell testing with single and upto 7 combined trace species added to the fuel; 3) determine mechanisms of interaction, the contaminant tolerance levels, and model the fuel cell performance effects due to all important, simultaneously combined interactions.

BACKGROUND

Coal-gas contaminants may affect the carbonate fuel cell in many ways, such as through:

a) increased <u>anode polarization</u> when foreign ions dissolve in the melt and chemisorb on active anode surfaces at certain competing threshold voltages;

b) aggravated hardware corrosion, resulting in shorter life and high contact resistance between cell components;
c) anode and gas passage plugging due to deposition of oxides, which reduce the effective size and porosity of the anode;
d) increased electrolyte loss, lowering anode melt content, effective ionic conductivity, and K^+ content.

The present project is a follow-up on earlier contaminant studies by Pigeaud and Patel in (1980, '85, '87, and '90). In 1987 MCFC effects due to ammonia, arsenic, zinc, lead, and mercury were studied. The impact of particulates in the gas stream and soot formation due to high carbon monoxide content, as well as several hydrocarbon gases, was also part of the early work. In this current study, five additional contaminants, H_2S, HCℓ, H_2Se, Cd and Sn, have now been studied for their various interactions and reactivities with fuel cell components.

PROJECT DESCRIPTION

Ten major (NH_3, H_2S, HCℓ), minor (Zn, Pb, As), and trace (Se, Cd, Sn, Hg) coal-derived contaminant species have been studied in this program which was subdivided into 5 main tasks:
1) to conduct a thorough literature survey and thermochemical analysis of all the possible interaction products which could conceivably be formed;
2) to perform out-of-cell testing of such interactions by isothermal (650°C) Thermogravimetric (TGA) experiments on various combinations of the contaminants with fuel cell components;
3) to perform in-cell testing in 300-cm^2, bench-scale, fuel cells both with single and with combinations of up to 7 contaminants simultaneously present;
4) to determine the tolerance levels for these contaminant species as derived from experimental and thermodynamic considerations;
5) to understand the various mechanisms of the interactions, model them, and assemble a computer software program capable of predicting the observed performance effects.

RESULTS

Computations on all the gaseous contaminant and fuel species have been performed using the SOLGASMIX (simultaneous thermochemical equilibrium) software program. This program was modified, as shown in Figure 1, to include the liquid carbonate melt phase as well as a reactive Ni-anode solid phase. The computations for free energy minimization of a complex, multispecies, 3-phase (solid/liquid/gas), interacting system of contaminants and reaction products, have been confirmed by many of the experimentally observed decay mechanisms.

Out-of-Cell TGA experiments to confirm individual reactions, and to investigate the elemental as well as product vapor formation reactions, have been performed to support both selection of the contaminant-addition temperatures and the various specific trace species activities at high temperature. For instance, Figure 2 illustrates data obtained to establish the addition reactor temperature for blending various amounts of Cd-vapor in different simulated (humidified) fuel gas stream.

Bench-scale Cell testing in seven, 300 cm^2, fuel cells for up to 4800 hours each, has been performed to directly study actual cell performance decay both with single and with multiple, combined contaminant, additions in a simulated fuel gas composition.

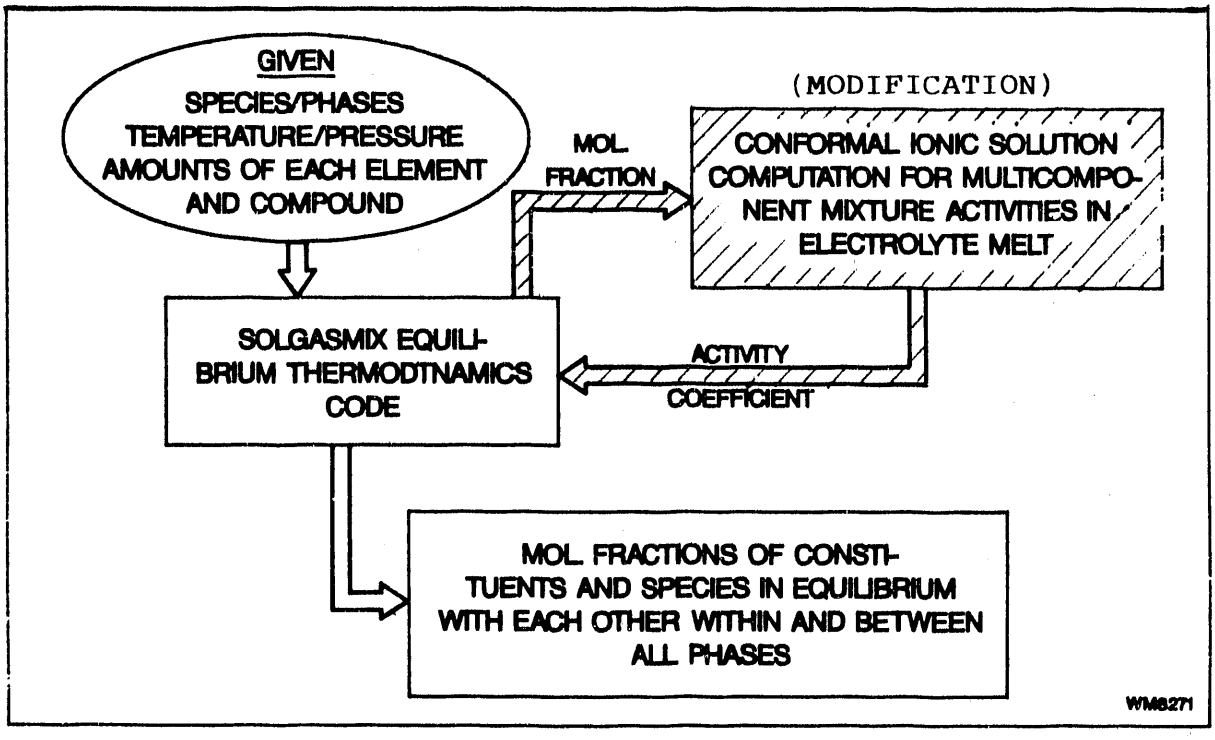

Figure 1. Equilibrium Thermochemistry Computations

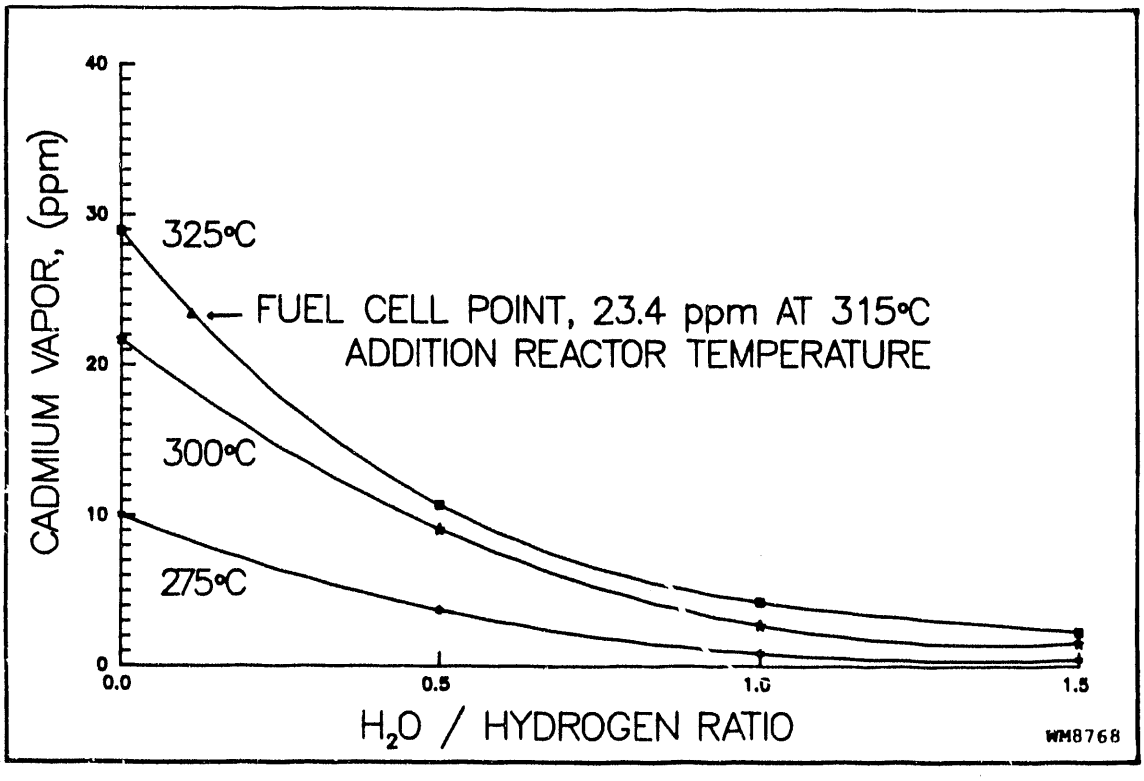

Figure 2. TGA Vapor Transpiration Data For Cadmium
(Vapor Pressure Varies With Fuel Gas Humidification and Temperature)

Figure 3 illustrates the lifegraph of one of the multiple contaminant cells which was operated on seven different contaminants simultan-eously. Tin (Sn), as our thermodynamic analysis in reducing environment had already indicated, did not appear to be transfered into the fuel cell when operating the addition reactor at a maximum 655°C.

Reaction mechanisms have been proposed and tolerance levels determined for the ten contaminant species conforming to the most recent experimental and theoretical evidence. Table 1 summarizes this information in terms of NO noticeable effects (i.e., NO limiting effects for 4 species), 4 species with significant effects, and 2 species causing minor effects.

This represents our current understanding of the tolerances due to the four primary mechanisms of interaction as illustrated in Table 2.

Three contaminant models have so far been developed for the four most important trace species affecting the carbonate fuel cell. Table 2 illustrates the key features and information used in assembling the computational models for providing cell performance data according to the given mechanisms. An example with regard to the performance decay due to 1 ppm HCl contamination of fuel gas is modeled in Figure 4. The model sofar has concentrated on calculating the increase in 'effective' anode resistance due to just the melt content of the anode decreasing because of the electrolyte depletion as a

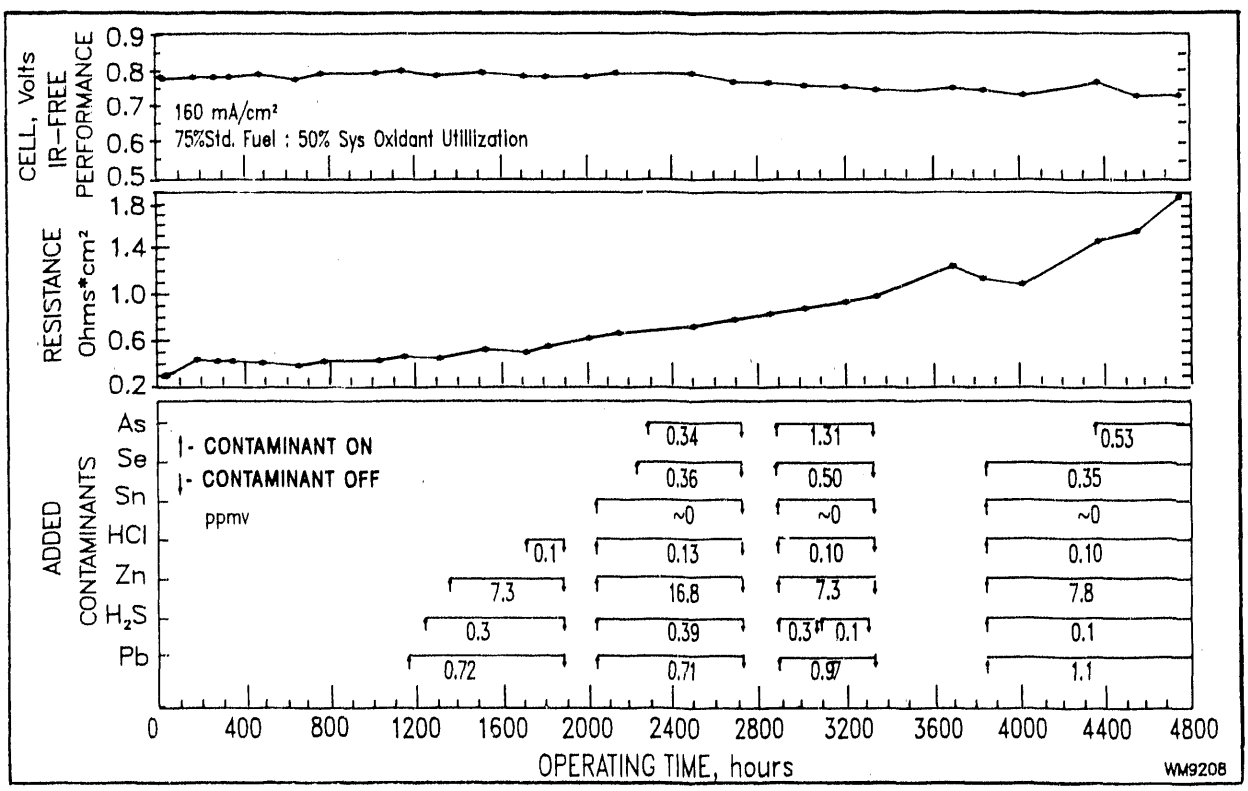

Figure 3. Lifegraph of Multiple Contaminant Test Cell
(Cumulative Effect of 7 Contaminant Species Simultaneously Added)

Table 1. PRESENT UNDERSTANDING OF INDIVIDUAL CONTAMINANT EFFECTS ON THE CARBONATE FUEL CELL

(Only 6 Out of the 10 Contaminants Studied Appear to be Important)

CONTAMINANT (ppm)	REACTION MECHANISM	TOLERANCE	CONCLUSIONS
NO NOTICEABLE EFFECTS			
NH_3 (10,000)	$2NH_3 \longrightarrow N_2 + 3H_2$	**~1 v/o NH_3**	No Effects
Cd (5)	$Cd + H_2O \longrightarrow CdO + H_2$	**~30 ppm Cd**	No Cell Deposits
Hg (1)	(Hg Vapor Not Reactive)	**35 ppm Hg**	No TGA Effects
Sn (3)	$Sn + H_2O \longrightarrow SnO + H_2$	**No Vapors @ 650°C**	No Cell Deposits
SIGNIFICANT EFFECTS			
H_2S (15,000)	$xH_2S + Ni \longrightarrow NiS_x + xH_2$	**~0.5 ppm H_2S**	Recoverable Effect
HCL (500)	$2HCl + K_2CO_3 \longrightarrow 2KCl\ (g) + H_2O + CO_2$	**<0.1 ppm HCl**	Long-Term Effect
H_2Se (5)	$xH_2Se + Ni \longrightarrow NiSe_x + xH_2$	**~0.2 ppm H_2Se**	Recoverable Effect
As (1?)	$AsH_3 + Ni \longrightarrow NiAs + 3/2H_2$	**<0.3 ppm As**	Long-Term Effect
MINOR EFFECTS			
Zn (100)	$Zn + H_2O \longrightarrow ZnO + H_2$	**<15 ppm Zn**	No Cell Deposits
Pb (15)	$Pb + H_2O \longrightarrow PbO + H_2$	**<1.0 ppm Pb**	No Cell Deposits

WM9207

Table 2. KEY FEATURES FOR ANODE PERFORMANCE MODELING

The Various Mechanisms can Independently Affect a Fuel Cell Anode

SPECIES	MODE	CHEMISTRY	APPROACH
H_2S, H_2Se	REVERSIBLE BARRIER FORMATION	CHEMISORPTION Ni–S_x FILM	NERST THRESHOLD POISONING
AsH_3 / As_2	IRREVERSIBLE BARRIER FORMATION	DIELECTRIC NiAs LAYER FORMATION	Ni–SURFACE DEACTIVATION FRONT
HCl	Cl^- ION FORMATION ELECTROLYTE VAPORIZATION	MAINLY KCl (v) DEPLETION Li/K DISPROPORTIONATION	MELT DEPLETION AND PHASE SOLIDIFICATION
Zn, Pb	PARTICULATE DEPOSITION IMPEDES GAS CIRCULATION	ZnO (s), PbO (s) DEPOSITION	ANODE PASSAGE & PORE OBSTRUCTION

NH_3, Cd, Sn, Hg NO EFFECTS

result of KCℓ vaporization. The dotted lines indicate supercooled melt condition which is probably not realistic, as a result of the electrolyte cation composition becoming greatly enriched in Li^+. In reality therefore, when the melt freezes at this point, the anode fill, ϵ, and hence cell current density will catastrophically drop to zero.

FUTURE WORK

Although the present effort has concentrated mostly on anode-side interactions and performance decay, near-term efforts will attempt to answer questions with regard to endurance effects and diffusion of melt and trace contaminant species across the electrolyte matrix.

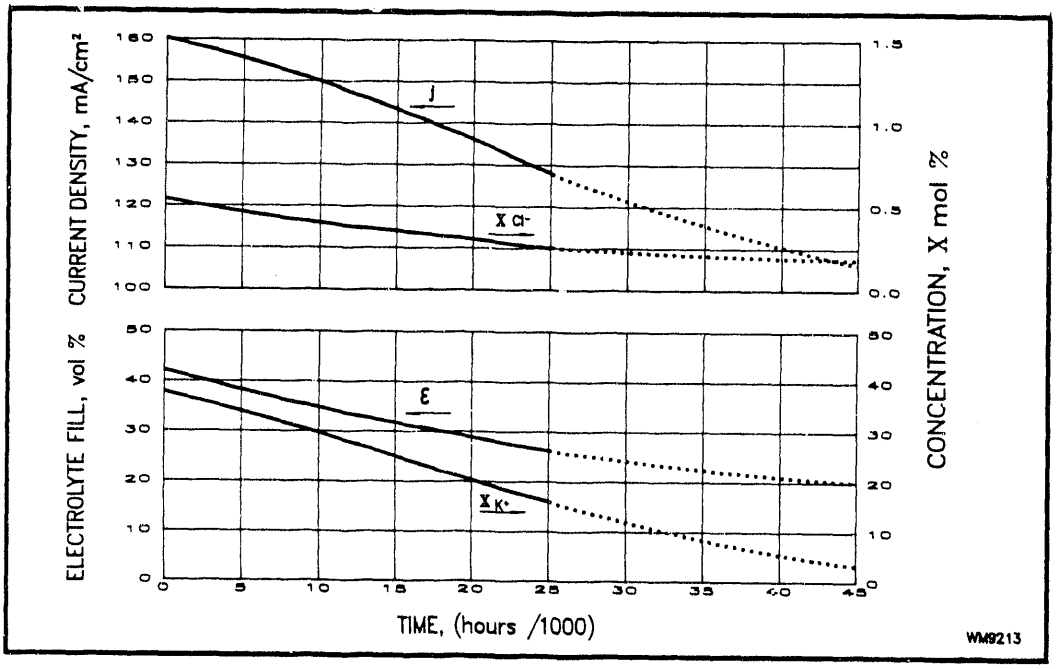

Figure 4. MODEL OF PERFORMANCE DECAY WITH 1 PPM HCℓ CONTAMINANT

(Current, j, may be Expected to Drop Suddenly When the Carbonate Content in Anode Freezes as a Result of Potassium Depletion)

REFERENCES

Pigeaud, A. et. al. 1980. "Development of MCFC Technology," Interim, Annual, and Final Reports to DOE under Contract No. DE-AC03-76ET11304.

Patel, P. et. al. 1985. "Trace Contaminant Removal from Hot Coal-gas for MCFC Application", Final Report to DOE (DE86001072).

Pigeaud, A. and Klinger, J. 1987. "Study of the Effects of Soot, Particulate and Other Contaminants on MCFCs Fueled by Coal-gas," Final to DOE (DE88001059).

Pigeaud, A. and Steinfeld, G. 1990. "Effects of Coal-derived Trace Species on the Performance of Molten Carbonate Fuel Cells", Reports to DOE under Contract No. DE-AC21-88MC25009.

Optical Diagnostics for Molten Carbonate Fuel Cells
Carbonate Movement and Contaminants

CONTRACT INFORMATION

Contract Number	A192
Contractor	Los Alamos National Laboratory P. O. Box 1663 Los Alamos, NM 87545 (505) 667-7121
Contract Project Manager	Richard C. Oldenborg
Principal Investigators	Byron A. Palmer David J. Funk
METC Project Manager	Curtis V. Nakaishi
Period of Performance	October 1, 1990 to May 31, 1991

Schedule and Milestones

FY91 Program Schedule

	O	N	D	J	F	M	A	M	J	J	A	S
Carbonate Movement	▬	▬	▬	▬	▬	▬	▬	▬	▬	▬		
Contaminant Processes									▬	▬	▬	▬

OBJECTIVES

Our research is directed toward developing optical diagnostics for molten carbonate fuel cells (MCFC). We are specifically developing diagnostics to measure major gas-phase species, alkali atom and salt concentrations, and techniques to elucidate contaminant problems and mechanisms.

The first phase of our work was to assess MCFC problems and come up with a set of diagnostic tools that could be applied to these problems. Our second objective is to use these tools to perform controlled laboratory experiments and investigate the important chemical and physical properties of MCFC materials and contaminants, and their role in carbonate transport and electrode deterioration. The third objective is to use these tools and measurements to assist in developing a model which describes the transport and deterioration phenomena. Our final objective is to use these diagnostics in a field environment to verify and/or correct the model.

These steps are not sequential and we plan to include industry in a collaborative effort that will help direct modelling, diagnostic development, and the determination of critical laboratory measurements.

BACKGROUND INFORMATION

Optical diagnostics have the advantage that they do not require a physical probe to be inserted into the region of interest (nonintrusive), they can have spatial selectivity, are species selective, can operate in harsh environments, and they can be very rapid. They do require optical access which can pose some technical difficulties (need to purge, etc.).

Optical diagnostics of the gas-phase species (CO_2 and H_2O) can be used to look at the micro efficiency of the MCFC during operation rather than the macro efficiency as given by the total current. These diagnostics can provide clues to the physical processes that are taking place by: 1) providing information concerning short-lived species in the reactions and 2) by elucidating the physical mechanisms associated with the problems of running an MCFC.

Optical diagnostics that measure gas phase alkali atoms and salts concentrations can help identify carbonate movement mechanisms and may be able to assist in the development of longer lived fuel cells. Finally, diagnostics that can elucidate the mechanisms of contaminant caused deterioration of the MCFC may be able to direct changes in the design to minimize these problems.

PROJECT DESCRIPTION

Problem areas observed in MCFC operation that optical diagnostics can address are: 1) the variation of the efficiency with position in the cell; 2) the movement of the electrolyte in the cell; 3) contamination processes and the mechanism involved in the efficiency reduction resulting from contamination; 4) the deterioration of the components in the MCFC.

The first effort in our research has been directed toward the measurement of CO_2 in MCFC. CO_2 is important in the MCFC because it is the primary product on the anode side and is consumed on the cathode side. Since it is observed on both sides of the cell and because the change in the CO_2 concentration is a direct measurement of performance at any given point in the cell, a technique for measuring CO_2 concentrations *in situ* would be very important as a diagnostic tool. The technique that we demonstrated was Coherent anti-Stokes Raman spectroscopy (CARS).

There are a variety of optical diagnostics available to aid in understanding the mechanism of carbonate movement. We evaluated a number of these including CARS, laser induced fluorescence (LIF), laser induced breakdown spectroscopy (LIBS), and photo-fragment fluorescence spectroscopy (PFFS). Each of these have advantages and disadvantages, which depend on species, concentrations, and the environment in which the species is found.

Because these techniques are molecule or atom specific we need to have some model that can predict what species might be present in the vapor phase that would contribute to contaminant movement. To do this we have looked at the processes in the MCFC and have developed a simple model to explain the movement.

We are now in the process of evaluating the techniques and refining the model based on laboratory experiments. What we hope to show with our diagnostics and laboratory measurements is how prevalent this process is and attempt to quantify reaction rates to enhance our model of carbonate movement.

Carbonate Movement Model

The model that we have chosen contains three basic assumptions:

1. The movement of the carbonate is related to the vaporization of alkali compounds.
2. The species involved may be any of several including halides and hydroxides.
3. Feed contaminants enhance this vaporization process.

Figure 1 shows the vapor pressures of the various species that we feel may be involved in carbonate movement. The metal atoms, if liberated from the carbonate, will not survive long in the environment of the MCFC. We expect that

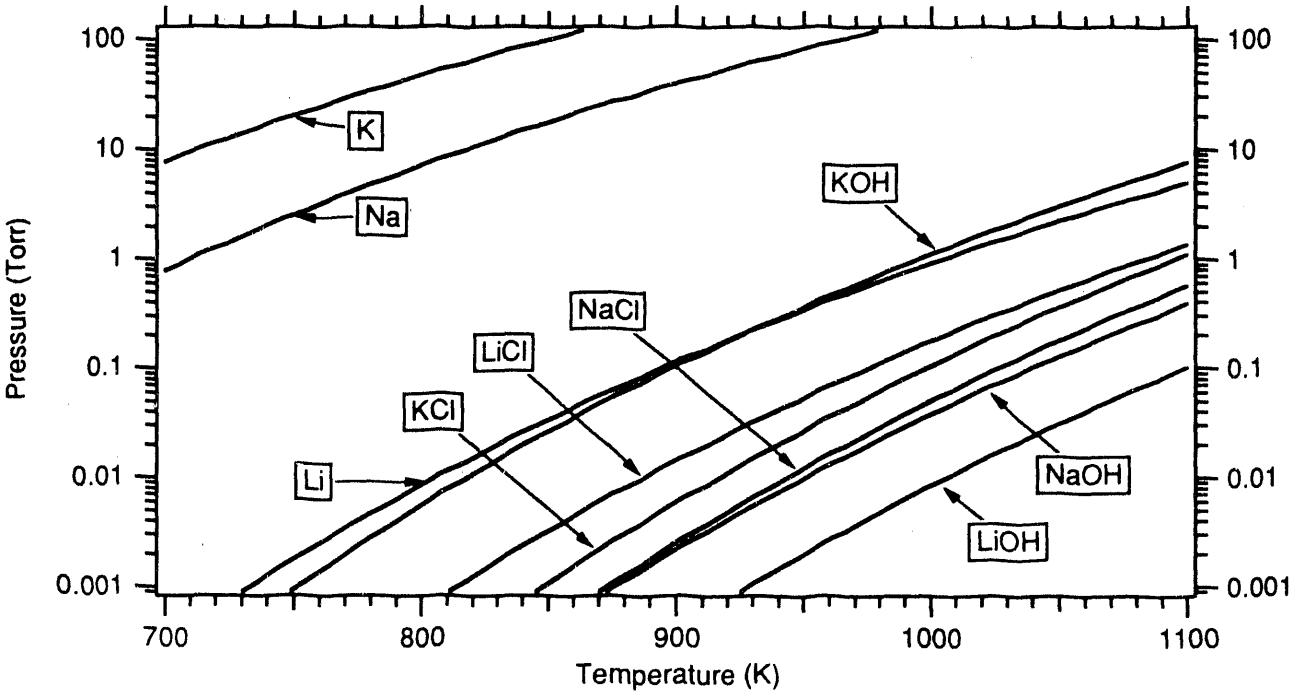

Fig 1. Vapor pressures of important species involved in carbonate movement.

they will be converted to the hydroxide or the chloride (if chlorine is present in some form). The formation of either the chloride or the hydroxide in the carbonate structure will lead rapidly to the release of the species into the vapor phase. Reactions may occur to drive the compound back to carbonate and redeposition of the alkali onto the carbonate but in the intervening time the alkali will have moved, resulting in carbonate movement.

We have investigated four techniques for measuring gaseous species using optical techniques. These techniques are described below. Each has its advantages and disadvantages.

Coherent Anti-Stokes Raman Spectroscopy

CARS is based on the combination of three photons interacting with the molecule of interest and the generation of a fourth photon, the signal. The strength of the signal beam, I_{as} at frequency ω_{as}, is given in Eq. 1.

$$I_{as} \propto \left(\frac{\chi^{(3)} P\, \omega_{as}\, \Delta_J}{T}\right)^2 I_p^2 I_s L^2 \qquad 1$$

where $\chi(3)$ is the nonlinear susceptibility of the gas, P is the partial pressure of the gas, T is the temperature, Δ_J is the difference in population of the two levels, I_p is the power of the pump laser at frequency ω_p, I_S is the power of the sample laser at frequency ω_S, and L is the length of the interaction zone of the two lasers. $\chi(3)$ is dependent on the molecule and the energy levels involved.

CARS has several advantages. It is species specific because of the $\chi(3)$ dependence. The signal light is generated in a coherent process and has the same properties as the incoming laser light, making it directional and allowing most of the signal to be detected. Because of the pressure and temperature dependence (including the temperature dependency in Δ_j), the temperature and pressure of the gas can be determined.

One disadvantage of CARS is that it requires two lasers, a pump laser and a Stokes laser. The pump laser is usually a Nd:YAG laser that has been frequency doubled to 532 nm. The Stokes laser is a dye laser that can be tuned to the required wavelength and is powered by part of the Nd:YAG 532 nm beam. Also, the limit of detection in a typical CARS setup is 10-1000 ppm and

is dependent on the other gases present. This is because the CARS technique generates a nonresonant background from all other gases (solids or liquids) present in the sampling volume. There are ways to minimize this nonresonant background but they require additional optics and more optical ports. Finally, CARS is sensitive to optical alignment since the beams are focussed into a small volume to get the signal strength higher. Because there are two beams, the two beams have to be focussed into the same point making optical alignment critical. Figure 2 shows a typical CARS setup and shows the large number of optical elements that have to be aligned for the experiment to work properly.

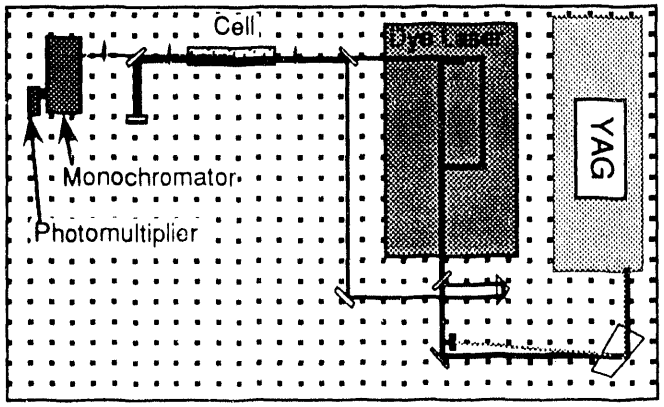

Figure 2. CARS setup.

Laser Induced Fluorescence

The second method that we considered was laser induced fluorescence (LIF) of the metal atoms. In this technique a laser is tuned to an optically allowed spectral line of the element of interest and populates an electronic excited state. The atom reemits the absorbed photon and a monochromator and detector look at the signal radiated perpendicularly to the laser beam and detect the fluorescence of the particular atom. This can be a very sensitive technique for determining metal atom concentrations (ppb level). Its major disadvantage is the Rayleigh scatter of the laser beam off of atoms and molecules in the beam path, with this scatter limiting the ultimate sensitivity of the technique. However, we do not expect to see alkali atoms present (in elemental form) in the MCFC , and we only briefly investigated the technique before proceeding.

Laser-Induced Breakdown Spectroscopy

A very promising technique that we think will prove very beneficial is called laser-induced breakdown spectroscopy (LIBS). In LIBS a laser (Nd:YAG at 1.06 μm) is focussed into the sample to generate a laser spark. Because of the large electric fields created by the intense laser energy, the gas (liquid or solid) breaks down the same way high voltage generates a spark. This spark creates a plasma which breaks all the molecular bonds apart and leaves only excited atoms. These atoms then emit light at their characteristic wavelengths. By tuning a monochromator to the particular wavelength emitted by an atom, you can detect the presence of those atoms in the material. Figure 3 shows the LIBS setup.

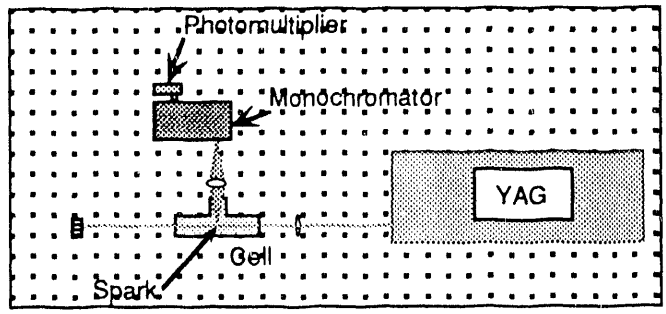

Figure 3. LIBS setup.

The advantages of this technique are that it is an elemental monitor and therefore is element specific. It has low limits of detection (20-100 ppb[weight to weight] in air for alkali metals). For example, Los Alamos has developed this technique into a continuous beryllium monitor. The setup is simple, inexpensive (only one laser is needed and that can have modest energy output), and small. Because there is only one beam and few optical elements, the setup is insensitive to alignment.

The disadvantages of LIBS are: 1) the signal is radiated in all directions (the smaller the field of view of the spark the less the sensitivity); 2) the

limits of detection can be high for some elements (examples of such elements are Cl, N, O, and S) due to the nature of their electronic structure; 3) Finally, because it does create a spark, it is not suitable for explosive environments.

Photo-Fragment Fluorescence Spectroscopy

The final technique that we looked at is photo-fragment fluorescence spectroscopy (PFFS). In this technique an ultraviolet laser beam of moderate to high energy passes through the gas. Most salts of the alkali metals molecules can absorb this ultraviolet light and dissociate leaving the individual atoms, with the alkali atom in an excited state. These atoms fluoresce as in LIBS and the light from this fluorescence can be detected using a monochromator and detector. By changing the energy or wavelength of the ultraviolet light, more strongly bonded species can be excluded. In this manner it is not only elemental specific but can be used to discriminate between molecular species. Figure 4 is the PFFS experimental setup.

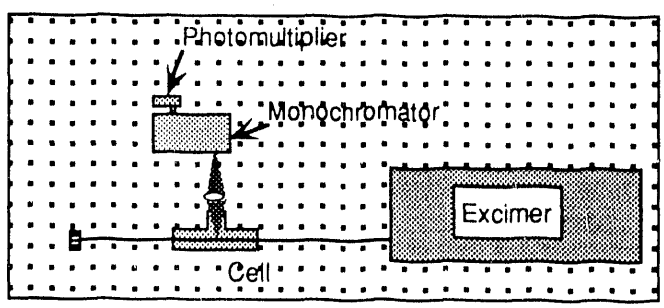

Figure 4. Photo-fragment fluorescence spectroscopy setup.

The advantages of PFFS are 1) it is a good alkali salt monitor (all the alkali salts break apart at a laser wavelength of 193 nm); 2) It is species specific within broad categories such as chlorides versus hydroxides; 3) Only one laser is required (typically an excimer); 4) It has low detection limits for alkali salts with detection limits less that 1 ppm possible. Because the beam does not have to be focussed as much as in CARS or LIBS, a larger volume is sampled so the signal is larger and detection limits are correspondingly smaller. There is however loss because not all of this extra light that is generated is able to be focussed through the slits of the monochromator.

The disadvantages of this technique are: 1) as in LIBS, the signal radiates in all directions; 2) Ultraviolet optics are required because of the wavelength of the laser. This poses a problem for high-temperature operation because quartz changes its transmission characteristics with increasing temperature. Therefore, small changes in the window temperature can change the power in the laser beam; 3) Finally, the laser is more complicated and expensive than the LIBS laser as it requires halogen and rare gases to operate and these gases have to be replaced regularly.

Experiment

All of the techniques described share a common data acquisition and instrument control setup. The signals are processed by box-car averagers and sampled by an A/D converter (13 bit, ±10V) connected to a computer. The computer controls the scanning of the laser and the monochromator as needed. The computer can signal average by recording multiple shots at any given laser or monochromator signal. Typically 5-20 laser pulses were averaged per setting. The dye laser was moved 0.048 nm per step when used in the CARS experiments. The monochromator was scanned to keep the signal beam centered in its band pass by the computer.

For the PFFS experiment the monochromator was stepped 0.25 nm per step and was a small double-pass instrument. A half-meter Ebert style monochromator was used for the LIBS experiments and had a much finer stepping control. The resolution of the LIBS data is much greater than the PFFS data due only to our experimental constraints. The excimer laser used in this experiment was run at low power (10 mj/cm$^{2)}$ to avoid adverse effects in the cell.

The cells that we used for these results were 8 cm long and 2.5 cm diameter quartz tubes with quartz windows. The cells were held in a small clam-shell heater and a thermocouple adjacent to the cell was connected to a temperature controller

for maintaining the appropriate temperature. Temperature variations during any given run were smaller than 10 K.

We used LiCl for these demonstrations because it has a large vapor pressure at moderate temperatures (for the alkali halides) and would not react with the quartz cell. A small amount (less than one gram) was loaded into the cell. The cell was then evacuated and filled with argon or carbon dioxide gas to a pressure of 760 Torr for LIBS and 100 Torr for PFFS. The cell was then heated to the appropriate temperature and the scan obtained.

RESULTS

The CARS work that we performed earlier on CO_2 showed that CARS is useful for major gaseous species but would not work for any of the carbonate movement measurements where high sensitivity is important. Therefore, we do not show any CARS results in this report. The previous report summarized our findings for CARS on CO_2.

An example of the LIBS data for LiCl is shown in Fig. 5. This data shows the increase in the signal in going between our estimated vapor pressures of 0.001 Torr to 0.080 Torr. This corresponds to a concentration of 1 ppm at the lower limit. Because we were using a very small slit (100 μm) and were not able to put much of the available light into the monochromator we estimate that we can reduce this by a factor of 20 with the appropriate optics and monochromator. This puts us in the range that other LIBS experiments. If we were able to dispense with the monochromator and used only an interference filter for removing the extraneous light we would do even better.

To better display the spectra, each of the plots are offset from the previous by 0.1 units in the intensity scale. The baseline of the spectra did not change with the temperature.

An example of PFFS spectra is shown in Fig. 6. Because of the larger volume probed by the laser, the wider slits on the monochromator (1 mm) and the better optical matching we were able to see signal down to the few parts-per-billion range. Because of the nature of the setup,

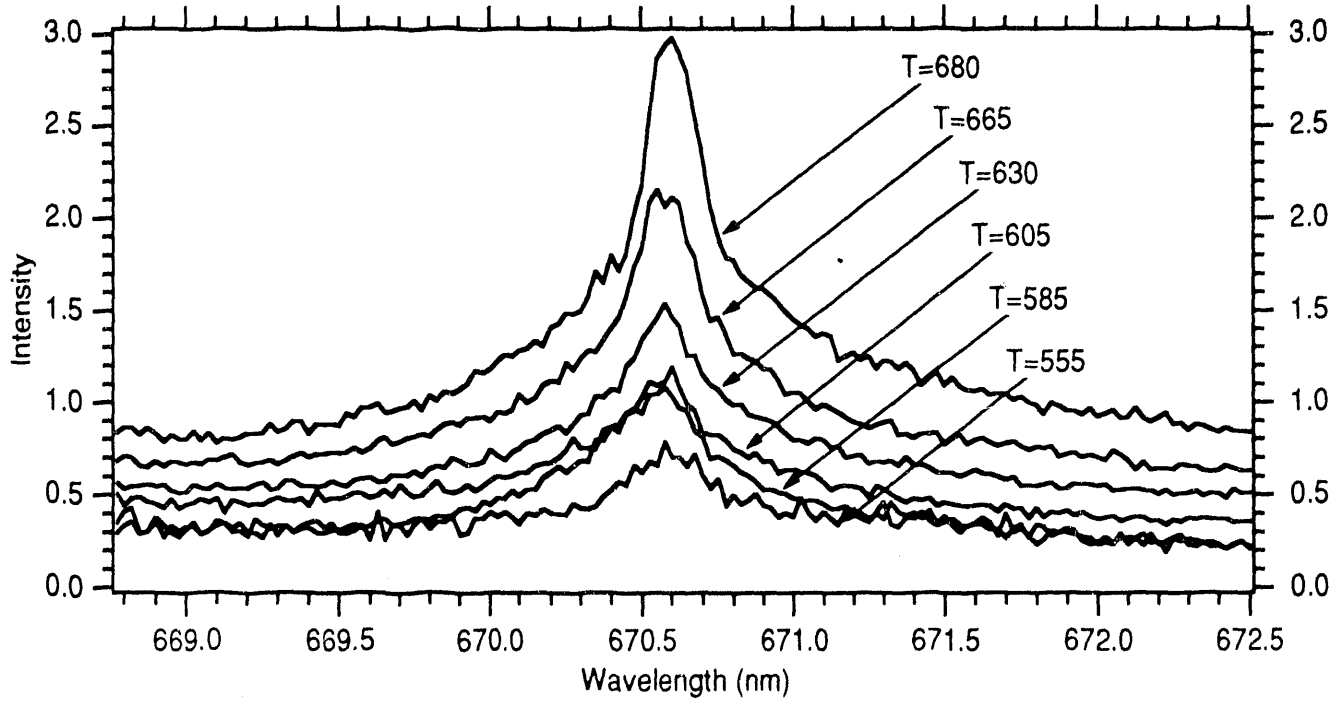

Figure 5. Laser induced breakdown spectra of LiCl

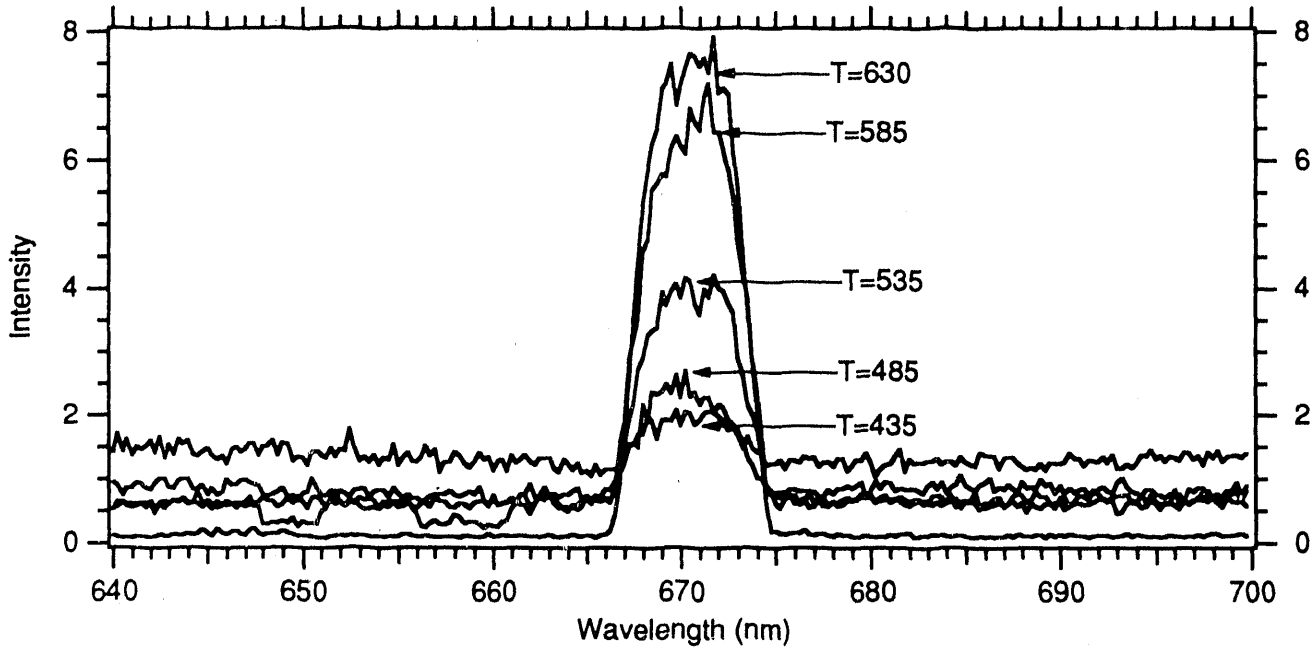

Figure 6. Photo-fragment fluorescence spectra of LiCl

the temperature was not as controlled as we need to be able to give a better value for the detection limit.

One of the problems we encountered with this cell was the deposition of the LiCl on the windows. Because the windows were at a lower temperature than the rest of the cell, the LiCl vapor would condense on contact with the windows. At higher temperatures when LiCl reached its melting point (883 K or 610 C) the windows would clear as the LiCl ran to the bottom of the cell. For the LIBS spectra, the energy of the laser focussed into a small circle managed to keep the window clean. But for the PFFS spectra, the coating on the window caused the background to rise. This rise in the background was caused by the scattered light from the fluorescence of the LiCl on the window and from the scattered laser light striking walls in the field of view of the monochromator. There was always some fluorescence from the cell windows.

We were unable to take the cell to temperatures higher than 630 C (903 K) because the LiCl in the vapor phase (or the windows, see below) absorbed all of the laser light before the interaction region. A simple plot of the intensity of the signal versus the pressure does not yield a straight line at the higher temperatures because of this effect. For our purposes this difficulty should not arise as the alkali chloride concentrations in a MCFC will never be as high as we had in the test cell. Other species may or may not be a problem. Further tests are needed to determine the exact effect and whether there are ways to circumvent the problem.

Another effect that we have not calibrated for yet is the temperature of the windows. Previous work indicates that quartz absorbs more of the 193 nm light from the excimer laser as it gets hotter. At 100 C the transmission is reported to have dropped to less than 50 %. But cold windows act as cryopumps for the vapor. We are looking at designs of the cell (i.e. purging) that will allow the window to be maintained at a reasonable temperature, remain clear, and not act as a trap for the vapor.

FUTURE WORK

We plan on continuing the studies of the vapor species that we have identified as problems in carbonate movement. These include the halides and the hydroxides. Hydroxides pose another problem in that at the temperatures that we operate the cell they decompose on many materials and react with most of the rest. Previous work in our laboratory indicates that silver may work as a containment vessel.

We will then apply the knowledge that we gained from investigating the individual species to studying the effects of the various compounds have in a carbonate mixture. This information will then direct us to the next step.

One of the experiments that we plan on carrying out is one in which a stream of chlorine (typically as HCl) is passed over the carbonate mixture, while we monitor the gas phase concentration of alkali chlorides using PFFS. This will help us determine the rates of carbonate movement as a function of chlorine concentration. It will also aid in identifying the chlorine species that present the greatest problem. In our model, chlorine contamination (HCl in the fuel gas) will promote carbonate movement. By studying the vapor phase concentration of the alkali atoms as a function of the chlorine concentration we can validate this model.

Assuming that our model, or a modified version, holds up through these tests, we propose to validate the model in field tests on actual MCFCs.

REFERENCES

Kinoshata, K., McLarnon, F. R., and Cairns, E. J., 1988. *Fuel Cells: A Handbook*, pp. 57-86. DOE/METC-88/6096. NTIC/DE88010252

Chase, M. W., Jr., C. A. Davies, J. R. Downey, Jr., D. J. Frurip, R. A. McDonald, and A. N. Syverud, 1985, *JANAF Thermochemical Tables*, J. Phys. Chem. Ref. Data, Vol. 14, Supl. 1, 1985.

Palmer, Byron., Richard C. Oldenborg, David J. Funk, 1990, In Situ Characterization of MCFC Using Optical Diagnostics, *In Proceedings of the Second Annual Fuel Cell Contractors Meeting*, ed. W. J. Huber, pp. 74-81. DOE/METC-90/6112 NTIC/DE90000490

Oldenborg, Richard C., and Steven L. Baughcum, 1986, Photofragment Fluorescence as an Analytical Technique: Application to Gas-Phase Alkali Chlorides, *Analytical Chemistry* 58(7): 1430-1436.

ERC's Carbonate Fuel Cell Power Plant Commercialization Progress

Bernard S. Baker
Energy Research Corporation

This presentation is intended as a status report on ERC's commercialization initiative. As things now stand, ERC is continuing a multifaceted parallel program effort directed at commercializing its Direct Fuel Cell based on carbonate fuel cell technology. The objective of this commercialization effort will lead to clean, cost competitive natural gas and coal gas fueled carbonate fuel cell power plants in the latter part of this decade. The five major categories of work are business activities, stack development and improvement, manufacturing, plant design and demonstrations.

BUSINESS ACTIVITIES

The business activities of ERC in the commercialization area fall into four categories, organizational, marketing, financial and scheduling.

Organizational

Since 1989 ERC has engaged in several major organizational activities. First, the manufacturing entity, Fuel Cell Manufacturing Corporation (FCMC), was organized as a 100% owned subsidiary of ERC in conjunction with financing provided by ERC, Messerschmitt-Bolkow-Blohm, GmbH (MBB) and Southern New England Telephone Company (SNET). Funding from ERC, MBB and SNET has been put into place to design and construct the manufacturing facility and to bring it to production readiness.

In 1990 the Fuel Cell Commercialization Group (FCCG) was formed by a group of municipal and investor owned utilities. This not-for-profit group, FCCG, under the Chairmanship of Robert Claussen of the Alabama Municipal Electric Authority has been working closely with ERC on many aspects of commercialization including marketing, sales, power plant design, contractual relationships and power plant demonstration plans. It presently has 23 members consisting of both investor-owned utilities and municipal utilities. The FCCG has formed four formal committees as shown in Figure 1 to work with ERC in these select areas.

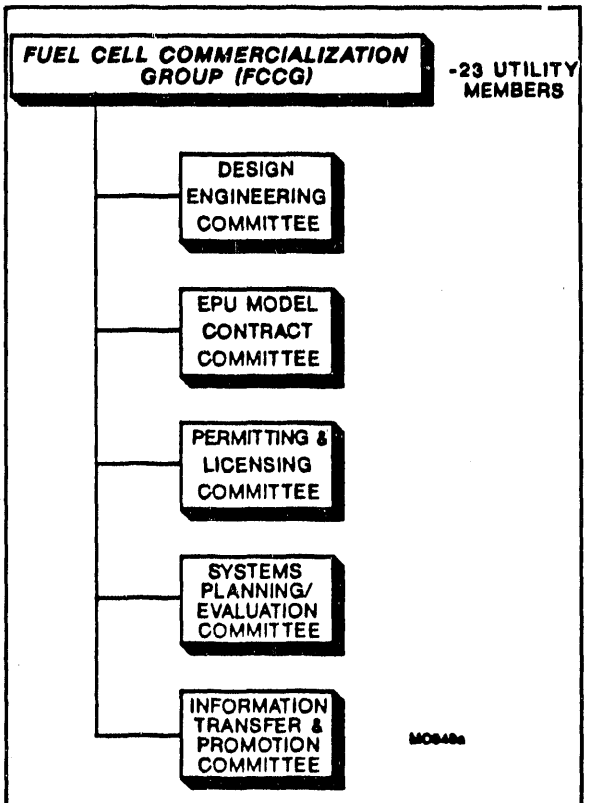

Figure 1. FCCG Organization

Derivative from FCCG is the Santa Clara Demonstration Group (SCDG) under the Chairmanship of Paul Eichenberger of the City of Santa Clara and consisting additionally of Southern California Edison Com-

pany, Southern California Gas Company, the Los Angeles Department of Water and Power, Pacific Gas and Electric Company (PG&E), the National Rural Electric Cooperative Association and Electric Power Research Institute (EPRI). The objective of SCDG is to have a 2MW natural gas fueled power plant in operation by 1994.

Also in 1990, a new company, Fuel Cell Engineering Corporation (FCEC), jointly owned by PG&E and ERC was formed to provide power plant design, construction and sales. With the formation of both FCEC as well as the aforementioned FCMC, the overall structure for ERC to initiate the commercialization of the Direct Fuel Cell is in place as shown in Figure 2.

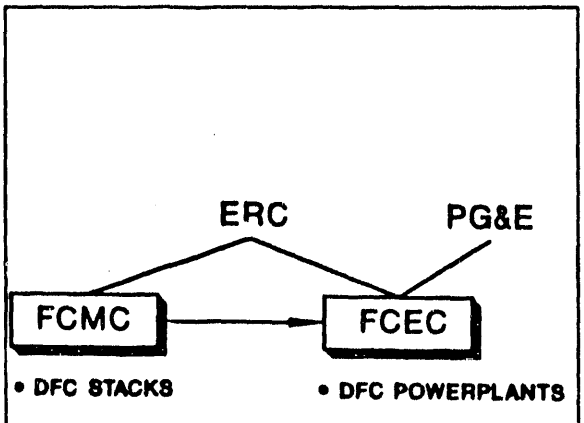

Figure 2. Overall Commercialization Structure

All of the above organizational activities were part of the process necessary to implement first the commercialization of natural gas power plants as a precursor to commercialization of the coal gasification carbonate fuel cell (CGCFC) power plants.

Marketing

ERC and its partners have initiated marketing studies on a worldwide and U.S. basis. Studies of the World and European market have been made by both MBB and Daimler Benz. The market for electric utility related equipment worldwide is large, estimated to be about $200 billion/year. While clearly the fuel cell must be competitive in every respect with other equipment, concerns about pollution and carbon dioxide production will benefit the fuel cell. Carbon related taxes already being considered in Europe will produce a tangible credit to the fuel cell power plant with a high efficiency potential. In some cases, existing studies have been used to guide the role for carbonate fuel cells in the marketplace and, in other cases, new market information is being sought. Initial focus is on smaller applications in the 2 to 10MW size range with a basic 2MW plant design. Such power plants will have market opportunity for municipal utilities, investor owned utilities as dispersed generators and for cogeneration. ERC is also studying larger natural gas and coal gas plants in the 200MW size range. In the U.S. the market potential is also largely made up from both growth in the electricity use and replacement of aging existing equipment. The former is estimated at about 2.3% annually and the latter can be estimated assuming a plant life of 40 years. Using 1997 as a start year for DFC sales the combined replacement-growth market is about 32 GW/year.

During 1990 ERC, together with the FCCG, hosted two electric utility briefings in Dallas, Texas. Response from the utilities was good and FCCG now has 22 members represented by a broad cross-section of U.S. municipal and investor-owned utilities as shown in Figure 3.

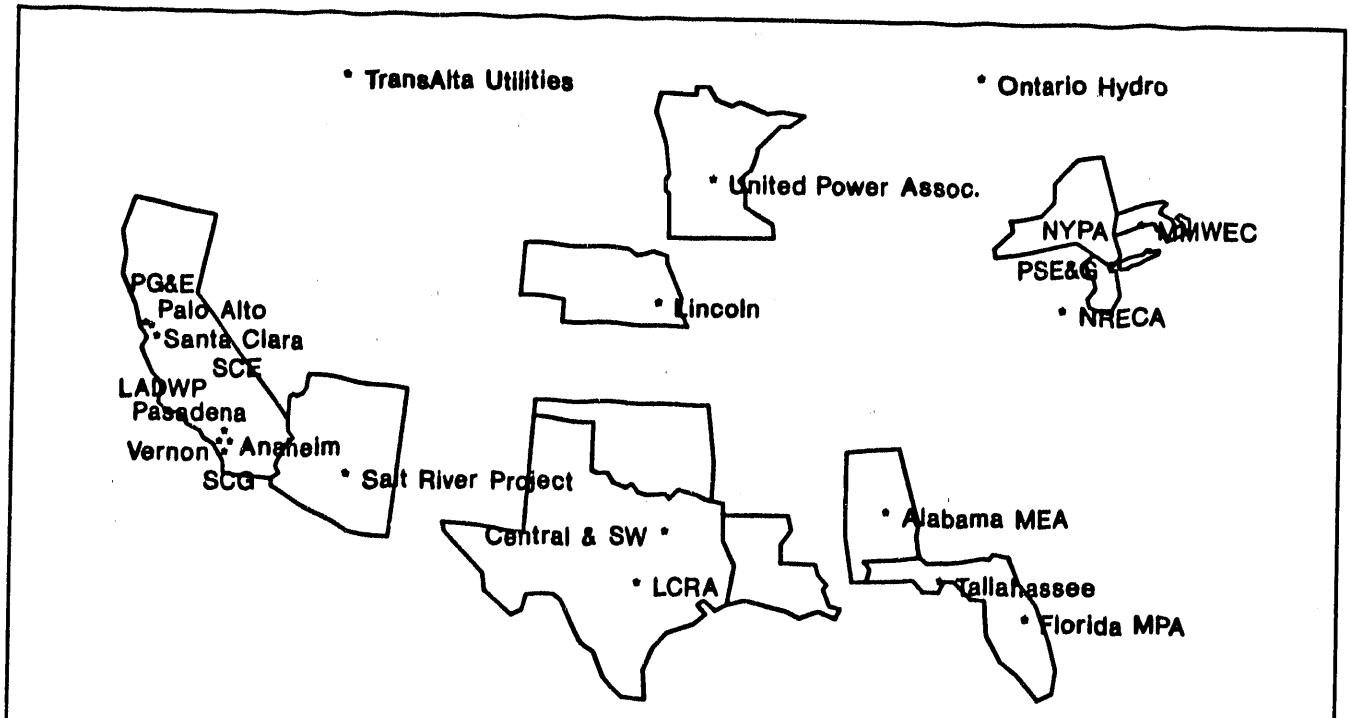

Figure 3. Geographical Distribution of FCCG Members

Financial

During 1989 and 1990, ERC was successful in raising private funding for FCMC and for FCEC. Additional private funding is required to pursue demonstration power plant financing and within a few years to seek private financing for the design and construction of commercial manufacturing and assembly facilities for carbonate fuel cell stacks and balance of plant (BOP) equipment respectively. Steps are being taken to raise this financing.

Schedule

ERC feels that its commercialization schedule, as shown in Figure 4, is still on track as planned with key items such as manufacturing facilities, demonstrations and development issues progressing as originally planned on a reasonably timely basis.

STACK DEVELOPMENT AND IMPROVEMENT

ERC is developing a common stack design for natural gas and coal systems. The current focus is on full height stack demonstrations. The overall approach and recent results are discussed in Dr. Farooque's paper.

MANUFACTURING

As discussed last year, ERC has completed a manufacturing plant design and now has under construction in Torrington, Connecticut, a 2MW/year carbonate fuel cell stack manufacturing plant. This existing 50,000-ft^2 facility has now been partially outfitted with specially designed manufacturing equipment and has a startup date of January 1992 which is presently on schedule. The present status of key manufacturing facilities is shown in Figure 5.

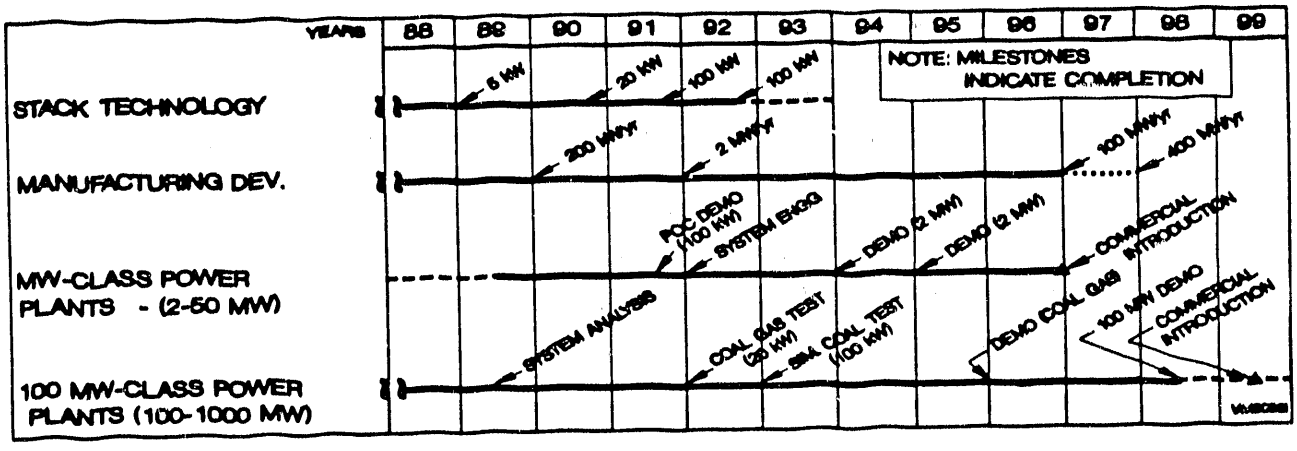

Figure 4. Commercialization Schedule

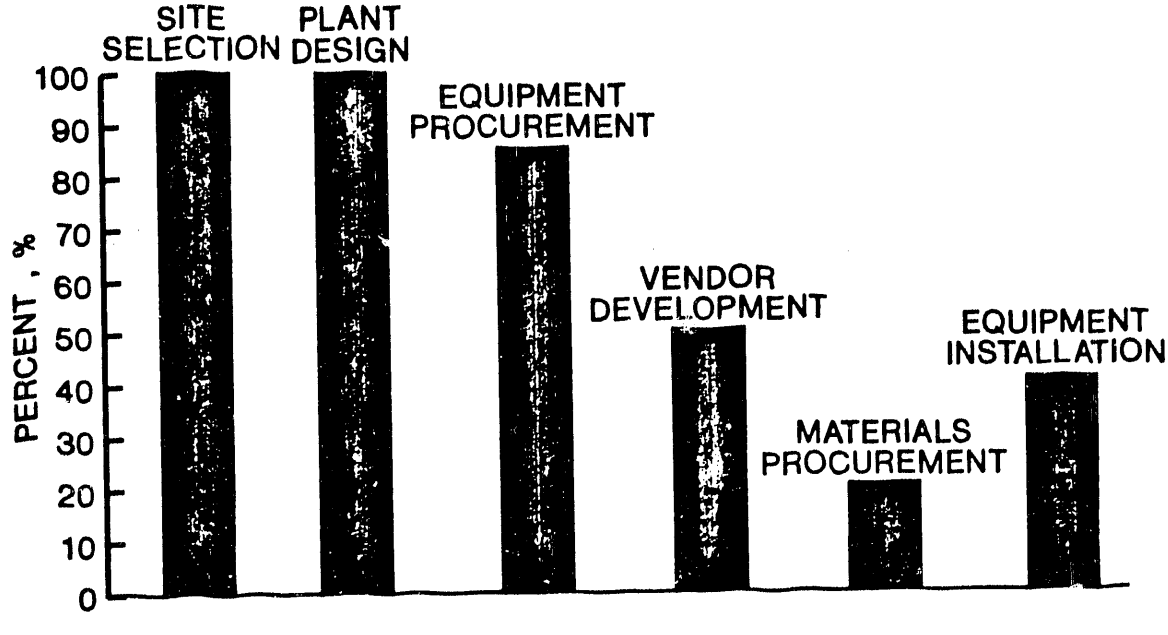

Figure 5. Status of Key Manufacturing Facilities

PLANT DESIGN

ERC is pursuing two different natural gas fueled 2MW plant designs, designated simplified and integrated. Both plants are based on the direct use of natural gas in the fuel cell stack. The major effort at present is on the simplified design and, in a joint effort with PG&E, the details of the early demonstration plant and early production unit design are being addressed. A schematic of the SCDG plant is shown in Figure 6. The DC power block consists of twenty 100kW stacks distributed on two 1 MW skids. The layout of one of these is shown in Figure 7.

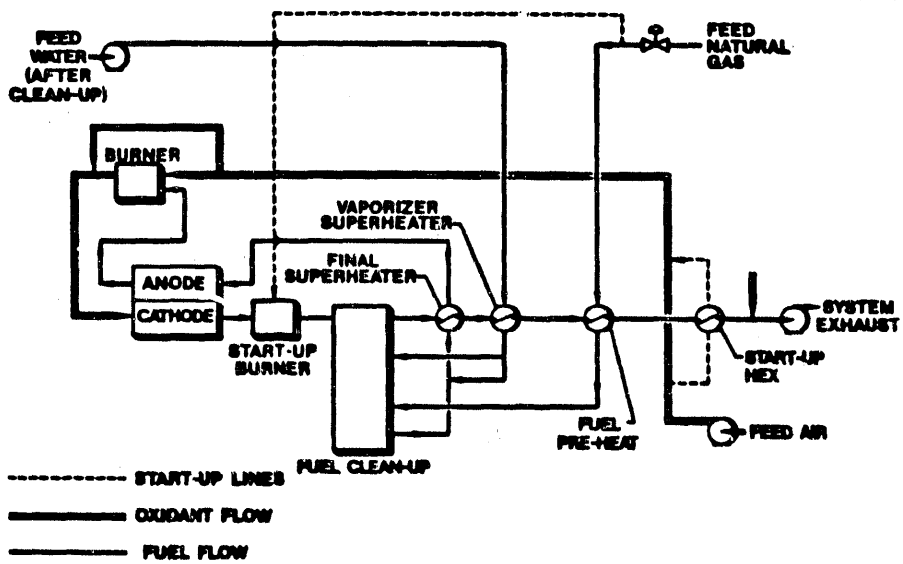

Figure 6. Simplified Power Plant Schematic

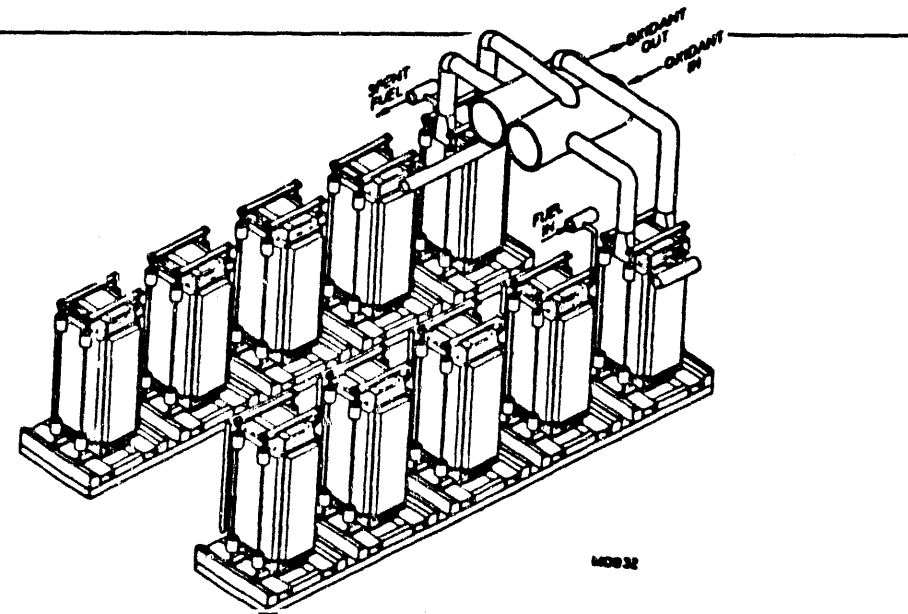

Figure 7. 1 MW SCDG Skid

On the coal gas front beginning with the rather complete studies undertaken for DOE[1], ERC working together with Fluor under EPRI contracts has configured a 52% efficient coal gas plant based on the British Gas Lurgi gasifier.

Additionally, under a new DOE Contract No. DE-AC21-90MC27227, ERC is working together with Fluor and the Energy and Environmental Research Center in North Dakota to configure a higher efficiency plant based on a methane producing gasifier highly integrated with the Direct Fuel Cell. The goal of this plant design would be to eliminate both the usual steam bottoming cycle and the oxygen plant to maximize efficiency and thereby minimize carbon dioxide production.

A block diagram for this type plant is shown in Figure 8. At least 55% efficiency appears possible based on these designs.

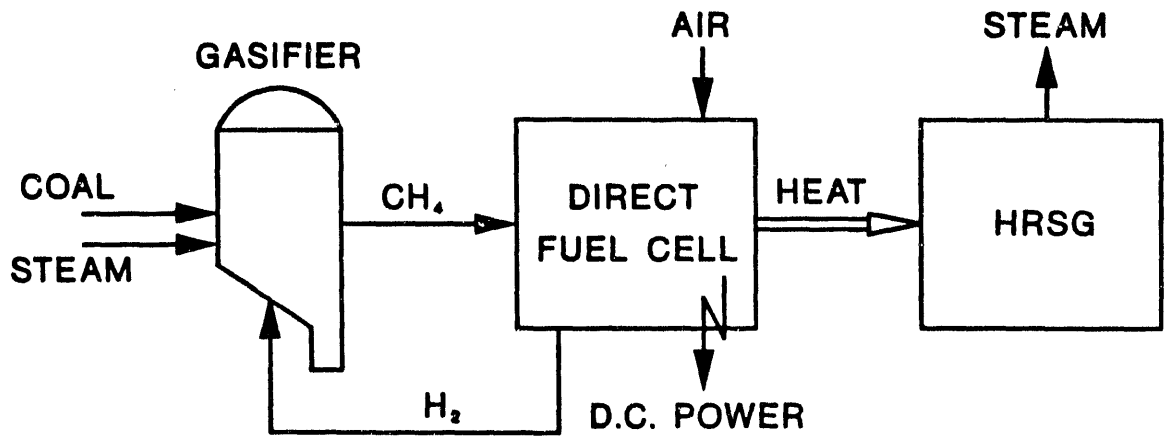

Figure 8. Conceptual Diagram of Advanced Coal Gasification Plant

DEMONSTRATIONS

To move into the demonstration phase, ERC has formed FCEC with PG&E to design and build initial 2MW power plant systems. The first such project will be submitted to the SCDG for review in May 1991. Other demonstrations are also planned through FCEC.

A subscale demonstration of the simplified plant will be operated at PG&E's San Ramon site this fall. This plant will demonstrate full height stack operation within the simplified system BOP framework. A 20kW stack packaged in the full size is shown in Figure 9 together with the BOP at PG&E's San Ramon site.

Figure 9. DFC Unit & BOP at San Ramon Test Site

A mini-version of a natural gas fueled grid-connected plant based on an earlier ERC integrated design[2] has been operating at Elkraft's Lyngby, Denmark power plant site since October 1990. This plant, with the BOP built by Haldor Topsoe A/S, as of March 1991, had accumulated over 3,500 hours of test time at design conditions after startup and short term testing at ERC in July 1990. The stack unit as shipped to Elkraft is shown in Figure 10.

Finally, on the demonstration front, the first real coal gas test will be conducted at Destec Energy, Inc.'s Plaquemine, LA site in 1992 using gas produced by their entrained gasifier. The BOP for this unit is being designed by Haldor Topsoe, Inc. This project is a joint effort of EPRI and DOE.

Other natural gas and coal gas demonstrations are being planned in Germany together with MBB, ERC's European partner.

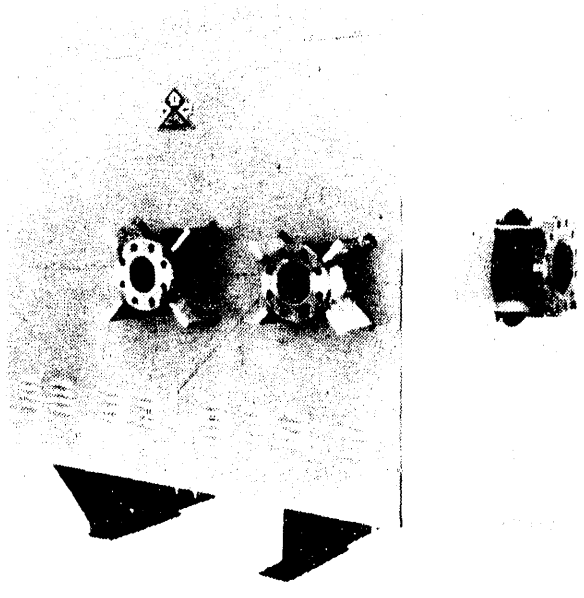

Figure 10. DFC Stack Tested at Elkraft Power Company Ltd.

REFERENCES

1. Farooque, Steinfeld, McCleary, Kremenik. 1990. Assessment of Coal Gasification/Carbonate Fuel Cell Power Plants. Topical Report.
   DOE/MC/23274-2911
   NTIS/DE90015579

2. Energy Research Corporation, Fluor Engineers, Inc. 1985. Parametric Analysis of a 6500-Btu/kWh Heat Rate Dispersed Generator. Final Report.
   EPRI EM-4179

Commercialization Aspects of the IMHEX CFC Power Plants

CONTRACT INFORMATION

Contract Number		DE-RA21-90MC27394
Contractor		M-C Power Corp. 8040 S. Madison St. Burr Ridge, IL 60521 (708) 986-8040
Project Manager	M-C Power ABB, Inc. ABB, Inc.	Lee H. Camara M.W. Snow R.R. Woods - Business Dev. & Marketing
METC Project Manager		Mark Williams
Period of Performance		September 14, 1990 - September 14, 1993

Schedule and Milestones

IMHEX CFC Commercialization Program Schedule

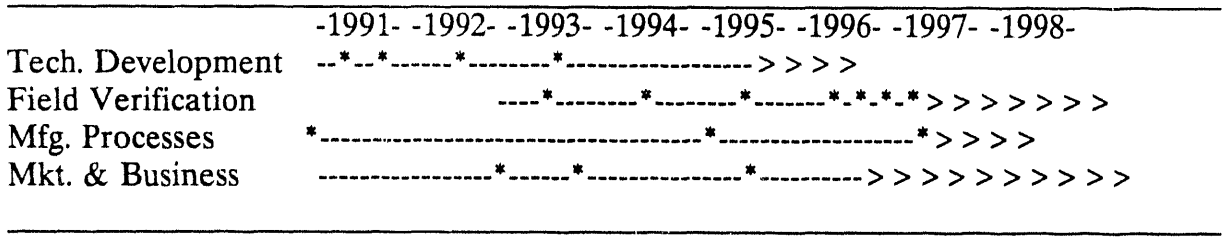

OBJECTIVES

The IMHEX (Internally Manifolded Heat Exchanger) Carbonate Fuel Cell (CFC) Commercialization Program was designed to consolidate and ensure coordination of the various activities, bringing this technology to the marketplace. The objective of this *overall program* is to develop the technical, market and business structures required to successfully commercialize IMHEX CFC power plants.

Inclusive programs are sponsored currently by several organizations which include the Department of Energy (DOE-METC), Gas Research Institute (GRI), Electric Power Research Institute (EPRI), State of Illinois, San Diego Gas and Electric (SDG&E), Southern California Gas Company (SoCalGas), UNOCAL, the South Coast Air Quality

Management District (SCAQMD), Public Service Gas & Electric and Florida Power Corporation. The *program* consists of developmental efforts by all the United States members of the IMHEX development team, M-C Power Corp., Asea Brown Boveri Inc. (ABB Inc.) and Institute of Gas Technology (IGT) and also includes parallel component development by our international partner, Ishikawajima-Harima Heavy Industries, Ltd. (IHI).

BACKGROUND INFORMATION

The IMHEX team was established in the late 1980's by IGT, a not-for-profit contract research organization which has been developing CFC technology for over 20 years. Recognizing the significant advantages of their internally manifolded carbonate fuel cell technology, IGT established M-C Power Corporation in early 1988 for the sole purpose of manufacturing, assembling, marketing and selling CFC stacks incorporating IGT's IMHEX concept. M-C Power currently has three major shareholders, IGT, ABB Inc. and IHI. The capital and technology infusion from these shareholders has enabled M-C Power to gain and maintain a leading position in CFC stack materials, manufacturing methods and techniques. To date, M-C Power has completed construction and initial operation of a facility in Burr Ridge, Illinois with the capacity of producing approximately 3 MW per year of CFC stacks and components.

IGT will continue as a strong technical partner in the IMHEX team and is responsible for the advancements in fuel cell component technology. Qualification of such critical technical issues as stack endurance and performance will be their goal over the next several years. Advancements achieved in IGT's laboratories will be transferred to M-C Power who will translate these technology cornerstones into commercial components and manufacturing processes.

ABB Inc. is responsible for developing the balance-of-plant and subsystem component technologies required to transform the IMHEX CFC stacks manufactured by M-C Power into complete power generation systems which meet marketplace requirements. In consideration of these evolving developments and of ABB Inc's equity in M-C Power and substantial contract cost-sharing, M-C Power has entered into an agreement with ABB Inc. that provides the latter with the marketing and distribution rights for the IMHEX technology in territories that include the United States. ABB Inc. is responsible for integrating M-C Power manufactured stacks and ABB Inc's balance-of-plant subsystems into commercially viable power plants, and marketing, sales and service of these power plants.

Asea Brown Boveri Inc. is the U.S. subsidiary of Asea Brown Boveri Ltd. which is a global $27 billion corporation serving electric power generation, transmission and distribution customers as well as industrial, environmental control and mass transit markets. ABB Inc is the parent of several companies in the USA including among others Combustion Engineering, Inc., the Transmission and Distribution Division formerly of Westinghouse Electric Corp. and several Asea Brown Boveri Ltd. subsidiaries in the USA. ABB Inc's Advanced Technology department, within the Power Plants business segment, has corporation-wide responsibility for CFC development and commercialization. Advanced Technology is drawing on experience and expertise across the Corporation to provide technologically superior, efficient and cost competitive components for CFC systems.

IHI is also a worldwide corporation

involved in diverse manufacturing industries, ranging from ships to heavy equipment with approximately $8 billion in revenues. They are one of the world's largest manufacturers of turbo-chargers and are a major player in the construction of electric generation power plants and chemical refineries. As a shareholder in M-C Power and one of the leading CFC developers in Japan, their role in the IMHEX team can provide several benefits. As an example, IHI plans to develop an advanced reformer subsystem based on in-house planar, catalytic combustion reformer developments.

PROJECT DESCRIPTION

The IMHEX CFC Commercialization program focuses on four major areas: Design and Development; Field Verification; Manufacturing Processes; plus Market and Business Development. These areas are interdependent, with the results from one area being used to guide activities in the other areas.

Design and Development - component and subsystem developments, systems integration testing, and field verification unit designs;

Field Verification - Proof-of-concept, field experiments, and prototype commercial unit testing;

Manufacturing Processes - Manufacturing technique development and quality assurance programs, design and construction of fabrication facilities; and

Market and Business Development - User involvement, product definition, market demand stimulation and business development activities, including assessing market and business issues and opportunities.

These combined areas form an aggressive RD&D program directed at developing the technology and stimulating the market demand required to commercialize the IMHEX carbonate fuel cell and related power plants. The program is estimated to cost approximately $175 M between 1990 and 1996.

Central to the program are the field verification activities. Beginning in 1993, the IMHEX team will field their first sub-scale proof-of-concept unit (approx. 250 kW) which is sponsored by the DOE, UNOCAL, SoCalGas and SCAQMD. Located at UNOCAL's R & D complex, this unit will operate on both simulated coal-gases and on natural gas. Incorporating the experience from this test, the team's second proof-of-concept is scheduled to begin operation in 1994 under the sponsorship of the GRI and SDG&E. These two tests should provide the IMHEX team with the experience necessary to design and construct commercial scale field experiment units during 1995. These units will fully reflect the performance and operational characteristics of the introductory commercial power plants and establish the bases for initial product orders. Following these tests the IMHEX team will transition through multiple unit field tests and into commercial deliveries during the last half of the 1990's. All results are focused on having the IMHEX CFC power plant commercially available by 1995 and producing and delivering a economically viable product by 1996/1997.

COMMERCIALIZATION STRATEGY

The IMHEX CFC Commercialization Program is based upon a technical/commercial assessment of the key forces likely to dictate the structure and focus of the power generation industry through the year 2000 and beyond. Those forces which have been determined to be

crucial to the development of the commercialization strategy include:

- Deregulation and the resulting increased competition in the power generation marketplace;
- Environmental policies and regulations stimulating the need for clean power technologies with improved efficiencies; and
- Fuel price projections which favor mid-term use of natural gas and long term use of coal gas.

By integrating these factors into IMHEX applications, technical and market developments will be responsive to future power generation requirements. Using functional building blocks of 250 to 500 cell stacks with one square meter active areas per cell, the IMHEX team envisions initial market entry power plants with capacities up to 2MW. With operational pressures of ≥ 3 atms and system components selected for optimal efficiency, these market entry power plants are projected to achieve approximately 50% (LHV) electrical efficiency and will provide the basis for expanded applications.

ABB Inc. views the initial market for IMHEX CFC power plants as a variety of dispersed site power applications. These include both cogeneration systems at large commercial buildings and industrial facilities plus electric utility applications at distribution substations. These markets will be based on natural gas fueled systems and may ultimately represent a substantial market opportunity. With the durability of these units demonstrated and an expanded manufacturing capability established around the turn of the century, the team envisions larger capacity natural gas units with higher electrical efficiencies for bigger dispersed site applications. Individual units with capacities of tens of megawatts will set the stage for a transition into coal-gas-fueled systems. Repowering applications and eventually greenfield central station plants represent exciting opportunities for CFC power plants with capacities up to several hundred megawatts.

Recognizing that this strategy is based primarily on expectations of technical progress and institutional perceptions, our utility sponsors and the IMHEX team established a group to represent the marketplace. ACCT, the Alliance to Commercialize Carbonate Technology, held its first organizational meeting in May 1991. ACCT's mission is to guide and support the commercialization of market responsive IMHEX CFC power plants through:

- Active participation in the IMHEX CFC Commercialization Program;
- Identification and representation of marketplace requirements;
- Integration of marketplace requirements into the technical developments; and
- Stimulation of market demand and commitments for initial market entry units.

ACCT's overall goal is to ensure the successful development and commercialization of IMHEX CFC products which are responsive to the specific opportunities and characteristics of members' business environments. Specific objectives of the organization are to exchange and assess technical information and market intelligence; to define market responsive products by late 1992 for subsequent initial commercialization and future product evolution; to support and participate in field verification activities, and collaborate with ABB to stimulate initial market demand and ensure sufficient initial product commitments.

There are several benefits to the participants in joining ACCT. The primary benefit is that the member companies may influence product design and operational characteristics. This will ensure that the product offered by the IMHEX team is responsive to their market requirements and issues. Secondly, participation in ACCT and sponsorship of program activities provides members with an opportunity to discuss with ABB the potential subdistribution, marketing, sales and service rights for IMHEX products in selected territories. This can provide new business opportunities and an industry leadership position for their company. Finally, ACCT members will be in a position to negotiate product delivery schedules that meet their market requirements.

CLOSING REMARKS

The IMHEX concept has progressed substantially from its origins in the laboratories of IGT in the 1980s. Today, a solid foundation has been established upon which the IMHEX team, users and sponsoring organizations can proceed to the realization of a commercially viable, market responsive IMHEX CFC power plant in the near future.

Construction of a full-area cell component manufacturing facility has been completed, which provides the basis for program activities and a foundation for transition into commercial scale production facilities. These facilities have also completed their initial verification runs with the successful fabrication of components, assembly and operation of a seventy cell tall stack which achieved 8 kW operation last month. The design for a full-area (one square meter) cell has been completed and components are presently being manufactured for the initial test of a 10 cell stack later this summer. Systems design and integration studies are progressing on schedule in preparation for a breadboard 20 kW system simulator test in 1992 and the 250 kW unit operation in 1993. An alliance of utilities and other users has been established to define user perspective for a market responsive product and to provide the foundation for initial market entry demand.

The corporate commitment of the IMHEX team members is high and their goal is to be the first and the best as the market for clean and efficient power generation equipment evolves during the 1990s.

Fuel Cell Commercialization Overview

William J. Lueckel, Jr.

International Fuel Cells Corporation
195 Governors Highway
South Windsor, CT 06074

International Fuel Cells (a subsidiary of United Technologies Corporation) is an industry pioneer whose product objectives are clean and efficient fuel cell power generators for the aerospace, defense and commercial utility markets. This paper summarizes recent activities and strategies aimed at commercializing two types of fuel cell plants--phosphoric acid and molten carbonate.

Phosphoric Acid Fuel Cell (PAFC) Power Plants

IFC is developing PAFC power plants for commercial applications ranging in size from 40 kilowatts to 11,000 kilowatts. These power plants are designed to operate cleanly and efficiently on hydrocarbon fuels and air. They are completely automatic and self-contained and require no operator control. An 11,000-kilowatt power plant is now operating at Goi, Japan as part of the Tokyo Electric Power Company (TEPCO) utility system. Four 200-kilowatt preprototype power plants have operated at user sites in Japan.

In late 1989 IFC established a subsidiary company called "ONSI Corporation." ONSI Corporation is dedicated to the business of manufacture and worldwide sales and service of fuel cell power plants for on-site energy service and supply. ONSI Corporation has recently completed the renovation and refitting of a 180,000-ft^2 production facility located in Middletown, Connecticut, dedicated to the manufacture and delivery of ONSI's PC25 power plant and capable of producing up to 200 units per year. The PC25 is a 200-kilowatt, phosphoric acid fuel cell power plant operating on natural gas. Orders have been received for 63 units for delivery in 1992 and early 1993. The customers for the PC25 include natural gas utilities throughout the European Continent, Japan, and the United States.

Molten Carbonate Fuel Cell (MCFC) Power Plants

Our strategy to commercialize MCFC plants parallels our strategy to commercialize PAFC plants, with modifications to account for differences in technology and potential customers. The key elements of the strategy are:

- A single MCFC Integrated Stack Unit (ISU) product to satisfy a wide range of potential market applications and operating with a wide range of fuels.
- An ISU with clean interfaces allowing "open power station architecture." (An engineer/constructor without special knowledge of MCFC technology can design a power station based on the IFC ISU).
- An ISU that can be manufactured, assembled and checked out at IFC in order to enhance product quality control and reliability, and to minimize expensive field labor.

- Controlled program risk. Utility demonstrations of MCFC power units only after an ISU unit of the same design has run successfully at IFC.
- Alliances with one or more foreign MCFC manufacturers/utilities in countries favorable to conducting high cost/high risk power plant demonstrations.
- The active participation of U.S. utilities, IPP's, and engineers/constructors in foreign demonstrations as the first step in establishing U.S. user acceptance of the IFC MCFC product.
- Outfit a production facility for MCFC ISU's only after the bill-of-material and/or manufacturing processes for MCFC cells, stack and accessories has been fully verified, and initial production orders are in hand.

Session 2

Solid Oxide Fuel Cells

High Temperature Solid Oxide Fuel Cell Power Generation System

CONTRACT INFORMATION

Cooperative Agreement No.	DE-FC21-91MC28055
Contractor	Westinghouse Electric Corporation Science and Technology Center 1310 Beulah Road Pittsburgh, PA 15235 (412) 256-2125
Contractor Project Manager	Emerson R. Ray
METC Project Manager	David A. Berry
Project Performance	April 1, 1991 to November 30, 1995

Schedule and Milestones

FY91 Program Schedule

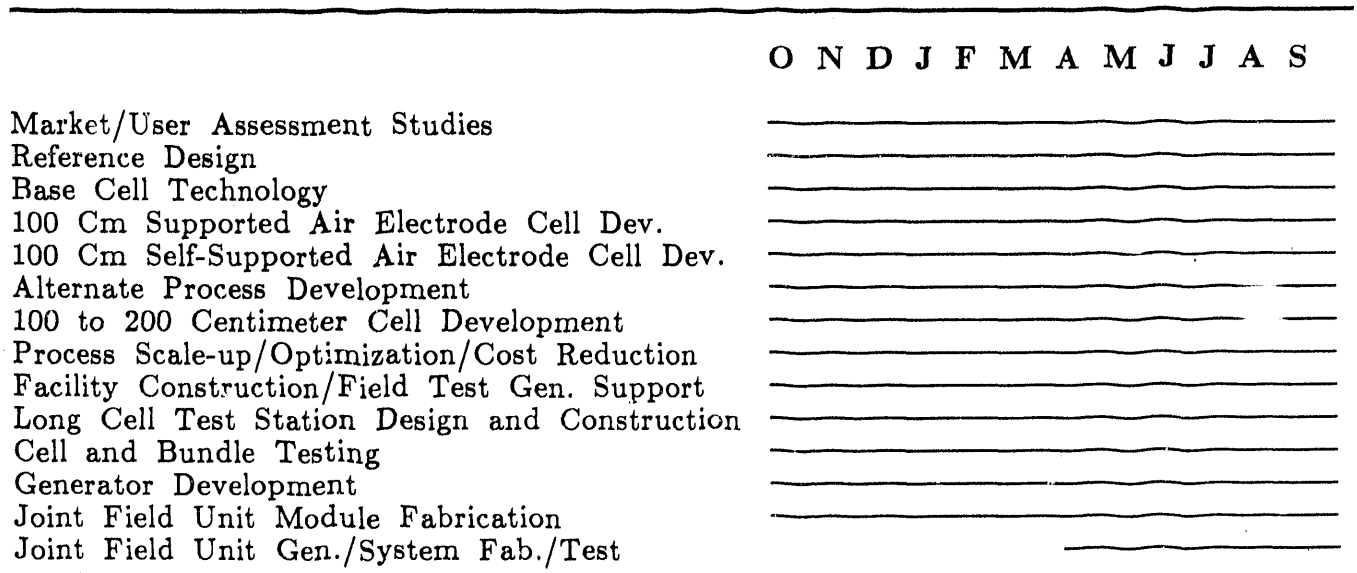

OBJECTIVES

This paper presents an overview of the Westinghouse tubular Solid Oxide Fuel Cell (SOFC) technology, the development status, results of the Multi-Kilowatt Generator (MKG) testing program, and a discussion of the present and planned Field Test Programs. All-electric and cogeneration applications for natural gas and coal derived fuel gas SOFC systems are also identified.

BACKGROUND INFORMATION

Advancements under this continuing program have resulted in the development of cells with greatly improved performance, reduced rate of degradation and increased life as well as the design, construction, and test of cell bundles and generator modules. Multiple single cell tests have now successfully exceeded 20,000 hours duration and generator test durations exceeding 6,800 hours have been achieved.

In 1980, a contract was initiated between Westinghouse and the U.S. Department of Energy and administered by the Morgantown Energy Technology Center. This cost share program centered on continuing to develop, improve, and scale-up the tubular SOFC technology for use with coal derived fuels. The most recent accomplishment of this program was the successful operation of a 20 kWe SOFC generator directly on pipeline natural gas.

In 1991, a Cooperative Agreement was initiated between Westinghouse and DOE-Morgantown Energy Technology Center, covering a project period through November 1995. Tubular SOFC technology is in the preliminary design stage of development and Westinghouse plans for field testing of multi-hundred kilowatt and multi-megawatt rated generators during the mid to latter-1990's. The ultimate objective of this program is to develop tubular SOFC technology to the point of acceptable risk for private sector commercialization.

PROJECT DESCRIPTION

Development of the tubular solid oxide fuel cell technology is being supported by the Westinghouse Electric Corporation, the United States Department of Energy (DOE), and various utility and industry sources. The Cooperative Agreement between Westinghouse and DOE is administered by the Morgantown Energy Technology Center (METC).

The potential to reform natural gas on the cell surface coupled with inherent modularity and simplicity of system configuration makes the tubular SOFC generator system a candidate for use in smaller on-site power plants as well as large scale electrical power plants. Because of the high operating temperature, there exists the concurrent potential for the cogeneration of usefully applied thermal energy in addition to electricity.

In the latter part of 1986, Westinghouse signed a contract with the Gas Research Institute to develop SOFC technology specifically for use with natural gas and directed toward applications in the commercial and industrial cogeneration market (20 kWe to 2 MWe). The primary objective of the GRI contract was the development of an SOFC generator that can consume natural gas directly - without the need for a separate fuel processing system. A 3 kW generator was designed, fabricated and successfully tested at Westinghouse as part of the GRI program. The GRI program was expanded in mid 1987 to include the study of applications and markets, and the development of conceptual designs and cost estimates for on-site cogeneration applications in the power range from 20 kWe to several megawatts. This effort was sponsored by a consortium of gas utilities in Japan (The Tokyo Gas Company, The Osaka Gas Company, and The Toho Gas Company) in cooperation with the Japanese New Energy and Industrial Development Organization (NEDO).

In 1989/90, the GRI program was further expanded to study alternate means of introducing fuel gas into the SOFC generator. Combined with the concept of

spent fuel recycling, Westinghouse is continuing to develop distributed reforming under sponsorship from DOE.

The continuing DOE program, along with several utility sponsored programs, are integral parts of the Westinghouse Commercialization Plan for the tubular SOFC technology.

The successful commercialization of the SOFC technology during the 1990's depends on the ability to produce cost competitive systems that can operate for five to ten years before replacement of the SOFC module(s). A thorough understanding of the phenomena that limits cell and generator lifetime is required in order that new processes and/or materials, as may be needed, can be developed. Furthermore, a detailed understanding of the manufacturing cost of cells and generators is also required in order that more cost effective processes and procedures can be implemented.

RESULTS

Our goal is to develop a cell that can operate for 50,000 to 100,000 hours with a voltage degradation rate less than 1% per 1000 hours. During 1990, an improved process cell (Figure 1) surpassed 20,000 hours of operation with a voltage degradation rate of 1.4% per 1000 hours. This cell was the longest running SOFC in the world - it was recently shut down for detailed examination (the cell could have operated longer) in order that improvements can be made in future cells. Eight additional improved process cells are presently under test for more than 17,000 hours with degradation rates ranging from 0.5% to 1.5% per 1000 hours.

Engineering studies indicate that the present cell cross-section (approximately 0.5 in. diameter) is satisfactory for commercial use but that cell length and power density need to be increased. Longer, higher power density cells will make an important contribution to practical and cost effective commercial systems. The majority of the cells utilized in the research phase of the program through 1986 were 30 cm. in length; 36 cm. long cells were demonstrated in The Tokyo Gas Company and The Osaka Gas Company 3 kW SOFC units operated in 1987/1988.

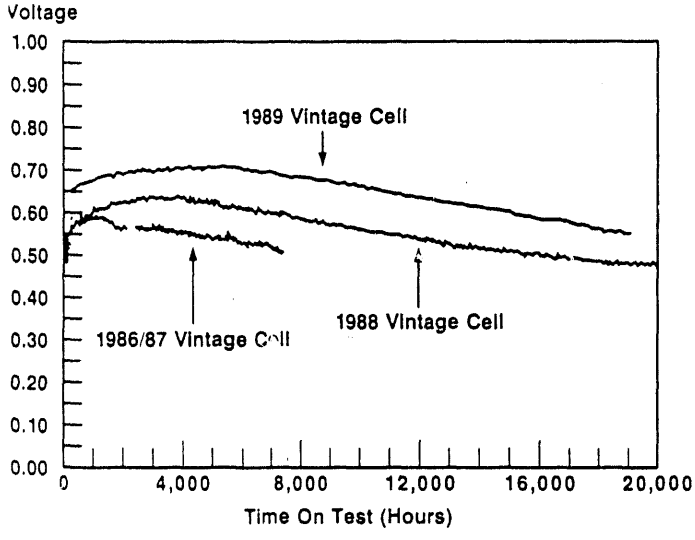

Figure 1. Cell Test Data Verifying Improved Cell Performance and Life

A major step in the commercialization program was construction of the 28,000 square foot Pre-Pilot Manufacturing Facility (PPMF) shown in Figure 2. This facility is located near Pittsburgh and is dedicated to the SOFC technology. The PPMF provides the opportunity to move the technology from a laboratory environment to a manufacturing environment, and enables the processes and quality control programs to be put in place that will be required to commercialize the technology during the 1990's. All equipment for the production and quality control of multi-hundred

kilowatt SOFC modules containing 1 meter long cells is in place.

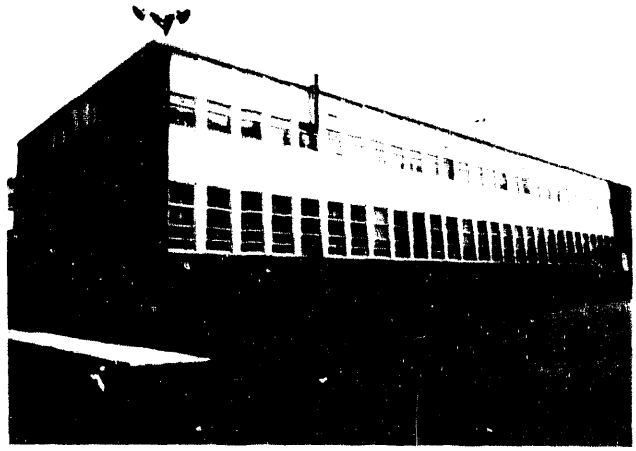

Figure 2. Photograph of the Westinghouse Pre-Pilot Manufacturing Facility

Bundle Test Four (BT-4), the first SOFC test article fabricated at the PPMF, consists of two bundles of eighteen 50 cm long cells. This test article was fabricated during 1989 and was designed to demonstrate that the transfer of technology from the laboratory to PPMF had been successfully accomplished. BT-4 has completed over 6,840 h of stable operation including eight planned thermal cycles (from room temperature to 1000°C and return to room temperature). The successful thermal cycling tests indicate that the SOFC technology has the potential for numerous start-ups and shutdowns similar to more conventional power generation equipment.

An air electrode supported cell (high power density) of 77 cm active length has accumulated more than 4000 h of operation at 0.647 V and 450 mA/cm^2 with no signs of voltage degradation. This cell has demonstrated a peak power (watts/cm) which exceeds cells made with porous support tubes by approximately 50%. For a fixed generator output, one-third of the cells in the generator could be eliminated by using air electrode supported cells.

Cells of 1 m length will be investigated at the PPMF during 1991. Our engineering studies indicate that this cell length can satisfy the commercial cogeneration market requirements of the 1990's and beyond. Future manufacturing programs will address still longer cells, which will further improve the economics for large central station electric utility power plants. The design of equipment to produce 2 m long cells was initiated during 1990 and is continuing. In addition, two test stands were also fabricated during 1990 which have the initial capability to test 1 m long cells and with modification, the capability to test cells up to 2 m long.

A major milestone of the SOFC program was the fabrication of the multi-kilowatt generator (MKG) (Figure 3). The MKG, rated at 20 kW, contains five hundred and seventy-six 50 cm long cells. The MKG was successfully started in November and has operated more than 1700 h on pipeline natural gas. The design, fabrication, and testing of the MKG was a primary objective of the past phase of the development contract with DOE.

The ability of the SOFC generator to operate on pipeline natural gas was demonstrated in the 1988/1989 time frame with single cell testing, bundle testing, and testing of a 3 kW SOFC generator as part of a contract funded by the Gas Research Institute (GRI). The 3 kW SOFC generator was operated for more than 5000 hours on pipeline natural gas. This development is being continued with the initiation of the design of the 100 kW SOFC generator for DOE. This generator will ultimately be part of a 100 kW

SOFC system planned for operation at a customer's site.

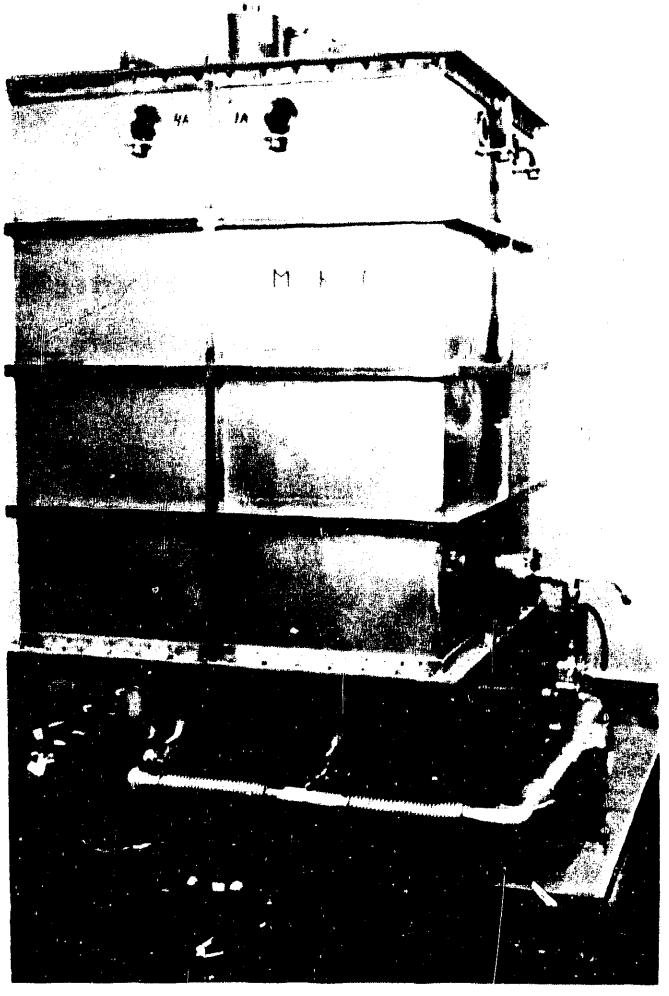

Figure 3. 20 kW SOFC Module

Twenty-five kW SOFC systems (Figure 4) are currently being fabricated at the PPMF. The first unit, which will produce only electric power, will be delivered in 1991 to The UTILITIES, a consortium of The Kansai Electric Power Company, The Tokyo Gas Company, and The Osaka Gas Company. The second unit, a cogeneration system producing both electric power and intermediate pressure steam, will be delivered to the Joint Gas Utilities, a consortium of The Tokyo Gas Company and The Osaka Gas Company. These units represent another order of magnitude scale-up in the SOFC technology committed to the field and make use of the lessons learned in designing, manufacturing, and operating the MKG generator (20 kW) at Westinghouse in Pittsburgh.

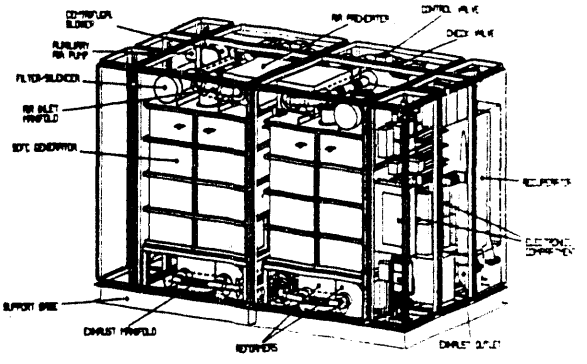

Figure 4. 25 kWe SOFC Field Unit

SUMMARY

A summary of significant developments and accomplishments which have recently occurred throughout the tubular SOFC program include:

- Demonstration that thousands of tubular solid oxide fuel cells can be fabricated with consistent and reproducible performance.
- Continuous operation of a 3 kWe tubular SOFC system for over six months at a customer's test site.
- Demonstration of stable performance and lifetime in excess of 5,300 hours for a 3 kWe generator module, operating directly on non-humidified desulfurized natural gas.
- Demonstration of stable performance and life times in excess of 20,000 hours in multiple single cell tests.

- Design, construction and operation of a dedicated cell, module and generator Pre-Pilot Manufacturing Facility (PPMF).

- Successful 6,840 hour bundle tests of 50 cm cells produced at the PPMF.

- Significant improvements in cell performance and life and marked reduction in cell degradation.

- Design, construction and successful operation of a 20 kWe tubular solid oxide fuel cell generator module.

- Development of a conceptual design for a 250 MWe tubular SOFC power plant fueled with coal-derived fuel gas.

Table 1 below summarizes the recent major accomplishments of the past and the current commitments.

FUTURE WORK

The existing Cooperative Agreement between Westinghouse and the Department of Energy was initiated in April, 1991 and will continue through November 1995. This five year program includes considerable financial contributions from Westinghouse, from domestic and foreign utilities, and from other agencies, in addition to the U.S. Department of Energy. Under this program Westinghouse will continue development of the tubular solid oxide fuel cell technology and generator systems. Field testing of multi-hundred kilowatt and multi-megawatt rated generators is planned during the mid to latter-1990's. The ultimate objective of this program is to develop tubular SOFC technology to the point of acceptable risk for private sector commercialization.

Table 1. Summary of Recent Westinghouse Program Accomplishments and Commitments

Event	Achieved	Committed
Cell-33 Watt, 36 cm Length, (20,000 Hours continuous electrical testing)	1990	
36 Cell, 50 cm Length Bundle Test, PPMF Produced Cells (6,840 Hrs.)	1990	
Additional single cell tests reaching 20,000 Hours continuous electrical testing	1991	
SYSTEM EXPERIMENTAL UNITS:		
TVA 400 Watt (1,760 Hrs.)	1986-7	
Osaka Gas 3 kWe (3,000 Hrs., Training Generator - >2,600 hrs.	1987-8	
Tokyo Gas 3 kWe (4,900 Hrs.)	1987-8	
36 Cell Bundle Test, Natural Gas Fuel (1,800 Hrs.)	1988	
Pre-Pilot Manufacturing Facility Construction	1988	
Pre-Pilot Manufacturing Facility Operation	1989	
GRI Natural Gas Fueled 3 kWe Generator (5,500 Hrs.)	1989	
Multi-kW Generator (DOE 20 kWe)	1990-1	
The UTILITIES (The Kansai Electric Power Company, The Tokyo Gas Company, and The Osaka Gas Company) 25 kWe Field Unit		1991
The Joint Gas Utilities (The Tokyo Gas Company and The Osaka Gas Company) Field Unit		1992

Alternative Materials for Solid Oxide Fuel Cells: Chromite Interconnections

CONTRACT INFORMATION

Contract Number (FTPA)	13822
Contractor	Pacific Northwest Laboratory Operated for the U.S. Department of Energy by Battelle Memorial Institute under contract DE-AC06-76RLO 1830 P. O. Box 999 Richland, Washington 99352 (509) 375-2579
Contractor Project Manager	J. Lambert Bates
Principal Investigators	Larry A. Chick J. Lambert Bates
METC Project Manager	David Berry/William Huber
Period of Performance	April 1, 1990 to April 1, 1991

Schedule and Milestones

FY-91 Program Schedule

	S O N D J F M A M J J A S
Synthesis and Processing of Air-Sinterable Chromite Powders as Interconnections	———————
Thermal Properties of Chromites	———————
Electrical Properties of Chromites	———————
Electrochemical Behavior of Alternative Materials	———————

OBJECTIVES

The research objectives are to:

- Develop a broader selection of alternative solid oxide fuel cell current interconnections and air electrode materials with improved electrical, thermal and electrochemical properties leading to enhanced and long-term performance.

- Develop new synthesis and processing methods for both state-of-the-art and new interconnection and air electrode materials that can be reproducibly and economically consolidated in air with the electrolyte and/or electrodes into a SOFC below 1823 K with a minimum number of fabrication steps.

BACKGROUND INFORMATION

Solid oxide fuel cells (SOFCs) are emerging as an attractive, clean, and efficient technology for the direct conversion of hydrogen and gaseous fossil fuels to electrical energy. The major challenge in producing SOFCs is to develop materials with acceptable electrical, thermal and electrochemical properties that can be synthesized, processed and fabricated as high-performance fuel cell at low cost (Bates 1989). Although the same materials may be utilized for all three major design concepts (tubular, monolithic, and planar), each generally can be fabricated by different processing methods.

The use of these different chromite, manganite, nickel-zirconia and zirconia materials as interconnections, electrodes and electrolyte combinations can result in several fabrication and performance-related limitations. The most critical problems are the thermal expansion compatibility between these materials and the complex fuel cell fabrication and process steps required. Critical thermal, electrochemical and electrical properties may be compromised in order to achieve compatibility between materials, cell fabrication and fuel cell performance.

An important key to developing low-cost, high-performance SOFCs is the ability to sinter the interconnection in air at temperatures between 1723 and 1823 K. The lanthanum manganites now used as the air electrode are unstable at low oxygen partial pressures. Reduction results in structural, property and composition changes that cannot be reversed by reoxidation. Therefore, the $La(Sr)MnO_3$ must be fabricated in high oxygen partial pressures. In contrast, the $La(Mg)CrO_3$ or $La(Sr)CrO_3$ used as the interconnection sinters best to high density under highly reducing conditions. However, because the chromites are stable in the oxidizing and reducing conditions required for SOFC interconnection use, significant economic benefits would result if the chromites interconnects could be simultaneously sintered with the electrodes and/or electrolyte in air below 1823 K into the SOFC.

The availability of high-quality, homogeneous, ultra-fine ceramic powders

using the Glycine-Nitrate Process[a] (GNP) developed at Pacific Northwest Laboratory [Chick et al. (1989) and Chick et al. (1990)] has opened avenues for studying the factors influencing the air sintering of the chromite, the air-sintering mechanism(s), and the role(s) of these factors on the chromite properties [Bates, Chick and Weber (1989), and Bates and Chick (1990)]. By understanding the air sintering of chromites, compositions, materials processing and synthesis might be altered to increase sintered densities, lower sintering temperatures, reduce open porosity, and improve electrical, thermal and structural properties of materials useful for all SOFC concepts.

PROJECT DESCRIPTION

This research and development is directed to modification of state-of-the-art and to development of analogous and alterative materials as SOFC electrodes and interconnections and consists of three tasks:

- **Electrical and Thermal Properties** of state-of-the-art and alternative interconnection materials as functions of composition, structure, synthesis and processing methods.
- **Materials Synthesis and Processing Methods** to produce state-of-the-art and alternative interconnection chromite and manganite materials that can be sintered in air below 1550°C without the use of additives.
- **Electrochemical Behavior** of materials interfaces to understand the kinetics and electro-chemical and chemical processes.

This report discusses R&D directed toward understanding the factors that affect air sinterability, sintering mechanisms and the thermal expansion of $La_{1-x}Sr_xCrO_3$ and $Y_{1-x}Ca_xCrO_3$.

RESULTS

Air Sintering of Chromites

Important materials characteristics have been identified that influence the air sintering of chromites [Bates, Chick and Weber (1989); Bates and Chick (1990); and Chick et al. (1989)]. Factors include powder morphology, particle composition, impurities, second phases and cation ratio. The sintering environments found to influence chromite sintering in air include temperature, vaporization and time. Many of these factors are synergistic. The roles of alkaline-earth substitution, cation ratio and air flow on air-sintering of $La_{1-x}Sr_xCrO_3$ and $Y_{1-x}Ca_xCrO_3$ are summarized in this paper. Details are reported elsewhere [Chick, Bates and Maupin (1991)].

Experimental. The $La_{1-x}Sr_xCrO_3$ and $Y_{1-x}Ca_xCrO_3$ powders were synthesized using the GNP. These powders were homogeneous, softly agglomerated, single-phase, crystalline perovskite structures with crystallite sizes between 20 and 50 nm. The as-synthesized GNP chromite powders were uniaxially pressed at 35 MPa and isostatically pressed at 140 MPa. The sample discs were placed on end on chromite setting-sand with sides exposed to the atmosphere of the furnace. The

[a] The Glycine-Nitrate Process was developed at Pacific Northwest Laboratory. Applications for U.S. and foreign patents have been filed for the United States Government and Battelle Memorial Institute.

temperatures were increased at 300°C/h to 1550°C and held for 8 hours and cooled at 300°C/h. Sintering was conducted in either stagnant air or in 0.25 l/s flowing air. Densities were determined by immersion and compared with the theoretical densities determined by X-ray diffraction. These chromite powders can be sintered in air at 1550°C to greater than 96% TD.

Alkaline-Earth Substitution. The air sinterability of $La_{1-x}Sr_xCrO_3$ increases with increasing Sr substitution, reaching a maximum in density at $La_{0.76}Sr_{0.24}CrO_3$ with airflow and at $La_{0.7}Sr_{0.3}CrO_3$ without airflow, as shown in Figure 1. Similar trends are observed for $Y_{1-x}Ca_xCrO_3$ with highest sintered densities at x = 0.2 and x = 0.3 with and without air flow, respectively (Figure 1). Note that the sintered densities for both chromite systems are the same in both stagnant and flowing air at x = 0.3. For $Y_{1-x}Ca_xCrO_3$ with

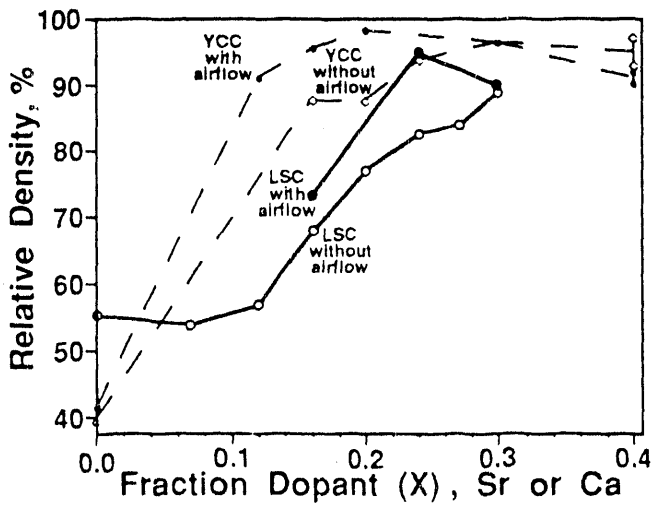

Figure 1. Sintered density as function of Sr content for $La_{1-x}Sr_xCrO_3$.

x > 0.3, the achieved sintered densities without air flow are higher than those in air flow.

Densification During Air Sintering. The shrinkage during air sintering was measured using a push-rod dilatometer from room temperature to 1550°C with heating rate of 3°C/min. The shrinkage rate for $LaCrO_3$ increases smoothly, suggesting a simple solid state diffusion process. This is typical for most ceramics. However, the shrinkage of $La_{1-x}Sr_xCrO_3$ with $x \geq 0.12$ shows a number of pronounced inflections during heating as shown in Figure 2. Sintering is enhanced at low temperatures near 1100°C. Two higher temperature inflections occur but the temperature of the inflections varies with composition. The inflection near 1250°C is attributed to the presence and melting of $SrCrO_4$ or its derivatives. This phase and its disappearance during sintering has been confirmed by both room-temperature and high-temperature x-ray diffraction. The causes for the inflections near 1100 and 1400°C for x=0.24 and 1550°C for x=0.27 are presently unknown.

The shrinkage of $Y_{1-x}Ca_xCrO_3$ during densification increases very rapidly with increasing Ca content at temperatures between 1000 and 1100°C, with shrinkage increasing proportionally to the Ca concentration as shown in Figure 3. This rapid densification is attributed to liquid-phase sintering. During the combustion synthesis of $Y_{1-x}Ca_xCrO_3$ in the GNP, temperatures near 1450°C are attained. At these temperatures, the Ca is completely substituted into the yttrium chromite, perovskite lattice. However, during heating at lower temperatures between 900 and 1100°C, the Ca solubility decreases and is

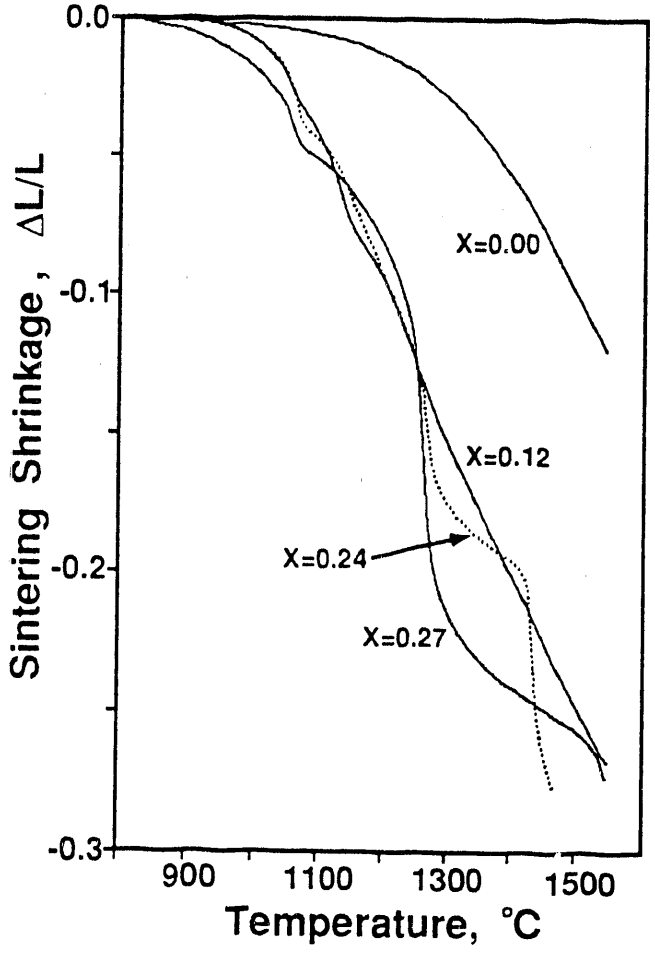

Figure 2. Shrinkage of $La_{1-x}Sr_xCrO_3$ as a function of temperature during sintering in air.

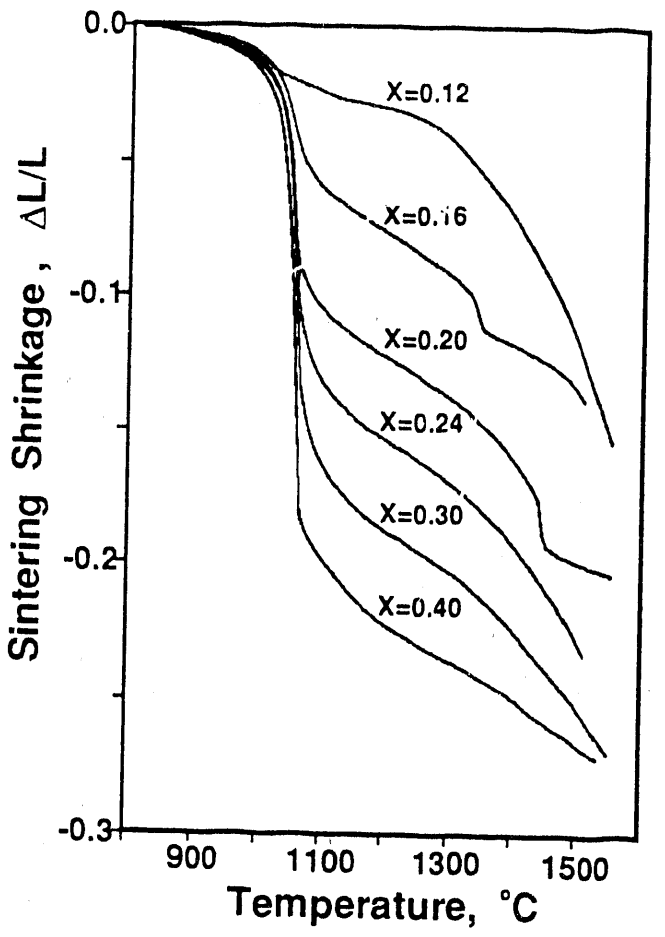

Figure 3. Shrinkage of $Y_{1-x}Ca_xCrO_3$ as function of temperature during sintering in air.

exsoluted as $CaCrO_4$. This chromate phase melts near 1020°C and acts as a transient-liquid sintering aid. As the sintering temperatures increase, the Ca is again fully substituted into the perovskite phase. In addition, a pair of higher-temperature inflections occur for Ca = 0.16 and Ca = 0.20 which also appear to influence sintering. Similar solubility and exolution occurs for $La_{1-x}Sr_xCrO_3$, with the $SrCrO_4$ melting near 1250°C.

Cation Ratio. Very large differences in sintering density can result from only small changes in the cation ratios, (La + Sr)/Cr and (Y + Ca)/Cr. For this study, Sr and Ca are assumed to substitute only on the "A" site of the ABO_3 lattice, thus cation ratios less and greater than unity are assumed to be Cr rich and Cr depleted, respectively. The effects of Cr enrichment and Cr depletion for $[La_{0.76}Sr_{0.24}]_{1-y}Cr_yO_3$ and $[Y_{0.6}Ca_{0.4}]_{1-y}Cr_yO_3$ in both stagnant and flowing air are shown in Figure 4. In stagnant air, the $[La_{0.76}Sr_{0.24}]_{1-y}Cr_yO_3$ has maxima in sintered densities when the (La + Sr)/Cr is 0.98 and 1.04. A minimum occurs near 1.0. Significantly higher density occurs when chromite is Cr depleted.

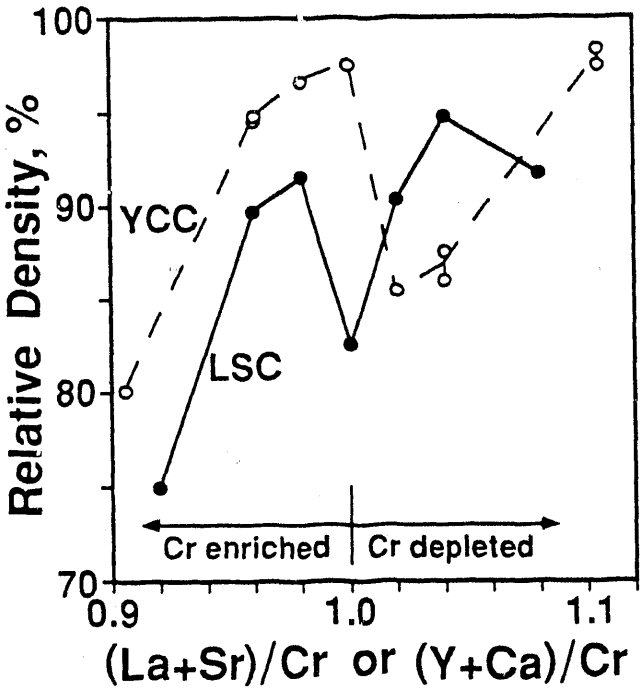

Figure 4. Sintered densities of $[La_{0.76}Sr_{0.24}]_{1-y}Cr_yO_3$ and $[Y_{0.6}Ca_{0.4}]_{1-y}Cr_yO_3$ as a function of chromium enrichment and depletion, stagnant air.

Similar variations in sintered density are observed for $[Y_{0.6}Ca_{0.4}]_{1-y}Cr_yO_3$. Maximum sintered densities occur when (Y+Ca)/Cr is near 1.0 and 1.1 in stagnant air.

The sintered density is very sensitive to flowing air and near the minima at 1.0 and 1.02 for $[La_{0.76}Sr_{0.24}]_{1-y}Cr_yO_3$ and at 1.02 for $[Y_{0.6}Ca_{0.4}]_{1-y}Cr_yO_3$. In flowing air, the minima has been suppressed or is not present; the highest sintered densities are near 1.04 and 1.1 for $[La_{0.76}Sr_{0.24}]_{1-y}Cr_yO_3$ and $[Y_{0.6}Ca_{0.4}]_{1-y}Cr_yO_3$, respectively. These effects remain under investigation. Chromium enrichment for both chromites significantly reduces the air-sintered densities. In contrast, Cr depletion enhances the air-sintered densities.

Significant differences are also observed in the microstructure of the sintered chromites as the (La+Sr)/Cr and (Y+Ca)/Cr are varied. The resulting structures often contain minor second phases not associated with impurities. Chromium enrichment or depletion strongly influence sintered microstructure and appears related to vapor (weight) loss. For example, with small depletions of Cr in $[Y_{0.6}Ca_{0.4}]_{1-y}Cr_yO_3$ the sintered body has a fully dense surface and a low-density, inhomogeneous interior that is slightly depleted in Cr. In contrast, the $[Y_{0.6}Ca_{0.4}]_{1-y}Cr_yO_3$ with high depletion of Cr is near theoretical density, but the interior contains a Y_2O_3 second phase.

The microstructure of the chromites with Cr depletion contain the oxide phases of La_2O_3 and Y_2O_3. The presence of La_2O_3 is deleterious, since it easily hydrates in moist air at room temperature, thus limiting use in SOFCs to compositions rich in Cr. Y_2O_3 is stable in water and compositions depleted in Cr can be used as SOFC interconnections. These are also the compositions with the best sinterability.

The sintered density is very highly sensitive to small changes in composition and requires good control of the starting chromite powder compositions. This is essential for controlling density and microstructure of the $La_{1-x}Sr_xCrO_3$ and the $Y_{1-x}Ca_xCrO_3$. For the GNP, stock solutions of metal nitrates are used to prepare the starting glycine-nitrate solutions. The nitrate compositions are determined accurately by an EDTA titration analysis

with ± 0.3% relative or better [Chick et al. 1990].

Weight Loss and Volatility. The air sinterability of chromites appears dependent upon volatilization and vapor transport, as indicated in the higher sintered densities achieved in flowing air. The weight loss, assumed to result from vaporization during sintering, is highly dependent and proportional to Cr enrichment in $La_{1-x}Sr_xCrO_3$, but the dependence is weak in $Y_{1-x}Ca_xCrO_3$. The Cr enriched chromites are difficult to sinter to near full density in air, however. This is attributed to vapor-phase transport resulting from the volatility of chromium oxides, such as CrO_3 as reported by Anderson (1978) and Meadowcroft and Wimmmer (1979). Vapor phase transport is consistent with the decreases in density with increased Cr.

For both $La_{1-x}Sr_xCrO_3$ and $Y_{1-x}Ca_xCrO_3$ vapor-phase transport is complicated by the formation of second phases and liquid-phase sintering. Potential deleterious effects of Cr vapor loss may be overshadowed by the formation of liquid phases at low temperatures. For example, enhanced surface sintering resulting from the lower-temperature, liquid-phase sintering in $Y_{1-x}Ca_xCrO_3$ may inhibit the transport of O_2 to the liquid-phase-forming $CaCrO_4$ which requires excess oxygen. Evidence of such effects are seen in sintered chromite microstructure.

Summary: Air Sintering Chromites

The air sintering characteristics of $La_{1-x}Sr_xCrO_3$ and $Y_{1-x}Ca_xCrO_3$ are summarized as follows:

- Sintered densities increase with increasing alkaline-earth substitution.
- Highest sintered densities are a function of cation ratio and generally increase with increase in (La+Sr)/Cr and (Y+Ca)/Cr with highest densities occurring with chromium depletion.
- Large differences in sintered density result from small differences in cation ratio, particularly in chromium-rich compositions.
- Sintered densities are higher in flowing air than in stagnant air when Cr rich and appears related to vaporization loss during sintering, with effects greater for $La_{1-x}Sr_xCrO_3$ than for $Y_{1-x}Ca_xCrO_3$.
- The microstructure of sintered chromites is a function of composition, sintering temperature, cation ratio and vaporization (weight loss).
- Low-temperature sintering of chromites, particularly $Y_{1-x}Ca_xCrO_3$, results from liquid-phase sintering in which the chromate acts as a transient liquid, sintering aid.
- The roles of vapor-, liquid- and solid-phase transport in the air sintering and densification of $La_{1-x}Sr_xCrO_3$ and $Y_{1-x}Ca_xCrO_3$ are not fully understood, but appear to be synergistic. More than one mechanism may be operative.

Thermal Expansion

The thermal expansion of chromites is critical for SOFC fabrication and stability during operation. The thermal expansion of

the SOFC interconnection should match that of the Y_2O_3 stabilized ZrO_2 (YSZ) electrolyte and other SOFC material components over the temperature range of fabrication and application. The YSZ thermal expansion is also a reference for comparing electrode and chromite interconnection materials and should be accurately determined. Thermal expansion is often reported as the thermal expansion coefficient, which is determined from the thermal expansion ($\Delta L/L$) between two temperatures. Reported values vary widely generally between 10 and 11.8 x 10^{-6}. The variations probably occur because different temperature ranges were used to calculate the average thermal expansion coefficient. The temperature range must be defined since the thermal expansion generally does not vary linearly with temperature. The best data for matching thermal expansions are obtained by comparing both the magnitude and shape of the $\Delta L/L$ versus temperature curves.

Experimental. The thermal expansion of air-sintered $La_{1-x}Sr_xCrO_3$ and $Y_{1-x}Ca_xCrO_3$ were measured in air using a push-rod dilatometer from near-room temperature up to 1550°C. The heating and cooling rates were 100°C/h. For convenience in comparing SOFC electrode and interconnection materials, only data to 1150°C are reported.

Y_2O_3 Stabilized ZrO_2. The thermal expansion of single crystal and polycrystalline Y_2O_3 stabilized ZrO_2 was determined. The polycrystalline oxide was an 8% Y_2O_3 stabilized ZrO_2 sintered from a TOSOH powder that is used by most U.S. investigators as the SOFC electrolyte. The shapes of the $\Delta L/L$ curves are similar, with very small decreases in thermal expansion as the amount of Y_2O_3 is increased from 8 to 24 mole%. The thermal expansion of the sintered polycrystalline ZrO_2 containing 8% Y_2O_3 is used for comparing the thermal expansion of the chromite interconnection materials. The thermal expansion coefficient between 25 and 1550°C increases with increasing temperature.

$La_{1-x}Sr_xCrO_3$ and $Y_{1-x}Ca_xCrO_3$. The thermal expansion of the air-sintered $La_{1-x}Sr_xCrO_3$ and $Y_{1-x}Ca_xCrO_3$ with cation A/B ratios of unity are summarized in Figures 5 and 6. The thermal expansion of $La_{1-x}Sr_xCrO_3$ and $Y_{1-x}Ca_xCrO_3$ increase with increasing Sr ($0.00 \leq x \geq 0.0.24$) or Ca ($0.00 \leq x \geq 0.04$) substitution. The $\Delta L/L$ versus temperature curve for $Y_{0.6}Ca_{0.4}CrO_3$ is identical, within experimental error, to that for 8% Y_2O_3 stabilized ZrO_2. At the higher Ca content of x = 0.5, the thermal expansion decreases. This decrease maybe related to a phase separation that occurs at this composition, where two phases with nearly identical compositions are observed by microscopy.

The thermal expansion of $La_{1-x}Sr_xCrO_3$ with $0.1 \geq x \leq 0.4$ is similar to that for $Y_{1-x}Ca_xCrO_3$, increasing with increasing Sr substitution. When $La0.84Sr_{0.16}CrO_3$ and $La_{0.76}Sr_{0.24}CrO_3$ are compared with the 8% Y_2O_3 stabilized ZrO_2, the thermal expansion of the state-of-art $La_{0.84}Sr_{0.16}CrO_3$ is lower than that for the Y_2O_3 stabilized ZrO_2, especially at high temperatures. In contrast, the thermal expansion of $La_{0.76}Sr_{0.24}CrO_3$, like that of the $Y_{0.6}Ca_{0.4}CrO_3$, matches closely the thermal expansion of 8% Y_2O_3 stabilized ZrO_2. The $La_{0.76}Sr_{0.24}CrO_3$ also exhibits the best air-sintering characteristics.

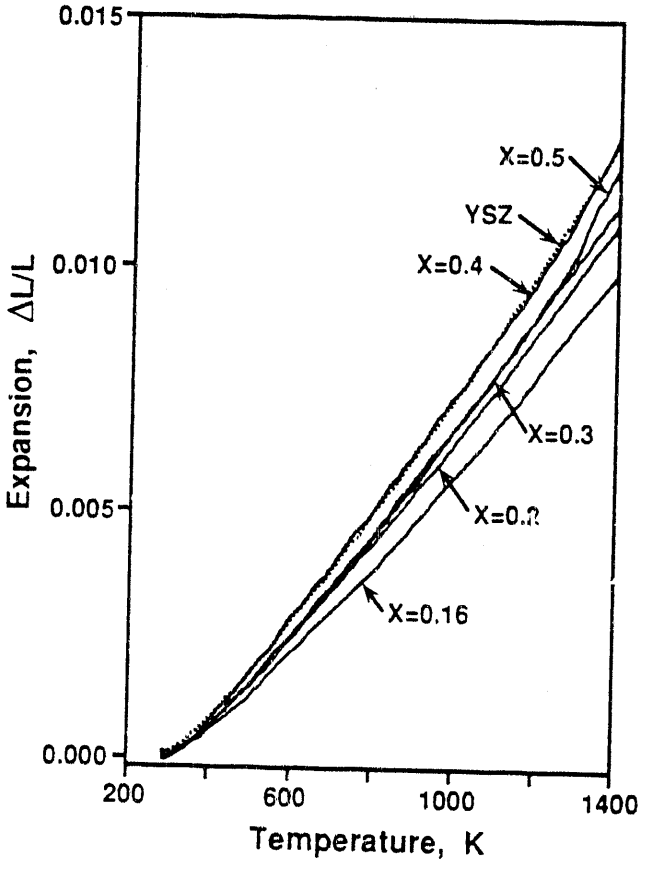

Figure 5. Thermal expansion of $Y_{1-x}Ca_xCrO_3$ as a function of Ca content compared with polycrystalline 8% Y_2O_3 stabilized ZrO_2.

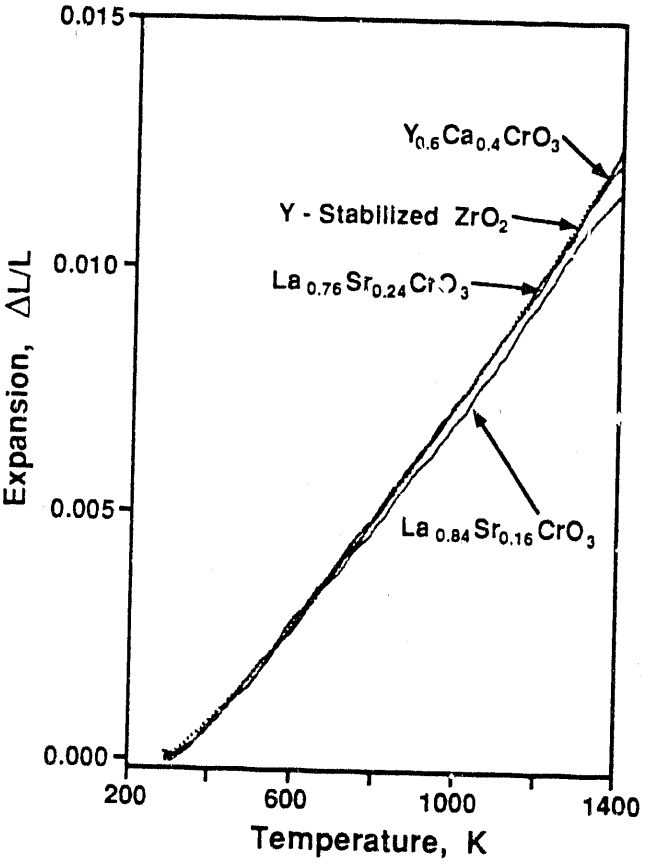

Figure 6. Thermal expansion of $Y_{0.6}Ca_{0.4x}CrO_3$, $La_{0.76}Sr_{0.24}CrO_3$ and $La_{0.84}Sr_{0.16}CrO_3$ compared with 8% Y_2O_3 stabilized ZrO_2.

CONCLUSIONS

The following conclusions are made for selecting compositions of $La_{1-x}Sr_xCrO_3$ and $Y_{1-x}Ca_xCrO_3$ as current interconnections for SOFCs. These preliminary conclusions are based upon current air-sintering, thermal expansion and electrical conductivity data. The potential reduction in thermal, structural, and chemical stabilities that might result from increased concentrations of alkaline-earth are not considered. The recommended compositions are:

$La_{0.76}Sr_{0.24}CrO_3$ with (La+Sr)/Cr of 0.98 in stagnant air; and $Y_{0.6}Ca_{0.4}CrO_3$ with (La+Ca)/Cr of 1.0 or 1.1 in stagnant air.

FUTURE WORK

Material Synthesis and Processing

The research to further understand roles of vapor loss, second phases and cation ratios on the air sinterability of $La_{1-x}Sr_xCrO_3$ and $Y_{1-x}Ca_xCrO_3$ will continue. The effects of these factors on the thermal, electrical and electrochemical properties will be studied in an effort to increase sintered density and reduce sintering temperatures.

Electrical and Thermal Properties

The effects of composition, synthesis and fabrication, and structure on the electrical transport and thermal expansion characteristics of the chromites will be determined.

Electrochemical Processes

The electrochemical interaction studies of these alternative $La_{1-x}Sr_xCrO_3$ materials and interfaces between the SOFC electrodes will be initiated.

REFERENCES

Anderson, H.U. 1978. "Fabrication and Property Control of $LaCrO_3$ Based Oxides". In **Processing of Crystalline Ceramics**. 1. ed. H. Palmour, R.F. Davis and T.M. Hare. Plenum Press, N.Y. 469-477.

Bates, J. Lambert. 1989. Solid Oxide Fuel Cells: A Materials Challenge. **In Energy Technology XVI: Energy Progress and Environmental Protection, Proceedings of Sixteenth Energy Technology Conference** February 28 - March 2, 1989, Washington DC., pp 205-219. Government Institutes, Inc., Rockville, Md.

Bates, J.L., L.A. Chick and W.J. Weber. 1989. "Alternative Materials for Solid Oxide Fuel Cells". In **Proceedings of the First Annual Fuel Cells Contractors Review Meeting**. ed. W.J. Huber, p. 54 to 63. DOE/METC-89/6105. NTIS/DE89011600.

Bates, J.L. and L.A. Chick. 1990. In **Proceedings of the Second Annual Fuel Cells Contractors Review Meeting**. ed. W.J. Huber, p. 159 to 170. DOE/METC-90/6112. NTIS/DE90000490.

Chick, L.A., J.L. Bates, L.R. Pederson and H.E. Kissinger. 1989. "Synthesis of Air-Sinterable Lanthanum Chromite Powders". In **Proc. First International Symposium: Solid Oxide Fuel Cells**, Subhash C. Singhal, Ed. p. 170-187. Electrochemical Society, Inc. Pennington, NJ.

Chick, L.A., J.L. Bates and G.D. Maupin. 1991. "Air-Sintering Mechanisms of Chromites". **Proc. Second International Symposium on Solid Oxide Fuel Cells**, Pieter Zegers and Subhash Singhal Eds. Athens Greece, July 2-5, 1991.

Chick, L.A., L.R. Pederson, G.D. Maupin, J.L. Bates, L.E. Thomas and G. J. Exarhos. 1990. "Glycine-Nitrate Combustion Synthesis of Oxide Ceramic Powders". **Materials Letters. 10** [1,2]. pp. 6-12.

Meadowcroft, D.B. and J.M. Wimmer. 1979. "Oxidation and Vaporization Processes in Lanthanum Chromite". **Bull. J. Am. Cer. Soc. 58** [6]. 610-615.

Contaminant Effects in Solid Oxide Fuel Cells

CONTRACT INFORMATION

Contract Number	DE-AC21-89MC26355
Contractor	Westinghouse Science and Technology Center 1310 Beulah Road Pittsburgh, PA 15235 (412) 256-2125
Contractor Project Manager	Emerson R. Ray
Principal Investigators	Nicholas J. Maskalick Charles J. Spengler
METC Project Manager	David A. Berry
Period of Performance	October, 1989 to February, 1992

Schedule and Milestones

Program Schedule

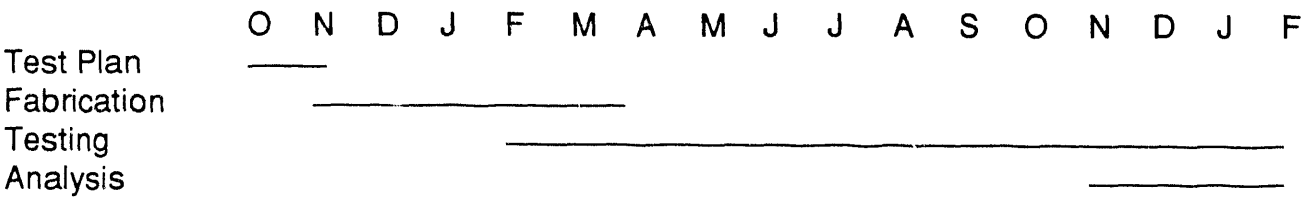

OBJECTIVES

The objectives of this study were to learn whether the fuel-side materials of the SOFC, comprising Ni, stabilized ZrO_2 and Mg-doped $LaCrO_3$ would be affected by contact with the coal gas impurities NH_3, HCl and H_2S, and to describe any interaction in terms of SOFC performance change and/or direct structural or chemical changes.

BACKGROUND INFORMATION

The subject tests provide a basis for estimating short-term effects in the presence of the specific coal gas impurities NH_3, HCl and H_2S. This theoretical/experimental study relates to the DOE mission as follows:

- It augments SOFC technology development work, providing information

and guidance toward materials and designs that adapt best to coal gas impurities.
It contributes to the development of an efficient and environmentally acceptable SOFC power generation system by establishing coal gas clean up criteria for system engineering.

PROJECT DESCRIPTION

The experimental apparatus is shown schematically in Figure 1. It comprises an alumina muffle tube which contains the test cell in such a way that fuel gas flows upward over the cell exterior while air is admitted to the cell interior. The air is pre-heated within an alumina air feed tube; initially contacts the cell air electrode at the closed, or lower end; then reverses direction and flows toward the open end, where partially spent air and fuel mix and combust. The fuel cell produces both electrical and thermal energy.

The apparatus employs nickel bus bars for current leads to a controlled-resistance external load. Platinum leads measure terminal voltage (V_T) directly at the cell anode and cathode. The muffle tube is contained within a 3-zone furnace. Cell temperatures are measured within the air chamber with a Pt, Pt/10% Rh thermocouple. Control over the fuel/H_2O ratio fed to the cell is accomplished by bubbling fuel through water which is thermostatically controlled at a temperature corresponding to the desired water partial pressure.

Fuel gases are obtained by blending CH_4, CO_2, CO, N_2, and H_2 to represent either of two types of gasified coal: air blown or oxygen-blown. In some cases, H_2 alone is used as a fuel in order to isolate cell electrochemical degradation due to contaminants versus slowing cell kinetics due to the inhibition of CH_4 reformation. Fuel is admitted to the cell anode at flow rates designed to keep fuel utilization at a constant value (85%) for different cell operating currents. Similarly, air flow varies with cell current to provide for constant air utilization (25%). The remainder of the fuel is combusted downstream of the cell. In these experiments, a constant cell current of 350 mA/cm^2 was maintained. Cell active areas were all nominally 188 cm^2.

The mass flow controllers employed to blend the fuel gas constituents, including each specific impurity, are Sierra type 830 or 840 or Tylan type 260 or 280. These controllers sense mass flow through a heated capillary tube by measuring the temperature change at each end of the tube with resistance thermometers. The temperature/resistance change is related to the molar specific heat and thermal conductivity of each gas. Mass flow control is achieved through a valve control circuit responding to output of the resistance thermometers.

Two types of coal derived-gas blends were chosen for these tests:

- air-blown, as exemplified by a composition from a KRW (Kellogg-Rust-Westinghouse) fluidized bed, specified at 1167°F.
- oxygen-blown, exemplified by a composition from a Texaco entrained bed, specified at 776°F.

Fuel Gas Species	Composition (mole %) Air-Blown	Oxygen-Blown
CH_4	1 5	0.3
CO_2	10.7	14.2
CO	14.4	36.7
H_2	17.7	33.6
N_2	47.1	2.1
H_2O	8.6	13.1

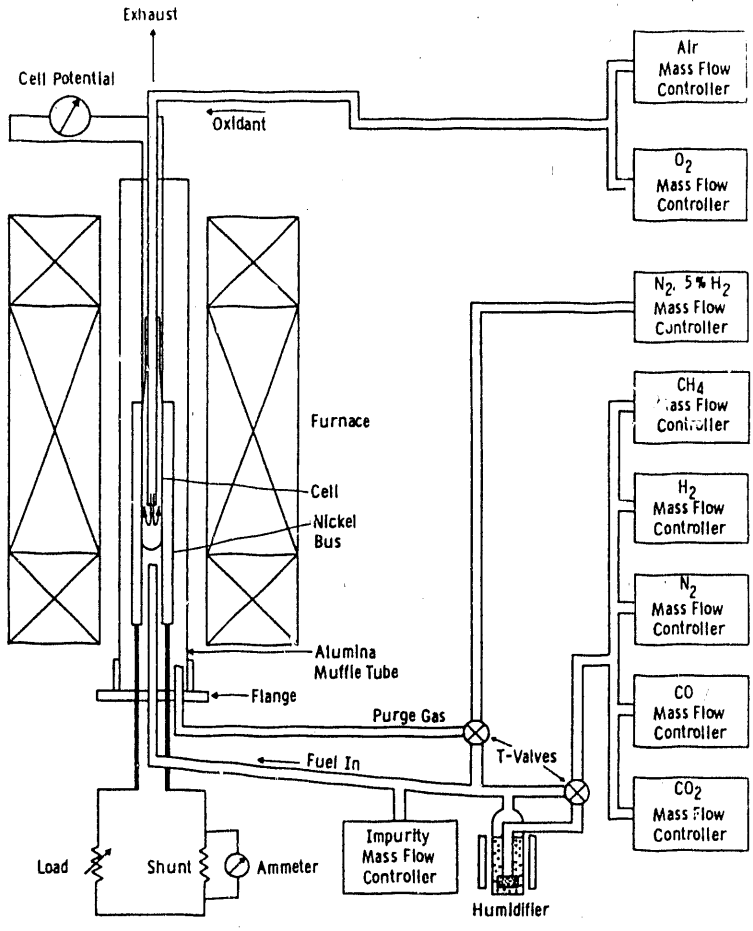

Figure 1. Fuel cell test stand schematic.

The fuel impurities NH_3, HCl and H_2S are introduced as dilute blends of each impurity in nitrogen. Each tank of gas blend is analyzed after preparation to verify impurity concentration.

Experimental values of total cell resistance, R, are obtained in most cases by using a high frequency ac method which minimizes disturbance of the current distribution. This method, CRM (continuous resistance measurement), and an alternate method employing oscilloscope tracking of rapid voltage change upon current interruption are in reasonable agreement with calculations based upon the dimensions of the cell, the known resistivity of the electrolyte, and estimates of electrode resistivities.

As a first approximation, local values of E and I are assumed to be unaffected by the contaminant; the change of IR and η (polarization) comprises the total observed drop in terminal voltage, ΔV_T. The polarization effect due to contamination is then obtained by:

$$\Delta\eta = - \Delta V_T - \Delta IR \qquad (1)$$

After operation in contaminated fuels, cells were examined by standard metallographic analysis using light optical microscopy, scanning electron microscopy.

Coupled with cell electrical testing results, evidence collected using these techniques was used to characterize the interactions of fuel impurities with cell components.

RESULTS

NH_3 Impurity in Coal Gas

High temperature cell testing indicates that NH_3 in synthetic coal gas has no observable effect on SOFC performance at 1000°C up to 5000 ppm NH_3, a typical concentration found in gasified coal. Figure 2 illustrates that the major observable effect of NH_3 is to add to the fuel value, increasing the terminal voltage (V_T) of the cell under load at 350 mA/cm^2 by several millivolts. In Figure 2 examples of this effect are shown for an air-blown coal gas composition at 950°C. A direct analysis was conducted of NH_3 (initially at 5000 ppm) in a sample from the fuel stream adjacent to the cell for 880°C O_2-blown coal gas. The results produced are listed in Table 1.

Table 1. NH_3 Concentration from Optical Absorbance at 40 nm

Sample Site	Gas Temp. Prior to Quench	Cell Mode	ppm of NH_3
Inlet gas	880°C	350 mA/cm^2	2990
Exit gas	880°C	350 mA/cm^2	50
Exit gas	880°C	Open Circuit	360

Much of the NH_3 content has decomposed upon reaching 880°C at the inlet, decreasing to approximately 2990 ppm. Most of the balance of NH_3 may be assumed to decompose to N_2 and H_2 in transit over the anode surface of the cell, finally exiting at approximately 50 ppm. When the cell is placed on open circuit, exit gas NH_3 concentration increases, indicating either that some NH_3 may function directly as fuel, or simply that the decomposition is favored when O_2 (as H_2O and CO_2) is present.

Table 2 contains an outline of the periods of time during which this cell was exposed to various levels of NH_3 impurity for specific temperatures and gas compositions. Throughout a total of almost 3200 hours of operation, no significant change in performance level or of resistance index could be detected. During this time, a cumulative period of ~1358 hours of operation in NH_3 containing fuel were recorded. Post-test examination of this test cell revealed no evidence of abnormal structure in any of the component materials.

Table 2. SOFC Operation Chronology at 350 mA/cm^2, 85% Fuel Utilization, 4 Stoichs, Air

Fuel Type	NH_3 (ppm)	Temp. (°C)	Time (h)
Air-blown	1000	1000	97.4
Air-blown	300	1000	21.6
Air-blown	3000	1000	50.0
Air-blown	5000	1000	101.0
Air-blown	5000	950	122.6
Air-blown	5000	950	209.6
Air-blown	5000	880	41.5
Air-blown	5000	880	71.2
Air-blown	5000	880	212.0
Oxygen-blown	5000	880	425.8
Oxygen-blown	5000	880	5.2

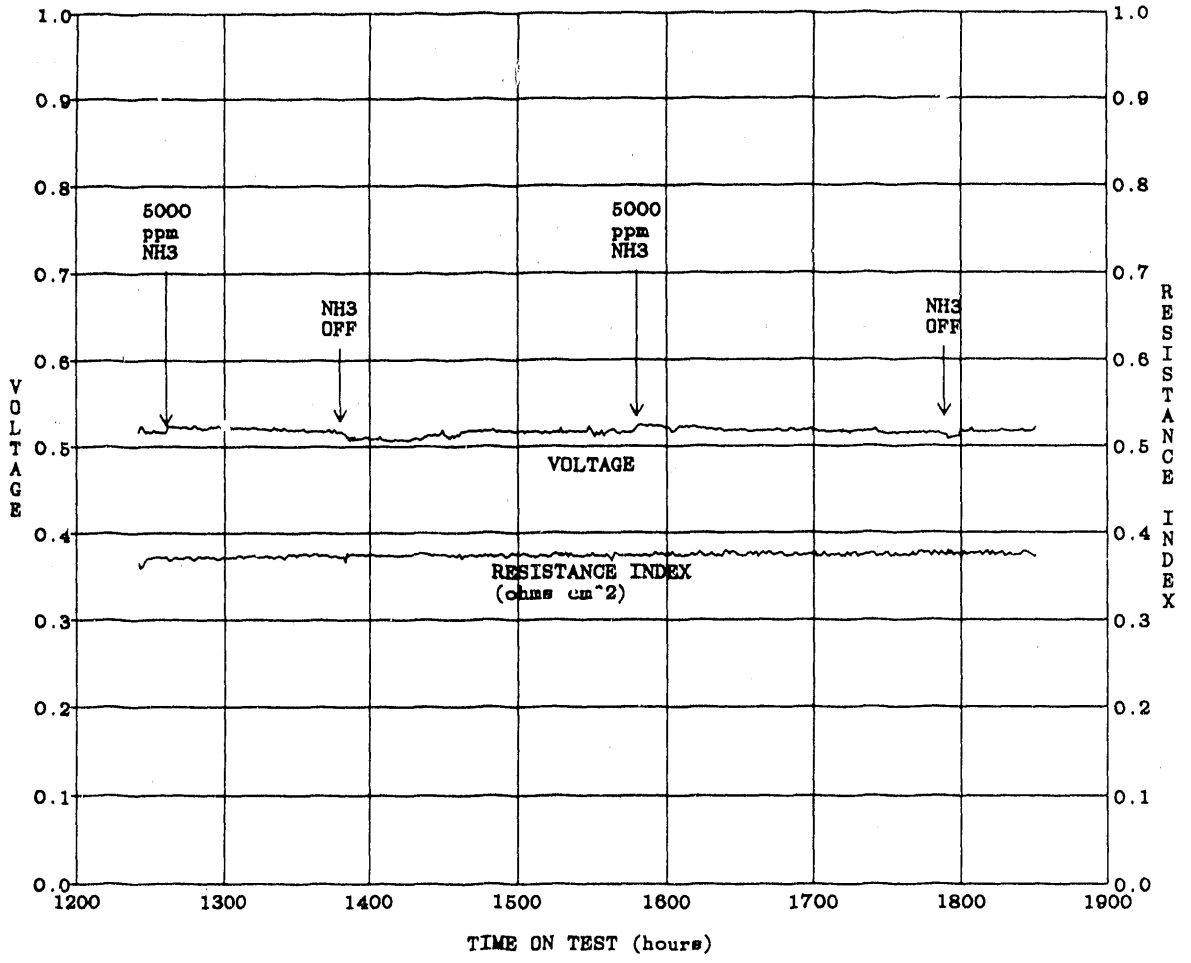

Figure 2. SOFC, SOA fuel electrode performance at 950 °C and 350 mA/cm^2, 85% fuel utilization. Fuel = simulated air-blown coal gas containing 5000 ppm HN_3.

HCl Impurity in Coal Gas

At 1000 °C, operation of an SOFC at 350 mA/cm^2 and 85% fuel utilization in HCl-containing fuel revealed no permanent response in cell performance up to 100 ppm of HCl in simulated oxygen-blown fuel. Figure 3 exemplifies a period of exposure at 1000 °C in oxygen-blown coal gas fuel containing various concentrations of HCl. In each instance, the performance trend seems unaffected by the HCl concentration or by removal of HCl.

Note that each time the concentration of HCl is increased, the performance declines slightly then quickly recovers. These transient negative effects on V_T appear to diminish appreciably after extended exposure to HCl. Figure 3 also contains cell resistance index data taken concurrently. These resistance index data indicate no change over approximately 650 hours of testing in fuel containing HCl at 1000 °C.

At 1050 °C, periods of exposure to simulated oxygen-blown fuel containing 25 ppm and 100 ppm of HCl were monitored. In

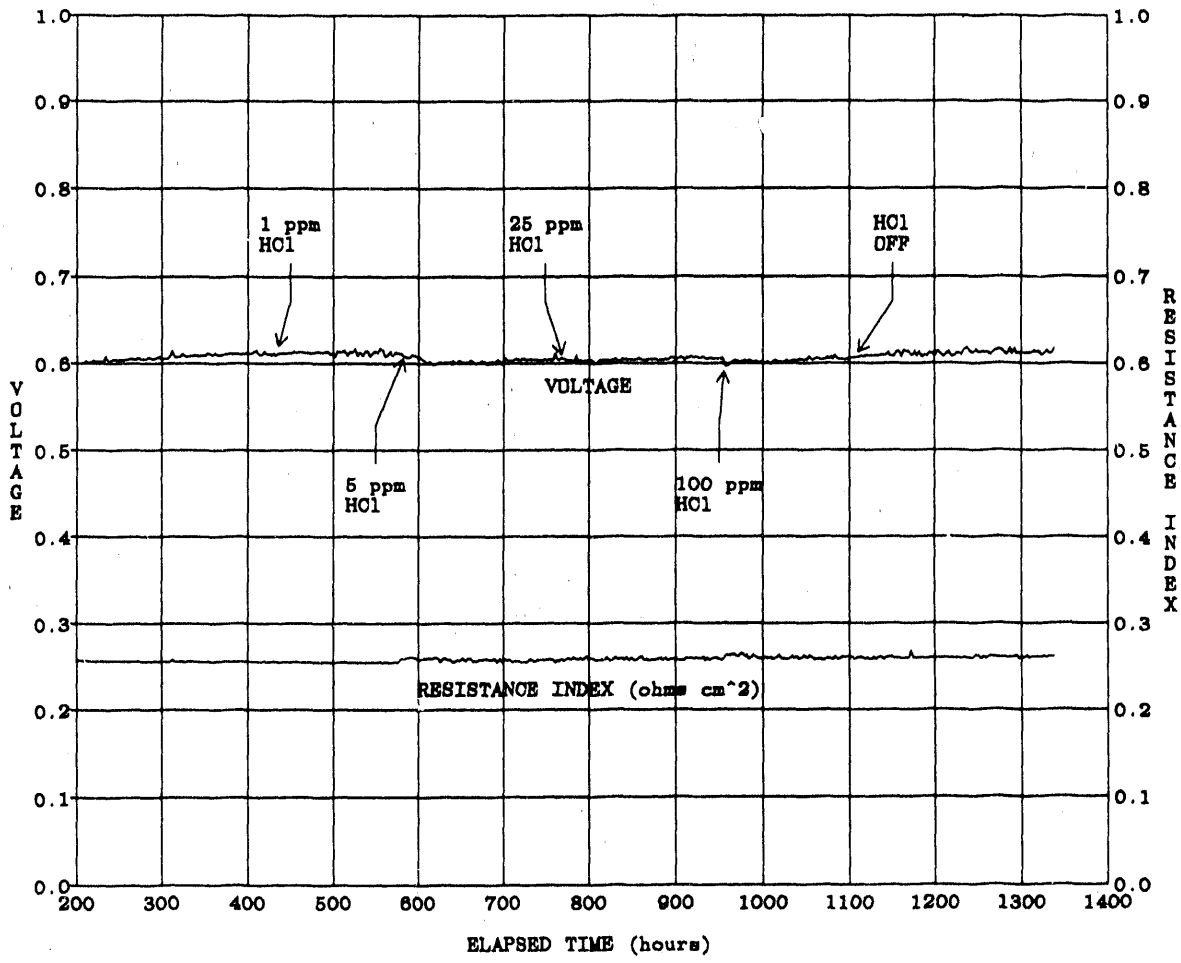

Figure 3. SOFC, SOA fuel electrode performance at 1000°C and 250 mA/cm^2, 85% fuel utilization. Fuel = simulated oxygen-blown coal gas containing up to 100 ppm HCl.

this case cell terminal voltage declined very slightly. This decline was accounted for by a concurrent increase in cell resistance index. When HCL was removed, cell voltage did not recover, but remained essentially the same. The data at 1050°C indicate that HCl interaction with the SOFC may be greater than at 1000°C.

Post-test microscopic examination of this cell revealed that nickel had migrated within the fuel electrode and that zirconia skeleton erosion had occurred (Figure 4). Figure 5 illustrates the condition of a similar fuel electrode at the same point in life (2000 hours) under similar conditions, but with no HCl contaminant.

H_2S Impurity In Coal Gas

H_2S is known to affect methane reformation to H_2 and CO, the fuel species that are most efficiently utilized in the SOFC. Therefore, to obtain data directly related to cell degradation uncomplicated by passivation effects which inhibit methane reformation kinetics, cell operation in H_2S impurity was conducted in hydrogen as the fuel of choice.

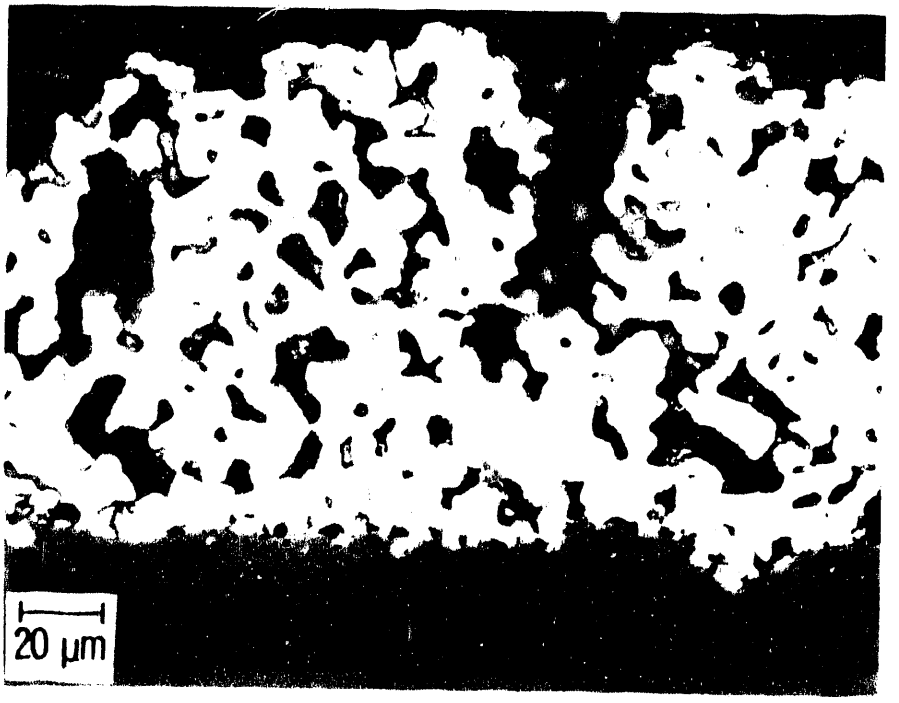

Figure 4. SOFC, SOA fuel electrode after testing in simulated oxygen-blown fuel gas containing up to 100 ppm HCl at 1000°C and 1050°C.

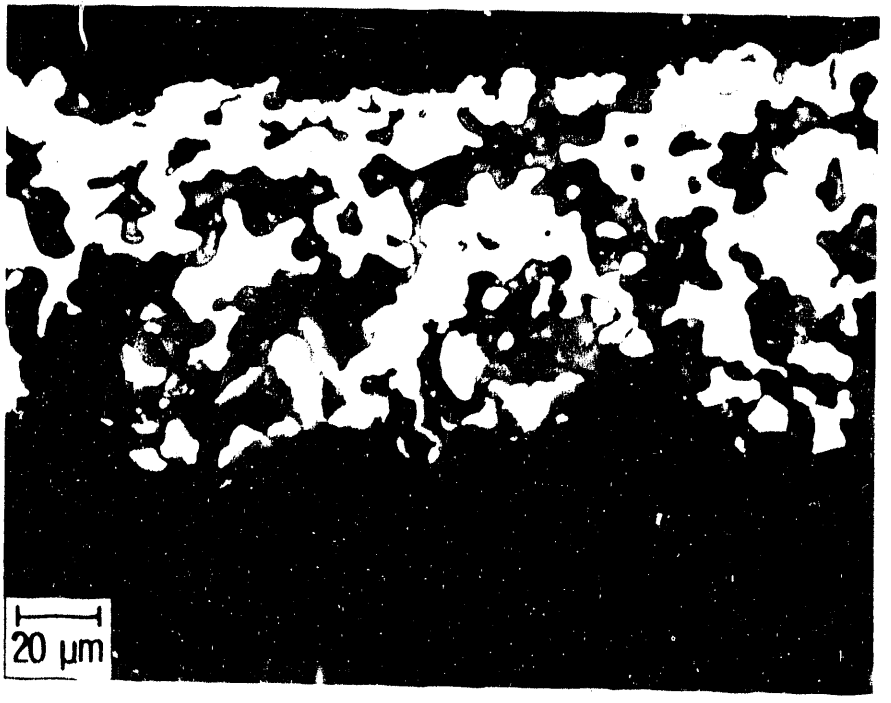

Figure 5. SOFC, SOA fuel electrode after testing at 1000°C in pure H_2, 11% H_2O fuel gas for approximately 2000 hours.

H_2S Impurity in Hydrogen Fuel

In hydrogen, SOFC response to H_2S was greatest at 900°C, the lowest test temperatures employed. At 1000°C the effect of H_2S on cell voltage was more moderate. Figure 6 illustrates operation at 1000°C initially in 5 ppm H_2S, followed by approximately 320 hours in 1 ppm H_2S. Response to H_2S was also sensitive to the particular type of SOFC employed. Specifically, an SOFC employing cell modifications exhibited more resistance to performance degradation than SOFC, SOA (Figure 7). In both cases, the losses in V_T experienced upon exposure to H_2S were fully recovered when the H_2S was removed, indicating that performance loss mechanisms were essentially reversible. No sulfur could subsequently be found if a cell had been degassed; i.e., operated without H_2S until recovery was demonstrated.

The major accomplishments of this work can be summarized in the following conclusions:

1) Ammonia impurity up to 5000 ppm in air or oxygen-blown gasified coal does not present a measurable contribution to SOFC degradation. Rather, NH_3 improves performance, apparently because it contributes actual fuel value.

2) HCl impurity up to 100 ppm in oxygen-blown gasified coal may not have an effect on SOFC degradation when used as fuel over short-term tests at 1000°C, but may affect the microstructure of the fuel electrodes enough to contribute to degradation over the long term. Further HCl concentration/temperature evaluation is needed to specify conditions which are appropriate for long-term testing.

3) H_2S impurity in hydrogen fuel can be tolerated up to 1 ppm by state-of-the-art technology SOFCs with moderate (~50 mV) degradation at 350 mA/cm^2 that can be fully reversed by subsequent operation in clean fuel. Up to 5 ppm of H_2S in hydrogen fuel has been demonstrated to result in stable, though slightly reduced (~20 mV) performance at 350 mA/cm^2 in modified SOFCs, also with fully reversible operation when H_2S is removed.

FUTURE WORK

Initiate a program to identify the long-term tolerance of the tubular solid oxide fuel cell (SOFC) to coal-derived fuel gas containing a mixture of three impurities: hydrogen sulfide (H_2S), hydrogen chloride (HCl), and ammonia (NH_3).

As a prelude to long-term testing of the three impurities, HCl, H_2S and NH_3, initiate additional short-term tests to a) verify the results already obtained, b) collect additional data, and c) make a decision regarding which of two SOFC designs should be chosen to be placed on long-term test. The SOFC design judged most successful will then be operated on a life test schedule in a two-cell, series-connected configuration.

Initiate testing to identify the short-term tolerance of the SOFC to six other coal-derived fuel gas impurities identified in the study conducted in Task 1. These contaminants, silicon (Si), alkali (K), calcium (Ca), aluminum (Al), zinc (Zn), and iron (Fe) are commonly present as oxides, halides, sulfates or carbonates in coal gas particulate matter.

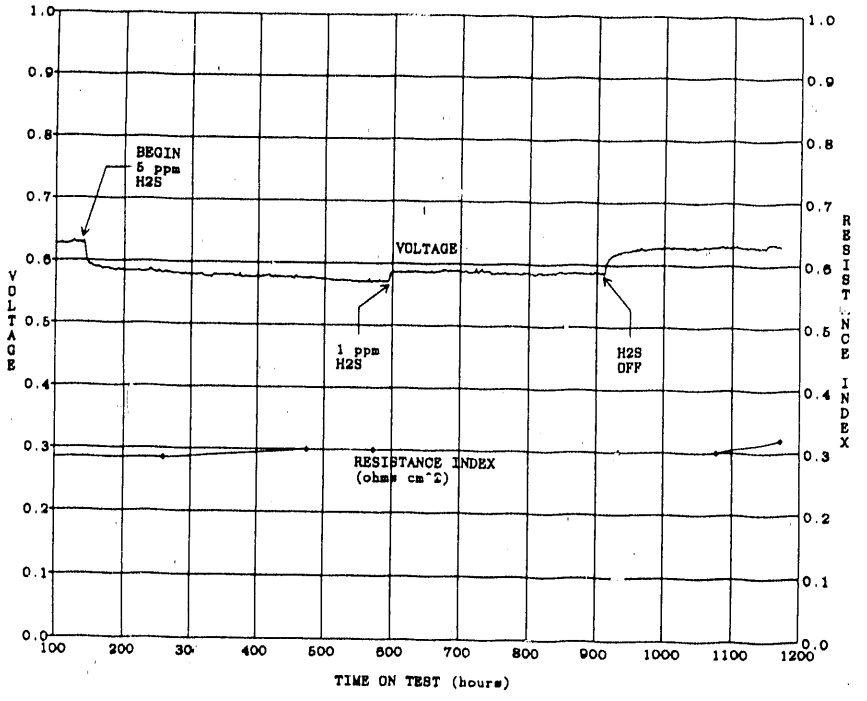

Figure 6. SOFC, SOA fuel electrode performance at 1000°C and 350 mA/cm^2. Fuel = H_2, 11% H_2O containing 5 ppm and 1 ppm H_2S.

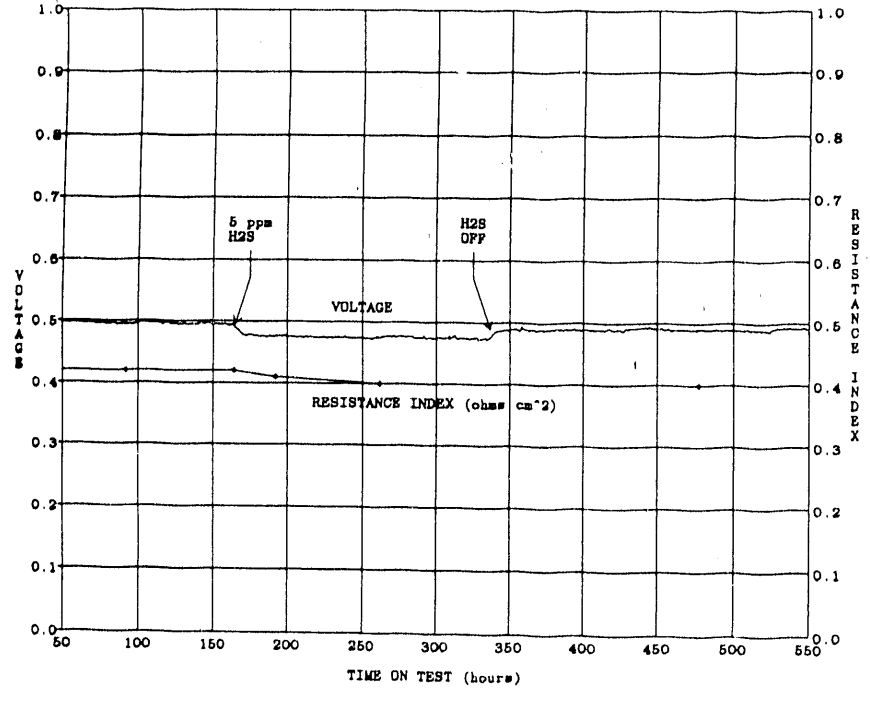

Figure 7. SOFC, modified fuel electrode performance at 1000°C and 350 mA/cm^2. Fuel = H_2, 11% H_2O containing 5 ppm H_2S.

Intermediate Temperature Electrolyte for SOFC

CONTRACT INFORMATION

Contract Number	49639
Contractor	Argonne National Laboratory 9700 South Cass Avenue Argonne, IL 60439 (708) 972-4516
Contractor Project Manager	Kevin M. Myles
Principal Investigators	Ira Bloom and Michael Krumpelt
METC Project Manager	William J. Huber
Period of Performance	April 1, 1990 through April 1, 1991

Schedule and Milestones

FY91 Program Schedule

	S	O	N	D	J	F	M	A	M	J	J	A	S
Prepare and Test New Electrolytes	----------												
Prepare and Test New Electrodes									----------				

OBJECTIVE

The objective of this work is to identify a new set of materials that would allow the operation of the solid oxide fuel cell in the 500-800°C temperature range.

BACKGROUND INFORMATION

The high operating temperature (1000°C) of current solid-state fuel cells limits the number of materials that can be used for cell interconnect and structural support. Lowering the operating temperature to the more moderate range of 500-800°C would allow much greater flexibility in engineering the fuel cell stack and would increase the cell efficiencies. At these

lower temperatures, however, the yttria-doped ZrO_2 (YSZ) electrolyte material does not have sufficient conductivity to make it practical. It would therefore be desirable to find a material that has a conductivity comparable to the high-temperature conductivity of YSZ (10^{-1} $\Omega^{-1}cm^{-1}$ at 1000°C) in the temperature range of interest.

PROJECT DESCRIPTION

This work is directed to exploring materials which do not crystallize in the calcium fluoride (cf. ZrO_2) structure. In this work, the evaluated materials include those that exhibit oxygen substoichiometry or have some crystallographic feature that may be conducive to rapid ionic transport. These materials should be stable in hydrogen and oxygen and have a conductivity of close to 5 x 10^{-2} $\Omega^{-1}cm^{-1}$ in the temperature range of interest.

RESULTS

Two hypotheses are being used in the search for candidate electrolyte materials. The first hypothesis arose from an observation regarding the dependence of conductivity on the strength of the metal-oxygen interaction in a given type of material. The free energy of formation (ΔG_f) values of the known oxide conductors, yttria-doped ZrO_2, CeO_2, and Bi_2O_3, are given in Table 1 along with their respective conductivities at 700°C [1].

As indicated by the data in Table 1, the oxides with smaller ΔG_f values tend to be more conductive. Yttria-doped ZrO_2, with the highest ΔG_f value, is the least conductive and yttria-doped Bi_2O_3, with the lowest ΔG_f value, is the most conductive. However, these materials are unacceptable for practical use because they are not stable in H_2 and O_2. Therefore, a candidate material would have to have a conductivity value similar to that of Bi_2O_3 and yet have sufficient stability for practical use.

Table 1. ΔG_f values for selected metal oxides and their respective conductivities [1,2].

Material (Y-doped)	ΔG_f/mol O_2 at 727°C, kcal/mol	Conductivity, $\Omega^{-1}cm^{-1}$ at 700°C
ZrO_2	-220	1.8 x 10^{-2}
CeO_2	-208	2.5 x 10^{-2}
Bi_2O_3	-58	1.6 x 10^{-1}

A companion to the above hypothesis is the degree of "openness" inherent to the lattice. It is reasonable to expect that oxide ion transport will be easier in a lattice which contains a fair amount of open space than in a tight lattice. The degree of openness is reflected in the geometry of the crystal structure. For example, in the ABO_3 perovskite structure, the movement of oxide ions can be visualized as the passage of the ion through a passageway formed by two A cations and one B cation. The size of the passageway, r_o, can be calculated from the radius of cation A, r_A, the radius of cation B, r_B, and a_0. The parameter a_0 is given by

$$a_0 = \left[\frac{V}{Z} \right]^{1/3}$$

where V is the volume of the unit cell, and Z is the number formula weights per unit cell. If the perovskite does not crystallize with a cubic unit cell, then a_0 represents the edge of a hypothetical cube containing one formula weight of the material. Using these definitions, the parameters r_o and r_c, measures of the passageway size, can be defined as [3]

$$r_o = \frac{0.75a_0^2 + \sqrt{2}(a_0)(r_B) + r_B^2 - r_A^2}{2r_A + \sqrt{2}\,a_0 - 2r_B}$$

and

$$r_c = \frac{r_o}{r_{oxide}}$$

where r_{oxide} is the radius of an oxide ion, 1.26 Å. Since r_c is the relative size of the passageway compared to the size of an oxide ion and may be more intuitively understood, it will be used hereafter to facilitate comparison of the passageway size among different perovskites. The larger the value of r_c is, the easier the jump to the next vacant site would be. With facile jumping, the conductivity would be expected to be high.

The second hypothesis used in finding candidate materials relates to the actual mechanism of ionic transport and represents a radical departure from the usual mechanism of anionic conductivity observed in vacancy conductors. The hypothesis is based on what has been observed in ion exchange resins and in zeolites. These materials consist of a structural polymer or framework with fixed, charge-bearing sites. For instance, in oxide-ion transport applications, the fixed charge-bearing site would have to be positively charged, and the framework would have to be able to accommodate the large oxide ion. In contrast to the vacancy-hopping mechanism observed in fluorites, such as yttria-doped ZrO_2 and CeO_2, the new mechanism would involve the transport of interstitial ions.

In this proposed mechanism for conduction, the materials must contain structural features, such as tunnels and sheets, in their crystal structure which have the ability to facilitate ionic transport. The exact nature of the mobile ion depends on how the material is made; theoretically, the mobile ion could be a proton or oxide or hydroxide ion. The transport of a mobile ion in, for example, a tunnel may produce the sought-after increase in conductivity. This mechanism is embodied in what has been termed "framework" materials. No reports of this sort of mechanism for the transport of oxide ions through a ceramic have appeared in the open literature.

Besides the above geometric considerations, the thermodynamics of the material have to be considered for the development of electrolyte materials. Unfortunately, most thermodynamic properties for the framework materials of interest are not known. Thus, the thermodynamic properties of the framework materials have to be gauged indirectly, as was done in the discussion of the first hypothesis above. As with all simplifications of this nature, any additional stabilization energies from lattice interactions are ignored.

For the sake of clarity, the remaining discussion will be divided according to material studied.

Perovskites

By using appropriately chosen perovskites, we tested the hypotheses regarding the effects of metal-oxygen interaction and amount of openness in the crystal structure. For this work, two perovskite systems were selected, Sr-Zr-O and $XAlO_3$ (X = La, Gd).

$SrZrO_3$ has a fair amount of open space (r_c value= 0.644) and, based on the thermodynamics of its constituent oxides, the ΔG_f value of the perovskite would be expected to be large and positive. There have been some reports in the literature on the effects of dopants on the perovskite, $SrZrO_3$. Usually, the method chosen to increase conductivity is to dope the

lattice with a lower-valent ion and thereby increase the vacancy population. However, this may not necessarily be the complete explanation of the effects of different dopants on conductivity. The change in conductivity reflects the net metal-oxygen interaction and net value of r_c, in addition to the change in vacancy population. If effects occurred other than vacancy population change, one would not expect a dependence of conductivity on the dopant used. Experimentally, these other effects have been found. For the sake of illustration, only the effects of trivalent dopants (on Zr site in $SrZrO_3$) on conductivity will be considered.

In our tests, $SrZrO_3$ had a conductivity of 7.35×10^{-7} $\Omega^{-1}cm^{-1}$ at 600°C and an ionic transference number (t_i) of 0.89. Ideally, the value of t_i should be one, but, at this stage of materials development, values 0.9 or greater are acceptable. A value of 0.89 is within experimental error of the acceptable range and indicates that the conduction mechanism in the material is predominantly ionic. However, the overall conductivity is low. The activation energy of this material was 1.76 eV, indicating that the potential barrier opposing the jump of the vacancy is large.

Takahashi has reported conductivity data for $SrZr_{0.9}In_{0.1}O_{2.95}$ [4]. He reported conductivity data in the 700 to 1000°C temperature range. For the sake of comparison, we have extrapolated his conductivity data to 600°C and have calculated the energy of activation from the slope of the line derived from

$$\ln(\sigma) = \ln(A) - \frac{E_a}{R}\left[\frac{1}{T}\right],$$

where σ is the conductivity, A is a constant, E_a is the activation energy, R is the gas constant, and T is the absolute temperature. From the data, the calculated conductivity of the material at 600°C would be 1.21×10^{-3} $\Omega^{-1}cm^{-1}$, and the energy of activation would be 0.37 eV.

The conductivity of a closely related material, $SrZr_{0.8}Yb_{0.2}O_{2.9}$, was reported to be 4×10^{-4} $\Omega^{-1}cm^{-1}$ at 600°C with an activation energy of 0.8 eV [5]. No value of t_i was given.

To further illustrate the effect of dopant, the compound $SrZr_{0.9}Y_{0.1}O_{2.95}$ was made and characterized in terms of conductivity. At 600°C, this material had a conductivity of 2.20×10^{-5} $\Omega^{-1}cm^{-1}$, a t_i value of 0.77, and an activation energy for conduction of 0.96 eV.

In the above series of compounds, the value of r_c does not change markedly. The r_c values are 0.644, 0.645, and 0.646 for the compounds $SrZrO_3$, $SrZr_{0.8}Yb_{0.2}O_{2.9}$, and $SrZr_{0.9}Y_{0.1}O_{2.95}$, respectively. No crystallographic data were reported for $SrZr_{0.9}In_{0.1}O_{2.95}$. Based on the relative sizes of the dopant ions (Yb, Y and In), the r_c value for this perovskite is expected to be only slightly larger, possibly 0.647 or 0.648. However, the ΔG_f values for these dopant ions do change markedly. These ΔG_f values, along with the conductivity values from the resulting perovskite, are given in Table 2.

Table 2. ΔG_f values of dopant oxides used in $SrZrO_3$ and the conductivity of the resulting perovskite [?].

Dopant Oxide	ΔG_f of dopant oxide at 727°C, kcal/mol O_2	Conductivity of perovskite, $\Omega^{-1}cm^{-1}$ at 600°C
In_2O_3	-100	1.21×10^{-3}
Yb_2O_3	-208	4×10^{-4}
Y_2O_3	-246	2.20×10^{-5}

Comparing the conductivity of the perovskite with the ΔG_f value of its respective dopant indicated a direct relationship between the two. The indium-doped perovskite is the most conductive (lowest ΔG_f) and the yttrium-doped, the least (highest ΔG_f). A similar trend can also be seen when comparing the activation energy and the ΔG_f values.

Extending the trend between average metal-oxygen bond strength led to another method that has the potential to increase the conductivity of $SrZrO_3$. The new method was to combine $SrZrO_3$ in a solid solution with another perovskite which had a weaker metal-oxygen bond. Based on lattice parameters and metal-ion sizes, $SrSnO_3$ was chosen to test the hypothesis. At 600°C, $SrSnO_3$ had a conductivity of $1.63 \times 10^{-5}\ \Omega^{-1}cm^{-1}$ and a t_i of 0.15. The activation energy for conduction was 1.01 eV. This conductivity was better than that of $SrZrO_3$, but it was not good enough for practical use.

The solid solution $SrSn_{0.9}Zr_{0.1}O_3$ had a conductivity of $1.96 \times 10^{-4}\ \Omega^{-1}cm^{-1}$ at 600°C, a t_i of 0.15, and an activation energy for conduction of 0.71 eV. These values show a 10-fold increase in the conductivity as compared to $SrSnO_3$ with no net change in transference number and a 100-fold increase in ionic conductivity (t_i x total conductivity) compared to that of $SrZrO_3$. At the same time, there was a substantial decrease in activation energy.

More Zr was then added to $SrSnO_3$ in order to increase the t_i value of the stannate. The solid solution $SrZr_{0.5}Sn_{0.5}O_3$ had a conductivity of about $2.54 \times 10^{-5}\ \Omega^{-1}cm^{-1}$ and a t_i of 0.69 at 600°C. The activation energy for conduction was 0.29 eV. Comparing these data to those from $SrZrO_3$ and $SrZr_{0.9}Y_{0.1}O_{2.95}$, a 25- and a 1.25-fold increase was seen in ionic conductivity, respectively, as well as a 6- and 3-fold decrease in activation energy, respectively. Clearly, formation of a solid solution in the Sr-Zr-Sn-O system improved the ionic conductivity over that observed in either $SrZrO_3$ or $SrSnO_3$. The improvement was better than that obtained by substituting lower-valent elements on the Zr site.

Of the materials evaluated in the Sr-Sn-Zr-O system, $SrZr_{0.5}Sn_{0.5}O_3$ had the highest ionic conductivity. But, because of a possible low concentration of mobile vacancies, its conductivity was not high enough for practical use. As a means of determining the effect of a larger vacancy concentration on conductivity, a pellet with the stoichiometry, $SrZr_{0.5}Sn_{0.4}Y_{0.1}O_3$, was made. At 600°C, the pellet had a conductivity value of $4.40 \times 10^{-5}\ \Omega^{-1}cm^{-1}$ and t_i value of 0.50. Comparing the conductivity and t_i values of $SrZr_{0.5}Sn_{0.5}O_3$ and $SrZr_{0.5}Sn_{0.4}Y_{0.1}O_3$, an approximately 2-fold increase in total conductivity and a decrease in ionic transference can be seen in the Y-doped material. The net ionic conductivity of the Y-doped material is slightly larger than that observed for $SrZr_{0.5}Sn_{0.5}O_3$, indicating that the additional vacancies do not significantly improve the conductivity. The metal-oxygen interaction strength appears to be the dominant factor improving the conductivity of the material.

In the literature, there have been reports that a fair amount of open space would permit the facile diffusion of oxide or hydroxide ions through the perovskite lattice. This is a geometric simplification of a very complex situation. To illustrate how complex conductivity in the perovskite lattice can be, two perovskites with approximately similar thermodynamic properties were examined: $LaAlO_3$ and $GdAlO_3$. The only difference in the materials is the amount of open space in the lattice, with the Gd perovskite having more. As undoped materials, their conductivities are in the 10^{-7} to $10^{-6}\ \Omega^{-1}cm^{-1}$ range at 1000°C.

Takahashi and Iwahara [6] have reported that, after the La perovskite was doped with Ba, the conductivity improved by a factor of 1000. However, when we doped the Gd perovskite with Ba, its conductivity did not increase; instead, it decreased.

The above results indicate that conductivity in perovskites is far more complex than either of the hypotheses would imply. Conductivity depends on many factors besides openness and metal-oxygen interaction strength. These factors include vacancy interactions, metal ion polarizability, and the exact distribution of space in the crystalline lattice. The results do, however, validate the initial hypotheses, i.e., the dependence of vacancy conductivity on openness and interaction strength.

Based on the above principles and results, another orthorhombically distorted, perovskite-based material was selected for assessment. It contains the thermodynamic features described in the Zr-Sn system and a fair amount of open space. The conductivity of the material is about $9 \times 10^{-2}\ \Omega^{-1}cm^{-1}$ with a t_i value of 0.7 at 800°C in an oxygen gradient. Based on these data, the material is a promising candidate for fuel cell applications. Issues that need to be addressed include its electrochemical and chemical behavior in the fuel cell environment.

Garnets

Using some of the ideas described in the perovskites section of this report about modifying metal-oxygen interaction strength to increase ionic conductivity, we characterized a series of compounds based on yttrium aluminum garnet ($Y_3Al_5O_{12}$, YAG) and yttrium iron garnet ($Y_3Fe_5O_{12}$, YIG). YAG is, essentially, a nonconductor, whereas YIG is a very good electronic conductor. The 50:50 mixture of the two has been found to be a moderate ionic conductor. The fact that we have any ionic conduction at all validates our hypothesis even further. However, the magnitude of the ionic conductivity was too small to be of practical use.

Framework Materials

In general, framework materials possess or can be made to possess fixed, charge-bearing sites. In addition, these materials have structural features native to their crystal structures, such as tunnels and sheets, which may be amenable for facile ion transport.

Apatite

Apatite materials have a large channel running along the crystallographic c-axis. Apatites which contain Cl^-, O^{2-}, CO_3^{2-} or OH^- ions are also known [7]. Hydroxylapatite, $Ca_5(OH)(PO_4)_3$, for example, is the major constituent of human bones. Hydroxyl- and oxyapatites may have one major advantage over the other framework materials mentioned. The crystal chemistry of the material is right for anionic conduction, either as diffusing O^{2-} or OH^- species. Since apatites may contain OH^- groups, proton-mediated conduction is also possible. The protons on adjacent hydroxyl groups may be close enough to form bridges between adjacent groups, creating a path for facile transport.

As a starting point, we have made fine-grained $Sr_5(OH)(PO_4)_3$ by solution techniques and have sintered it into pellets with 93-95% of theoretical density. Quite unexpectedly, we found that the crystals of $Sr_5(OH)(PO_4)_3$ were preferentially oriented with the c-axis (contains the channel) parallel to the surface of the pellet.

Even so, the material still had a fair amount of ionic conductivity: $2.58 \times 10^{-4}\ \Omega^{-1}cm^{-1}$ at about 780°C with a transference number of 0.59. This conductivity value is about 100-fold greater than that obtained by Takahashi et al. [8] and may be attributed to differences in fabrication techniques.

Another material which also has the above structural features was selected for evaluation. It had a conductivity of $3 \times 10^{-2}\ \Omega^{-1}cm^{-1}$ and a transference number close to one at 800°C. This material represents a new class of conductors and may be the first example of an interstitial proton conductor.

FUTURE WORK

The above descriptions clearly indicate that many materials other than fluorites can be good ionic conductors. Once the effects of parameters such as powder synthesis and fabrication techniques on conductivity and ceramic quality are understood, it is reasonable to expect that materials with even higher conductivities can be found.

We plan to continue to evaluate and to improve the properties of two candidate materials mentioned above. These materials had conductivities of at least $10^{-2}\ \Omega^{-1}cm^{-1}$ at 800°C.

This work was performed under the auspices of the U.S. Department of Energy under contract No. W-31-109-Eng-38 and also supported by the Electric Power Research Institute and the Gas Research Institute.

REFERENCES

[1] These conductivity values were taken or calculated from:
ZrO_2: D. W. Strickler and W. G. Carlson, J. Am. Cer. Soc., 48 (1965) 286.
CeO_2: T. Kudo and H. Obayashi, J. Electrochem. Soc., 122 (1975) 142.
Bi_2O_3: T. Takahashi, H. Iwahara, and T. Arao, J. Appl. Electrochem., 5 (1975) 187.

[2] The ΔG values were calculated from data given in Thomas R. Reed, Free Energy of Formation of Binary Compounds: An Atlas of Charts for High-Temperature Chemical Calculations, MIT Press, 1971, Cambridge, MA, p. 7ff.

[3] A. Sammells, private communication.

[4] T. Takahashi and H. Iwahara, Revue de Chemie Minerale, 17 (1980) 243.

[5] K. W. Browall and O. Muller, Mat. Res. Bull., 11 (1976) 1475.

[6] T. Takahashi and H. Iwahara, Energy Conversion, 11, (1971) 105-111.

[7] I. Naray-Szabo, Inorganic Crystal Chemistry, translated by P. Hedvig and G. Zentai, Akademiai Kiado Budapest, 1969, p. 319ff.

[8] T. Takahashi, S. Tanase, and O. Yamamoto, Electrochim. Acta 23 (1978) 369.

Perovskite Electrolytes for SOFC

CONTRACT INFORMATION

Contract Number	DE-FG02-90ER80910
Contractor	Eltron Research, Inc. 4260 Westbrook Drive Aurora, IL 60504 (708) 898-1583
Contract Project Manager	Anthony F. Sammells
Principal Investigator	Anthony F. Sammells
METC Project Manager	William I. Huber
Period of Performance	July 23, 1990 to February 14, 1991

Schedule and Milestones

FY90 Program Schedule

	J	A	S	O	N	D	J	F
Electrolyte Preparation	———							
Electrolyte Characterization		———	———	———				
SOFC Testing			———	———	———	———	———	———

OBJECTIVES

The object of this program was to experimentally determine the utility of selected perovskite related solid electrolytes for application in SOFC's operating at 600°C. Specific technical objectives addressed in this program were:

- Synthesize selected single phase perovskite related solid electrolyte powders with the potential for i) a low activation energy (E_a) for ionic conduction, and ii) a high population of ionic charge carriers.
- Prepare sintered solid electrolyte disks and determine their ionic conductivity.
- Incorporate solid electrolytes demonstrating acceptable ionic conductivity into SOFC's operating at ≅600°C and determine electrochemical performance.

BACKGROUND INFORMATION

Because of the relatively high E_a for ionic conduction in yttria stabilized zirconia (YSZ) corresponding to ≅0.8eV, it is necessary to operate fuel cells incorporating this material

at 1000°C where this oxygen anion conducting solid electrolyte possesses an ionic conductivity of 2 x $10^{-1}\Omega^{-1}cm^{-1}$. Operation of fuel cells utilizing YSZ at 600°C, where its ionic conductivity would be only 3 x $10^{-3}\Omega^{-1}cm^{-1}$, would restrict operation to low current densities as a result of high IR polarization losses.

As a consequence of the above, there are strong incentives to identify alternate solid electrolytes possessing sufficiently high ionic conductivities to facilitate practical fuel cell operation at 600°C or below. Such a goal might be addressed by developing a systematic approach into the dependency between E_a for ionic conduction, metal oxide lattice parameters and, for example, the characteristics of ions occupying specific lattice sites within the unit cell of a given solid electrolyte. Such an approach is currently evolving at Eltron Research, Inc. (ERI) for the systematic selection of perovskite related solid electrolytes with the potential for achieving ionic conduction significantly larger than currently found with YSZ based materials.

PROJECT DESCRIPTION

Perovskite solid electrolytes selected for this investigation were based upon rationale currently under evolution at ERI which had previously shown[1] correlation between activation energy (E_a) for ionic conduction in perovskite lattice and the 'free volume' present in the perovskite unit cell crystal lattice, as defined by the unit cell volume subtracted by the ionic volume of constituent ions. It was in general found for $A^{2+}B^{4+}O_3$ perovskites that larger 'free volumes' favored progressively lower activation energies for ionic conduction. This insight into the rational selection of anion conducting perovskite solid electrolytes has now been extended to include a number of other parameters shown to systematically influence E_a and thereby permitting us to more rationally select solid-state lattice possessing enhanced overall ionic conductivity.

Parameters of particular interest have included: 1) the perovskite lattice average metal-oxygen bond energy, 2) the lattice free volume previously discussed, 3) the parameter $r_{critical}$ (r_c) corresponding to the radius of the opening between the two A site cations and one B site cation through which the mobile anion must pass, and 4) the overall lattice polarizability towards anion migration.

The expression for ionic conductivity in a solid electrolyte, as derived from random walk theory, may be given by:[2,3]

$$\sigma T = A \exp(-\Delta H_m/KT) \quad (1)$$

where

$$A = (Z\lambda^2 e^2/6v_a K)C(1-C)v_a \exp(\Delta S_m/K) \quad (2)$$

and $-\Delta H_m$ (equivalent to E_a) and ΔS_m are, respectively, enthalpies and entropies for activation, C is the fraction of available sites occupied by mobile ions, λ the jump distance, Z the number of jump directions, v_a the molar volume, K the Boltzmann constant and e the electronic charge.

Examining relationship (1) above, we see that overall ionic conductivity σ is influenced both by an exponential and a preexponential term A. Performing a study on the influence of perovskite lattice parameters and ionic constituents upon E_a only addresses the exponential component of this relationship. The preexponential term A is related to the number of charge carriers present in the solid-state lattice. As a consequence, experimental investigations were extended to also include perovskite related lattice where a high population of oxygen vacancies were intrinsic, thereby con-

tributing to the possibility of high ionic conductivity. This general approach resulted in our investigating materials based upon the brownmillerite structure $A_2B_2O_5$, which may be considered to be derived from the perovskite structure by removing 1/6 of the unit cell oxygen atoms.

To address these complimentary approaches, solid electrolytes studied have included the prototype materials $BaTh_{0.9}Gd_{0.1}O_3$, $BaCe_{0.9}Gd_{0.1}O_3$, $Sr_2Gd_2O_5$ and $Sr_2Dy_2O_5$.

RESULTS

Ionic conductivity measurements for intermediate temperature fuel cells incorporating these solid electrolytes were obtained both from DC current-voltage curves performed on H_2/O_2 cells of general configuration:

$$\underset{(3\%H_2O)}{H_2,Ni(\text{or Pd})}/\underset{(A_2B_2O_5)}{ABO_3}/\underset{(\text{or Ag})}{La_{0.9}Sr_{0.1}CoO_3},\underset{(3\%H_2O)}{O_2}$$

and using an impedance/gain-phase analyzer.

For the prototype solid electrolyte $BaTh_{0.9}Gd_{0.1}O_3$, ionic conductivities up to 8.7 x $10^{-2}\Omega^{-1}cm^{-1}$ at 550°C and $\cong 10^{-1}\Omega^{-1}cm^{-1}$ at 600°C were found for single phase material as extrapolated from the slope of the current-voltage curves shown in Figure 1 at these two respective temperatures. Parasitic electronic conductivity, as determined by differences between theoretical and experimentally determined open-circuit potentials for the H_2/O_2 couple, were subtracted from the overall measured conductivity to determine true ionic conductivity. Ionic conductivity (t_i) was found to vary for 12 fuel cells investigated between 85 and 95% of total conductivity.

We have found E_a values for this solid electrolyte to most frequently vary between 0.3 and 0.6eV with $\cong$0.5eV being an average value for 12 fuel cells incorporating this solid electrolyte.

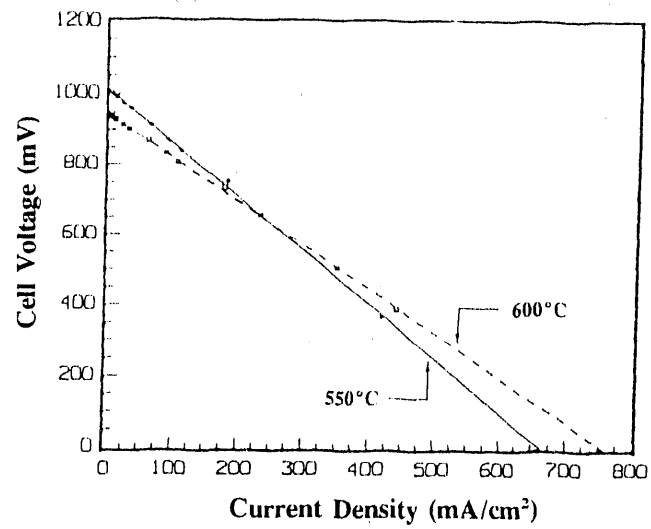

Figure 1. Current-voltage curve for the cell: $H_2(3\%H_2O)Pd/BaTh_{.9}Gd_{.2}O_2/La_{.9}Sr_{.1}CoO_3,O_2$at A) 550°C, σ = 8.7 x $10^{-2}\Omega^{-1}cm^{-1}$, and B) 600°C, σ = 1.03 x $10^{-1}\Omega^{-1}cm^{-1}$.

For intermediate temperature fuel cells incorporating prototype perovskite solid electrolytes like $BaTh_{0.9}Gd_{0.1}O_3$, which have a particularly large calculated lattice free volume (57Å^3), it was instructive to gain insight into whether this material was predominantly an O^{2-} or proton (OH^-) conductor. This was addressed by fabricating concentration cells possessing the general respective configurations:

$$O_2(He),Ag/BaTh_{0.9}Gd_{0.1}O_3/Ag,(He)/O_2$$

and

$$H_2(He)Pd/BaTh_{0.9}Gd_{0.1}O_3/Pd,(He)H_2$$

to determine whether the concentration cells possessed Nernstian type behavior to one or both of these species. For oxygen concentra-

tion cells no concentration dependency was observed up to 100% O_2 on one side and O_2/He mixtures on the other. In comparison, a Nernstian concentration dependency was observed for the hydrogen concentration cell. Such experimentally observed concentration dependency towards hydrogen in these cells was supportive of predominantly proton transport across $BaTh_{0.9}Gd_{0.1}O_3$. This implied that intermediate temperature fuel cells incorporating this solid electrolyte would only produce steam at their cathode from OH^- species mediated from anode to cathode regions.

Ionic conductivity in the perovskite related brownmillerite solid electrolyte $Sr_2Gd_2O_5$ was performed using a cell of configuration:

$$\underset{(3\%H_2O)}{H_2,Ni/Sr_2Gd_2O_5/La_{0.9}Sr_{0.1}CoO_3/}\underset{(3\%H_2O)}{O_2}$$

giving a value of 2 x $10^{-2}\Omega^{-1}cm^{-1}$ at 600°C from both the slope of the current-voltage curve (Figure 2) and impedance measurements.

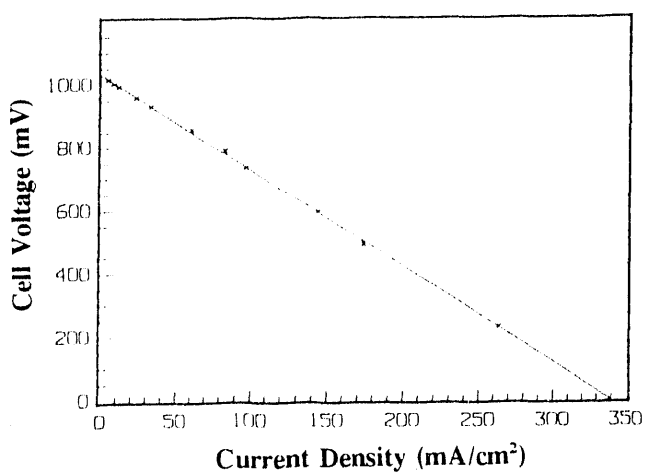

Figure 2. Current-voltage curve for the cell: $H_2(3\%H_2O)Ni/Sr_2Gd_2O_5/La_{0.9}Sr_{0.1}CoO_3,(3\%H_2O)O_2$ at 600°C.

For the closely related solid electrolyte $Sr_2Dy_2O_5$, initial ionic conductivity measurements were performed using the fuel cell:

$$H_2(3\%H_2O),Ni/Sr_2Dy_2O_5/Ag(3\%H_2O),O_2$$

The corresponding current-voltage curve for this cell is shown in Figure 3 at 625°C where an ionic conductivity of 3.65 x $10^{-1}\Omega^{-1}cm^{-1}$ was found. This was found in general agreement with impedance plots performed on this cell.

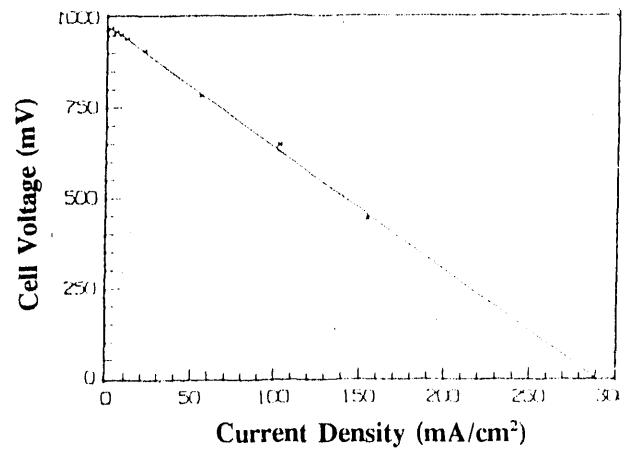

Figure 3. Current-voltage curve for the cell: $H_2(3\%H_2O)Ni/Sr_2Dy_2O_5/Ag(3\%H_2O),O_2$ at 625°C.

While many other perovskite related solid electrolytes are currently being investigated in our laboratory, the above selected materials illustrate the point that complimentary strategies which both lower E_a for ionic conduction and increase the available popuiation of carrier sites, can result in the identification of materials possessing potentially high ionic conductivities. Although this previous statement may be considered somewhat a truism, the ease with which perovskite lattice constituents can be varied permit us to conveniently systematically adjust solid-state properties towards achieving this goal.

Some of our considerations used for predicting perovskite related solid electrolytes include:

a) That cations introduced into perovskite A and B lattice sites were absent of multiple oxidation states, thereby minimizing electronic transport via this mechanism.

b) Ensuring that the perovskite crystallographic lattice possesses a relatively open structure or 'free volume' compatible with facilitating high ionic mobility.

c) That weak association is present between mobile anions and the lattice bulk.

d) Ensuring that the aliovalent dopant cation introduced into the B lattice site for creation of oxygen vacancies necessary for promoting anionic conduction will possess a similar ionic radii to the B-cation it replaces. When the dopant radii is significantly different,[4] an increase in E_a for anion conduction may result from association between the mobile anion and dopant.

e) That the saddle point critical radius (r_c) formed by two A and one B lattice site, through which mobile anions must pass between vacancies, are large enough so that minimal disturbance of the lattice occurs.

f) That the solid-state lattice through which the mobile anion migrates does not unduly polarize the latter species.

Empirical parameters shown by us to exhibit correlations to E_a for anion transport in perovskite solid electrolytes have included:

- The average metal-oxygen bond energy in the perovskite.
- Calculated lattice free volumes, obtained by subtracting ionic volumes of cations and O^{2-} in the unit cell from the overall crystallographic unit cell,
- The parameter $r_{critical}$ (r_c) which corresponds to the radius of the opening between the two A site cations and one B site cation through which the mobile anion must pass.
- Lattice polarizability towards anion migration.

We will now briefly discuss our current insight into each of these correlations to E_a for anion conduction in perovskite solid-state lattice.

A. Average Metal-Oxygen Bond Energy

To estimate oxygen binding energies within perovskite solid electrolytes, we selected a relationship from which the average metal-oxygen bond energy (ABE) could be calculated from the starting oxide heat of formation, the metal heat of sublimation and the oxygen dissociation energy.[5,6] For perovskites where the A site cations are 12 coordinate and those for B sites 6 coordinate, the average perovskite bond energy can be given by:

$$ABE = \frac{1}{12 \cdot m}\left(\Delta H_{A_mO_n} - m\Delta H_A - \frac{1}{n} D_{(O_2)}\right) + \frac{1}{6 \cdot m}\Delta H_{B_mO_n} - m\Delta H_B - \frac{1}{n} D_{(O_2)} \quad (3)$$

where $\Delta H_{A_mO_n}$ and $\Delta H_{B_mO_n}$ are the heats of formation of the A_mO_n and B_mO_n oxides, respectively, ΔH_A and ΔH_B are the heats of sublimation of the metals A and B, respectively, and $D_{(O_2)}$ is the oxygen dissociation energy. These calculated average metal-oxygen bond energies were found to be linearly related to experimentally determined activation energies for anion transport in perovskite solid electrolytes as shown in Figure 4.

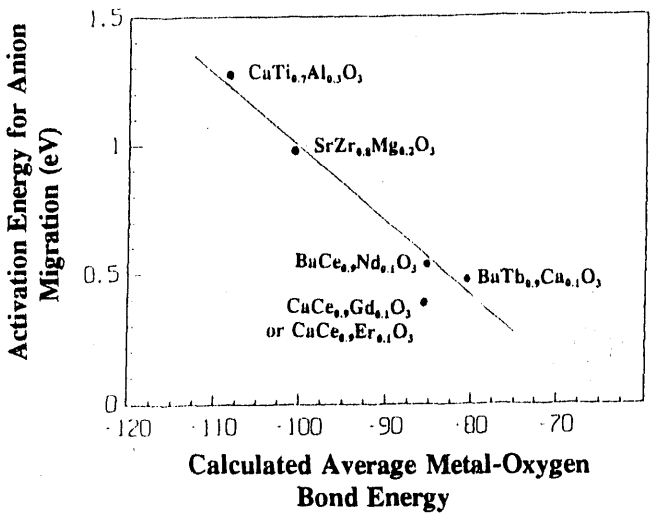

Figure 4. Relationship between average perovskite metal-oxygen bond energy and E_a. We assume A site cations are 12 coordinate and B sites 6 coordinate.

B. Lattice Free Volumes.

Another parameter found correlatable to E_a for anion transport through perovskite solid-state lattice is the crystallographic free volume (FV) which we here define as the difference between perovskite unit cell volume and the summed volume occupied by all ions present within the perovskite unit cell of interest. Here, tabulated empirical ionic radii values were used[7] and corresponding perovskite unit cell volumes calculated from:[8]

$$a_0^3 \text{ (unit cell lattice edge)} = 2.37r_B + 2.47 - 2.00\,(S^{-1}\text{-}1) \qquad (4)$$

which relates the ionic radii of the ions A_{n+} (r_A), B^{m+} (r_B) and O^{2-} with the corresponding perovskite unit cell volume, where S is the Goldschmidt Tolerance Factor.[9] Lattice free volumes were calculated with the assumption: $0.75 < S < 1.05$; $1.5 < r_A < 0.8$Å; $1.0 < r_B < 0.45$Å; $r_A > r_B$; and $a_0 \leq 5$Å for ideal $A^+B^{5+}O_3$, $A^{2+}B^{4+}O_3$ and $A^{3+}B^{3+}O_3$ perovskites with the assumption that the A lattice site was 12 coordinate. Using this assumption, predicted and closest match perovskites have been calculated and gave the respective values:

	(Å)	FV(Å^3)	r_A(Å)	r_B(Å)	S
Predicted:					
$A^+B^{5+}O_3$	4.298	34.2	1.57	.75	.98
$A^{2+}B^{4+}O_3$	4.745	68.2	1.46	1.09	.81
$A^{3+}B^{3+}O_3$	4.419	56.8	1.18	.99	.76
Closest Match:					
$RbUO_3$	4.314	34.1	1.6	.75	.99
$BaThO_3$	4.484	57.9	1.42	1.0	.83
$LaPrO_3$	4.424	57.2	1.18	.997	.76

From Figure 5 we can see that both $BaTh_{.9}Gd_{.1}O_3$ (E) and $BaCe_{.9}Gd_{.1}O_3$ (D) were found to fit well into this empirical prediction. It should be noted that both of these were $A^{2+}B^{4+}O_3$ perovskites. We have found, however, in our investigations that for $A^{3+}B^{3+}O_3$ perovskites the trend appears to proceed in parallel to the fluorites corresponding to higher E_a values as FV increased as shown in Figure 6. This suggests that there may be an optimum FV value for perovskites in the 50-57Å^3 range beyond which other factors become dominant. For $A^{2+}B^{4+}O_3$ materials it may be that inherent lattice constriction is the dominant factor influencing E_a, whereas at higher FV values for $A^{3+}B^{3+}O_3$ materials solid-state lattice polarization related effects may become more dominant.

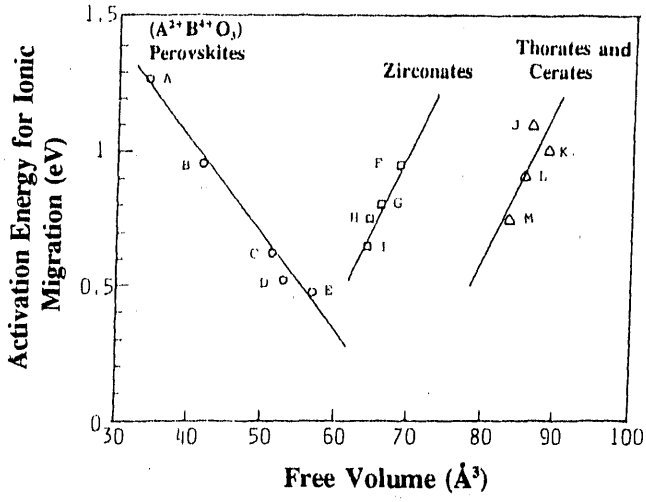

A. $CaTi_{0.7}Al_{0.3}O_3$
B. $SrZr_{0.8}Mg_{0.2}O_3$
C. $SrCe_{0.9}Yb_{0.1}O_3$
D. $BaCe_{0.9}Gd_{0.1}O_3$
E. $BaTh_{0.9}Gd_{0.1}O_3$
F. $Zr_{0.82}Sm_{0.18}O_{1.82}$
G. $Zr_{0.84}Y_{0.16}O_{1.84}$
H. $Zr_{0.85}Yb_{0.15}O_{1.85}$
I. $Zr_{.82}Sc_{0.18}O_{1.82}$
J. $Th_{0.95}Ca_{0.05}O_{1.95}$
K. $Th_{.85}Y_{0.15}O_{1.85}$
L. $Ce_{0.8}La_{0.2}O_{1.8}$
M. $Ce_{0.85}Ca_{0.15}O_{1.85}$

Figure 5. Correlation found at ERI between activation energies for anion migration in perovskite and fluorite solid oxide electrolytes as a function of free volume. (Free Volume = unit cell volume - lattice volume.)

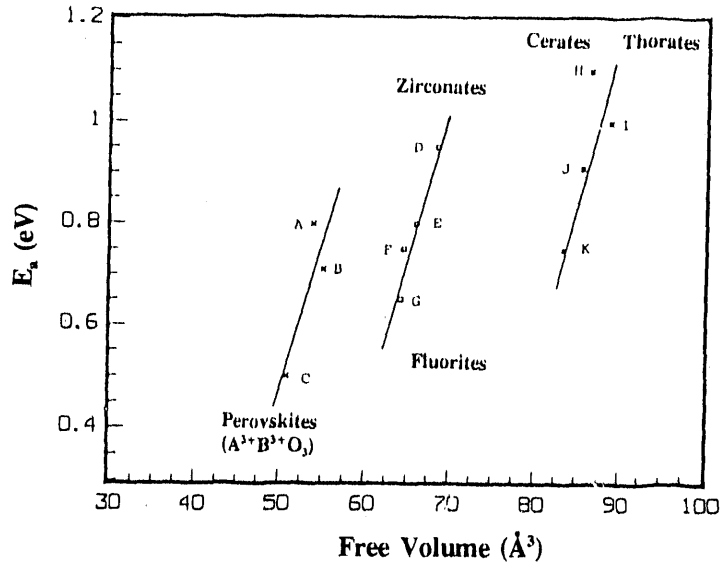

A. $LaGd_{0.9}Ca_{0.1}O_3$
B. $LaSm_{0.9}Ca_{0.1}O_3$
C. $LaEr_{0.9}Ca_{0.1}O_3$
D. $Zr_{0.82}Sm_{0.18}O_2$
E. $Zr_{0.84}Y_{0.16}O_2$
F. $Zr_{0.85}Yb_{0.15}O_2$
G. $Zr_{0.82}Sc_{0.18}O_2$
H. $Th_{0.95}Ca_{0.05}O_2$
I. $Th_{0.85}Y_{0.15}O_2$
J. $Ce_{0.8}La_{0.2}O_3$
K. $Ce_{0.85}Ca_{0.15}O_2$

Figure 6. Comparison of free volume vs E_a for O^{2-} migration for high free volume perovskite $A^{3+}B^{3+}O_3$ and fluorite solid electrolytes compared to fluorites.

C. A-A-B Perovskite Crystallographic Saddle Point r_c.

An empirical relationship between E_a and the saddle point associated with r_c in the perovskite lattice has also been suggested. Here previous work[10,11] examining anion (F^- and O^{2-}) migration through perovskite lattice has implied that this process occurs i) via a vacancy mechanism, and ii) most readily along the <110> edges of the BO_6 octahedra. Here it was shown that the saddle point for ionic migration between two anionic sites occurs via a triangle formed by two A site cations and a B site cation (Figure 7). The radius of a circle just touching the radii of these three cations is defined as r_c. We have calculated r_c values for

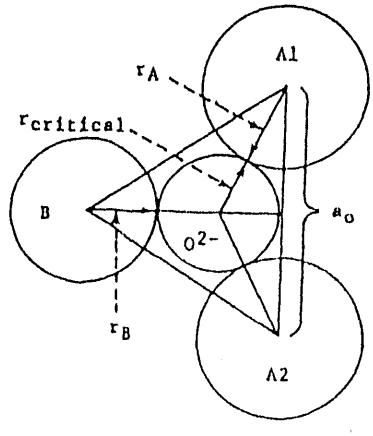

$$r_{critical} = \frac{r_A^2 + \frac{3}{4}(a_o^2) - \sqrt{2}(a_o)(r_B) + r_B^2}{2(r_A) + \sqrt{2}\,a_o - 2(r_B)}$$

Figure 7. Geometry and calculation used for determining $r_{critical}$. (O^{2-} not to scale.)

over 400 ($A^{3+}B^{3+}O_3$ and $A^{2+}B^{4+}O_3$) perovskites and found that the value of this parameter does not exceed 1.1Å while ionic radii for, respectively, OH^- and O^{2-} correspond to 1.37 and 1.4Å. Thus, the crystallographic dimensions of the A-A-B saddle point through which migration proceeds would reasonably be expected to influence E_a.

With this thought in mind we have plotted E_a for O^{2-} (or OH^-) migration through the perovskite lattice versus r_c for known O^{2-} (or OH^-) conducting perovskite electrolytes. Since r_c for OH^- and O^{2-} are so close, general trends found for perovskites conducting either one or both of these species and E_a would be similar. Results assuming O^{2-} conduction in all these perovskite lattice are shown in Figure 8. Here E_a for anion migration appears to depend upon the level of constriction it encounters at the AAB saddle point. Again in an analogous manner to the previously discussed FV case, a distinct difference is experimentally observed between $A^{2+}B^{4+}O_3$ and $A^{3+}B^{3+}O_3$ perovskites where higher E_a values are observed for the latter materials which, in fact, would be expected to possess a more open lattice. This may signify increasing E_a control by solid-state host lattice polarization phenomenon towards the mobile anion.

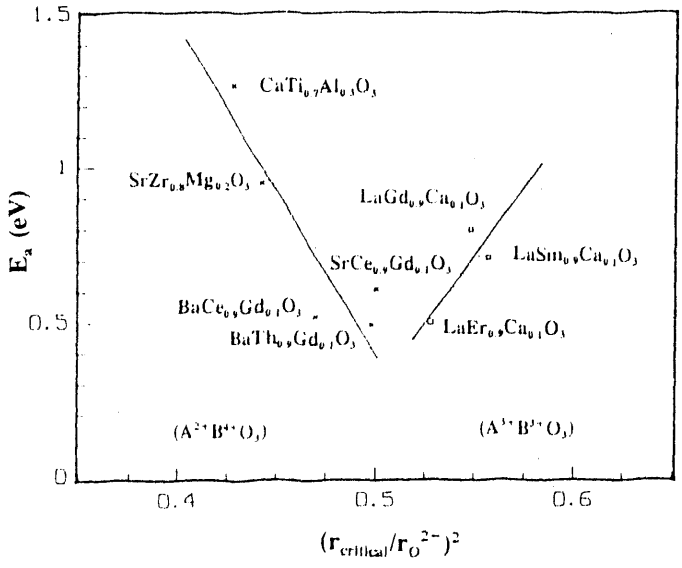

Figure 8. Comparison of $(r_{critical}/r_O^{2-})^2$ vs E_a for O^{2-} migration through perovskite lattice having constricted $(r_{critical}/r_O^{2-})^2 < 0.5$, $A^{2+}B^{4+}O_3$) and open $(r_{critical}/r_O^{2-})^2 > 0.5$, $A^{3+}B^{3+}O_3$ for A-A-B saddle points.

D. Perovskite Lattice Polarizability.

The influence of solid electrolyte lattice polarizability upon anion migration has also been studied. Here lattice polarizability can be calculated from the relationship:[12]

$$\frac{\alpha_c}{\alpha_f} = \left(\frac{r_c}{r_f}\right)^3 \qquad (5)$$

where α_c is the electric polarizability of the ion in the ionic lattice of interest, and α_f is the calculated electronic polarizability given from the quadratic Stark effect[13] by:

$$\alpha_f = \frac{c}{Z - S_R} \text{ and } S_R = S_{RO} - (Z - Z_o)\Delta S_R \qquad (6)$$

Many solid-state ionic lattice electronic polarizabilities have been shown to be additive. For perovskites it has been shown that:[14]

$$\alpha_{ABO_3} = \alpha_A^{2+} + \alpha_B^{4+} + 3\alpha_O^{2-} \qquad (7)$$

By plotting polarizability (Å^3) versus E_a (Figure 9), we see that activation energy for anion migration decreases upon increasing lattice polarizability leading, in principle, to materials possessing high ionic conductivity.

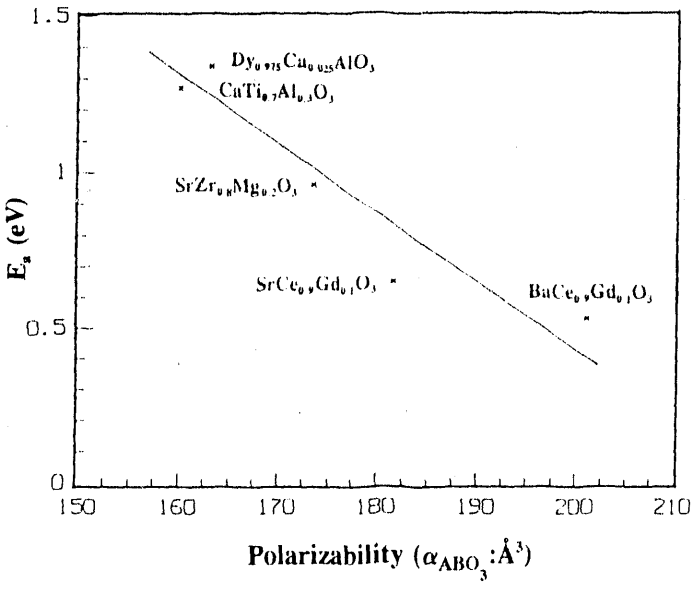

Figure 9. Correlation of lattice polarizability with activation energies for O^{2-} migration in perovskites.

E. Support for OH^- Conduction in 'Proton' Conducting Solid Electrolytes.

Both O^{2-} and OH^- have nearly identical radii corresponding to 1.4 and 1.37Å, respectively. Hence, migration through the perovskite lattice by these two negatively charged species might be expected to result in somewhat similar conductivities. If OH^- is the species responsible for ionic conduction when experimental conditions favor proton conduction in these perovskite solid electrolytes, then one might search for evidence implying a somewhat weak association by this species with the bulk perovskite lattice. Evidence in support of this expectation is as follows:

- For acceptor doped $KTaO_3$ which is a known proton conductor, both H and D directly introduced into single crystal material[15] give rise to very sharp IR spectra at, respectively, 3472cm^{-1} (OH^-) and 2565cm^{-1} (OD^-). Furthermore, these stretching frequencies seemed to be unaffected by the presence of dopants Cu^{2+}, Fe^{3+} or Ni^{3+} introduced into the bulk perovskite lattice, suggesting little direct association between OH^- and OD^- and the bulk lattice.
- EPR spectra performed on Fe^{3+} in Fe^{3+} doped $KTaO_3$ has been found to be significantly changed under conditions which experimentally resulted in either the incorporation or removal of OH^- from the perovskite lattice.[16]
- The spectroscopic constants found for hydroxyl ions from H, D and T in $KTaO_3$ gave IR bands at 77°K due to OH^-, OD^- and OT^- which were found to be extremely narrow, suggesting that interactions between the hydroxyl ions and the surrounding perovskite lattice were weak.[17] In fact, no other IR transitions in the solid-state have been reported as narrow.
- Hydrogen could be directly incorporated as OH^- into Fe^{3+} doped $KTaO_3$ by heat treatment of the latter in H_2O vapor, air or H_2. Heat treatment in Ar or O_2 resulted in removal of OH^- from the perovskite crystal.[18]

The above discussion is supportive of OH^- being the conducting species in perovskite solid electrolytes under experimental conditions conducive to proton mediation.

F. Summary

For the prototype perovskite solid electrolyte $BaTh_{0.9}Gd_{0.1}O_3$, ionic conductivities (predominantly OH^-) up to 8.7 x $10^{-2}\Omega^{-1}cm^{-1}$ at 550°C and $10^{-1}\Omega^{-1}cm^{-1}$ at 600°C were measured. Perovskite lattice parameters which favored low activation energies for anion migration included 1) that the overall lattice possess a moderate metal-oxygen binding energy, 2) perovskite solid electrolytes possess free volumes 50-57Å^3, 3) that the lattice minimally polarizes the mobile anion, and 4) pre-

ferred $(r_{critical}/r_O^{2-})^2$ ratios for A-A-B saddle points $\cong 0.5$. High ionic conductivities were also achieved for the perovskite related brownmillerites $Sr_2Gd_2O_5$ and $Sr_2Dy_2O_5$ which possessed a high intrinsic population of anion vacancies in their lattice and demonstrated respective ionic conductivities of 2 and 3.65 x $10^{-2}\Omega^{-1}cm^{-1}$ at 600°C. Unoptimized fuel cells were experimentally shown to deliver current densities $\cong 200mA/cm^2$ at 0.7V and 600°C.

FUTURE WORK

This will be addressed by i) selecting an optimum perovskite related solid electrolyte, ii) optimize preparation techniques for perovskite solid electrolytes and other components to be incorporated into the intermediate temperature fuel cell, iii) perform an in-depth electrochemical study on fuel cells incorporating preferred selected solid electrolytes and electrocatalysts, and iv) incorporate preferred components into a fuel cell stack which will be subjected to extensive performance testing at intermediate temperatures.

REFERENCES

1. R.L. Cook and A.F. Sammells, Solid State Ionics, accepted for publication (1991).
2. P. McGeehin and A. Hopper, J. Mater. Sci., 12, 1 (1977).
3. J.B. Goodenough, Proc. Royal Soc., (London), A393, 215 (1984).
4. J.A. Kilner and R.J. Brook, Solid State Ionics, 6, 237 (1982).
5. A.A. Appen, V.B. Glushkova and s.S. Kayalove, Izv. Akad. Nauk SSR Neorgan. Mater., 1, 576 (1965).
6. R.J.H. Voorhoeve, J.P. Remeika and L.E. Trimble, Ann. N.Y. Acad. Sci., 272, 3 (1976).
7. R.D. Shannon, Acta. Crystallogr., A32, 751 (1976).
8. O. Fukunaga and T. Fujita, J. Solid State Chem., 8, 331 (1973).
9. V.M. Goldschmidt, Akad. Oslo I, Mat. Natur., 2, 7 (1926).
10. J.A. Kilner, P. Barrow and R.J. Brook, J. Power Sources, 3, 67 (1978).
11. J.A. Kilner, Philosophical Magazine, 43, 1473 (1981).
12. J. Shanker and S.K. Agarwal, J. Phys. Chem. Solids, 37, 443 (1976).
13. L. Pauling, Proc. Roy. Soc., London, A114, 181 (1927).
14. S. Roberts, Phys. Rev., 76, 1215 (1949).
15. H. Engstrom, J.B. Bates and L.A. Boatner, J. Chem. Phys., 81, 2528 (1984).
16. M.M. Abraham, L.A. Boatner, D.N. Olson and U.T. Hochli, J. Phys. Chem., 81, 2528 (1984).
17. H. Engstrom, J.B. Bates and L.A. Boatner, J. Phys. Chem., 73, 1073 (1980).
18. R. Gonzalez, M.M. Abraham, L.A. Boatner and Y. Chen., J. Phys. Chem., 72, 660 (1983).

Planar Solid Oxide Fuel Cell Technology

CONTRACT INFORMATION

Contract Numbers	DOE DE-FG01-90ER81010 EPRI RP8002-26
Contractor	Ztek Corporation 460 Totten Pond Road Waltham, MA 02154 (617) 890-5665
Contractor Project Manager **Principal Investigator**	Michael Hsu Michael Hsu
Project Managers	METC William I. Huber EPRI Richard H. Goldstein
Period of Performance	July 23, 1990 to April 30, 1991
Schedule and Milestones	FY90-91 Program Schedule

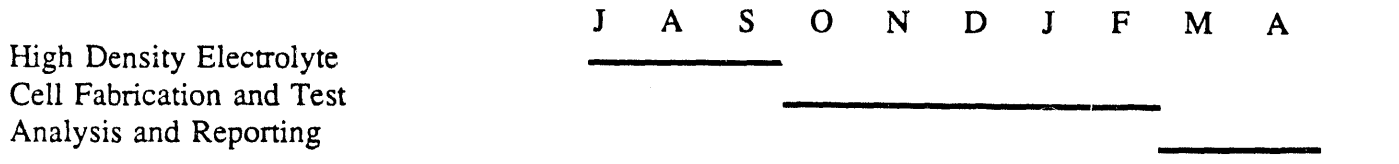

OBJECTIVES

The successful implementation of solid oxide fuel cells (SOFC) in the power generating industry will require a reliable device that can be fabricated at low cost, scalable to the desired size by incorporating modularized construction, and demonstrate high performance in operation.

The objective of this project is to develop advanced fabrication technique and configuration, leading to cost reduction while achieving high performance.

BACKGROUND INFORMATION

Among the three cell configurations current under development in the SOFC industry, namely the planar, the tubular and the monolithic designs, Ztek has been pursuing the planar approach which has the potential to be the most viable technology to compete in cost, performance, reliability and scalability for commercial applications. Listed below are the distinctive ceramic techniques associated with the three general approaches:

Configuration	Feature Technique
• Tubular	• EVD
• Monolithic	• Tape Co-firing
• Planar	• Plasma Deposition
	Tape cast

Ztek's planar stack has been under development since 1975, Ref. 1,2,3,4,5,6. The patented Ztek baseline technology comprises:

- Free-standing electrolyte plate with electrode coatings
- Free-standing interconnector plate
- Internal manifolding
- Seal by compression contact and flux

A prototype stack of 10 cells was successfully constructed and thoroughly tested. In the continuing effort for cost reduction and performance enhancement, an advanced method suitable for fast turn-around, mass production of the free-standing electrolyte/electrodes plate was evaluated in this effort. The results are reported here.

PROJECT DESCRIPTION

Tri-layer plates were fabricated by an advanced technique, in which the three components (electrode/electrolyte/electrode) of drastically different fabrication characteristics were formed in consecutive steps in a single fabrication setup. For cost considerations, no post process action was applied. The challenge of this task was in forming intact dense electrolyte layer over a surface up to a 12cm diameter. Furthermore, as an interim step of forming the electrolyte layer in the fabrication sequence, it should not affect the formation states of the electrodes. Mechanical and fuel cell tests were carried out for material characterization. The cell performance was evaluated utilizing a fuel cell diffusion analysis.

RESULTS

During this effort, Ztek has successfully made dense yttria-stabilized zirconia electrolyte layers of large size (12cm in diameter) using the advanced technique. The cross-sectional micrograph of a tri-layer plate is shown in Figure 1, where the thickness of the electrolyte layers is about 150um. No cracks are visually detectable either at the interfaces or in the material bulks. The results indicate generally that the adhesion between the electrolyte layer and the electrode layer is strong and that the electrolyte layer has good mechanical integrity. The electrolyte exhibits extremely fine pore structure. Visual pore analysis has classified it at 0.98 volumetric density. The thermal/structural property of the electrolyte plate as determined from flexural measurement is shown in Figure 2. The electrolyte is capable of sustaining an in-plane temperature difference of 200°C, a requirement in realistic power device design.

Based on the open circuit voltage measurements as shown in Figure 3, the effect of gas cross-over through the tri-layer plate, represented by the voltage reduction from the theoretical value, is at an acceptable level as the electrolyte thickness is greater than 150um. The measured power output, the current-voltage characteristics, is shown in Figure 4, which indicates that the performance reduction due to the gas cross-over of a 200um thick electrolyte is minimal under a current loading condition. At 200mA/cm^2, the overvoltage induced by the gas cross-over is estimated to be 12mV. The cell exhibits a resistance of 1.1 Ohm/cm^2. The overall technical accomplishments are summarized below:

1. Tri-layer plates (cathode/electrolyte/anode) of 12cm diameter have been fabricated with facility suitable for mass production.

2. The tri-layer plates have demonstrated to simultaneously satisfy the following conditions:

   - Low gas cross-over
   - High surface power density
   - Good thermal shock resistance
   - Excellent structural integrity

Based on the procedures developed in this effort, the advanced technique can be further developed into an economical, high yield process for mass production of the planar solid oxide fuel cells.

FUTURE WORK

The continuing effort will apply the state-of-the-art fabrication technique and configuration in a prototype demonstration, leading toward the product commercialization. The immediate emphases are:

- Perform extended test on components and prototype stack.
- Design scalable module suitable for field applications.
- Establish cost data on module construction and system integration for near term commercial applications.

REFERENCES

1. "High-Efficiency Electrochemical Plant," M. Hsu, et al., Record of the 10th Intersociety Energy Conversion Engineering Conference, University of Delaware, Aug. 1975.
2. "Electrochemical Power and Hydrogen Generation from High Temperature Electrolytic Cells, " M. Hsu and T.B. Reed, Record of the 11th Intersociety Energy Conversion Engineering Conference, State Line, NV, Sept. 1976.
3. "Status of Solid-oxide Fuel Cell Development at Lincoln Laboratory," M. Hsu, Lincoln Labs. Technical Memorandum, 16 Nov. 1981.
4. "Zirconia Fuel Cell Power System," M. Hsu, National Fuel Cell Seminar, Tucson, AZ, May 1985.
5. "Zirconia Fuel Cell Power System, Planar Stack Development," M. Hsu, Fuel Cell Seminar, Tucson, AZ, Oct. 1986.
6. "Planar Solid Oxide Fuel Cell Technology, Cell Stack Test and Evaluation," M. Hsu, Fuel Cell Seminar, Long Beach, CA, Oct. 1988.
7. "Planar Solid Oxide Fuel Cell Development," M. Hsu, EPRI Report GS-6504, prepared by Ztek Corporation, Oct. 1989.
8. "Planar Solid Oxide Fuel Cell Technology Development," M. Hsu, Fuel Cell Seminar, Tucson, AZ, Nov. 1990.

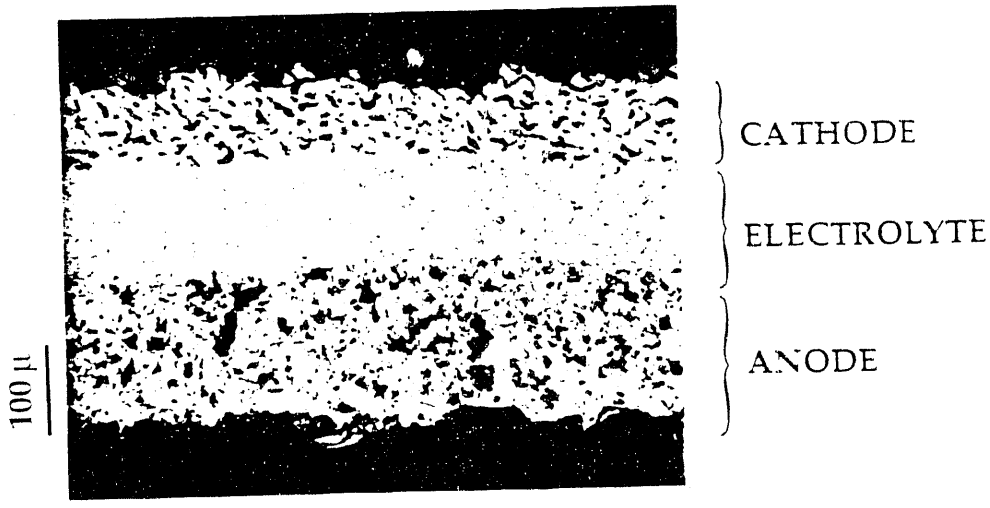

Figure 1 Cross-Section of the Tri-Layer Plate

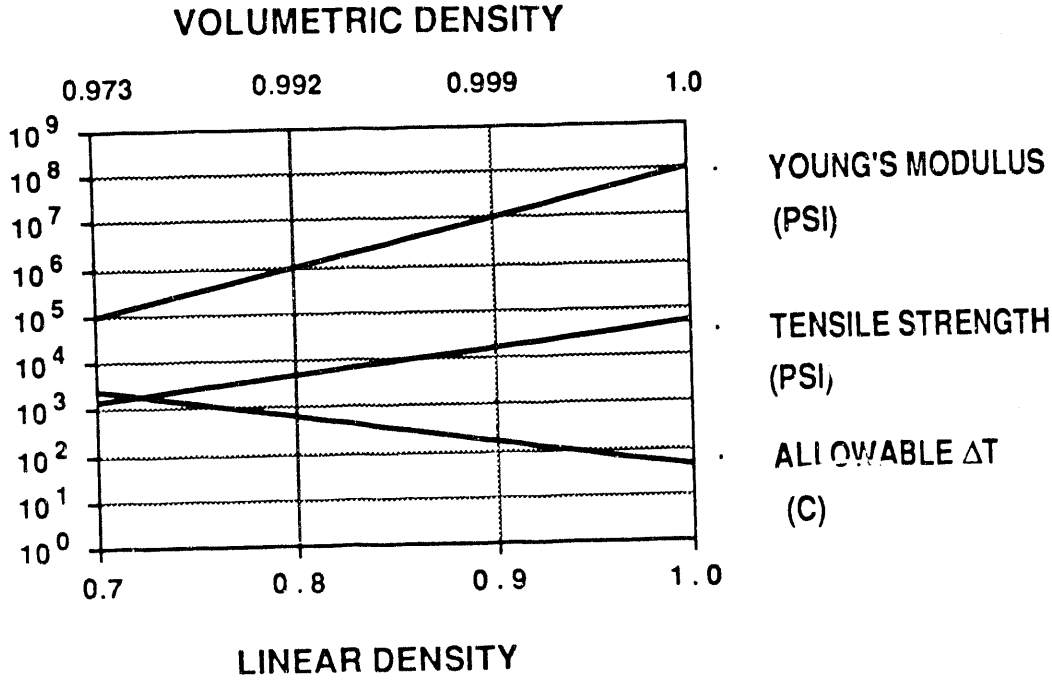

Figure 2 Material Properties Correlation - Zirconia Electrolyte

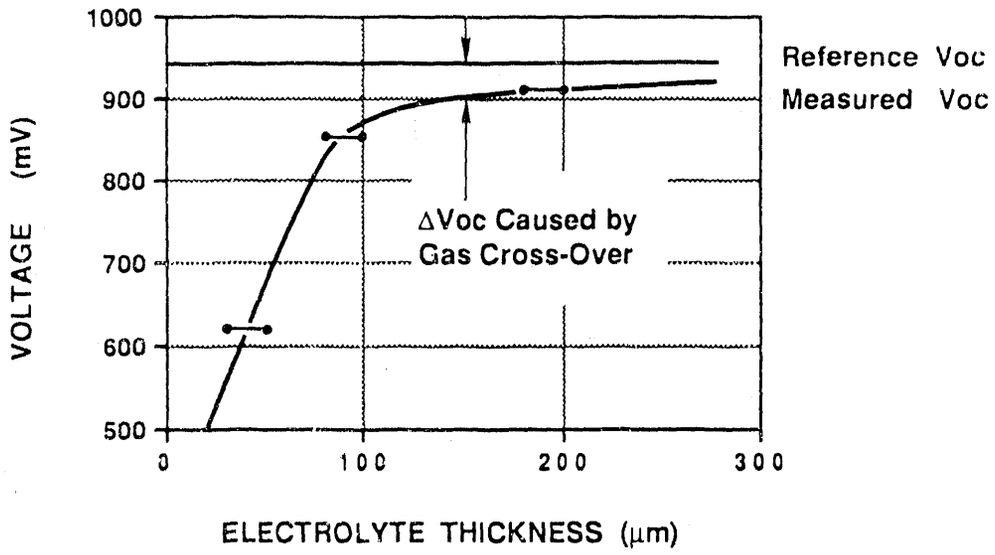

Figure 3 Measured Open Circuit Voltage - Tri-Layer Plate

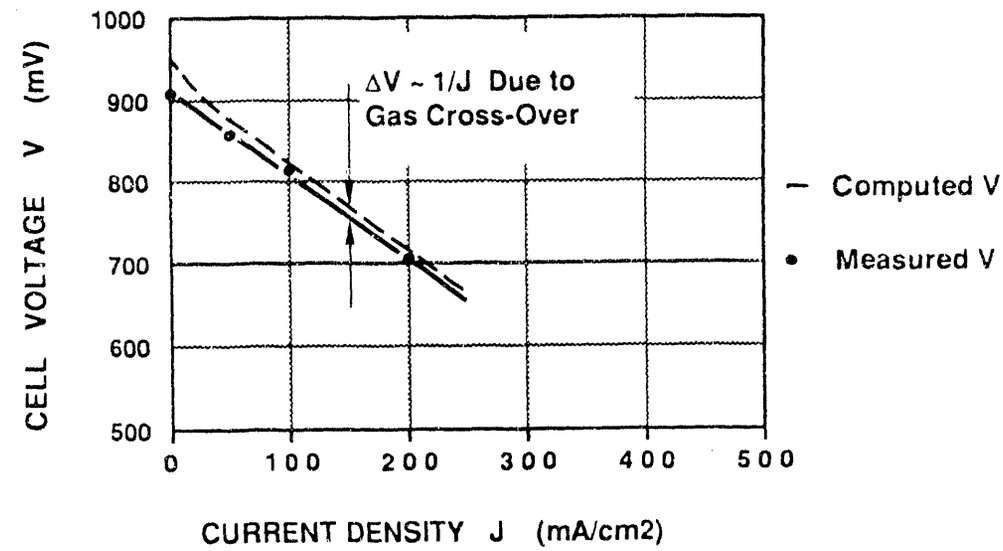

Figure 4 I - V Characteristics - Tri-Layer Plate

Sealant Research for SOFC

CONTRACT INFORMATION

Contract Number	49638
Contractor	Argonne National Laboratory 9700 South Cass Avenue Argonne, IL 60439 (708) 972-4516
Contractor Project Manager	Kevin M. Myles
Principal Investigators	Ira Bloom and Michael Krumpelt
METC Project Manager	William J. Huber
Period of Performance	February 1, 1991 through April 1, 1991

Schedule and Milestones

FY91 Program Schedule

	S	O	N	D	J	F	M	A	M	J	J	A	S
Glass Sealants													
Ceramic Sealants													
Commercial Sealants													

OBJECTIVES

The objective of the sealant work is to develop materials that can form gas-tight seals in a solid oxide fuel cell (SOFC). These materials must be chemically and thermally stable at 1000°C in H_2, O_2, and water vapor and must be compatible with the fuel cell components. The key to the development of suitable sealing materials is the matching of chemical and thermal properties of the materials involved.

BACKGROUND INFORMATION

Solid-oxide fuel cells are potentially more durable than other types of fuel cells because the solid electrolyte cannot evaporate, corrode, or leak and should achieve a long and

trouble-free service life. SOFCs have the additional advantage of being able to run directly on hydrocarbon and CO fuels. This, in turn, simplifies system design and assures lower capital cost. However, state-of-the-art SOFCs operate at 1000°C. At that rather high temperature, it is difficult to find materials to seal the edges and the manifolds of the fuel cell stack.

To circumvent this problem, cell designs that do not need seals have been developed. Because an engineering approach was used to solve a materials problem, however, the cell has become complicated and expensive. As fuel cells approach commercialization, new, less-expensive designs are being proposed. The monolithic SOFC and several flat-plate configurations are good examples. In these cell configurations, gas-tight seals have to be formed at the edge of each electrode and between the manifold and the stack.

In general, the sealant material (hereafter called "cements") must be compatible with the cell components and with the fuel cell environment. For example, the cement must not only be chemically compatible with the cell components for good wetting, but also have a coefficient of thermal expansion (CTE) similar to that of the cell component. If the cement has these properties, several mechanical failure routes may be eliminated.

PROJECT DESCRIPTION

The scope of this project includes the evaluation of commercially available cements and novel cement materials. There are three basic groups of novel cement materials according to their as-applied state: polycrystalline (heat and water-activated), glassy, and a composite of the two. During the course of seal formation, the exact nature of the material may change. This possibility will be addressed if it arises in tests of seal formation.

During the initial part of the project, the cement itself and the seal that it makes to anode, cathode, and interconnect materials, as well as to their pairwise combinations, will be characterized by standard electrochemical and materials science methods. At present, it is unknown whether one material can form an acceptable seal between all these combinations of materials. A family of materials may have to be developed to be compatible with implicit differences in materials and their related surface chemistries.

RESULTS

Commercial cements

As the first step in finding a suitable sealant for the solid oxide fuel cell, we completed a comprehensive survey of commercially available high-temperature cements. Many commercial high-temperature cements are available, but most contain high levels of SiO_2 (~10-50 wt%). Because SiO_2 is volatile under reducing conditions and can contaminate fuel cell components, these cements were considered unacceptable and were not obtained for testing. Two commercial cements rich in calcium aluminate have been obtained and are being tested. These cements have been used to bond together fired disks of electrolyte, anode, and cathode materials. After curing, the bonded disks were heated to 1000°C and held for 24 h. In both cases, strong bonds were formed. While the thermal expansions of the cements have not yet been measured, no problem was encountered with cracking of the disks, suggesting that a mismatch in thermal expansion is not a serious problem.

Novel materials

Reactive glasses were selected as the first novel material to evaluate. The glasses should be chemically compatible with the fuel cell gases and both chemically and thermally compatible with the ceramic components of the cell. Chemical compatibility with cell gases implies that, for example, the activity of SiO_2 must be kept low in these materials. The glass must also form the seal at temperatures below the sintering temperatures needed to form the component.

Three different glass compositions (designated A, B, and C) were made and characterized in terms of their CTEs and their compatibility with yttria-doped ZrO_2, the present electrolyte material in SOFCs. A plot of their relative thermal expansions versus temperature is given in Figure 1. From the figure, it can be seen that the thermal behavior of the three glasses is quite similar, with CTEs in the 7-8 x 10^{-6}/°C range. These CTEs are lower than that for ZrO_2, 10 x 10^{-6}/°C. The wetting angles of these glasses on ZrO_2 were in the range of 15-18°.

Even though the CTEs of the glasses and their wetting angles on ZrO_2 were very similar, the interactions between the glasses and electrolyte material were very different. Under the optical microscope, Glass A was seen to wet the surface of the ZrO_2 coupon very well and formed a thin reaction zone. Glass B had a more extensive reaction zone, which was about 1.5 μm thick. Glass C had the most extensive reaction zone, with clear evidence of intermediate compound formation along the glass-ZrO_2 interface.

As expected, the extent of the interaction between the glass and ZrO_2 is composition dependent. From the above results, finding glasses which are thermally compatible with ZrO_2 is not a problem. Surface and materials chemistry seem to be more important than an exact matching of CTEs. Issues which still need to be addressed include controlling the interaction between the materials and determining compatibility with the other fuel cell components.

FUTURE WORK

Once the bonding characteristics of the commercial cements have been determined, the seals will be tested for integrity under operating conditions. These conditions include thermal cycling and the presence of humidified H_2/O_2.

In the area of novel materials, a material or group of materials that can make a gas-tight seal between fuel cell components will be identified and then tested under similar conditions. It is hoped that one material or group of materials will be shown to be superior to the others.

This work was performed under the auspices of the U.S. Department of Energy under contract No. W-31-109-Eng-38.

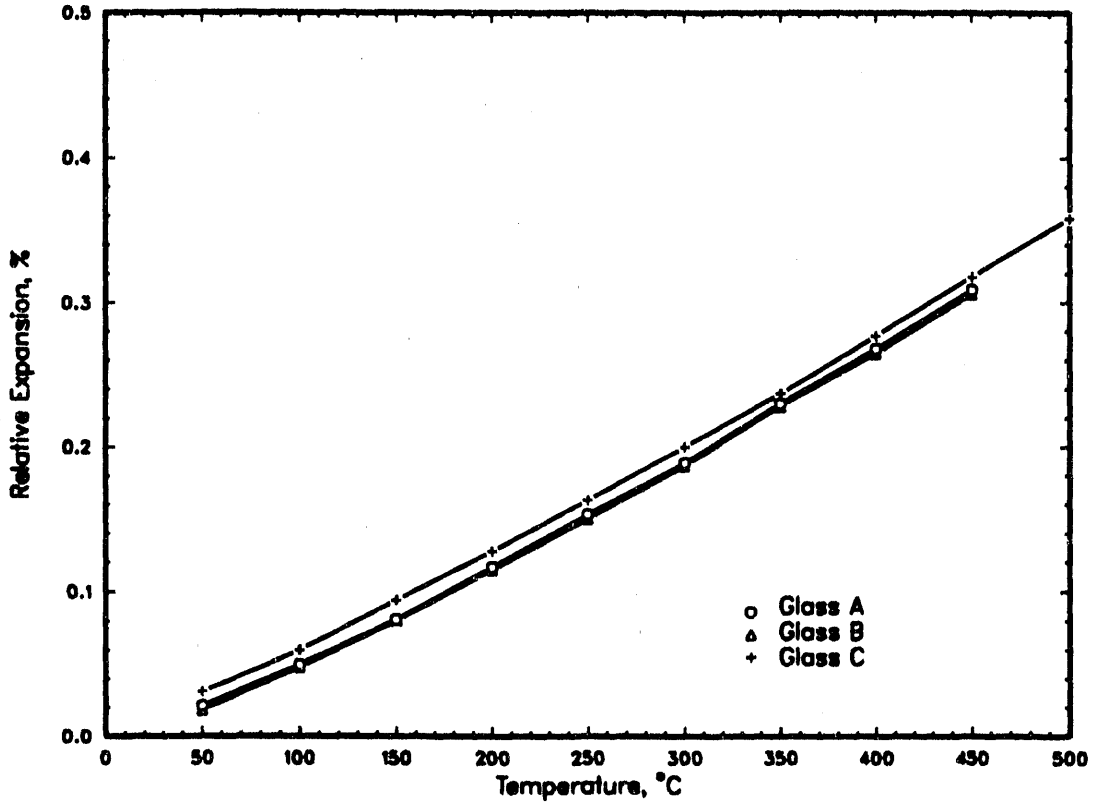

Fig. 1. Relative Thermal Expansion versus Temperature for Glasses A, B, and C. Even though their compositions are different, their thermal behaviors are quite similar.

Progress in MSOFC Technology and Analysis

CONTRACT INFORMATION

Program Title	MSOFC Technology Advancement For Coal-Based Power Generation
Contract Number	DE-AC-21-89MC26006
Contractor	Allied-Signal Aerospace Company AiResearch Los Angeles Division 2525 West 190th Street Torrance, CA 90509
Contractor Project Manager	Dr. Richard A. Gibson
Principal Investigators	Dr. Nguyen Q. Minh
METC Project Manager	Mr. Edmund F. Beyma
Period of Performance	September 27, 1989 to September 27, 1992
Schedule and Milestones	

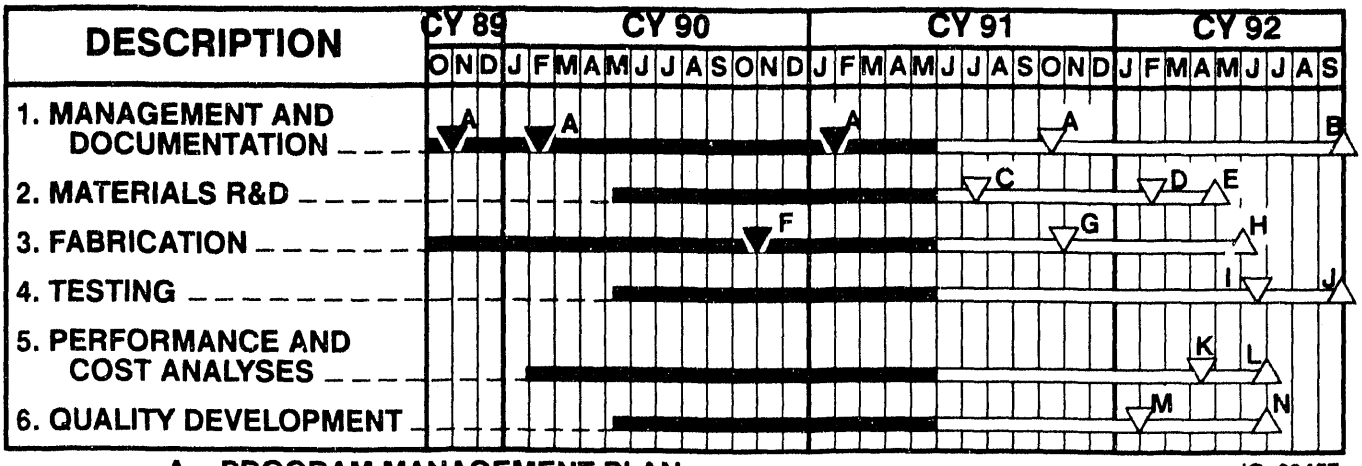

MILESTONES

- A PROGRAM MANAGEMENT PLAN
- B FINAL REPORT
- C INTERIM SPECIFICATION, INTERCONNECT AND CATHODE
- D PRELIMINARY SPECIFICATION, ANCILLARY MATERIALS
- E SPECIFICATION, OPTIMUM MATERIALS AND MICROSTRUCTURES
- F PRELIMINARY SPECIFICATION, MATERIALS AND PROCESSES
- G DEMONSTRATION, 100-W STACK FABRICATION
- H DEMONSTRATION, 250-W STACK FABRICATION
- I DEMONSTRATION, MSOFC LIFE TEST
- J DEMONSTRATION, 250-W STACK OPERATION
- K UPDATED MANUFACTURING COST
- L TOPICAL REPORT, SYSTEM CONFIGURATION AND MARKET ASSESSMENT
- M SPECIFICATION, MICROCRACK CONTROL METHODS
- N NDE METHOD SPECIFICATION

Program Schedule

OBJECTIVES

The overall objective of this program is to advance materials and fabrication methodologies to develop a monolithic solid oxide fuel cell (MSOFC) system capable of meeting performance, life, and cost goals for coal-derived fuel applications. The technical effort of this program is aimed at creating a technology base that will be used to extend MSOFC development from proof of concept toward practical application.

BACKGROUND INFORMATION

The MSOFC is an all-ceramic structure in which cell components are configured in a compact, corrugated array. The MSOFC produces a direct current by electrochemically combining fuel and oxidant across the zirconia solid electrolyte at an operating temperature of about 1000°C. There are two versions of the monolithic fuel cell, coflow (Figure 1) and crossflow (Figure 2). The crossflow approach is used in this program because it is more straightforward to manifold and fabricate. As can be seen from the figures, the MSOFC is made of two types of multilayer structures, each composed of three ceramics—anode/electrode/cathode and anode/interconnect/cathode. The anode/electrolyte/cathode composite represents a single cell. The function of the anode/interconnect/cathode composite is to connect the cells in electrical series to build voltage. In the MSOFC, the anode and cathode layers must be porous to allow gas transport to the reaction sites, while the electrolyte and interconnect layers must be dense to prevent gas mixing. Design goals for layer thicknesses and cell-to-cell distance are 25 to 100 μm and 1 to 2 mm, respectively. The MSOFC design eliminates inactive structural support, increases active surface areas, and lowers voltage losses due to internal electrical resistances. The monolithic fuel cell, thus, has high efficiency, excellent performance, and high power density. The MSOFC can be integrated with coal gasification plants and is expected to have high overall efficiency in the conversion of the chemical energy of coal to electrical energy.

The materials currently used for building the MSOFC are Y_2O_3-stabilized ZrO_2 for electrolytes, Ni/Y_2O_3-ZrO_2 cermet for anodes, doped $LaMnO_3$ for cathodes, and doped $LaCrO_3$ for interconnects. These materials are known to possess adequate levels of conductivity, and they are compatible and stable under cell operating conditions. The challenge is to develop ways to form the materials into thin components and to incorporate these components into the monolithic structure. A fabrication scheme for the MSOFC must incorporate each materials such that none of the fabrication steps will diminish the desired materials characteristics of any of the component layers. The fabrication of the MSOFC must

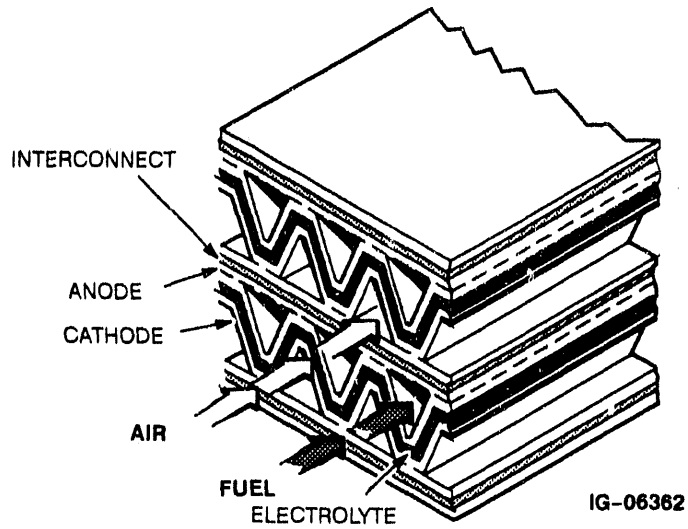

Figure 1. Coflow MSOFC

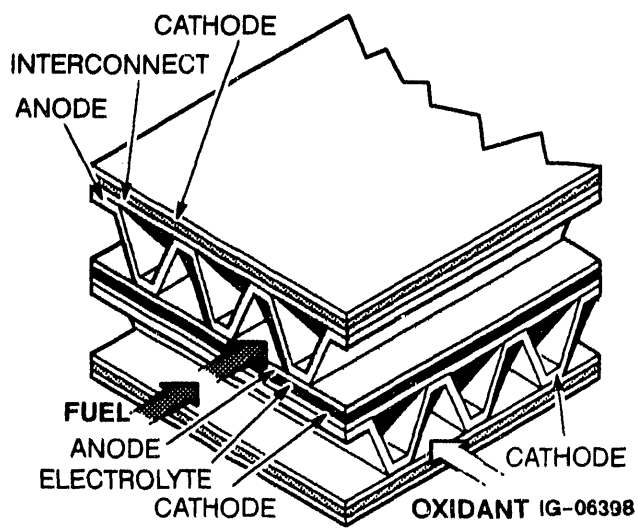

Figure 2. Crossflow MSOFC

achieve the following: (1) high-density electrolyte and interconnect, along with porous anode and cathode layers, (2) good interfacial bonding between adjacent layers, (3) insignificant reaction and interdiffusion between neighboring layers, and (4) a defect-free structure. At present, the development of suitable materials and the fabrication of the intricate structure are the main foci of the MSOFC development effort.

PROJECT DESCRIPTION

This program is performed by a team comprising the AiResearch Los Angeles Division of the Allied-signal Aerospace Company and Argonne National Laboratory (ANL). The technical effort of the program is organized around five work tasks as follows:

(a) Materials research and development: This task concentrates on development of materials suitable for the unique MSOFC structure and environment. The work addresses several identified material issues such as interconnect sinterability, material stability and performance (especially in coal gas), and current collector materia s.

(b) Fabrication: This task is aimed at demonstrating MSOFC fabrication and fabrication reproducibility and reliability. The fabrication process will be scaled up to produce MSOFC stacks of increasing power output. This effort also involves definition of optimal fabrication parameters, defect analysis, development of material and process specifications, and material supplier identification.

(c) Testing: This task verifies the performance and life of the MSOFC with coal-derived fuels. MSOFC cells and stacks are tested under specified conditions, and posttest analyses are carried out to provide information for explaining observed behavior and identifying degradation mechanisms.

(d) Performance and cost analysis: This task involves performance, system, and cost analysis of the MSOFC in coal-based applications. The emphasis of performance analysis is on development of an MSOFC performance model. System and cost analysis defines MSOFC system configurations and MSOFC manufacturing and system costs.

(e) Quality development: This task concentrates on developing methods for ensuring the quality of fabricated MSOFC stacks. This effort involves evaluation of NDE methods, stress analysis, and microcrack control.

The overall program is expected to resolve several material and fabrication issues and to result in a technology base that will be used to bring the MSOFC technology toward practical application.

RESULTS

The team's approach to MSOFC development involves tasks undertaken at several different levels, as follows:

- Fabrication of single cells and stacks for performance and structural evaluation
- Off-line analysis and testing for resolving key technology issues identified during performance and structural evaluation
- Applied research for long-term basic technology development to improve MSOFC performance, life, and robustness, and reduce costs

Recent effort in MSOFC development has centered on development of material, processes, and techniques for fabricating MSOFC stacks. The two key issues are the development of a suitable integral interconnect and the development of MSOFC structures that incur minimal damage during firing. Two approaches for the development of an integral interconnect are being pursued, cosintering and two-step co-firing. In the cosintering interconnect approach, the MSOFC stack is fired as a single monolithic structure. In the two-step co-firing process, interconnects and single-cell modules are fired separately, and then assembled with a bonding formulation and fired a second time, forming a monolithic structure.

Progress made at each of the three levels is discussed below.

Fabrication Effort

During the past year, fabrication of defect-free single cells (anode/electrolyte/cathode trilayer discs) has become routine. Also, defect-free single-cell modules (trilayer cells with top and bottom corrugated electrodes) are produced with high yield. However, when top and bottom cathode and anode flat plates are cosintered with the single-cell module (forming a so-called single-cell stack), the number of defects significantly increases.

The most serious defects observed are fracturing of the cathode and anode at the electrode corrugate-trilayer (A/E/C) interface. This leads to high internal resistance and poor cell performance. To analyze this problem and suggest solutions, a stress model was developed to predict

stress levels throughout the stack incurred during the cool-down phase of the firing cycle, when stresses are believed to be highest.

Currently, AiResearch is attempting to experimentally verify its analytical results by incorporating design changes suggested by model predictions into single-cell stacks. Recently, using model guidelines to redesign the stacks, cell fracturing has been reduced (Figure 3). The performance of the improved single-cell stacks is currently under evaluation.

Off-Line Analysis and Testing

The key to fabricating stacks via the two-step cofiring process is to find a strong, conducting bond for assembling the single-cell modules and interconnects. Identifying and characterizing these bonding formulations has been the subject of a set of designed experiments at AiResearch. Several bonding formulations were evaluated in a set of 18 experiments to test the effects of seven key factors on the strength of the bond and its conductivity. The best bonding formulation was then incorporated in a two-cell stack. The performance of this stack is currently under evaluation at AiResearch.

To analyze MSOFC system performance, a comprehensive, accurate stack model is essential. A stack model originally developed at ANL has been upgraded to include operation on coal gas as well as hydrogen and provide more accurate heat transfer calculations. The simulated performance of a stack is displayed in Table 1. The program also makes three-dimensional plots of the current density, fuel partial pressure, Nernst potential, and electrolyte temperature. A plot of the current density for the simulated stack is displayed in Figure 4.

The long-term stability of the cathode was determined by analysis of ac impedance tests on cathode/electrolyte/cathode composites (Figure 5). Analysis of the test results predicts a fuel cell performance degradation of less than 15 percent after 23,000 hr of operation.

Applied Research

A key hurdle in fabricating multicell stacks via the cosintering process is the development of an interconnect that will densify at moderate temperatures ($\leq$ 1400°C) in air. The approach has been to use dopants and sintering aids to form a liquid phase to enhance the sintering process. It has been found that doping $LaCrO_3$ with calcium and cobalt produces interconnect material which, when fired by itself, meets the above criteria. However, when the interconnect is fired with adjacent anode and cathode layers, the interconnect does not densify and morphological changes occur in the anode and cathode. Recently,

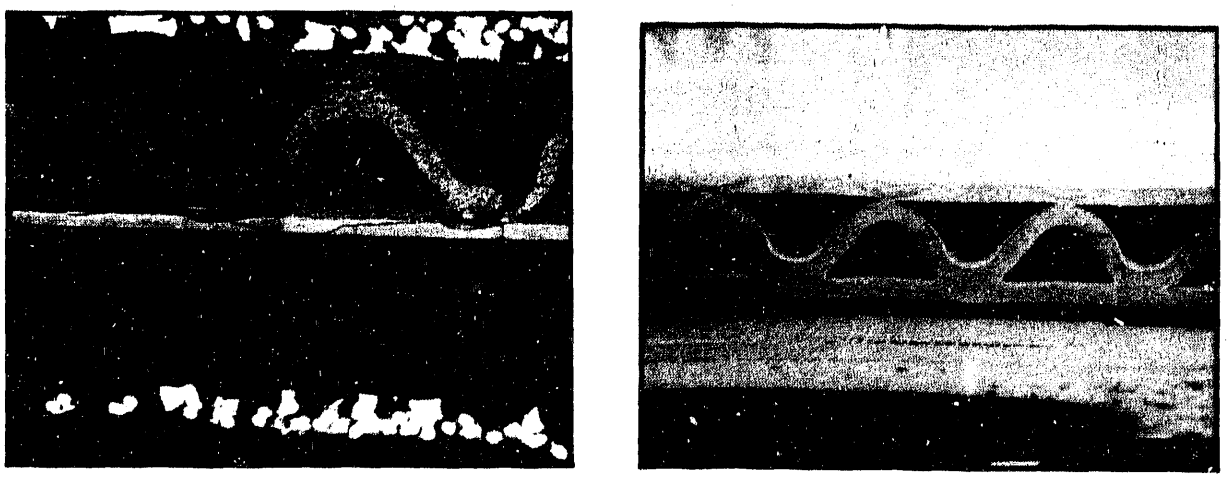

Figure 3. Better Single-Cell Stack Design has Led to Reduced Cell Fracturing

Table 1. Selected Results from a Stack Model Simulation

Item	Results: Coal Gas	Results: Humid H_2
Cell dimensions, cm x cm	9 x 9	9 x 9
Fuel flow rate, l/hr	9.5	11.5
Fuel composition, vol percent:		
H_2	33	97
H_2O	17	3
CO	15	—
CO_2	27	—
CH_4	8	—
Airflow rate, l/hr	281	433
Cell voltage, v	0.75	0.75
Fuel utilization, percent	85.0	85.0
Maximum temperature, °C	1050	1050
Cell efficiency, percent	46.7	49.5
Fuel efficiency, percent	55.0	58.2
Average Nernst potential, v	0.839	0.883
Average current density, ma/sq cm	192	280
Gross power, w (per cell)	11.6	17.0
Net power, w (per cell)	11.4	16.3

AiResearch has made encouraging technical progress with a new proprietary, interconnect formulation. With this approach, the interconnect will densify with adjacent (porous) anode and cathode layers (Figure 6). Currently, AiResearch is evaluating the resistivity and materials compatibility of this promising new material.

FUTURE WORK

Future plans include progress toward a 100-W-Class stack via both two-step co-firing and cosintering interconnect processes. An updated assessment of the costs of producing MSOFC stacks will be performed, building on the study completed in the previous program with METC. Life testing of stacks and an evaluation of NDE methods will also be performed in the near future.

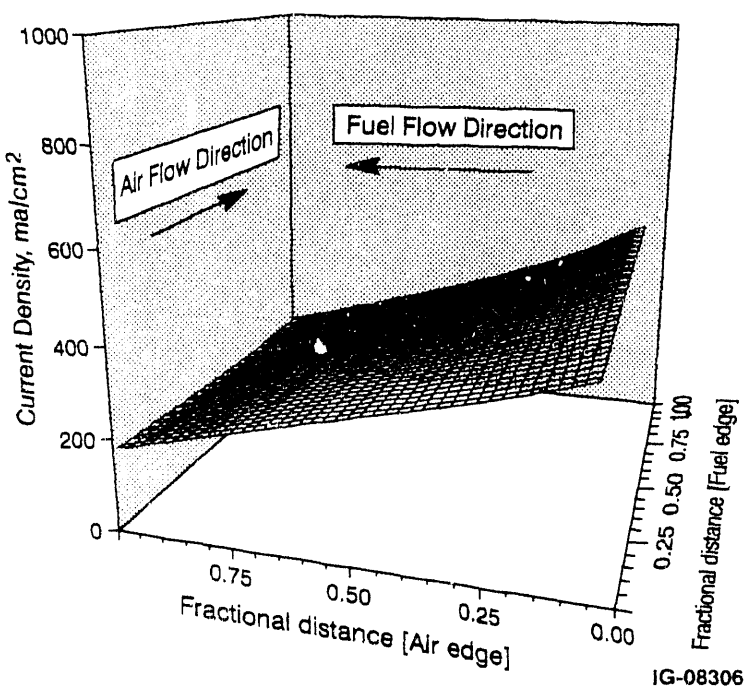

Figure 4. A Comprehensive Stack Performance Model Has Been Developed

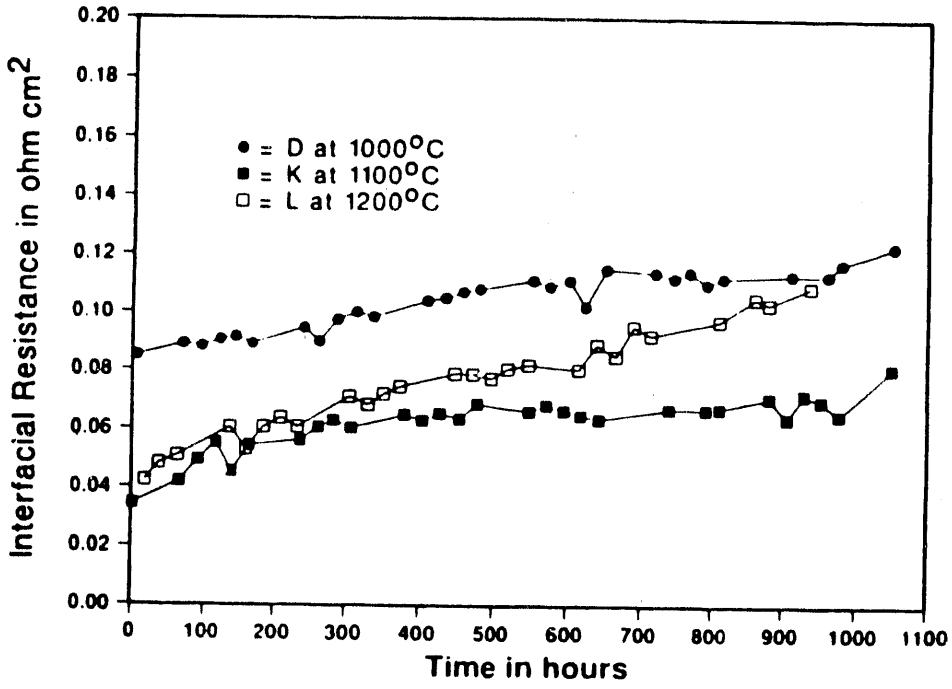

Figure 5. Long-Term Cathode Stability is Shown by Test Data

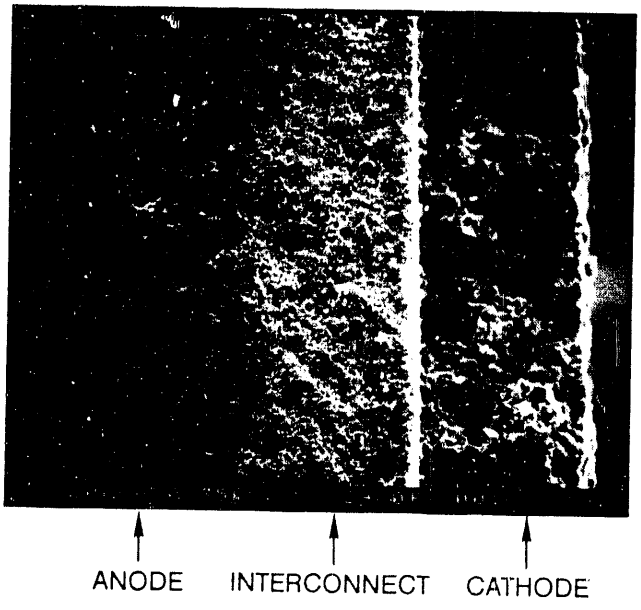

Figure 6. Anode/Interconnect/Cathode Trilayer Showing Dense Interconnect and Porous Electrodes

Session 3

Phosphoric Acid Fuel Cells

Advanced Water-Cooled Phosphoric Acid Fuel Cell Development

1. CONTRACT INFORMATION:

Contract Number: DE-AC21-88MC24221

Contractor: International Fuel Cells Corporation (IFC)
P.O. Box 739
195 Governors Highway
South Windsor, CT 06074
(203) 727-2212

Contractor Program Manager: Fred S. Kemp

Principal Investigators: Glenn W. Scheffler

METC Project Manager: Edmund F. Beyma

Period Of Performance: April 1988 to April 1992

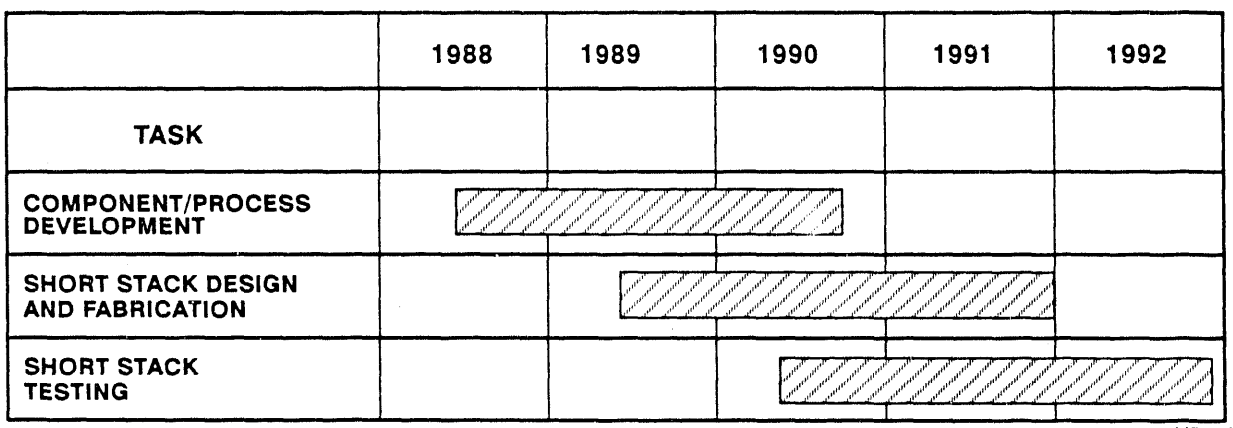

HP265
R911005

2. OBJECTIVES

The objective of this research and development effort is to improve the performance and minimize the cost of the existing water-cooled electric utility, phosphoric acid fuel cell stack technology. The improved stack technology shall be capable of demonstrating a power density of at least 175 watts per square foot over a 40,000 hour useful life and a projected manufactured cost of less than $400 per kilowatt in initial production.

3. BACKGROUND

An advanced phosphoric acid fuel cell design was developed and verified in DOE Contract DE-AC21-82MC24222. This effort was part of an atmospheric pressure on-site fuel cell technology development program which was jointly funded by DOE and the GAS RESEARCH INSTITUTE (GRI). The key feature of this design is that low cost cell component materials are utilized without compromising performance. Other features associated with this design are an ad-

vanced separator and a thin matrix which contribute to additional cost reduction and improved performance. The new cell concept has been fabricated into short stacks with small area (3-5 ft^2) cells and successfully operated at ambient pressure conditions.

4. PROGRAM DESCRIPTION

A conceptual design was created to guide the development effort toward the program goals. The design uses 10-ft^2 cells operating at 300 watts per square ft to meet the manufactured cost goal for electric utility applications. As shown in Figure 1, 300 watts per square foot is equivalent to 400 ASF at 0.75 volts per cell with the projected performance of pressurized cells. This design is periodically updated as the technology developed in the early phases of the program are incorporated into short stacks for evaluation.

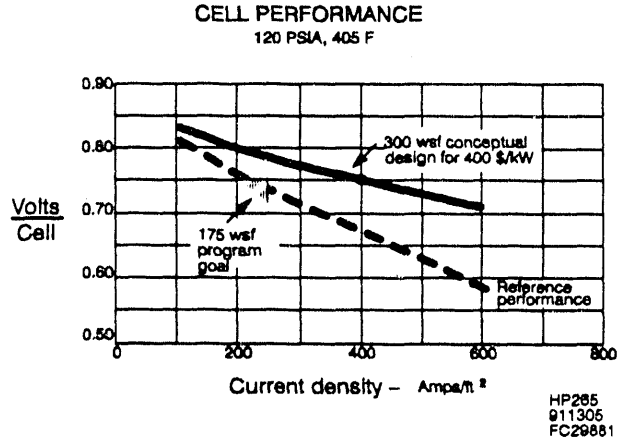

Figure 1. Power Density Goal

The technology effort included both component and process development. The goals of these activities were directed toward reducing the processing cost of cell components, improving the integrity of cell parts for pressurized operation, and scaling up for the manufacture of the larger electric utility size 10-ft^2 parts. Component development consisted of the examination of alternative cell material such as substrate precursors, commercially available components and alternative resin system for graphite components, and the verification of promising configurations in subscale single cell tests. Process development activities included investigation of alternative processing approaches for substrates, integral separator plates, seals, matrices, and coolers.

Following the technology development effort, design and fabrication tasks incorporated the newly developed features into two short stacks: a small area development stack and a 10–ft^2 subscale stack. Later in the program, a third short stack (known as the small area on–site stack) will be fabricated to test further advancements in component technologies.

The final task of the program addresses the testing of the three short stacks described above. The overall objective of this series of short stack tests is to verify the operation of the advanced cell design at both on–site and electric utility operating conditions. The small area development stack was operated first at atmospheric pressure (to compare its characteristics to previous atmospheric tests) and then at electric utility pressurized conditions of 120 psia to examine its ability to operate at these conditions. The 10-ft^2 stack is being run at pressurized conditions to verify the scaling characteristics of the features developed in this program. The final small area stack will be tested at on–site conditions.

5. RESULTS

The small area development stack was assembled and successfully tested for 3,050 hours. The first 2,380 hours of testing was conducted at atmospheric pressure, and the final 670 hours was at 120 psia pressurized conditions. As shown in Figure 2, performance was stable throughout testing. Intermediate and post test inspections of the stack showed parts to be in generally good condition with no anomalies.

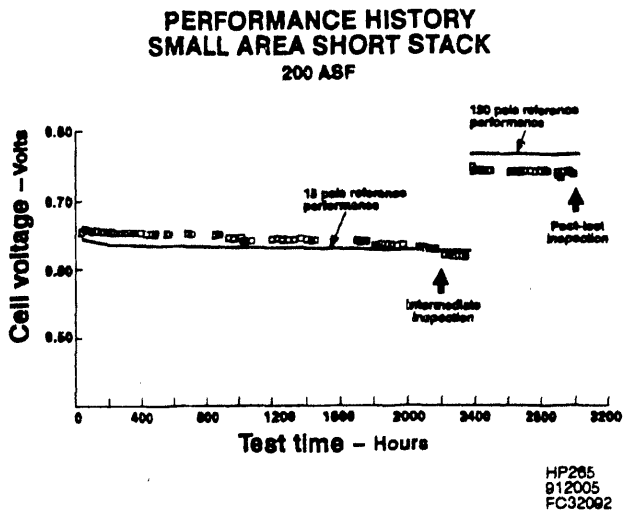

Figure 2. Small Area Development Stack Performance History

The first 10–ft^2 Configuration–B subscale stack was assembled and testing is in progress. (Figure 3 shows the stack mounted in the pressure vessel).

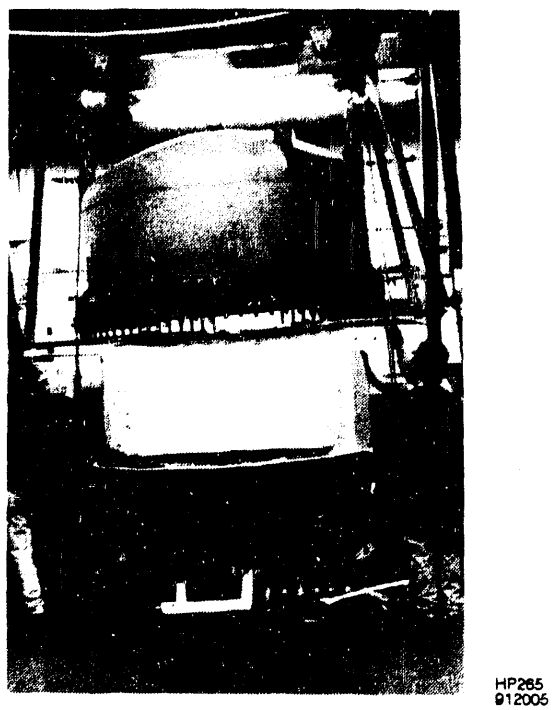

Figure 3. 10-Ft^2 Subscale Stack

As shown in Figure 4, the 10–ft^2 subscale stack has been operated up to 400 ASF, and a power density of approximately 285 wsf (60% over goal) has been achieved.

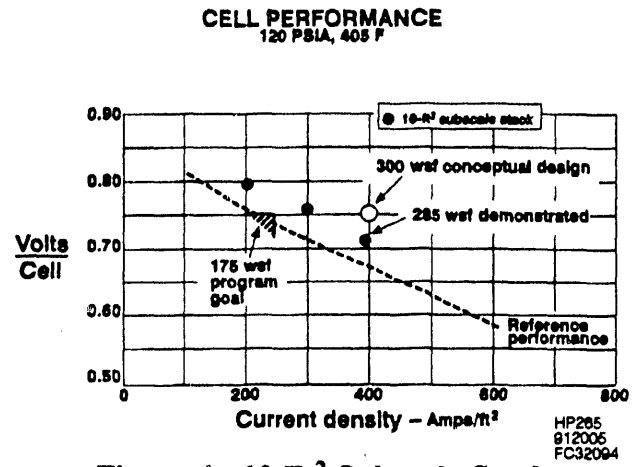

Figure 4. 10-Ft^2 Subscale Stack Performance

6. FUTURE WORK

Testing of the 10–ft^2 subscale stack will continue for a total of approximately 3,000 hours. Post test analyses will be run on the components to determine the effect of operating at the Electric Utility condition. Next, a small area short stack will be assembled and tested at on-site atmospheric conditions for approximately 3,000 hours. The purpose of this short stack is to incorporate and evaluate recent technology advancements.

Corrosion-Resistant Catalyst Supports for PAFC

CONTRACT INFORMATION

Contract Number	DE-FG02-90ER80861
Contractor	Giner, Inc. 14 Spring Street Waltham, MA 02254-9147 (617) 899-7270
Contractor Project Manager	John A. Kosek
Principal Investigators	John A. Kosek Cecelia Cropley
DOE Project Manager	James Carr
Period of Performance	March 08, 1990 to March 07, 1992

Schedule and Milestones

FY91 Program Schedule

	S	O	N	D	J	F	M	A	M	J	J	A	S
1. Optimize Characteristics	———	———	———	———	———								
2. Production and Fabrication Methods	———	———	———	———	———	———	———	———	———				
3. Fuel Cell Testing							———	———	———	———	———	———	———
4. Cost and Systems Analysis											———	———	

OBJECTIVES

The overall objective of this SBIR Phase II program is to develop low cost corrosion-resistant catalyst support (CRCS) materials as replacements for the carbon materials currently used as cathode catalyst supports in phosphoric acid fuel cells (PAFC). The CRCS materials are prepared using a low-cost, energy efficient, self-propagating, high-temperature synthesis (SHS) method. To meet this objective the properties and SHS production methods of CRCS materials are being developed and optimized, along with methods of catalyzing the support. The specific objectives of the present program are to:

- increase the support surface area
- enhance the electrochemical stability of the CRCS material
- optimize the structure of gas-diffusion electrodes prepared from platinized CRCS materials
- define and scale up processes for low-cost SHS production of these materials

BACKGROUND INFORMATION

The introduction of supported catalysts, e.g., 10% platinum dispersed on a high-surface-area carbon black, was an important milestone in the development of phosphoric acid fuel cell (PAFC) technology, allowing the total precious metal content of the electrodes to be lowered from 20 mg/cm^2 of Pt to 0.75 mg/cm^2. Concurrent with the development of the supported catalyst were investigations into identifying an optimum support material for the catalyst itself. Ideally, the support material should possess a high surface area, electrical conductivity, resistance to chemical dissolution and electrochemical oxidation (corrosion) and be low cost.

High-surface-area carbon blacks such as Vulcan XC-72 (Cabot Corp.) have found widespread applications as catalyst supports in fuel cells. However, such carbon blacks do not always have adequate resistance to electrochemical oxidation. Thermodynamically, carbon as a material is unstable at the air cathode potential in hot phosphoric acid. The kinetics of the electrochemical oxidation at the temperatures and potentials that are presently being used are sufficiently slow so that carbon can be used as a catalyst support. Nevertheless, this adds to the various modes of fuel cell performance decay (such as increased platinum migration due to undercutting, increased diffusional losses due to disruption of the carbon-Teflon interface) and puts a fundamental limitation on the lifetime of the fuel cell electrodes.

The recent trend in fuel cell operation is towards increased temperature and pressure, leading to higher cathode potentials. In addition, part-load operation utility stacks will require that during a certain percentage of time the oxygen electrode will be at potentials in excess of 0.8 V. These conditions are severe from the viewpoint of corrosion of the catalyst support. Recognizing drawbacks of the presently utilized catalyst support materials, DOE and PAFC manufacturers are seeking to replace carbon components and catalyst supports with low-cost, corrosion-resistant materials.

The feasibility of using low-cost CRCS materials prepared by SHS as replacements for the cathode carbon support materials was demonstrated in a SBIR Phase I program (DOE Contract DE-AC02-89ER 80807). The SHS method was selected due to the promising surface area, conductivity and corrosion resistance of materials prepared by this method and to the inherent advantages of the SHS method. These advantages include simplicity, safe non-corrosive reactants, low energy consumption, high purity, high yield and cost-effectiveness.

The SHS process has been highly developed in the Soviet Union, where it has been used to produce more than 200 ceramic and refractory compounds in the laboratory and is being used to produce at least two materials industrially (Crider, 1982). Little research on this process has been conducted in the United States, but it has great promise for becoming a major ceramic manufacturing technique. Crider (1982) sites several advantages of the SHS process over currently used ceramic production methods, including: a) simplicity, including elimination of high-temperature furnaces and complex processing equipment, b) rapid production of large quantities of high-purity ceramics, and c) significant energy savings.

Self-propagating high-temperature synthesis was originally developed in the Soviet Union by Merzhanov and Borovinskaya (1972) as a technique to prepare ceramic material by spark or resistance heating of packed reactant powders. It has been used to fabricate SiC (Yamada, et al., 1985; Yamada, et al., 1986), TiB_2 (Zavitsanos and Morris, 1983) and Ti-B-C mixtures (McCauley, et al., 1982). Although the technique was developed to form dense, hard ceramics by pressure compacting the starting materials, Riley, et al. (1987) has reported the formation of loose TiC powder by SHS. The final particle size was similar to the initial particle size of the carbon material, 2 microns, although the titanium powder particle size was much larger, 30-50 microns. Riley proposed that the Ti melts and diffuses into the carbon, which remains solid, and creates TiC which retains the general shape of the precursor carbon. Submicron SiC has been

fabricated by Yamada, et al. (1986) by using submicron starting materials.

The general method of manufacture is to a) physically blend powders of the starting materials, b) compact the blended powders into a pressed pellet and c) ignite the pressed pellet with a resistance heated coil inserted at one end of the reaction vessel (Crider, 1982). Alternatively, an electric spark can be passed through one end of the compacted pellet (McCauley, et al., 1982). The reaction proceeds through the pellet from one end to the other spontaneously, due to the heat generated by the exothermic combustion. The process generally results in a nearly complete transformation with 0.2 wt% or less unreacted residue. The process is usually run under an argon atmosphere to preserve the product purity; performing the reaction under a nitrogen atmosphere will result in nitride formation/contamination. It is a simple energy-efficient process for producing ceramic materials. A schematic drawing of the reaction apparatus used in our laboratory is shown in **Figure 1**.

Using the SHS technique, high-surface-area, conductive CRCS materials were produced in the Phase I program. The electrochemical stability of select CRCS materials in hot concentrated phosphoric acid was greater than that of the reference Vulcan and equivalent to that of heat-treated Black Pearls 2000 (HTBP), a state-of-the-art cathode catalyst support. The CRCS materials were approximately 5 times more conductive than Vulcan or HTBP. The oxygen reduction activity of select platinized CRCS materials was superior to that of platinized carbon (Vulcan) at low current densities.

PROJECT DESCRIPTION

To achieve the objective of developing CRCS materials prepared by SHS as low-cost corrosion-resistant cathode catalyst supports, four tasks are being conducted:

- Optimize the surface area and electrochemical stability of CRCS materials in hot concentrated phosphoric acid, while maintaining high electrical conductivity. For this optimization, the parameters being evaluated include: type and particle size of reactants, form and processing conditions of the reactant sample, product purity and product morphology.

- Develop and optimize methods for scaling-up SHS production of CRCS materials and for platinizing the CRCS support. We will also define the optimum hydrophilic/hydrophobic nature of the Teflonized catalyst to obtain efficient, high-current-density gas diffusion electrodes from the platinized CRCS material.

- Evaluate the electrochemical performance of selected catalyzed support materials in laboratory size single-cell PAFCs. Fuel cell tests of up to several hundred hours will be used to evaluate selected support materials, the effectiveness of platinization methods, and variations due to electrode fabrication procedures. Longer term testing under both atmospheric and pressurized fuel cell conditions will be used to evaluate the performance and stability of the optimum catalyzed CRCS material.

- Conduct a preliminary cost and systems analysis to determine the impact of using CRCS materials as cathode catalyst supports on the capital and operating costs of a PAFC. The study will determine the PAFC system size at which the enhanced stack life and possible enhanced cell performance due to CRCS materials outweighs the possible initial higher cost of the CRCS support.

Experimentally, selected variations in reactant composition and SHS processing conditions are used to produce the CRCS materials. Initial evaluation of the materials consists of surface area and electrochemical stability measurements. Promising samples are then further evaluated for purity, morphology, and particle size. Electrical conductivity is also measured. Selected samples are platinized using proprietary Giner, Inc. techniques and evaluated for O_2 reduction activity and electrochemically active surface area.

The support surface area is determined by the BET (Brunauer, et al., 1938) N_2 adsorption technique using a Micromeritics Flowsorb II 2300 instrument. As a screening test for electrochemical stability, the corrosion current of samples in N_2-purged 190°C, 100% H_3PO_4 at a potential of 1.0 V vs. a dynamic hydrogen electrode (DHE) is monitored for 1000 min. X-ray diffraction is used to determine chemical phases and lattice parameters. Particle size and morphology are observed by transmission electron microscopy (TEM). The electrical (dc) conductivity is determined by passsing a known current through a compressed powder sample and measuring the voltage drop. The O_2 reduction activity of platinized samples is measured using the floating electrode half-cell technique (Giner and Smith, 1967) with 100% H_3PO_4 at 190°C. Electrochemically active surface area is determined using a hydrogen stripping voltammetry technique of hydrogen deposition and oxidation.

RESULTS

The effort in this program to date has been concentrated on developing CRCS materials with desirable support properties, i.e., high surface area, electrochemical stability and conductivity, and on developing methods for platinizing the CRCS supports. Additionally, initial scale-up of batch size from 3-5 g/batch to 30 g/batch has been successful.

Although the SHS reaction is conceptually very simple, materials with a wide range of properties may be produced by varying the type, particle size, and ratios of the reactants, and the form and processing conditions of the reactant sample. These properties determine the rate, extent and temperature of the reaction since once the SHS reaction has been initiated, it is self-propagating and is not externally controlled. By varying the initial conditions, we have produced CRCS materials with a wide range of BET surface areas, to a maximum of 100 m^2/g, and corrosion currents after 1000 min. to a low of 1 $\mu A/mg$. Some of this variation in properties has been found to be due to incomplete conversion of the reactants.

Several CRCS materials with surface area, electrochemical stability, and conductivity characteristics desirable for PAFC cathode catalyst supports have been produced. In general, the surface areas of the CRCS materials are lower than those of Vulcan and HTBP, with typical surface areas of 15-25 m^2/g. The support surface areas are high enough to provide good dispersion of small Pt crystals as discussed below. Electrical conductivities of all of the CRCS materials developed are several times higher than those of the carbon supports.

The corrosion currents of many CRCS samples after 1000 min. in hot H_3PO_4 at 1.0 V vs. DHE are lower than that of Vulcan, and several samples have corrosion currents comparable to that of HTBP. Typical results are shown in **Figure 2**.

Selected samples with relatively high surface area and low corrosion currents were catalyzed with 4 to 15 wt% Pt using standard proprietary Giner, Inc. techniques.

To date, electrodes prepared from several CRCS-supported catalysts have performance superior to or comparable to that of 10% Pt/Vulcan XC-72, the baseline PAFC O_2 reduction catalyst. **Figure 3** compares the performance of the baseline catalyst with 15% Pt/CRCS-57 and 15% Pt/CRCS-45. The Pt loadings of these electrodes are 0.5 mg/cm^2 for the baseline Vulcan-supported electrode and approximately 3 mg/cm^2 for the CRCS electrodes.

Lower Pt loadings on CRCS supports also provide high electrochemical activity, as shown in Figure 3. The performance of CRCS Sample 22, with 4% Pt yielding a Pt loading of 0.8 mg/cm^2, was $\approx$50 mV lower than that of 10% Pt/Vulcan on O_2 at 100 mA/cm^2. With optimization of Pt deposition and electrode fabrication parameters, it is likely that the performance of $\approx$5 wt% Pt/CRCS will be comparable or superior to the Pt/Vulcan at the low noble metal loading level (0.5 mg Pt/cm^2).

The electrochemically active surface area of selected platinized CRCS electrodes was determined using a hydrogen stripping voltammetry technique. For the supports catalyzed with 15% Pt, the electrochemically active surface area is typically between 65 m^2/g and 85 m^2/g, while the electrochemically active surface area of 10% Pt/Vulcan is ≈ 120 m^2/g Pt. Although the electrochemically active area of the platinized CRCS supports is somewhat lower than that of Pt/Vulcan, likely due to heat treatment of the CRCS supported catalysts as part of the platinization procedure, the surface area indicates that Pt is adequately dispersed on the CRCS support. This was confirmed by TEM of several platinized CRCS samples which showed good dispersion of very small Pt crystallites on CRCS crystals. Studies of methods of further improving the electrochemically active Pt surface area of the platinized CRCS supports, such as modifications to the platinization procedure and increasing the CRCS surface area are continuing.

In summary, high-surface-area, conductive, corrosion-resistant catalyst supports can be prepared by the simple, efficient, SHS technique. The electrochemical stability of a CRCS material in hot, concentrated H_3PO_4 was greater than that of Vulcan and equivalent to that of HTBP. The O_2 reduction activity of platinized CRCS was superior to that of platinized carbon.

FUTURE WORK

Development and optimization of the CRCS materials will continue with emphasis on increasing the surface area and electrochemical stability of the supports.

Evaluation of support platinization procedures will continue. Methods of increasing the electrochemically active area of platinized CRCS will be investigated. Following further floating electrode half-cell evaluations of electrochemical activity, several of the platinized CRCS supports providing the highest activity at 200 mA/cm^2 will be evaluated in laboratory-size single-cell phosphoric acid fuel cells under typical atmospheric pressure operating conditions for durations of up to several hundred hours. Following these tests, a platinized CRCS support will be selected for longer term evaluation under both atmospheric and pressurized PAFC conditions. The effect of cell operation on the characteristics of the Pt deposit will be evaluated using cyclic voltammetry and electron microscopy.

Concurrent with the evaluation of platinization methods, procedures for fabrication of gas diffusion electrodes for the catalyzed CRCS materials will also be evaluated. Electrode Teflon content, hydrophobic/hydrophilic balance, and sintering conditions will be modified to provide peak performance in floating electrode half-cell testing and in fuel cell testing.

A cost and systems analysis will be initiated to determine the overall impact on the capital and operating costs of a PAFC of using CRCS materials produced by SHS as a cathode catalyst support. A realistic cost basis for production of CRCS materials by SHS will be developed. This will be used to determine the PAFC system cut-off size for the economical application of CRCS supports.

REFERENCES

Brunauer, S., P.H. Emmett, and E. Teller, *J. Am. Chem. Soc.*, **60**, 309 (1938).

Crider, J.G., *Ceram. Eng. Sci. Proc.*, **3**, 519 (1982).

Giner, J., and S. Smith, *Electrochem. Technol.*, **5**, 59 (1967).

McCauley, J.W., N.D. Corbin, T. Resetar and P. Wong, *Ceram. Eng. Sci. Proc.*, **3**, 538 (1982).

Merzhanov, A.G., and I.P. Borovinskaya, *Dokl. Chem.* [Eng. Trans.], **204**, 429 (1972).

Riley, E., R.J. Wright, and M.A. Riley, "A Novel Method for Generation of Submicron Carbides and Borides," Paper presented at the 18th Annual Meeting of the Fine Particle Society, Aug. 3-7, 1987, Boston, MA.

Yamada, O., Y. Miyamoto, and M. Koizumi, *Am. Ceram. Soc. Bull.*, **64**, 319 (1985).

Yamada, O., Y. Miyamoto, M. Koizumi, *J. Mater. Res.*, **1**, 275 (1986).

Zavitsanos, P.D., and J.R. Morris, Jr., *Ceram. Eng. Sci. Proc.*, **4**, 624 (1983).

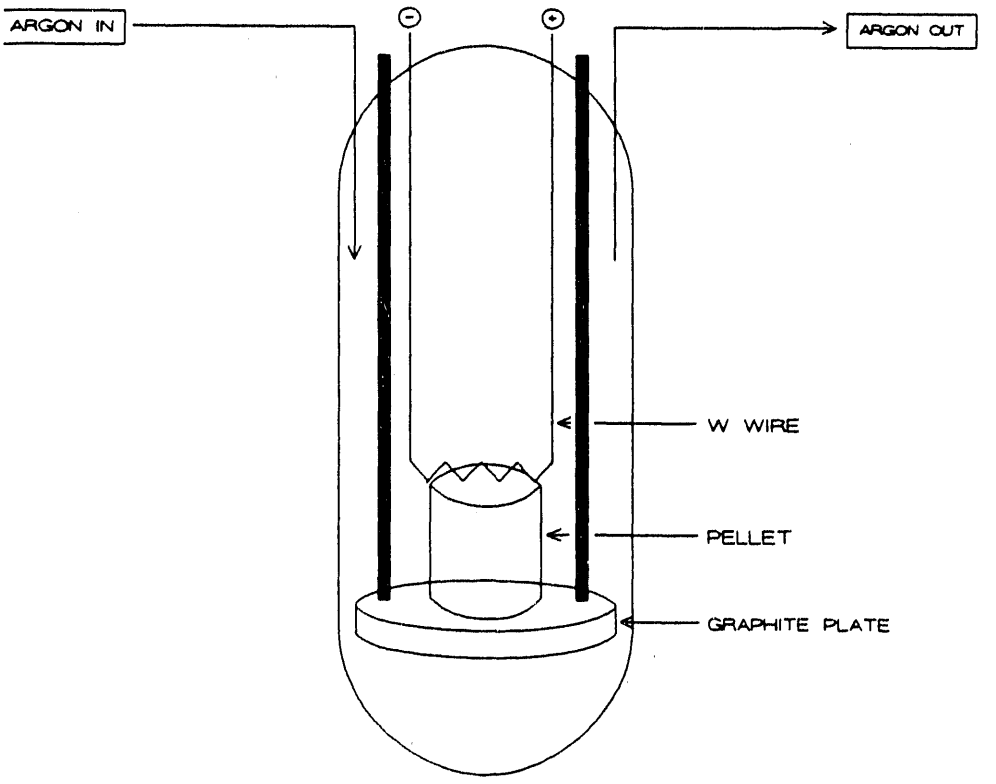

Figure 1. SHS Reactor Assembly

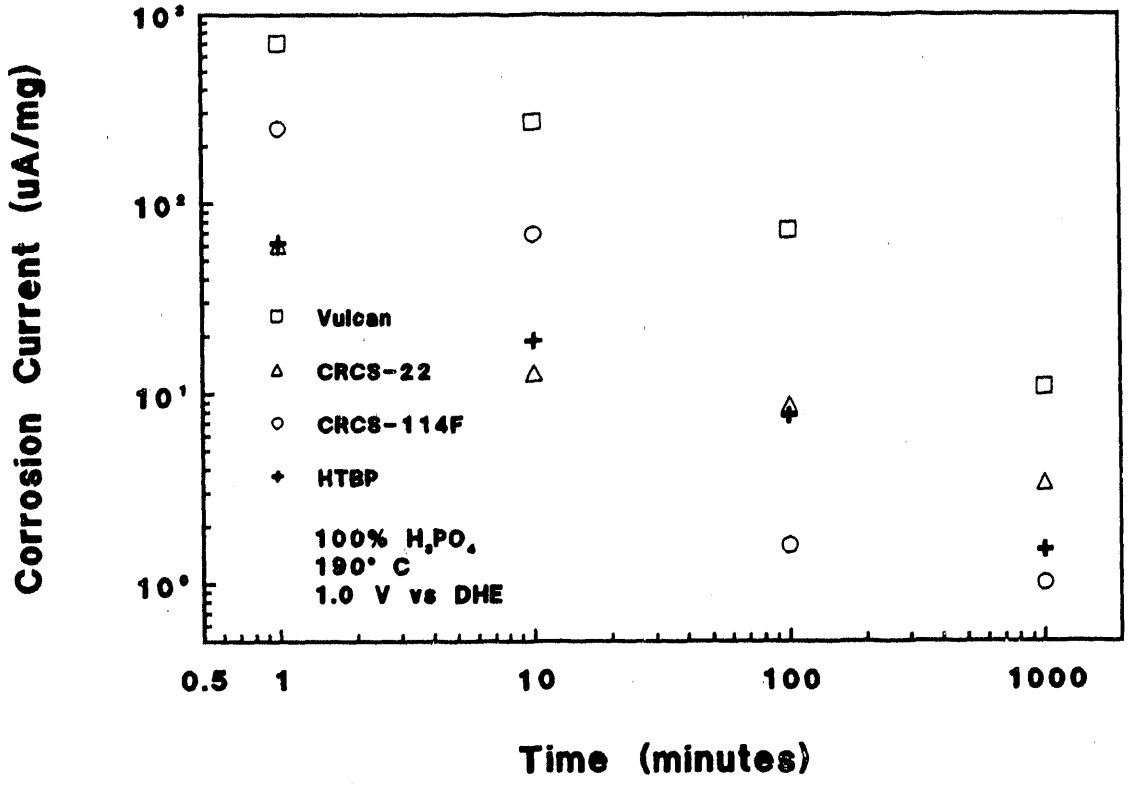

Figure 2. Comaprison of Corrosion Currents of CRCS Materials, HTBP and Vulcan

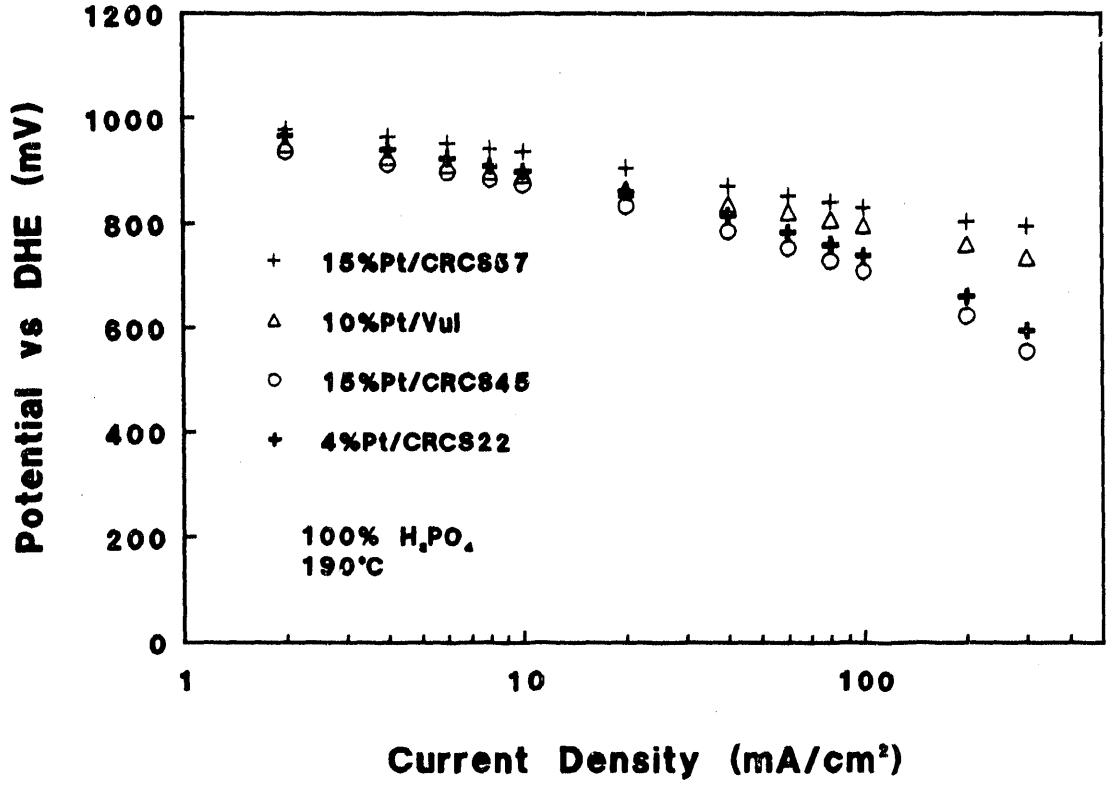

Figure 3. Comparison of Oxygen Reduction Activity of Pt/CRCS to Pt/Carbon

Corrosion Resistant Support for Air Cathodes in PAFC

CONTRACT INFORMATION

Contract Number DE-FG01-90-ER81077

Contractor

The Electrosynthesis Co., Inc.
P.O. Box 430
East Amherst, NY 14051
(716) 684-0513

Contractor Project Manager Dr. Norman L. Weinberg

Principal Investigators

Dr. Norman L. Weinberg
Dr. J. David Genders
Richard M. Baran
Dan M. Hartsough

METC Project Manager James P. Carr

Period of Performance September 14, 1990 to September 13, 1992

Schedule and Milestones

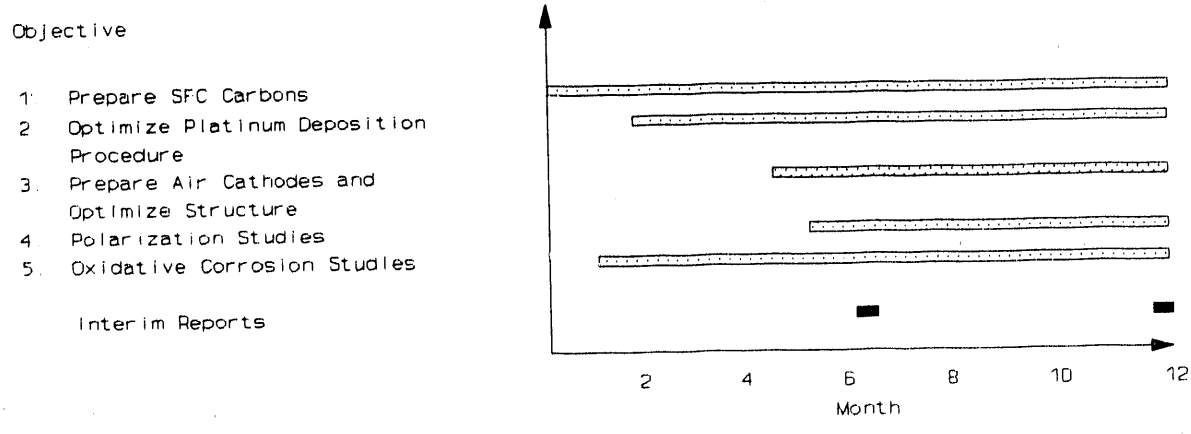

OBJECTIVES

The primary objective of this work is to produce a corrosion resistant carbon suitable for use as a catalyst support material in phosphoric acid fuel cell cathodes. This is to be achieved by the use of Specifically Fluorinated Carbons (SFC™ materials).

BACKGROUND INFORMATION

The oxidation of carbon in the concentrated phosphoric acid electrolyte of the acid fuel cell has previously been investigated by Kinoshita and Bett [1,2] and by Stonehart [3]. At long corrosion times the principal reaction was found to be the evolution of CO_2, and the amount formed, together with other surface oxide species, was shown to be strongly dependent on the type of carbon used. Stonehart [3] reported that graphitized carbons show the least amount of corrosion. It is thought that the graphitization process reduces the number of edge sites available to oxidative attack. Therefore, it would be reasonable to expect that if these same edge sites could be converted to stable carbon fluorine functionality, then the resultant carbon would exhibit enhanced stability.

PROJECT DESCRIPTION

Specifically Fluorinated Carbons (SFC™ materials) [4] provide a method of manufacturing a corrosion resistant carbon without substantially changing the dimensional or physical characteristics of the starting material. Therefore it should be possible to produce a catalyst support material that retains its high surface area while also being corrosion resistant.

Carbon blacks are the preferred materials for use as catalyst supports. In common with most carbon forms, these contain oxide groups on the carbon surface. These functionalities, which generally occur at the edge sites, dislocations and grain boundaries, also provide high energy sites at which oxidative corrosion of the carbon can occur. The premise of this work is to convert the surface oxide groups, present as carboxylic acids, phenols, quinones and lactones, into stable carbon fluorine bonds. See Figure 1. The resultant SFC™ carbon has previously been shown to be highly oxidation resistant [5].

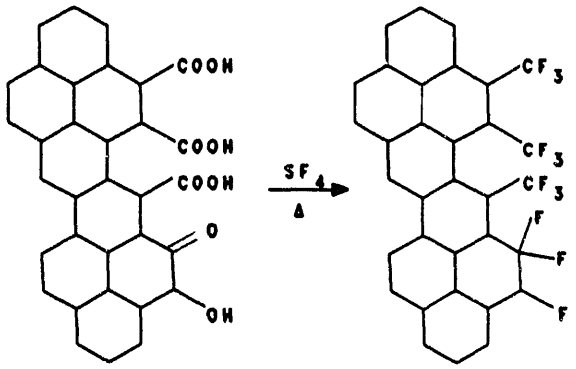

Figure 1. Fluorination of Oxide Functionality

RESULTS

Carbon Preparation

A series of commercially available carbon blacks have been fluorinated to produce a group of SFC carbons. Carbons were fluorinated in their untreated state as well as in a pre-oxidized form. The latter step develops inherently unstable sites and increases the available oxide sites on the carbon and therefore increases the amount of fluorine that can be introduced. Oxidation was carried out by immersion in 1M ammonium persulfate for two hours at 70°C, followed by filtering, washing, and drying.

The specific fluorinations were accomplished using a PARR Model 4621 High Pressure Reactor, a caustic scrubber system, and piping and valves for delivery of fluorinating gas and inert purge gas. Carbon samples were oven dried at 100°C before sealing them in the reactor. The reactor was purged with argon several times and then charged with the appropriate amount (ca. 100 g) of mild fluorinating agent (SF_4). The reaction

temperature (250°C) was maintained for one week. At the conclusion of a fluorination run the reactor was cooled to room temperature and the off-gases discharged through caustic scrubbers with a continuous stream of argon. Fluorinated carbons were then removed from the reactor and washed in a several step procedure to neutralize or remove carbon acyl fluoride and any adsorbed but unreacted fluorides.

Variations on this fluorination process are also practiced and these include the use of a catalyst to shorten fluorination time and/or post fluorination of the carbon with fluorine gas to remove any residual sulfur compound that may remain on the carbon surface.

The carbons are characterized by determining the oxide and fluorine content by standard analytical methods. The fluorinated carbon was pyrolytically decomposed by heating 0.200g to 540°C for two hours in a 1:1 mixture of potassium and sodium carbonates. This produces water soluble fluorides, the concentration of which can be determined by measurement with an Orion Research Digital Ionalyzer 501 and a fluoride ion selective electrode, the Orion 960900, versus an internal reference electrode. Comparison of the potential against a calibration curve made from standardized sodium fluoride solutions gave the fluorine content in each carbon. Oxide group analyses were performed by stirring aliquots of the carbon for 24 hours in solutions of sodium bicarbonate and sodium hydroxide, filtering off the carbon, washing and back-titrating the excess base with a standardized acid. $NaHCO_3$ will only react with the strong acid functionalities (carboxylic acid) on the carbon surface whereas NaOH will react with both strong and weak acid (phenolic) functionalities. Thus strong acid groups (COOH) and weak acid groups (OH) formed by oxidation could be determined. The types and amounts of surface groups were also confirmed by X-ray photoelectron spectroscopy (XPS) [6]. Fluorinated carbons prepared to date are shown in Table 1.

Carbon	BET Surface Area (m^2/g)	Fluorine Content (%)
Vulcan XC-72R	254	3.1
Pre-Oxidized Vulcan XC-72R		8.0
Shawinigan Acetylene Black (SAB)	80	0.8
Steam Activated SAB	261	2.4
Black Pearls 2000	1475	3.5
Ketjenblack EC300J	800	4.0
Pre-Oxidized Ketjenblack EC300J		6.8

Table 1. Fluorinated Carbon Analysis

As can be seen from the Table, the amount of pre-oxidation gives some control over the amount of fluorine that is introduced into the carbon. This is most evident from a comparison of the fluorination of pre-oxidized Vulcan XC-72R with the same carbon that had not been pre-oxidized.

Corrosion Tests

The stability of the SFC™ carbons has been evaluated by measuring the oxidative corrosion at 1V vs. RHE in 95% phosphoric acid at 200°C. This accelerated corrosion test has been reported by a number of groups [1-3] and is generally accepted as being a suitable method for screening of carbon stability. The corrosion measurements are generally run for a period of 100 minutes, or preferably, 1000 minutes, after which a Tafel plot is recorded. In the preferred configuration, the data is collected by a computer directly from the experiment at a sampling rate of one point per minute. Figure 2 shows a typical corrosion curve for the corrosion of Vulcan XC-72R and Figure 3 shows a typical Tafel plot recorded after the carbon had been corroding for 1000 min. Form this data the total charge associated with the corrosion of the carbon and the final corrosion current are determined. The Tafel data is used to calculate an extrapolated corrosion current at 0.7V vs RHE. Comparison of these values will give an estimation of the corrosion stability of the SFC carbons.

Figure 4 shows a comparison of the corrosion currents observed for Ketjenblack and SFC Ketjenblack after 100 minutes. It can be seen from this Figure that the corrosion current for the SFC carbon is significantly lower than that observed for the untreated Ketjenblack. Moreover, the overall charge associated with the corrosion curves for the SFC material is only 33% of that associated with the Ketjenblack. This result is very encouraging and indicates that the SFC process is successfully protecting the carbon from oxidative attack.

Polarization Measurements

Polarization measurements of oxygen depolarized cathodes have been made for a series of fluorinated and non-fluorinated carbons. It will be important to the success of the SFC carbons as catalyst support materials to show that the fluorination process does not adversely affect the catalyst performance. Figure 5 shows a typical oxygen reduction polarization curve for fluorinated and non-fluorinated Vulcan XC-72R. The effect of fluorination of the support carbon on the performance was relatively small in most cases. The performance curves are usually within about 20mV of each other.

FUTURE WORK

Future efforts will focus on the optimization of the fluorination process in an attempt to further improve the stability of the carbon. This effort will also concentrate on methods of obtaining higher fluorine coverage on the carbon surface and the removal of residual sulfur and/or sulfur species which remain after the fluorination process. The success of the optimization studies will be determined from further corrosion studies and surface analysis of the carbons.

Future efforts will also seek to optimize the catalyst deposition procedure onto the SFC carbons and hence the air cathode structure. Finally, long term stability measurements will be made on these cathodes.

REFERENCES

1. K. Kinoshita and J. Bett, Carbon, II, 237 (1973).

2. K. Kinoshita and J. Bett, in "Proceedings of the Symposium on Corrosion Problems in Energy Conversion and Generation", C. S. Tedmon, Editor, pp. 45-55, The

Electrochemical Society, Pennington, NJ (1974).

3. P. Stonehart, Carbon, 22, 423 (1984).

4. Weinberg,N.L. U.S. Patent 4,908,198, 1990. Others pending.

5. "Specifically Fluorinated Carbon Anodes for Ozone and Persulfate Electrogeneration", R.M.Baran, J.D.Genders and N.L.Weinberg, Nineteenth Biennial Conference on Carbon, Penn State University, June 1989.

6. W. Aldred, C.Fierro, D.Tryk, E.Yeager, Case Western Reserve University, Sub-Contract on DOE Contract No. DE-FG01-90ER81077.

Figure 2: Corrosion Study
Untreated Vulcan XC-72R

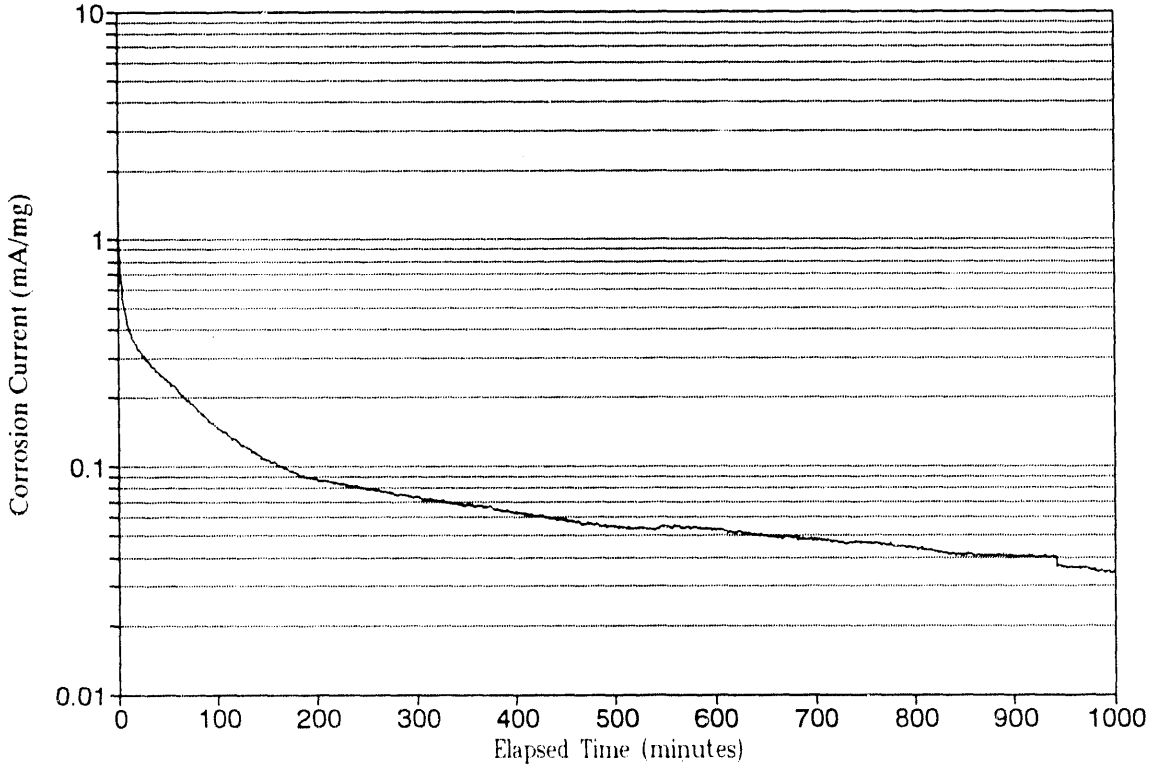

Figure 3

Tafel Plot #199-68

Untreated Vulcan XC-72R

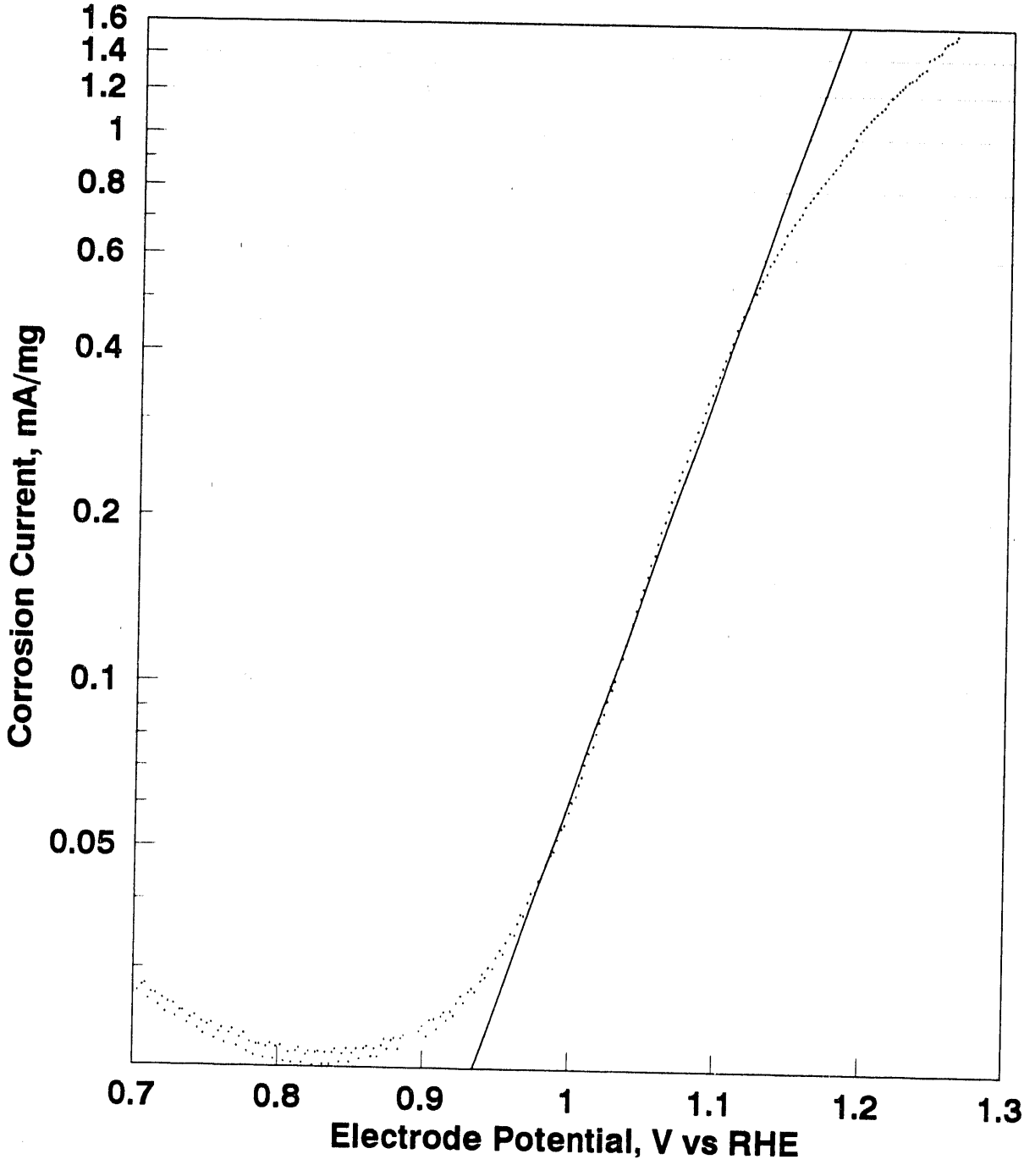

Figure 4. Corrosion Test Ketjenblack

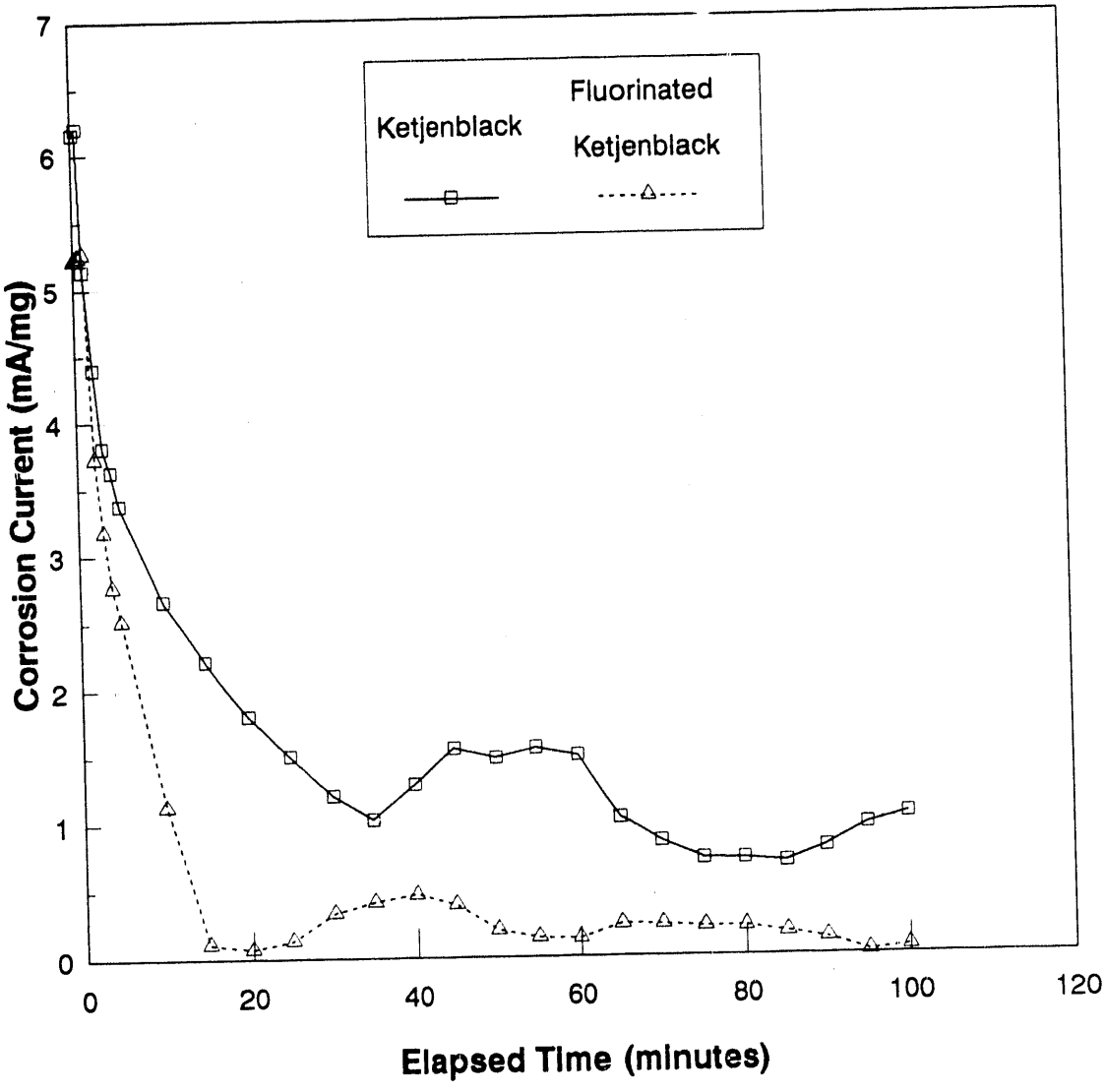

Figure 5
Oxygen Reduction Polarization Curves
Oxidized XC-72 / 10 wt.% Pt

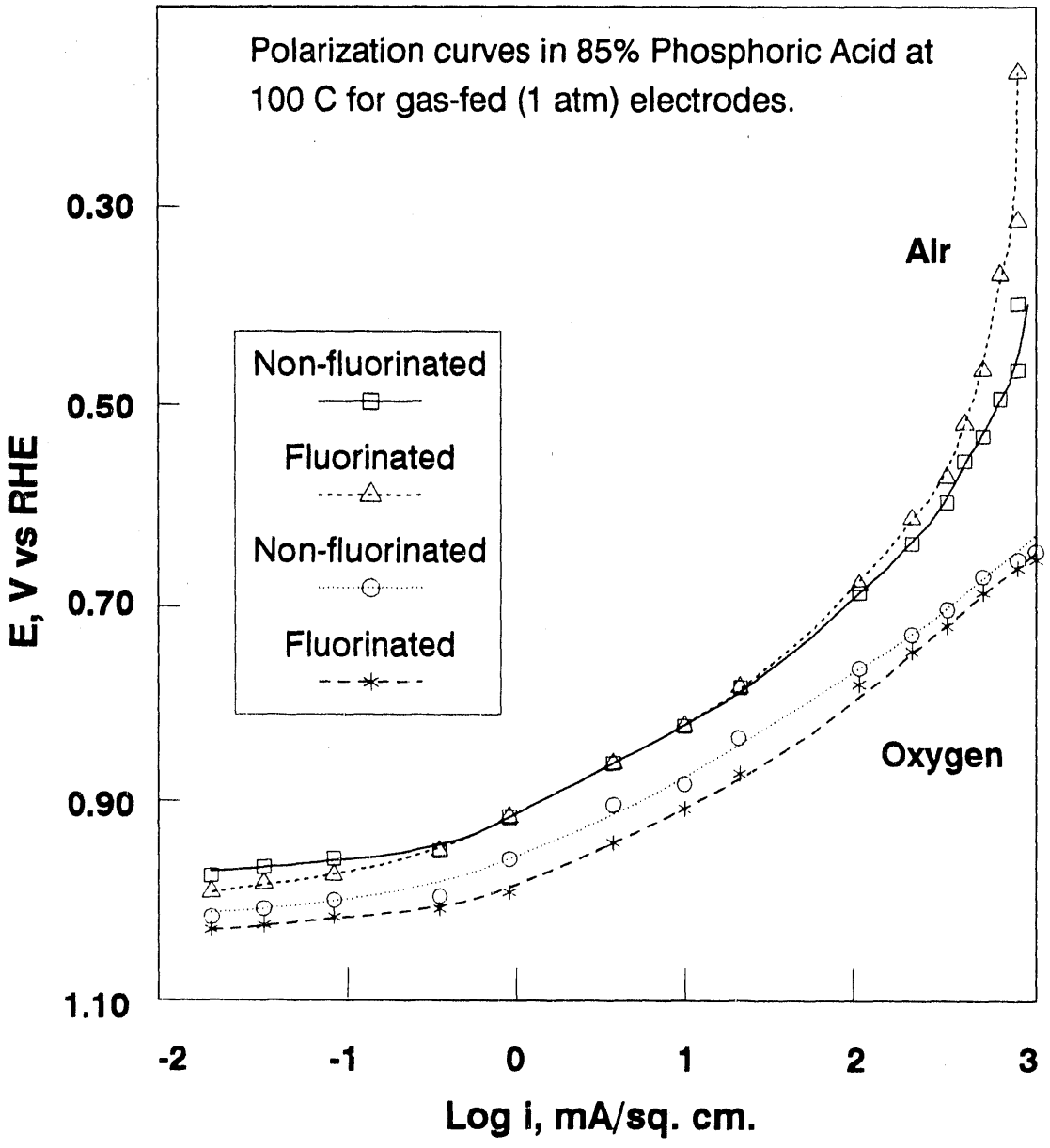

Novel Solid-State Proton Conductors

CONTRACT INFORMATION

Contract Number DE-AC21-88MC25169

Contractor

Center for Electrochemical Systems and Hydrogen Research
238 Wisenbaker Engineering Research Center
Texas Engineering Experiment Station
Texas A&M University System
College Station, TX 77843-3402
(409) 845-8281

Contractor Project Manager A. John Appleby

Principal Investigators

A.J. Appleby, E.R. Gonzalez, A. Parthasarathy and S. Srinivasan, Texas A&M University
M. Gillette, J.K. Ghosh and D.D. DesMarteau, Clemson University
A.G. Einset, M. Desai and V. Jalan, ElectroChem, Inc.

METC Project Manager William J. Huber

Period of Performance June 10, 1988 to June 9, 1991

Schedule and Milestones

TASK	MONTH FROM CONTRACT AWARD								
	0	3	6	9	12	15	18	21	24
1. **Preparation of Management Plan**	———								
2. **Preparation and Characterization of Proton Conducting Materials**	———	———	———						
3. **Preparation and Characterization of Polymer Conducting Materials**			———	———	———	———	———	———	———
4. **Reports, Deliverables**	———	———	———	———	———	———	———	———	———

OBJECTIVES

The objectives of the present work are the synthesis and characterization of polymer superacids derived from fluorinated sulfonimides, which are to be evaluated as suitable proton conducting electrolytes for high temperature (> 150° C) aqueous fuel cells.

BACKGROUND INFORMATION

The phosphoric acid fuel cell (PAFC) is presently in a more advanced state of development than those using other electrolytes. This fuel cell has several advantages, but a major drawback is the slowness of the oxygen reduction reaction (ORR) in this system. It has been recognized for some time that the ORR is much faster in certain superacids, such as trifluoromethanesulfonic acid and its polymeric equivalent, Nafion®[1]. This led to the development of the proton exchange membrane fuel cell (PEMFC), with a much higher power density than that of the PAFC. Like the PAFC, the PEMFC is CO_2 rejecting, but its relatively low temperature of operation (~ 80° C) means that it tolerates only minimal amounts of CO. Similarly, it does not allow the use of waste heat to generate steam. Furthermore, the PEMFC shows problems of water management and of membrane degradation.

More recent work has shown that fluorinated sulfonimides of the type (R_fSO_2) NH may be promising alternative electrolytes, which could be used as both bulk aqueous electrolytes and as additives to phosphoric acid[2,3]. Thus, it may be expected that these compounds will result in both enhanced ORR kinetics and higher operating temperatures (>150°C), which will improve the overall efficiency of the fuel cell.

PROJECT DESCRIPTION

Synthesis of Solid Proton-Conducting Polymer Electrolyte Compounds (Clemson University)

The purpose of this work is to synthesize ionene polymers of the type:

$CH_3SO_2[N(H)SO_2(CF_2)_4SO_2]_mN(H)SO_2CF_3$

using condensation polymerization of the difunctional monomers $FSO_2(CF_2)_4SO_2F$ and $Me_3SiN(Na)SO_2(CF_2)_4SO_2N(Na)SiMe_3$. The product is end-capped with CF_3SO_2NNa and CF_3SO_2, and the polymer indicated is obtained by acidification.

Organic impurities present in these compounds is eliminated by treatment with H_2O_2. NMR spectra is the technique used for characterization.

Electrochemical Characterization of Proton-Conducting Polymer Electrolytes (CESHR/Texas A&M University)

Because the aqueous solutions of the polymers will be in contact with platinum catalysts, the presence of impurities which may strongly adsorb on the electrode may result in major problems. Thus, as a first step, the purity of the solution is established by the use of cyclic voltammetric experiments at a platinum microelectrode in deoxygenated solutions.

The major transport parameters of dioxygen in these solutions (i.e., its solubility and diffusion coefficient) are determined by the use of chronoamperometry. These parameters are essential for the evaluation of ORR kinetics, and can be determined in a single experiment.

Finally, major aspects of the kinetics of dioxygen reduction at platinum are studied using the data from current-potential curves, which can furnish kinetic parameters such as the Tafel slope and exchange current density.

Evaluation of Proton-Conducting Polymer Electrolytes Under Fuel Cell Conditions (ElectroChem, Inc.)

This portion of the project involves evaluation of the proton-conducting polymers in a unitary fuel cell using an immobilized electrolyte matrix with high surface area electrodes. In this configuration, the large ratio of the electrocatalytist surface area to the electrolyte volume minimizes problems resulting from the presence of impurities. Optimization of the catalyst/electrolyte contact in the fuel cell using suitable techniques of electrode impregnation by electrolyte is necessary to obtain the highest performance.

RESULTS

Synthesis of Solid Proton-Conducting Polymer Electrolyte Compounds (Clemson University)

A large number of fluorinated sulfonimide compounds were prepared. Four were produced in appreciable quantities and supplied to CESHR/Texas A&M and ElectroChem, Inc. for evaluation. These were as follows:

$(CF_3SO_2)_2NH$ Monomeric acid (**1**)

$CF_3SO_2N(H)SO_2(CF_2)_4SO_2N(H)SO_2CF_3$

Dimeric acid (**2**)

$CF_3SO_2\big(N(H)SO_2(CF_2)_4SO_2\big)_3N(H)SO_2CF_3$

Tetrameric acid (**3**)

$CF_3SO_2\big(N(H)SO_2(CF_2)_4SO_2\big)_nN(H)SO_2CF_3$

Polymeric acid (**4**)

The synthesis procedure for Monomeric acid (1), bis(trifluoromethyl)sulfon)imide, has been already described [2,3]. Extension of the synthetic methodology to difunctional acids was conducted using two methods:

Method 1

$$FSO_2(CF_2)_nSO_2F\ (\mathbf{A}) \xrightarrow{NH_3} H_2NSO_2(CF_2)_nSO_2NH_2 \xrightarrow{NaOH}$$

$$Na(H)SO_2(CF_2)_nSO_2N(H)Na \xrightarrow{HMDS} Me_3Si(Na)SO_2(CF_2)_nSO_2N(Na)SiMe_3\ (\mathbf{B})$$

$$R_fSO_2F \rightarrow R_fSO_2(Na)NSO_2(CF_2)_nSO_2N(Na)SO_2R_f \xrightarrow{H^+} R_fSO_2(H)NSO_2(CF_2)_nSO_2N(H)SO_2R_f$$

Method 2

$$R_fSO_2N(Na)SiMe_3 \xrightarrow{\mathbf{A}} R_fSO_2(Na)NSO_2(CF_2)_nSO_2N(Na)SO_2$$

Methods **1** and **2** provided the conceptual basis for the formation of polymers (ionenes) of this class of material by step polymerization. After considerable trial and error, a reproducible method was developed to prepare the polymers of moderate molecular weight, together with a model compound containing four acid groups to provide a better understanding of the properties of the polymers, which would only be available as a mixture of compounds with varying chain length.

$$\mathbf{A} + CF_3SO_2N(Na)SiMe_3 \xrightarrow[80^\circ C]{CH_3CN} CF_3SO_2N(Na)SO_2(CF_2)_4SO_2F$$

1] **B**

$\rightarrow$ $CF_3SO_2N(H)[SO_2(CF_2)_4SO_2N(H)]_3SO_2CF_3$ (TETRAMER **3**)

2] H+

$$\mathbf{A} + \mathbf{B} \xrightarrow[80^\circ C]{CH_3CN} \begin{matrix} FSO_2(CF_2)_4SO_2N(Na)[SO_2(CF_2)_4SO_2N(Na)]_nSO_2(CF_2)_4SO_2F \\ Me_3SiN(Na)[SO_2(CF_2)_4SO_2N(Na)]_nSO_2(CF_2)_4SO_2N(Na)SiMe_3 \end{matrix}$$

1] CF_3SO_2F 2] $CF_3SO_2N(Na)SiMe_3$ 3] H+

$\rightarrow$ $CF_3SO_2N(H)[SO_2(CF_2)_4SO_2N(H)]_nSO_2CF_3$ (POLYMER **4**)

In much of the work with the polymer, a small excess of **A** was used to try to obtain FSO_2-end groups. It was realized that this would reduce the value of n, but it provided a basis for determining chain length by ^{19}F NMR. Values of n were typically an average of 40, but depending on the excess of **A**, values from 10 to 100 were obtained. In continuing work, considerable higher values of n will be possible by carefully controlling the stoichiometry of **A** and **B**. It is also possible to vary the $-(CF_2)-$ connecting links to both shorter and longer values, and work is continuing to prepare polymers containing $-(CF_2)_2-$ and $-(CF_2)_6-$.

The ionenes are somewhat soluble in water and behave as strong polyfunctional acids with all acid groups of equal acidity. They are stable to at least 320° C, as DSC has shown. The tetramer (n=3) melts sharply at 248° C, whereas the polymer (n=40) melts near 320° C with decomposition. These ionenes are unique in two respects. They are the only known examples of polyfluorinated ionenes, and they probably have the highest Bronsted acidity of any known ionenes.

Electrochemical Characterization of Proton-Conducting Electrolyte Polymers (CESHR/Texas A&M University)

Electrochemical experiments were first conducted with Compounds 1 and 4 (Monomeric and Polymeric acids), following a methodology already established for investigation of the platinum/aqueous acid and the platinum/Nafion® interface [4]. To obtain purified solutions, the acids were dissolved in water and treated with 30% H_2O_2 at 75°C, followed by pre-electrolysis with platinum electrodes at 1.7 V for 6 hours.

Figure 1 shows cyclic voltammograms at a platinum microelectrode for the monomeric and dimeric acids, and for H_2SO_4 at the same concentration for comparison. It is obvious that for the imide compounds, there is both a reduction in active area and a deformation of the voltammogram, which can be attributed to adsorption of the polymer and/or of impurities on the platinum surface.

Table 1 shows the mass transport parameters for dioxygen in the new acids determined by chronopotentiometry. It includes sulfuric acid results at the same concentration for comparison.

Table 1. Comparison of Mass Transport Parameters for Oxygen in Acid Electrolytes

Acid	Diffusion Coefficient cm^2/s	Solubility mol/cm^3
0.1 M Sulfuric Acid	9.2×10^{-6}	2.5×10^{-6}
0.1 M Monomeric Acid	8.8×10^{-6}	3.8×10^{-6}
0.1 M Polymeric Acid	3.5×10^{-6}	7.4×10^{-6}

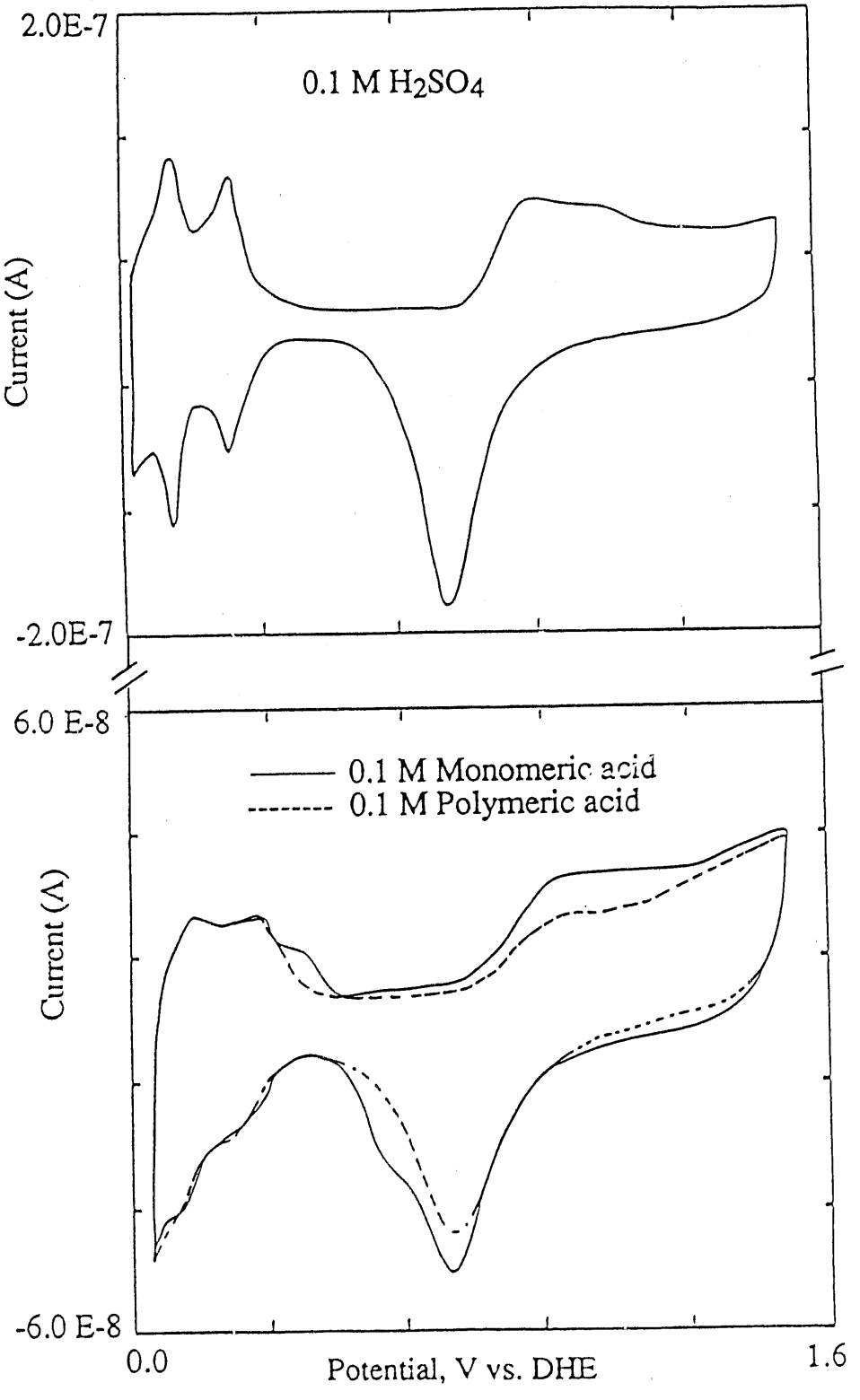

Fig. 1: Cyclic voltammograms at the Pt/acid interface.

From the results in Table 1 it is clear that the solubility of oxygen is higher in the presence of imide acids, even at the low concentrations examined. The diffusion coefficient does seems to have decreased for the polymeric acid, but this should not be a problem when gas diffusion electrodes of fuel cell type are used.

Figure 2 shows the mass transfer corrected Tafel plots for the imide acids at a platinum microelectrode, obtained from steady-state current-potential curves. The corresponding kinetic parameters are shown in Table 2, together with those for H_2SO_4.

In the imide acids it was not possible to detect the region corresponding to the surface partially covered by adsorbed oxygen, which shows lower Tafel slopes. This resulted from their low open circuit potentials, which for both acids were under 1.0 V vs. DHE. This effect may be due to the presence of impurities in the solution.

In the oxide-free region, the values of the Tafel slopes and exchange current densities are comparable to those observed in H_2SO_4. This is promising if one takes into account the presence of impurities, evidence of which is shown in the cyclic voltammograms obtained.

Table 2. Comparison of Electrode Kinetic Parameters for Oxygen Reduction at a Platinum Microelectrode/Acid Interface

Acid	Tafel slope mV/decade	Exchange Current density A/cm^2
0.1 M Sulfuric Acid	-69	7.21×10^{-10}
	-121	7.15×10^{-8}
0.1 M Monomeric Acid	-118	1.32×10^{-8}
0.1 M Polymeric Acid	-125	2.49×10^{-8}

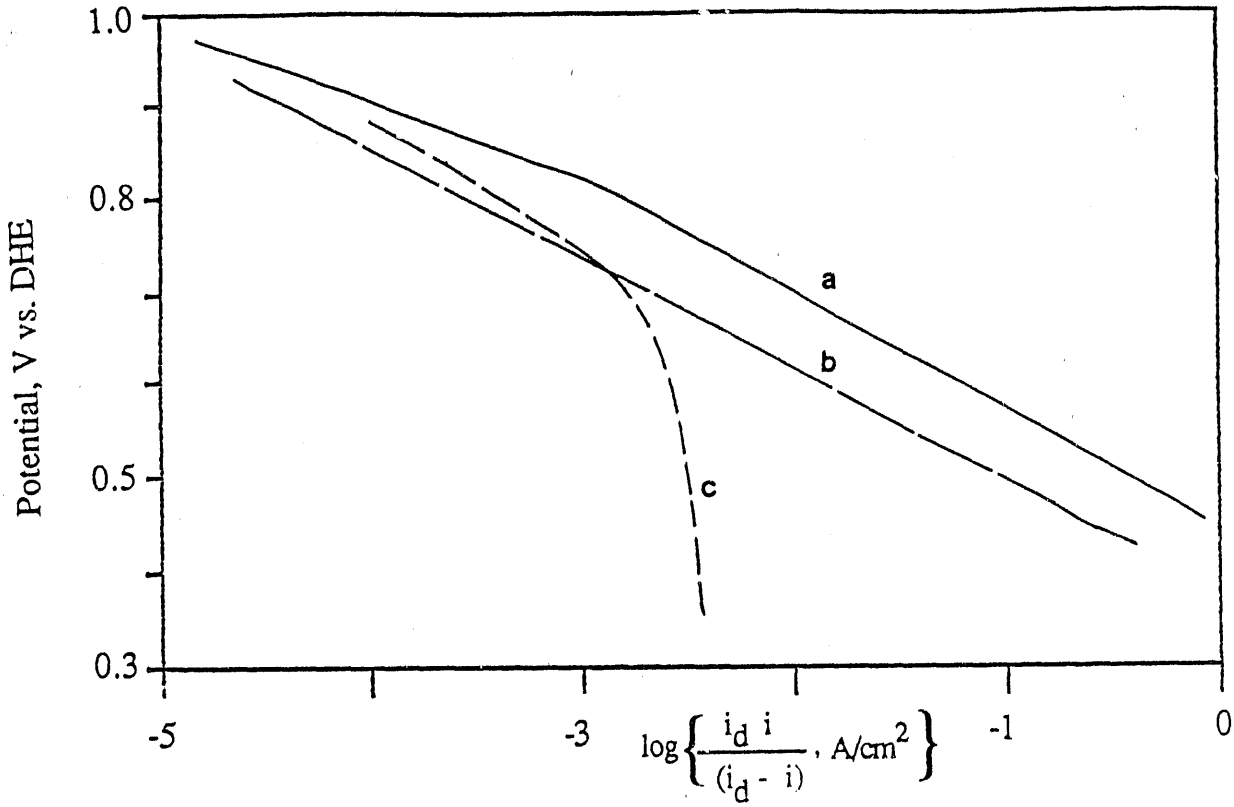

Fig. 2 Mass transfer corrected Tafel plots at the Pt/acid interface: (a) 0.1 M H_2SO4, (b) 0.1 M monomeric acid, (c) 0.1 M polymeric acid

Evaluation of the Proton Conducting Polymers Under Fuel Cell Conditions (ElectroChem, Inc.)

All four acids supplied to ElectroChem. Inc. from Clemson University were examined as additives at 2.5 wt % concentration in standard 100% phosphoric acid fuel cells. The performance of each was compared with that of a fuel cell containing pure 100% phosphoric acid as a control. Evaluations of all cells were carried out both at 190°C and at 75°C.

The open circuit voltage (OCV) for each cell is shown in Table 3. The lower molecular weight compounds studied in phosphoric acid solution (i.e., the Monomeric and Dimeric acids) have OCVs very similar to that of a cell containing 100% phosphoric acid. However the OCVs of the high molecular weight compounds (Tetrameric and Polymeric acids) were depressed by about 100 mV, perhaps because of the presence of impurities. Despite the depression of OCV, the performance of both the tetrameric and polymeric acid cells at high current density was superior to that of the other three electrolyte systems. Indeed, at 190°C and 200 mA/cm^2, the IR-corrected voltages of the stabilized polymeric and tetrameric acid cells was 20-30 mV higher than that of the 100% phosphoric acid fuel cell (Table 3). Although the lower molecular weight compounds showed high OCVs initially, their performance under load deteriorated with time. This deterioration also resulted in a depression of the OCV from 961 mV to 661 mV. This apparent load- and time-dependent effect could be reversed by polarization of the anode. Immediately after polarization, the IR-corrected voltage at 190°C and 200 mA/cm^2 was very similar to that of the pure phosphoric acid cell (Table 3). This suggests that the anode was poisoned in the imide acid solution, either by the low molecular weight compounds, or more likely by impurities which had not been removed by pretreatment.

Comparison of the Tafel plots obtained at 190°C and 75°C shows that the performance of all

five acids was much better at higher temperatures. However, at 75°C, only cells containing either pure phosphoric acid, Tetrameric acid or Polymeric acid could sustain a reasonable cell voltage at higher current densities (i.e., 100 mA/cm^2). High cell voltages could only be obtained after anodic polarization for the low molecular weight acids under these conditions (Table 3).

The IR-corrected voltages for fuel cell operation at 75°C show that the performance of Tetrameric, Polymeric and phosphoric acid cells are very similar under these non-stabilized conditions. The performances of Monomeric and Dimeric acid cells were much lower, especially at the lower temperatures. In fact, these low molecular weight acids have difficulty in sustaining a 200 mA/cm^2 current density at 75°C.

The cell resistance in the presence of the lower molecular weight acids was higher than that in the presence of those of high molecular weight. In addition, the fuel cells using electrolytes with low molecular weight acids displayed resistances which appeared to increase with decreasing temperature, however, the resistance of the cells containing the higher molecular weight acids was not similarly affected. This resistance effect could be the result of electrode poisoning, caused either by the formation of a high resistance film on the electrode surface, or a change in electrode morphology. This poisoning effect appears to be more acute at lower temperatures. The phosphoric acid cell showed a high cell resistance, but this was only a result of not using an optimized cell design.

Of all the acid electrolytes investigated in fuel cells, those which contained either Tetrameric or Polymeric acid appeared to be the most promising. In consequence, these cells were operated for approximately 100 hours at 200 mA/cm^2 a, during which they showed good performance stability.

The results obtained suggest that both Tetrameric and Polymeric acids show promise as new electrolytes. The Monomeric and Dimeric acids are not without promise, although poisoning of the anode is a problem. This could possibly be overcome by further removal of impurities.

Table 3. Comparison of Cell Open Circuit Voltage and Steady State Voltage at 200 mA/cm^2

Liquid Electrolyte	OCV	190°C		75°C	
		V(ir corr)	V	V(ir corr)	V
Phosphoric acid	950	732	618	657	569
Monomeric acid + H_3PO_4	961	728*	659	---	
Dimeric acid + H_3PO_4	988	732*	676	623*	536
Tetrameric acid + H_3PO_4	824	759	723	641	592
Polymeric acid + H_3PO_4	871	749	706	665	615

* after anode polarization
All cell voltages are in mV

FUTURE WORK

At Clemson University, work is in progress to obtain the 6-carbon analogs of the above acids, i.e., those containing $-(CF_2)_6-$ in dimer and polymer acids. Synthesis and testing of compounds containing the $-(CF_2)_2-$ fragment is expected to lead to conclusions concerning the optimum carbon chain length. Finally, efforts are continuing to obtain the structure of the Tetrameric acid as the Cs salt.

Future work at Texas A&M University will involve the purification and testing of solutions of the Dimeric and Tetrameric acids most recently received from Clemson University.

REFERENCES

1. E. A. Ticianelli, C. R. Derouin and S. Srinivasan. 1988. Localization of Platinum in Low Catalyst Loading Electrodes to Attain High Power Densities in SPE Fuel Cells. *J. Electroanal. Chem.* 251: 275-295.

2. M. Razaq, A. Razaq, E. Yeager, D. D. DesMarteau and S. Singh. 1987. Bis-((trifluoromethyl)sulfonyl)imide as an Alternate Electrolyte in Hydrogen-Oxygen Fuel Cells. *J. Applied ElectroChem.* 17: 1064-1069.

3. M. Razaq, A. Razaq, E. Yeager, D. D. DesMarteau and S. Singh. 1989. Perfluorosulfonimides as an Additive in Phosphoric Acid Fuel Cells. *J. ElectroChem. Soc.* 136: 385-390.

4. J. F. Foropoulos and D. D. DesMarteau. 1984. Synthesis Properties, and Reactions of Bis-((Trifluorom hyl)-sulfonyl)imide, $(CF_3SO_2)_2NH$. *Inorg. Chem.* 23: 3720.

5. M. Witz and D.D. DesMarteau. 1991. n-Fluoro-bis(trifluormethan sulfonyl)imide. An Improved Synthesis. *J. Fluorine Chem.* 52: 7.

6. A. Parthasarathy, C.R. Martin and S. Srinivasan. 1991. Investigations of the O_2 Reduction Reaction at the Platinum/Nafion® Interface Using a Solid-State Electrochemical Cell. *J. ElectroChem. Soc.* 138: 916-921.

Development of CO and H_2S Tolerant PAFC Anode Catalysts

CONTRACT INFORMATION

Contract Number	DE-AC02-87ER80493
Contractor	ElectroChem, Inc. 400 W. Cummings Park Woburn, MA 01801 (617) 932-3383
Contractor Project Manager	Vinod Jalan
Principal Investigators	Vinod Jalan, Jeffrey Poirier, Mahesh Desai, and Brian Morriseau
METC Project Manager	William J. Huber
Period of Performance	May 13, 1987 to June 8, 1990

Schedule and Milestones

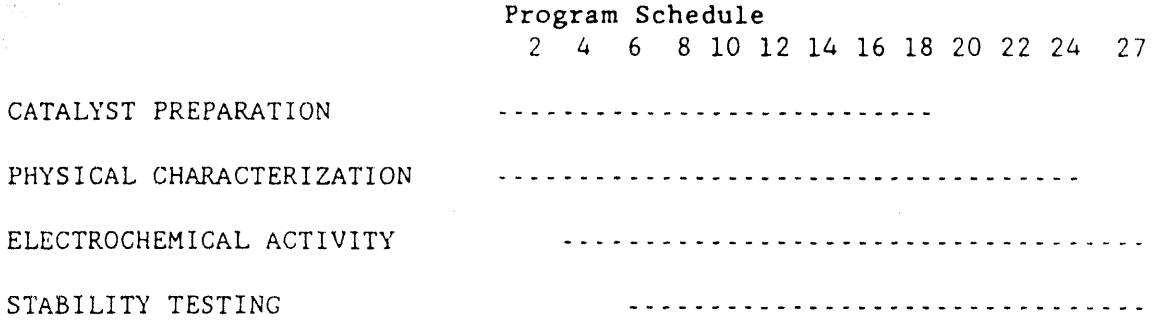

OBJECTIVES

The objective of this program is to develop improved anode electrocatalysts that are resistant to poisoning by coal gas contaminants, namely carbon monoxide and hydrogen sulfide. The benefits ultimately derived will be increased coal utilization and reduced fuel processing requirements.

BACKGROUND INFORMATION

Advances in PAFC technology over the past decade have brought it to almost commercial status. Present R & D efforts by DOE are directed toward advanced PAFC technologies that can be utilized for load leveling or for providing on-site electrical power to remote locations. The currently-used PAFC systems derive their oxygen from ambient air and hydrogen from relatively clean reformed fuel (methanol, natural gas, etc.). The commercial attractiveness of the PAFC system would be greatly enhanced if it could use coal gas from a gasifier as its fuel source. However, the presence of high levels of CO and H_2S in coal-derived gases causes much larger anodic polarizations than those obtained from reformed methanol or natural gas. This restriction to relatively clean fuel could be overcome and coal gas could be used in a fuel cell if the poison-

ing effects of CO and H_2S were reduced. An anode catalyst enabling PAFC operation on gasified coal represents a near term means of achieving efficient coal utilization as well as reducing the fuel processor requirements for sulfur containing reformed fuels while maintaining the same level of performance.

PROJECT DESCRIPTION

Our approach for reducing poisoning effects is to increase catalyst dispersion and, by alloying, decrease the adsorption affinity of the catalytic surface for CO and H_2S. At higher dispersion, the Pt catalyst has a greater number of active reaction sites and when alloyed with other metals, Pt has improved tolerance to poisoning by the adsorption of CO and H_2S.

Twenty-five anode electrocatalysts were prepared, characterized, and evaluated in the floating electrode half cell. In the presence of H_2S and CO, increased catalyst dispersion provided significantly lower anode polarization than the state-of-the-art catalyst. Further improvements in performance were realized by alloying. The effects on anode polarization of catalyst composition, surface area, support, and fuel gas composition were investigated in detail. The effects of contaminant concentration, temperature, pressure, and fuel utilization on an ultra-high surface area Pt catalyst were also examined in the full cell. A CO and H_2S tolerant high surface area binary Pt alloy was developed and evaluated in the full cell. Long term contaminant resistance and performance stability were demonstrated during atmospheric pressure life testing using a simulated coal gas mixture. Similar testing at increased pressure is currently underway.

RESULTS

Half Cell Catalyst Screening

Our approach has been to prepare and evaluate Pt based catalysts with increased dispersion and lower adsorption affinity for CO and H_2S. Half cell testing provided results to evaluate a large number of catalysts for their tolerance to CO and H_2S poisoning. Figure 1 summarizes the results in this area. The lower line depicts the activity for hydrogen oxidation (expressed as current density for 20 mV polarization) at 200°C using simulated coal gas (SCG: H_2 with 10% CO and 200 ppm H_2S) for three Pt catalysts showing an increase in activity with higher dispersion. Catalyst poisoning for anodic oxidation of H_2 based fuel containing CO or H_2S occurs by site blockage. Higher surface area provides more sites for hydrogen oxidation given the same fraction of total surface blocked by absorbed contaminants. The benefit of higher surface area is indicated by a higher reaction rate (current density) for the same driving force (20 mV).

Alloying with selected metals increases the hydrogen oxidation activity of a Pt catalyst in the presence of CO and H_2S by reducing the surface affinity for contaminant adsorption. This is shown by the upper line in Figure 1 (Pt alloys) which also indicates a dispersion effect similar to that of pure Pt. Reducing the affinity of the surface for CO and H_2S adsorption provides a larger effective area for hydrogen oxidation and thus a higher current density at constant polarization.

Figure 2 shows the anode polarization curves for a high surface area (HSA: 95 m^2/g) and an ultra-high surface area (UHSA: 143 m^2/g) Pt catalyst at 200°C using H_2 and simulated coal gas. Surface area had no

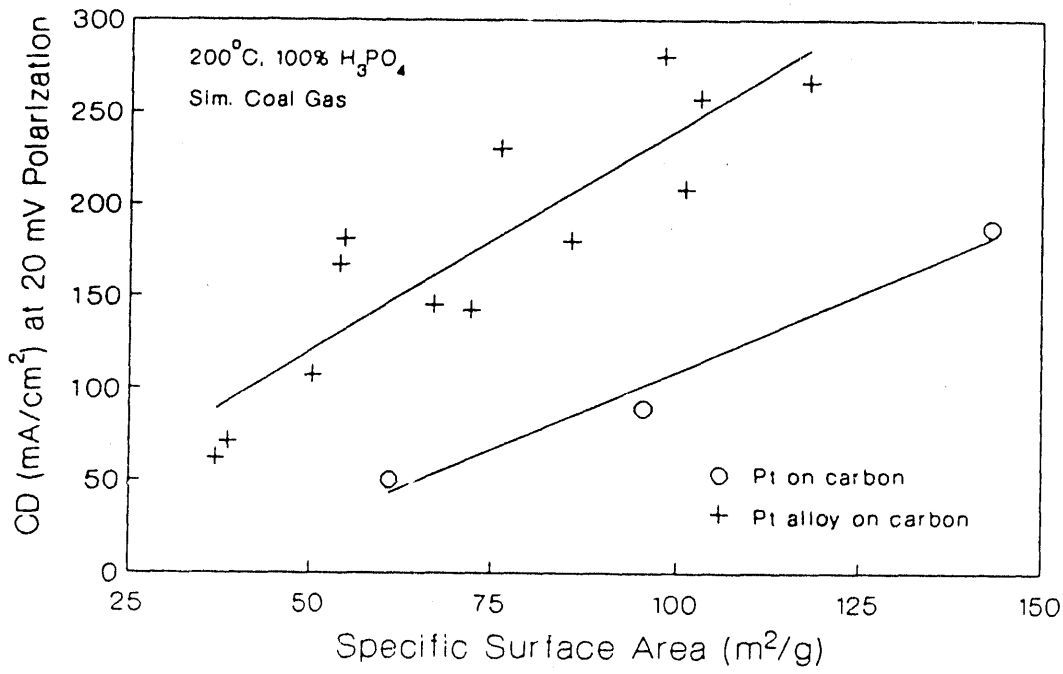

Figure 1. H_2 Oxidation Activity vs. Specific Surface Area for Pt and Pt Alloys

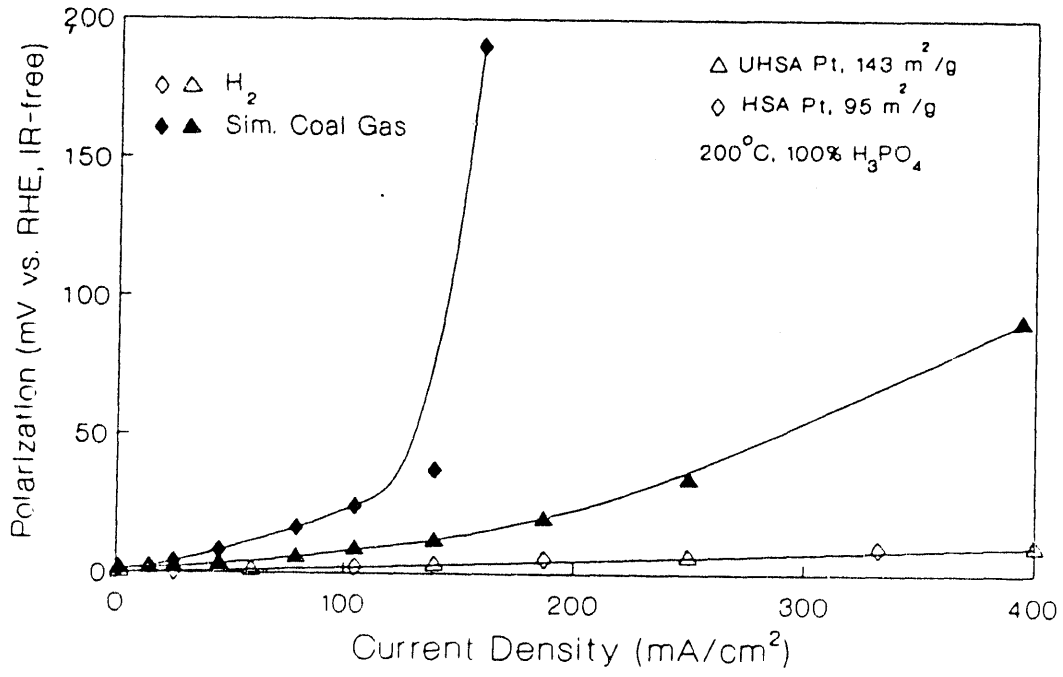

Figure 2. Anode Polarization for Pt

effect on performance on pure hydrogen, and the two catalysts had nearly the same polarization. On simulated coal gas however, the polarization for UHSA Pt was significantly lower than HSA Pt, especially at higher current densities.

Full Cell Testing of UHSA Pt

An ultra-high surface area Pt catalyst and a number of Pt alloys (prepared from UHSA Pt) having contaminant tolerance were selected for full cell testing. Full cell testing allowed verification of half cell results and investigation of operating a PAFC on simulated coal gas. We have studied the effect on performance of contaminant concentration, temperature, pressure, and fuel utilization of a complete fuel cell containing an UHSA Pt anode. This work forms a basis for gauging further development of anode catalysts.

The typical fuel cell test conditions are low utilization of the fuel and oxidant, 190°C cell temperature, 100% H_3PO_4 electrolyte, and 200 mA/cm^2 current density (CD). Both atmospheric and pressurized conditions have been used. In all tests, the cathode contained Pt-Ni-Co, a ternary Pt alloy catalyst.

Fuel cell testing for catalyst development focuses on evaluation of performance--the decrease in cell voltage when operating with H_2 containing 10% CO and 200 ppm H_2S (both singularly and in combination) as compared to operating on pure H_2 under the same conditions. The contaminant induced decrease in cell voltage, ΔE, is calculated with respect to operation on pure H_2. ΔE is a measure of the increase in anode polarization; a large drop in cell voltage due to catalyst poisoning is indicated as a large ΔE.

Effect of CD on ΔE. Figure 3 shows the decrease in cell voltage (ΔE) caused by 200 ppm H_2S and 10% CO, both singularly and in combination, for a fuel cell with an UHSA Pt anode operated at 190°C, 1 atm. The figure indicates that the fuel cell could not sustain higher current densities in the presence of these levels of CO and H_2S. With simulated coal gas or H_2 + H_2S as the CD increases the ΔE rises sharply. When both CO and H_2S are present, this sharp rise in ΔE occurs at a lower CD than with H_2S alone. The performance could be recovered by removing the contaminant gases from the anode feed. With CO alone as a contaminant, the cell could be operated to higher than 200 mA/cm^2 without this precipitous drop in performance.

Effect of Contaminant Concentration on ΔE. The effect of contaminant concentration on ΔE at 200 mA/cm^2 was determined. Figure 4 shows the effect of H_2S concentration on ΔE with and without 10% CO present in H_2. The ΔE is referenced to performance on pure H_2 in the case of H_2S alone and to performance on H_2 with 10% CO for H_2S and CO. In both cases, at higher H_2S concentrations, the ΔE rises abruptly. This drop in performance occurs above 240 ppm and above 160 ppm for H_2S alone and for H_2S with 10% CO, respectively. Figure 5 shows the corresponding effect of CO concentration with and without 200 ppm H_2S present in H_2. Without H_2S the cell could operate with up to 20% CO (the highest concentration tested) with no sharp drop in performance. With 200 ppm H_2S, greater than 2% CO caused ΔE to rise sharply.

Effect of Temperature on Cell Voltage. Figure 6 shows the effect of temperature on cell voltage for H_2 and H_2 + 10% CO, H_2 + 200 ppm H_2S, and SCG. Very little temperat-

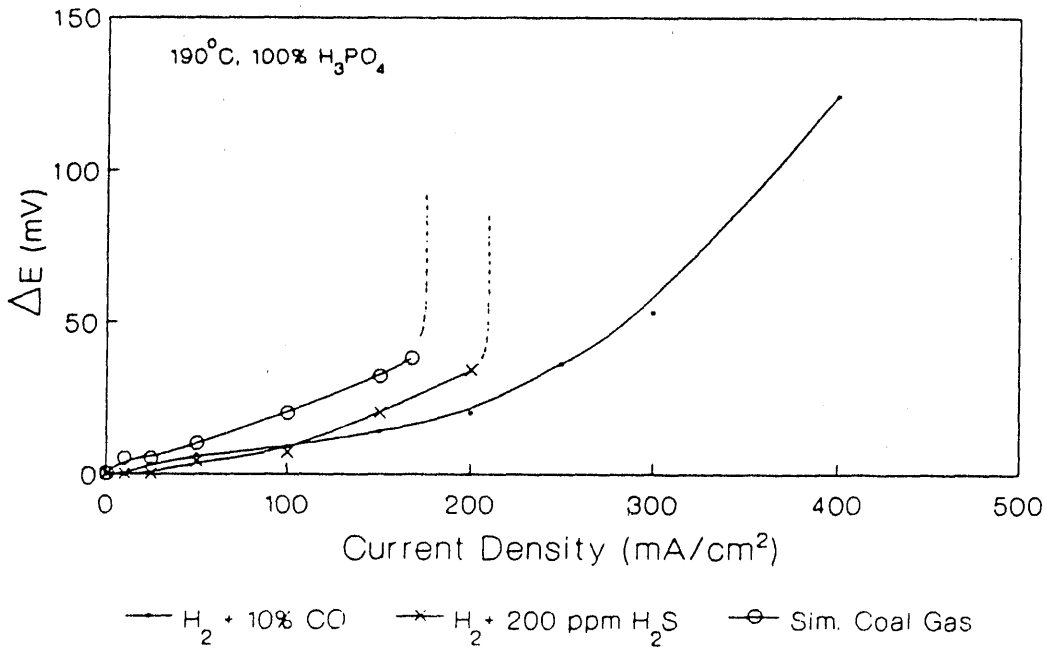

Figure 3. Effect of Current Density: UHSA Pt Anode

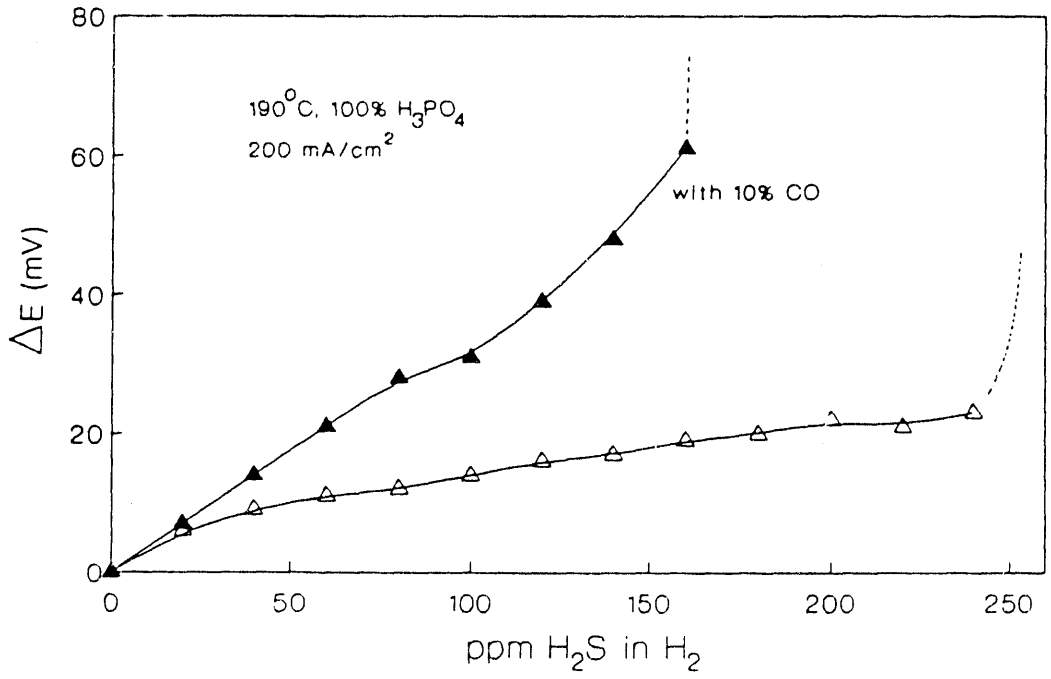

Figure 4. Effect of H_2S Concentration: UHSA Pt Anode

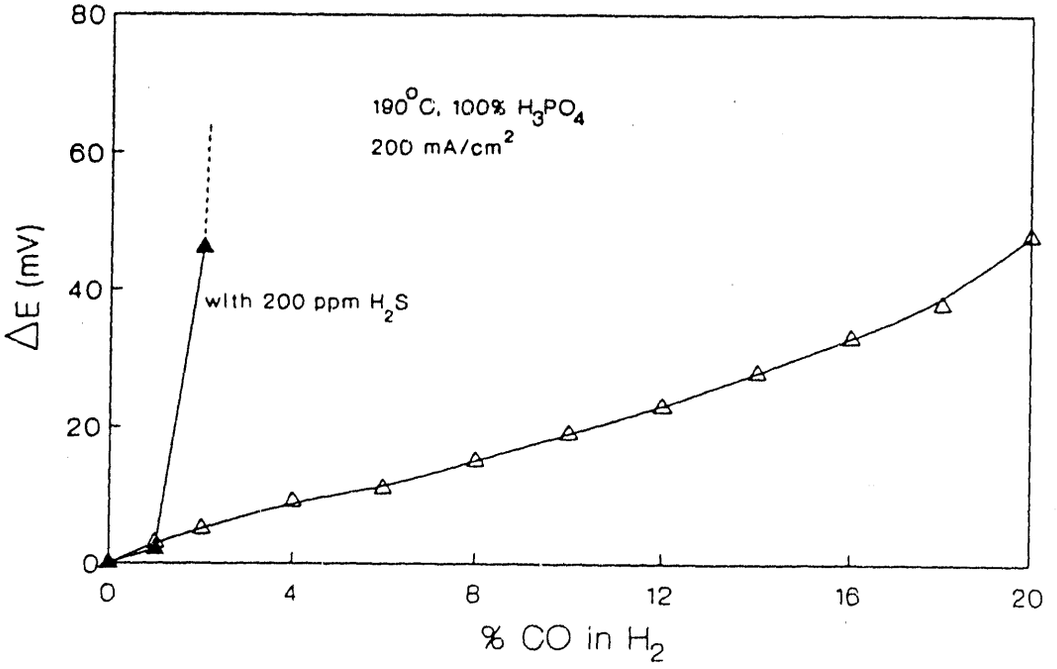

Figure 5. Effect of CO Concentration: UHSA Pt Anode

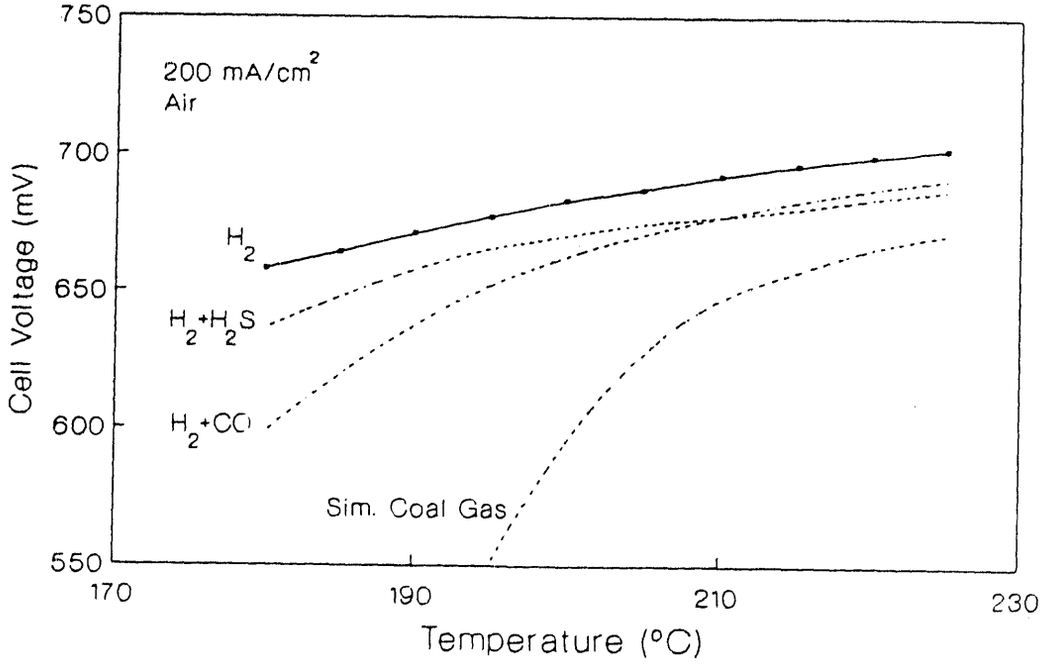

Figure 6. Effect of Temperature: UHSA Pt Anode

ure effect is seen for H_2 + H_2S. For H_2 + 10% CO, the cell voltage deviates more from pure hydrogen at lower temperatures. Higher temperature is beneficial to performance in the presence of CO due to reduced adsorption. For SCG, a strong temperature effect is seen; below 200°C cell voltage drops sharply to unacceptable levels. For the most part, the effect of the contaminants is not additive, indicating that there is an interaction between CO and H_2S.

Effect of Pressure on Cell Voltage. The cell was pressurized while operating at 190°C using SCG. At 70 psig, a polarization scan was obtained (Figure 7) showing much improved performance, and the cell was able to operate at much higher current densities compared to atmospheric pressure.

Effect of Hydrogen Utilization on Cell Voltage. The effect of hydrogen utilization on performance at 200 mA/cm^2, 190°C using SCG is shown in Figure 8. At up to 70% hydrogen utilization (the highest level tested), the cell could sustain 200 mA/cm^2, though the effect of utilization above 50% was greater.

Full Cell Testing of Pt Alloys

Through testing of a group of catalysts which were selected for CO and H_2S tolerance, we have developed a high surface area binary Pt alloy catalyst (designated EC-J1) that shows a significant improvement over the non-alloyed or pure Pt catalyst. This improvement is depicted in Figure 9 which shows that Pt has very high polarization losses when operated at current densities greater than 150 mA/cm^2 using SCG as fuel at 190°C, while EC-J1 can sustain more than 325 mA/cm^2 without excessive performance losses. The curve for EC-J1 does not show a radical drop in cell voltage at higher CD. In this case, a system operating limit was reached; it was indicated that the cell could have sustained even higher current densities if experimental conditions had not prevented it. As expected, performance of the Pt and Pt alloy catalysts on pure hydrogen is similar.

Figures 10 and 11 compare the performance at 190°C of UHSA Pt and EC-J1 using H_2 + 200 ppm H_2S and H_2 + 10% CO, respectively. Figure 10 shows a sharp drop in performance above 200 mA/cm^2 with H_2S present for UHSA Pt while EC-J1 can operate to much higher current densities. Figure 11 shows that, with 10% CO present, the Pt and Pt alloy catalysts can sustain high current densities with relatively small deviation from performance on pure H_2 and that the EC-J1 catalyst has better CO tolerance.

Long Term Performance Stability and Contaminant Resistance of EC-J1

The full cell tests used for catalyst screening and development were run for a few hundred hours under the changing conditions needed for evaluating performance. These tests demonstrated the CO and H_2S tolerance of the EC-J1 catalyst.

The long term performance stability (contaminant resistance) testing of the EC-J1 anode was carried out at atmospheric pressure using the simulated coal gas mixture (50% H_2 utilization) and air (25% O_2 utilization) at 190°C and 200 mA/cm^2. Figure 12 shows the life plot including data from a cell operated under the same conditions using H_2 as fuel. The cell was heated to 190°C under nitrogen and then switched to SCG and put under load. Figure 12 shows that performance improved initially due to wetting of the electrodes and then continued relatively constant for the duration of the test. Peak cell voltages were 670 mV

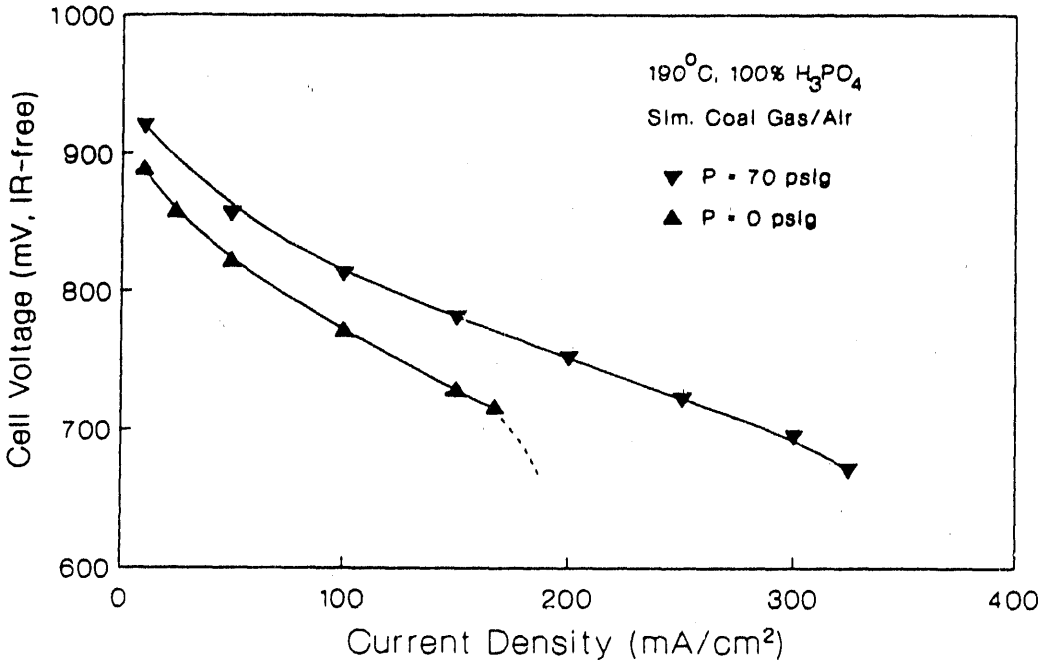

Figure 7. Effect of Pressure: UHSA Pt Anode

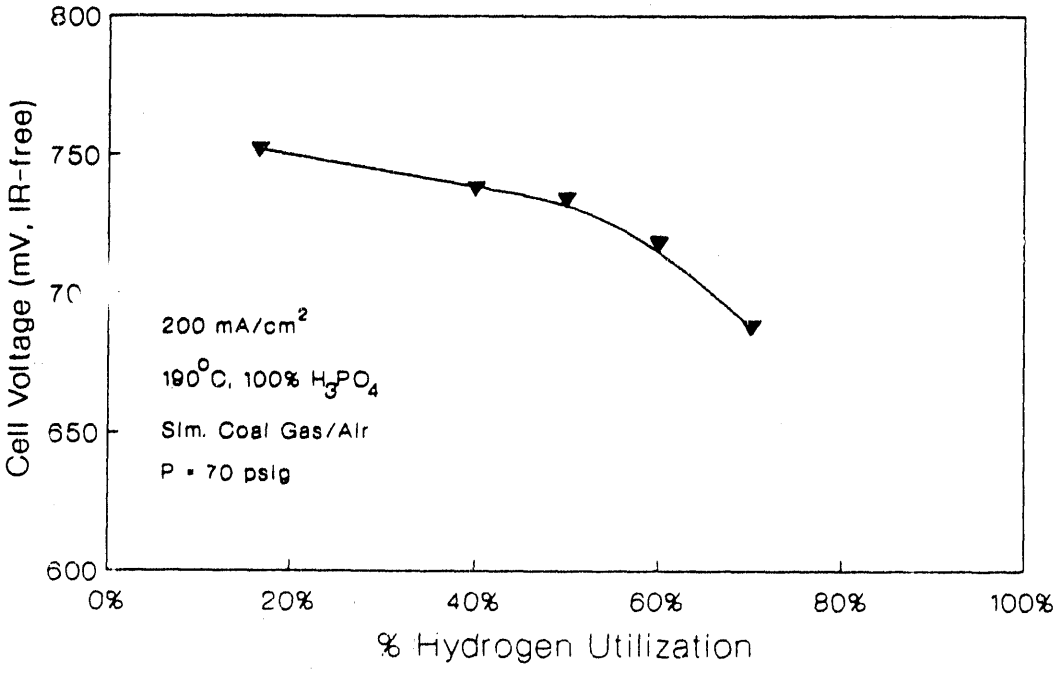

Figure 8. Effect of Hydrogen Utilization: UHSA Pt Anode

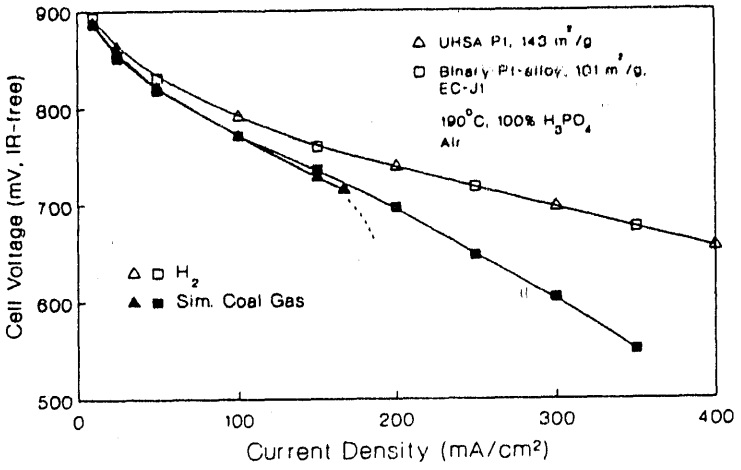

Figure 9. Effect of Simulated Coal Gas for Pt and Pt Alloy Catalysts

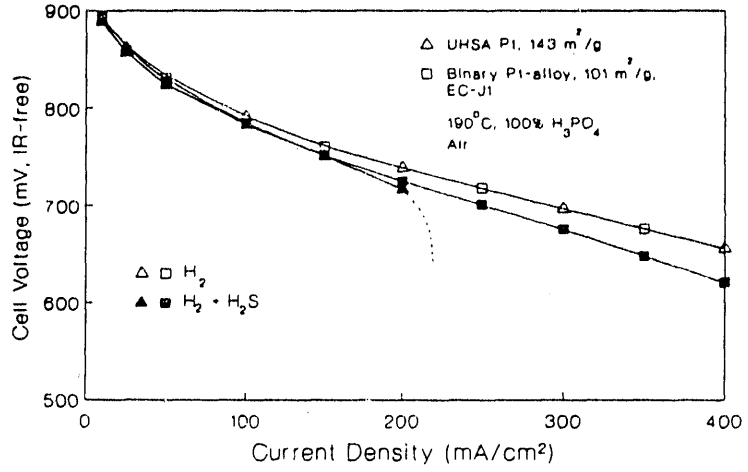

Figure 10. Effect of 200 ppm H_2S for Pt and Pt Alloy Catalysts

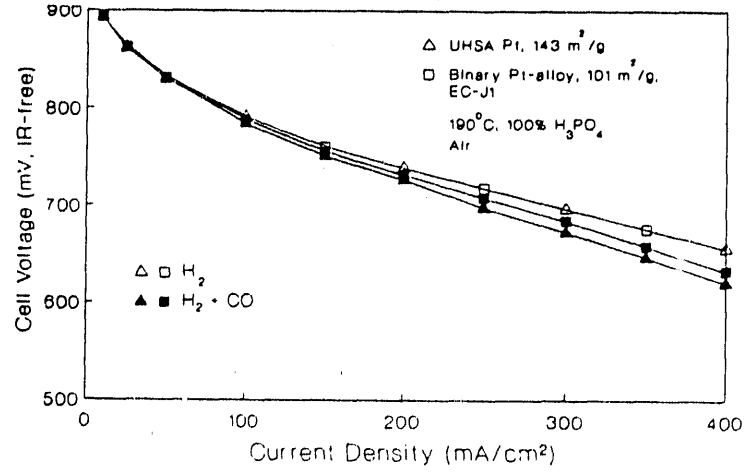

Figure 11. Effect of 10% CO for Pt and Pt Alloy Catalysts

on SCG and 695 mV on H_2. These results demonstrate the long term resistance and performance stability of the EC-J1 catalyst.

FUTURE WORK

Long term pressurized testing of the EC-J1 catalyst is underway.

ACKNOWLEDGMENT

We gratefully acknowledge the support for this work provided by the Department of Energy and we thank Mr. William J. Huber for his assistance. We also thank R. King and S. Srinivasan for valuable discussions.

REFERENCES

Jalan, V., J. Poirier, M. Desai, and B. Morriseau, "Operation of Phosphoric Acid Fuel Cells on Coal Gases," Proceedings of the First Annual Fuel Cells Contractors Review Meeting, ed. W.J. Huber, p. 259, DOE/METC-89/6105, DE89011699 (May, 1989).

Jalan, V. and J. Poirier, "Operation of Phosphoric Acid Fuel Cells on Coal Gases," Proceedings of the 24th Intersociety Energy Conversion Engineering Conference, ed. W.D. Jackson, vol. 3, p. 1565 (August, 1989).

Jalan, V., J. Poirier, M. Desai, B. Morriseau, R. Vora, and B. Burrell, "Operation of Phosphoric Acid Fuel Cells on Coal Gases," Proceedings of the EPRI/GRI Fuel Cell Workshop, ed. R. Goldstein (October, 1989).

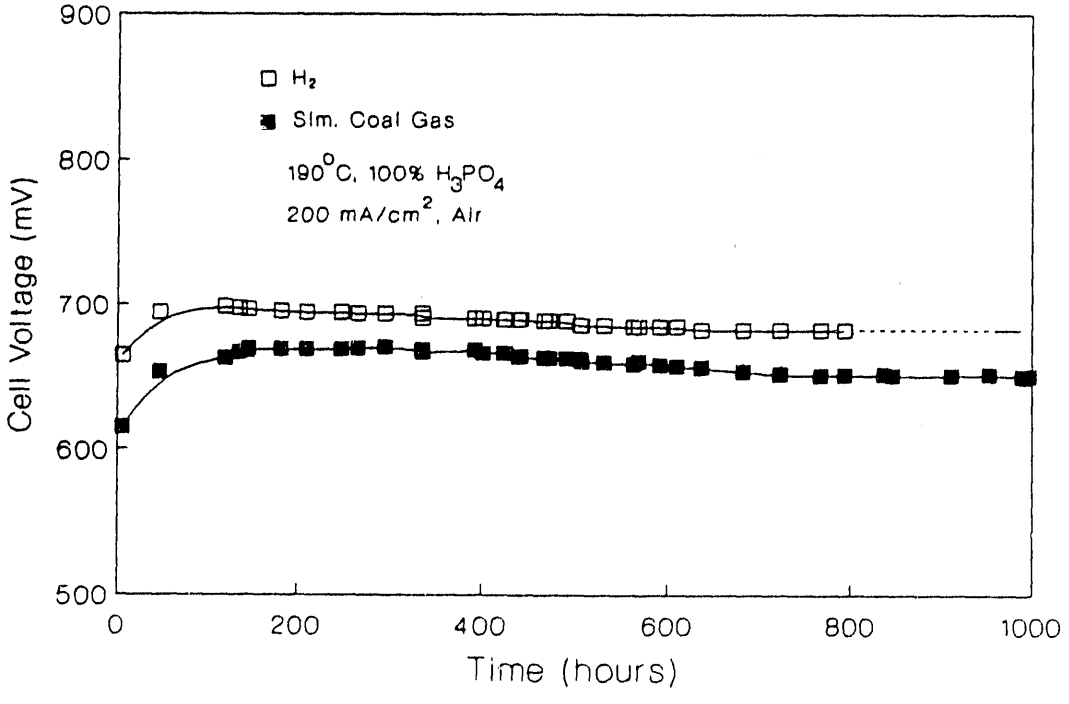

Figure 12. Life Plot of Pt Alloy Anode: EC-J1

Westinghouse Air-Cooled PAFC Technology Development Status

CONTRACT INFORMATION

Contract Number	DE-AC21-82MC24223
Contractor	Westinghouse Electric Corporation Nuclear and Advanced Technology Division Advanced Energy Systems Department Large, PA 15236-0864 (412)-382-5186
Contractor Program Manager	Jerome M. Feret
Principal Investigators	Jack L. Kelly Anthony J. Pereira Maynard K. Wright Ashok K. Kush (Energy Research Corporation)
METC Project Manager	Edmund F. Beyma
Period of Performance	May 14, 1982 to March 31, 1992

Schedule and Milestones

FY91 Program Schedule

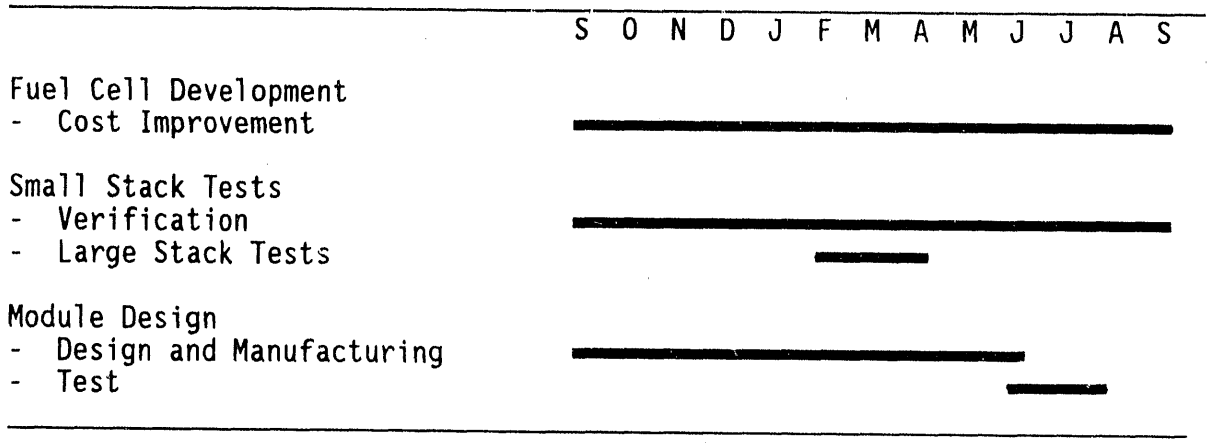

OBJECTIVES

The key objective of this contract is to develop the basic technology needed to demonstrate the air-cooled phosphoric acid fuel cell (PAFC) performance, performance stability and cost goals associated with successful energy service. In order to achieve the power plant performance and economic objectives, progressive fuel cell technology objectives were established. Initially, these objectives are: (1) average beginning-of-use performance of 690 mV at 267 mA/cm^2, 190^oC, 4.7 atmospheres, 83 percent hydrogen utilization using reformed natural gas and 50 percent oxidant utilization using air; (2) performance stability

consistent with a voltage loss of 8 mV/1000 hours; and (3) a 400 kW rated module that can be manufactured for $2600/kW without employing mass without employing mass production techniques. Modest performance and performance stability improvements to 705 mV and 4 mV/1000 hours, respectively, are needed to achieve the early commercial power plant requirements at the same operating conditions except for a 60% oxidant utilization.

BACKGROUND INFORMATION

Over the past 20 years, the Department of Energy (DOE), the Electric Power Research Institute (EPRI), the Gas Research Institute (GRI), private industry and others have been pursuing the development of fuel cells for use in environmentally clean electric utility and industrial power plants. These power plants are expected to be in the 3 MW to 50 MW range.

Of the several types of fuel cells, the PAFC technology is the furthest developed, and thus most mature in terms of readiness for commercialization. The Westinghouse Electric Corporation entered into a licensing agreement with Energy Research Corporation relative to their air-cooled PAFC technology. As a result of this agreement, Westinghouse has been developing for over a decade this most promising and highly efficient alternative power generation technology option.

PROJECT DESCRIPTION

The DOE-METC sponsored Technology Development Program consists of four logical units of work. These work elements are planned to reflect progressive stages of technology achievement via the demonstration of 2 kW, 10 kW, 32 kW, and 100 kW stacks and the end product or the 400 kW module.

The overall program consists of four primary work elements. These are fuel cell development and test, system engineering, facilities development and program management. Each of these top level work elements involves two or more subtasks depending upon the technology maturity. Three of the four planned logical units of work are complete with the fourth initiated in late 1987.

The successful completion of the Fourth Logical Unit of Work and therefore the Technology Development Program is dependent upon building on the current cell technology baseline that meets the initially established performance goals. This will be accomplished by the identification, development, and demonstration of appropriate solutions to major challenges such as: (1) scaling up the technology from a 100 kW stack comprised of multiple stack units to a single unit 100 kW stack and then to the 400 kW module, and (2) developing a module rated at 400 kW minimum that has the economic potential to be commercially manufactured.

Demonstrated proof that these challenges are met involves the manufacture, acceptance testing and suitable performance testing of stacks and modules.

RESULTS

The primary thrust of the development work over the past 24 months was directed towards improving the cell performance stability and production costs. Another most significant effort was concentrated on developing the designs for a single unit 100 kW stack and 400 kW module and their subsequent testing.

The component and processing development portions of the program to achieve the performance goals have been essentially completed. Extensive experiments, subscale cell screening tests, cell materials and component characterizations, and stack tests were performed. These various efforts resulted in the selection of an improved baseline cell technology and associated stack design to achieve the performance objectives.

The improved baseline cell technology selected includes advancements in the areas of design configuration, materials of construction, and component manufacturing processes. Several of the more important advancements include: (1) a better acid management system; (2) less expensive bipolar and cooling plate manufacturing process; (3) inverted cell configuration; (4) electrode integral cell seal; (5) improved lateral acid transport within a new cell matrix; and (6) other design configuration and process control enhancements.

To confirm the improved baseline cell technology selections made, two essentially identical 2 kW stacks were constructed for long term endurance testing. One of these stacks has completed its test objectives with having been tested for about 5,300 hours. The second stack has completed over 1700 hours with its testing still ongoing.

The beginning-of-life performance for each of these stacks is shown in Table 1.

Table 1. Small Stack Performance

Stack	Cell Voltage, mV
W010-34	703
W010-35	700

As shown in Figure 1, performance is very good and consistent from cell to cell for Stacks W010-34 and -35.

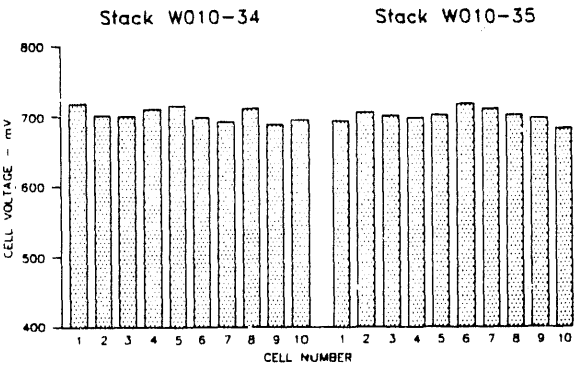

Figure 1. Stacks W010-34 and -35 Cell Variation

The performance decay for one of these stacks, namely Stack W010-34, is presented in Figure 2.

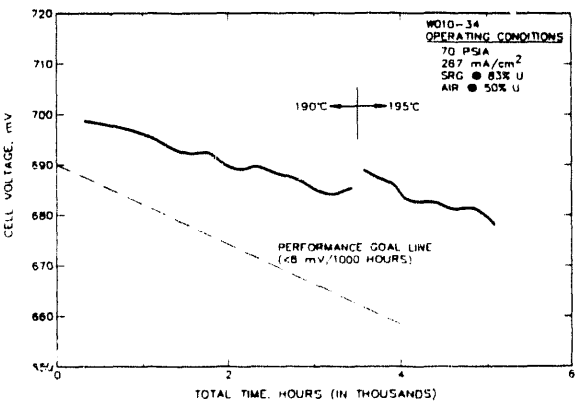

Figure 2. Stack W010-34 Performance Stability

A most recent key achievement of the program involves the design completion, manufacture and assembly of the first Westinghouse single unit 100 kW stack. The electrode, plate, and

matrix technology used in this stack is identical to that used in the 2kW stacks W010-34 and -35.

This 100 kW stack, designated W468-01 and shown in Figure 3, has nominally 468 cells stacked in a vertical arrangement. The cells are arranged into six cell thermal groups with an air cooling plate separating each thermal group. Thus, a typical stack has 78 thermal groups, but could vary by one or two depending upon production tolerance variations. The cooling air is fed to each stack by a central air plenum, passes through each stack and then is drawn down the outside of the stack.

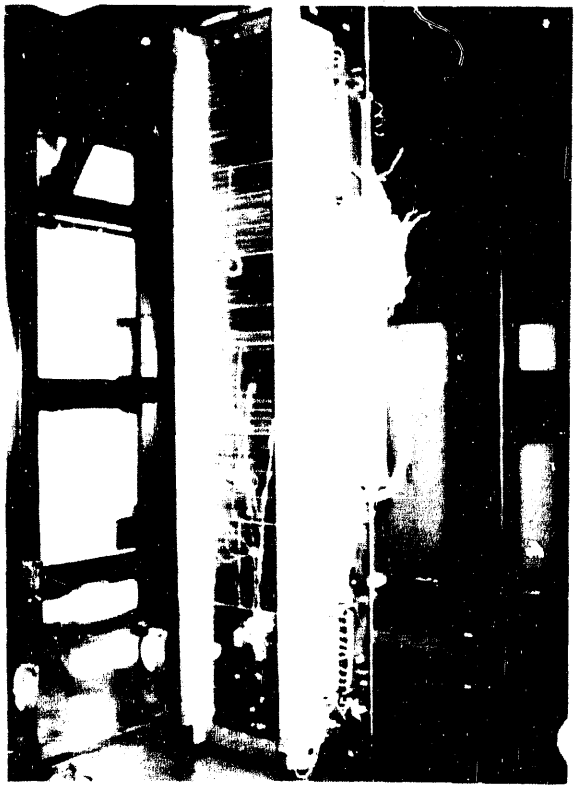

Figure 3. Stack W468-01

Process fuel gas is brought into the stack by a flexible hose connected to the anode inlet manifold which distributes the hydrogen fuel to each cell. An outlet manifold is provided to collect expended fuel gases and exhausts them through another flexible hose.

Process air is drawn from the exhaust cooling air at an intake manifold. The pressure drop across the graphite plates for the process air as well as fuel ensures the uniform distribution of these gas streams through all the cells. The outlet process air manifold collects the moisture laden exhaust gas and feeds it to a flexible hose for discharge outside of the pressure vessel.

The stack assembly is held in compression by two disc spring assemblies which straddle the graphite plates and keep a steady load on the cells and plates. This provides a creep follow system to maintain tight edge seals around the electrodes to prevent loss of the process gases.

Power is extracted by flexible cables at the top and bottom of the graphite plate assembly. The typical stack voltage and current at rated operating conditions are shown in Table 2.

Table 2. Stack Rated Operating Conditions

Operating Pressure	70 psia
Operating Cell Temperature	190°C
Fuel Utilization	90% H_2
Air Utilization	60%
Cooling Air Inlet/Outlet Temperature	147°C/186°C
Stack Voltage	325 V
Stack Current	327 A
Stack Power	106 kW

The top of the stack is equipped with acid feed tubes to each corner. Acid can be added throughout the stack operating lifetime to replenish the acid lost to evaporation. No other stack maintenance is required over its operating lifetime.

The manufacture of the first single unit 100 kW stack was successfully completed in November 1990. Stack testing was initiated in February 1991 and is now nearing completion of the planned 1000 hour test program. This stack along with three others, two of which are complete, will be used in the first 400 kW module produced.

The test operations to date have been proceeding quite well. The stack performance characteristics achieved are as projected and about the same early performance demonstrated for the two 2 kW stacks. Peak stack performance at rated conditions was 330 volts and 108 kW. The average cell performance is 705 mV and is very uniform to within 1.5 percent throughout the stack. Successful operational checkout of the Brassboard Power Management System and the Electrolyte Replenishment System have also been completed.

Module Description

The Westinghouse PAFC Module shown in Figure 4 is designed to provide a minimum electrical power output of 400 kW, under rated, full current, operating conditions at beginning-of-use (BOU). The module electrical output is based on a full current of 327 amperes; the voltage is about 1300 volts depending on what fuel is being used.

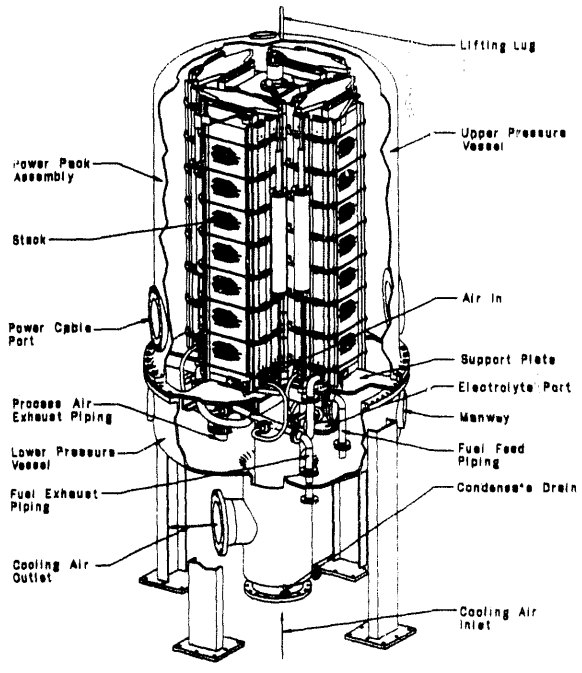

Figure 4. The Westinghouse PAFC Module

The module consists of two subassemblies, the Power Pack and the Lower Vessel Assembly. The Power Pack, which is a replaceable unit, contains four PAFC stacks, each nominally rated at 100 kW, stack support hardware, stack coolant air ducting, and the Upper Vessel Assembly. The Lower Vessel Assembly contains the fuel inlet and outlet headers and stack connection inlet/outlet pipes, process air outlet header and stack connection pipes, penetrations for the electrolyte replenishment system, electrical power leads, instrumentation, and the lower pressure vessel. The containment pressure vessel includes the stack support plate and the upper and lower vessel assemblies.

Gas Systems

Coolant air enters the module

at the bottom of the "Tee" in the Lower Vessel Assembly (LVA) and passes upward inside a coaxial duct to the coolant plenum within the stack assembly. The plenum serves both for coolant air distribution and for stack mechanical support. From the plenum, the coolant air passes through the stack coolant air passages to a space between the stacks and the UVA shell where a portion of it is extracted for process use. After exiting the stacks, the coolant passes downward past the stack support plate to the LVA where it continues downward past the process gas headers and leaves the module through the branch of the LVA "Tee".

Three process gas headers are located in the LVA and supported from flanges on the pipes which penetrate the lower vessel head. The larger diameter of these is the process air (cathode) exhaust header. This header contains air, depleted of oxygen, water vapor, and varying small concentrations of dilute phosphoric acid. The smaller two headers are the hydrogen inlet and outlet (anode) headers. The inlet header contains the fuel gas, while the outlet fuel header contains fuel depleted in hydrogen, water vapor and a small amount of dilute phosphoric acid. Each of the headers has four holes which mate with pipes connecting them with the stack manifolds.

Summary

Completion of the cell technology and manufacturing process developments and the supporting cell/stack engineering effort will culminate in the program's end product, namely the module. Two modules will be built and tested. The first is designated the Engineering Model Module (EMM), and the second the Demonstration Module DM). The EMM design is complete and its manufacture and assembly is nearly complete. The DM will be used for full power testing in the Norsk Hydro Power Plant Demonstration Project.

FUTURE WORK

Completion of the cell technology and manufacturing process developments and the cost improvement program will be achieved in parallel with the 400 kW manufacture and test program. The Engineering Model Module is being prepared for testing during the third quarter of 1991. The Demonstration Module is being manufactured for subsequent testing in early 1992.

REFERENCES

Various monthly and quarterly technical progress narratives pertaining to DOE Contract DE-AC21-82MC24223.

Feret, J.M. May 1989. *Westinghouse Air Cooled PAFC Status, Accomplishments and Issues. In Proceedings of the First Annual Fuel Cells Contractor's Review Meeting*, ed., W. J. Huber, p. 287-296. DOE/METC-89/6105 NTIS/DE89011699).

Kelly. J.L. May 1990. *The Westinghouse PAFC Design. In Proceedings of the Second Annual Fuel Cells Contractor's Review Meeting*, ed., W. J. Huber, p. 204-210. DOE/METC-90/6112 NTIS/DE90000490.

Appendices

Appendix A: Agenda

WEDNESDAY, JUNE 5, 1991

8:15 a.m. REGISTRATION/COFFEE

9:00 a.m. *DOE/METC Welcome & Overview*
Rita A. Bajura
Morgantown Energy Technology Center

9:20 a.m. *DOE/METC Perspective*
Manville J. Mayfield
Morgantown Energy Technology Center

9:35 a.m. *Electric Power Research Institute Perspective*
Daniel M. Rastler
Electric Power Research Institute

9:50 a.m. *Gas Research Institute Perspective*
Michael P. Whelan
Gas Research Institute

SESSION 1 – MOLTEN CARBONATE FUEL CELLS

Chairperson: Tom J. George

10:05 a.m. 1.1 *Full-Height Fuel-Flexible Carbonate Fuel Cell Stack Development*
Mohammad Farooque
Energy Research Corporation

10:35 a.m. 1.2 *Simulated Coal Gas MCFC Power Plant System Verification*
Thomas G. Benjamin
M-C Power Corporation

11:05 a.m. BREAK

11:25 a.m.	1.3	*IFC MCFC Stack Research Status* Carl A. Reiser International Fuel Cells
11:55 a.m.	1.4	*ANL's Development of Conductive Ceramic Components for MCFC* Gene H. Kucera Argonne National Laboratory
12:15 p.m.	1.5	*Effects of Coal-Derived Trace Species on the Performance of Carbonate Fuel Cells* A. Ed Pigeaud Energy Research Corporation
12:40 p.m.	1.6	*Optical Diagnostics for Molten Carbonate Fuel Cells Carbonate Movement and Contaminants* Byron A. Palmer (or Richard Oldenborg) Los Alamos National Laboratory
1:00 p.m.	LUNCH -- METC, "The Energizer"	
2:30 p.m.	1.7	PANEL DISCUSSION -- *MCFC Cathode Corrosion* Moderators: Mark C. Williams and Tom J. George

Chairperson: Mark C. Williams

3:15 p.m.	1.8	*ERC's Carbonate Fuel Cell Power Plant Commercialization Progress* Bernard S. Baker Energy Research Corporation
3:45 p.m.	BREAK	
4:00 p.m.	1.9	*Commercialization Aspects of the IMHEX CFC Power Plants* Richard Root Woods M-C Power Corporation
4:30 p.m.	1.10	*Fuel Cell Commercialization Overview* William J. Lueckel, Jr. International Fuel Cells
6:30 p.m.	SOCIAL HOUR & BANQUET -- Hotel Morgan Ballroom Speaker -- Thomas F. Bechtel, Director, METC	

THURSDAY, JUNE 6, 1991

8:15 a.m. REGISTRATION/COFFEE

9:00 a.m. *Welcome*
William J. Huber
Morgantown Energy Technology Center

9:05 a.m. *Gasification/Cleanup Overview*
Gerald Wheeler
DOE Headquarters

9:20 a.m. *Extraction Overview*
Hugh D. Guthrie
Morgantown Energy Technology Center

9:35 a.m. *Status of DOE Conservation Fuel Cell Program*
Pandit G. Patil
DOE Headquarters

SESSION 2 – SOLID OXIDE FUEL CELLS

Chairperson: David A. Berry

9:50 a.m. 2.1 *High Temperature Solid Oxide Electrolyte Fuel Cell Power Generation System*
Emerson R. Ray
Westinghouse Electric Corporation

10:20 a.m. 2.2 *Alternative Materials for Solid Oxide Fuel Cells: Chromite Interconnections*
J. Lambert Bates
Battelle Pacific Northwest Laboratory

10:40 a.m. 2.3 *Contaminant Effects in Solid Oxide Fuel Cells*
N. J. Maskalick
Westinghouse Electric Corporation

11:00 a.m. 2.4 *Intermediate Temperature Electrolytes for SOFC*
Ira D. Bloom
Argonne National Laboratory

11:20 a.m. BREAK

11:40 a.m.	2.5	*Perovskite Electrolytes for SOFC* Anthony F. Sammells Eltron Research, Inc.
12:00 p.m.	2.6	Planar Solid Oxide Fuel Cell Technology Michael Hsu Ztek Corporation
12:20 p.m.	2.7	*Sealant Research for SOFC* Ira D. Bloom Argonne National Laboratory
12:40 p.m.	2.8	*Progress in MSOFC Technology and Analysis* Richard A. Gibson Allied-Signal Aerospace Company
1:05 p.m.	LUNCH -- METC, "The Energizer"	

SESSION 3 – PHOSPHORIC ACID FUEL CELLS

Chairperson: Edmund F. Beyma

2:15 p.m.	3.1	*Advanced Water-Cooled Phosphoric Acid Fuel Cell Development* Glenn W. Scheffler International Fuel Cells
2:45 p.m.	3.2	*Corrosion-Resistant Catalyst Supports for PAFC* Cecelia C. Cropley Giner, Inc.
3:05 p.m.	3.3	*Corrosion Resistant Supports for Air Cathodes in PAFC* J. David Genders The Electrosynthesis Company, Inc.
3:25 p.m.	3.4	*Novel Solid-State Proton Conductors* S. Srinivasan Texas A&M
3:45 p.m.	BREAK	

4:00 p.m.	3.5	*Anode Catalysts for Coal Gas Fueled PAFC* Vinod Jalan ElectroChem, Inc.
4:25 p.m.	3.6	*Westinghouse Air-Cooled PAFC Technology Development Status* Jerome M. Feret Westinghouse Electric Corporation
4:55 p.m.	ADJOURN	

Appendix B: METC Participants

Cynthia L. Bageant, Civil Engineer
Coal Projects Management Division
304/291-4271, Mailstop D01

Rita A. Bajura, Director
Coal Projects Management Division
304/291-4109, Mailstop D01

Thomas F. Bechtel, Director
Morgantown Energy Technology Center
304/291-4511, Mailstop C02

Justin L. Beeson, Chemical Engineer
Gasification Section
304/291-4671, Mailstop C04

Damon S. Benedict, Mechanical Engineer
Process Technology and Engineering Branch
304/291-4546, Mailstop E01

Louis H. Berkshire, Program Analyst
Technology Applications Assessment Branch
304/291-4189, Mailstop E01

David A. Berry, Project Manager
Fuel Cells Branch
304/291-4430, Mailstop D06

Edmund F. Beyma, Project Manager
Fuel Cells Branch
304/291-4064, Mailstop D06

Charles W. Byrer, Project Manager
Unconventional Gas Projects Branch
304/291-4547, Mailstop E06

Morgan R. Clevenger, Public Affairs Specialist
Office of the Director
304/291-4307, Mailstop A03

Floyd W. Crouse, Director
Projects Management Branch
304/291-4535, Mailstop B06

Randy J. Dellefield, Chief
Fluidized-Bed Combustion Section
304/291-4725, Mailstop C04

Elizabeth Dolezal, Deputy Director
Office of Applied Science and Technology
304/291-4634, Mailstop B05

Lee D. Gasper-Galvin, Chemical Engineer
Transport and Separations Branch
304/291-4832, Mailstop N05

Rodney A. Geisbrecht, Chemical Engineer
Extraction Science and Engineering Branch
304/291-4058, Mailstop A04

Tom J. George, Project Manager
Fuel Cells Branch
304/291-4825, Mailstop D06

Frank D. Gmeindl, Chief
Technology Applications Assessment Branch
304/291-4751, Mailstop E01

Leonard E. Graham, Director
Systems and Technology Support Division
304/291-4714, Mailstop C02

Judy A. Gribble, Secretary
Fuel Cells Branch
304/291-4532, Mailstop D06

Hugh D. Guthrie, Director
Extraction Projects Management Division
304/291-4632, Mailstop E06

William J. Haggerty, Deputy Director
Extraction Projects Management Division
304/291-4526, Mailstop E06

Norman T. Holcombe, Project Manager
Gas Stream Cleanup Branch
304/291-4829, Mailstop E06

Nancy Houston, Attorney
Office of the Director
304/291-4081, Mailstop A03

William J. Huber, Project Manager
Fuel Cells Branch
304/291-4663, Mailstop D06

Gregg C. Huston, Research Chemist
Gas Stream Cleanup Branch
304/291-4047, Mailstop N03

Suresh C. Jain, Project Manager
Gas Stream Cleanup Branch
304/291-4446, Mailstop E02

Lisa A. Jarr, Patent Advisor
Office of the Director
304/291-4555, Mailstop A03

Doug M. Jewell, Project Manager
Projects Management Branch
304/291-4720, Mailstop D04

Thomas W. Keech, Chief
Process Technology and Engineering Branch
304/291-4291, Mailstop E01

Julianne M. Klara, Chemical Engineer
Process Technology and Engineering Branch
304/291-4729, Mailstop E01

Vijendra P. Kothari, Project Manager
Gas Stream Cleanup Branch
304/291-4579, Mailstop E02

Patrick H. Le, Mechanical Engineer
Process Technology and Engineering Branch
304/291-4324, Mailstop E01

George T. Lee, Chemical Engineer
Process Technology and Engineering Branch
304/291-4824, Mailstop E01

James R. Longanbach, Project Manager
Gasification Section
304/291-4659, Mailstop C04

Kanwal Mahajan, General Engineer
Technology Applications Assessment Branch
304/291-4965, Mailstop E01

Rodney D. Malone, Project Manager
Unconventional Gas Projects Branch
304/291-4723, Mailstop E06

Manville J. Mayfield, Chief
Fuel Cells Branch
304/291-4847, Mailstop D06

William R. Miller, General Engineer
Office of Applied Science and Technology
304/291-4827, Mailstop J02

Curtis V. Nakaishi, Project Manager
Gas Stream Cleanup Branch
304/291-4275, Mailstop E02

Stephen Noel, Electrical Engineer
Heat Engines Branch
304/291-4510, Mailstop E03

Benjamin T. Queen, Mechanical Engineer
Clean Coal Projects Division
304/291-4375, Mailstop E06

Larry K. Rath, Chief
Gasification and Combustion Branch
304/291-4094, Mailstop C04

Robert B. Reuther, Chemical Engineer
Coal Projects Management Division
304/291-4573, Mailstop D01

Steven W. Richardson, Mechanical Engineer
Gas Stream Cleanup Branch
304/291-4275, Mailstop C04

L. Carol Roberson, Technology Transfer Manager
Office of the Director
304/291-4308, Mailstop A03

Luke H. Rogers, Mechanical Engineer
Clean Coal Projects Division
304/291-4109, Mailstop D04

Louis A. Salvador, Associate Director
Office of Technical Management
304/291-4147, Mailstop B06

Ralph E. Schafer, Associate Director
Office of Resource Management
304/291-4472, Mailstop C01

Dale K. Schmidt, Project Manager
Projects Management Branch
304/291-4359, Mailstop D04

Harold D. Shoemaker, Project Manager
Unconventional Gas Projects Branch
304/291-4715, Mailstop E06

Larry D. Strickland, Acting Division Chief
Engineering Technology Division
304/291-4494, Mailstop N04

Fred A. Sudhoff, Chemical Engineer
Process Technology and Engineering Branch
304/291-4560, Mailstop E01

Venkat T. Venkataraman, Project Manager
Gasification Section
304/291-4105, Mailstop C04

Jan K. Wachter, Chief
Physical and Chemical Sciences Branch
304/291-4607, Mailstop N03

Paul R. Wieber, Associate Director
Office of Applied Science and Technology
304/291-4544, Mailstop B05

Mark C. Williams, Chemical Engineer
Fuel Cells Branch
304/291-4747, Mailstop D06

John S. Wilson, Deputy Director
Morgantown Energy Technology Center
304/291-4529, Mailstop A05

John Wimer, Project Manager
Morgantown Energy Technology Center
304/291-4505, Mailstop E02

Charles M. Zeh, Project Manager
Gas Stream Cleanup Branch
304/291-4265, Mailstop E02

Marie T. Zitterbart, Chemical Engineer
Physical and Chemical Sciences Branch
304/291-4192, Mailstop N03

Appendix C: Other Participants

JEREMIAH J AYRES
SR. VICE PRESIDENT
EQUITABLE RESOURCES, INC.
420 BOULEVARD OF THE ALLIES
PITTSBURGH, PA 15219
412-553-5728

CAROL J BAILEY
PROJECT MANAGER
SOUTHERN CALIFORNIA GAS CO.
3216 N. ROSEMEAD BLVD.
EL MONTE, CA 91731
818 307-2575

RICHARD BAJURA
ASSOC. PROVOST FOR RESEARCH
WEST VIRGINIA UNIVERSITY
105 STEWART HALL
MORGANTOWN, WV 26506
304-293-3449

BERNARD S BAKER
PRESIDENT
ENERGY RESEARCH CORP.
3 GREAT PASTURE ROAD
DANBURY, CT 06813
203-792-1460

U. (BALU) BALACHANDRAN
CERAMIST
ARGONNE NATIONAL LABORATORY
9700 SOUTH CASS AVE.
ARGONNE, IL 60439
708-972-4250

RICHARD BARAN
RESEARCH ASSOCIATE
ELECTROSYNTHESIS CO., INC.
P.O. BOX 430
EAST AMHERST, NY 14051
716-684-0513

BRIAN M BARNETT
DIR., ELECTROCHEMISTRY
ARTHUR D. LITTLE, INC.
15 ACORN PARK
CAMBRIDGE, MA 02140
617-864-5770

IRV BARRACK
ASSISTANT PATENT COUNSEL
OAK RIDGE OPERATIONS
125 DANA DRIVE
OAK RIDGE, TN 37830
615-576-1072

J. LAMBERT BATES
CHIEF SCIENTIST
BATTELLE PACIFIC NORTHWEST LAB
P.O. BOX 999
MSIN K2-45
RICHLAND, WA 99352
509-375-2579

THOMAS G BENJAMIN
PROJECT MANAGER
M-C POWER CORP.
8040 S. MADISON AVE.
BURR RIDGE, IL 60521
708-986-8040

RICHARD BILJETINA
ASST. VICE PRESIDENT
INSTITUTE OF GAS TECHNOLOGY
3424 S. STATE
CHICAGO, IL 60616
312-890-6418

RICHARD BLASHFIELD
GENERATION ECONOMY MANAGER
JERSEY CENTRAL POWER & LIGHT
310 MADISON AVE.
MORRISTOWN, NJ 07885
201-455-8722

IRA D BLOOM
CHEMIST
ARGONNE NATIONAL LABORATORY
9700 SOUTH CASS AVENUE
ARGONNE, IL 60439
708-972-4516

ANDREW S BOGUS
DIR., SPACE & ENERGY PROGRAMS
ALLIED-SIGNAL AEROSPACE CO.
1530 WILSON BLVD.
SUITE 1000
ARLINGTON, VA 22209
703-276-2167

CHARLES O BOUNDS
DIRECTOR, R&D
RHONE-POULENC
PROSPECT PLAINS ROAD
CN 7500
CRANBURY, NJ 08512
609-395-4548

DAVID BREEDEN
PATENT ADVISOR
OAK RIDGE OPERATIONS
OFFICE OF PATENT COUNSEL
125 DANA DRIVE
OAK RIDGE, TN 37830
615-576-1080

ALAN BROWN
ELECTROCHEMIST
ARGONNE NATIONAL LABORATORY
9700 S. CASS AVE.
ARGONNE, IL 60439
708-972-3838

PATRICK M BROWN
SENIOR TECHNICAL CONSULTANT
CYPRUS FOOTE MINERAL CO.
301 LINDENWOOD DRIVE
MALVERN, PA 19355
215-651-8407

JAMES E BRULE
PROJECT MANAGER
ABB, INC.
1000 PROSPECT HILL ROAD
WINDSOR, CT 06095
203-285-6689

PAUL E. C. BRYANT
DIR., ADVANCED TECHNOLOGY
ABB, INC.
1000 PROSPECT HILL ROAD
WINDSOR, CT 06095
203-285-9268

THOMAS L CABLE
SR. PROJECT LEADER
BP RESEARCH
4440 WARRENSVILLE CENTER RD.
CLEVELAND, OH 44128-2837
216-581-6356

ELIAS (LEE) H CAMARA
VICE PRESIDENT
M-C POWER CORP.
8040 S. MADISON AVE.
BURR RIDGE, IL 60521
708-986-8040

MICHAEL CAROLAN
SENIOR RESEARCH ENGR.
AIR PRODUCTS & CHEMICALS, INC.
7201 HAMILTON BLVD.
ALLENTOWN, PA 18195
215-481-2185

CHRISTOPHER H CHEH
SR. PROCESS DEVELOP. ENGR.
ONTARIO HYDRO
800 KIPLING AVE.
TORONTO, ONTARIO
CANADA, M8Z5S4
416-231-4111

DENNIS R CHENEY
PRINCIPAL PROJECT ENGR.
EG&G IDAHO
P.O. BOX 1625
IDAHO FALLS, ID 83401
208-526-9557

PAUL A CHOMKA
STAFF ENGINEER
CONSOLIDATION COAL CO.
4000 BROWNSVILLE ROAD
LIBRARY, PA 15129
412-854-6677

DAVID CLOUGH
MARKETING MANAGER
MAGNESIUM ELEKTRON, INC.
500 POINT BREEZE ROAD
FLEMINGTON, NJ 08822
908-782-5800

SAM CLOWNEY
DIR., GAS MEASUREMENT
TENNECO GAS
P.O. BOX 2511
HOUSTON, TX 77252-2511
713-757-3968

MICHAEL A COBB
PRESIDENT
MICHAEL A. COBB & CO.
1688 BROOKWOOD DRIVE
AKRON, OH 44313-5068
216-869-8046

CECELIA CROPLEY
PROJECT MANAGER
GINER, INC.
14 SPRING ST.
WALTHAM, MA 02254-9147
617-899-7270

SAMPA DAS
STUDENT
OAK RIDGE ASSOCIATED UNIV.
U.S. DEPARTMENT OF ENERGY
P.O. BOX 880, MS A04
MORGANTOWN, WV 26507-0880
304-291-4192

STEVE DATSKO
RESEARCH SPECIALIST
BABCOCK & WILCOX
1562 BEESON ST.
ALLIANCE, OH 44601
216-829-7528

JEFFREY C DEMOS
MARKET ANALYST
PSI
4350 LA JOLLA VILLAGE DR.
SUITE 300
SAN DIEGO, CA 92122
619-546-4432

VICTOR K DER
DIR., SPECIAL TECHNOLOGIES
U.S. DEPARTMENT OF ENERGY
OFFICE OF FOSSIL ENERGY
WASHINGTON, DC 20585
301-353-2700

DARRYL D DESMARTEAU
TOBEY-BEAUDROT PROFESSOR
CLEMSON UNIVERSITY
DEPT. OF CHEMISTRY
HOWARD L. HUNTER CHEMISTRY LAB
CLEMSON, SC 29634-1905
803-656-4705

NARAYAN DODDAPANENI
SR. MEMBER OF TECHNICAL STAFF
SANDIA NATIONAL LABORATORIES
ORGANIZATION 2523
ALBUQUERQUE, NM 87185
505-846-2653

WALTER J DOLLARD
MGR., ADVANCED ENERGY CONVER.
WESTINGHOUSE ELECTRIC CORP.
1310 BEULAH ROAD
PITTSBURGH, PA 15235
412-256-5300

RAYMOND D DUNLOP
DIR. OF RESEARCH & DEVELOP.
NEW ENGLAND ELECTRIC SYSTEM
25 RESEARCH DR.
WESTBOROUGH, MA 01582
508-366-9011

MOHAMMAD FAROOQUE
GEN. MGR., CARBONATE FUEL CELL
ENERGY RESEARCH CORP.
3 GREAT PASTURE ROAD
DANBURY, CT 06813
203-792-1460

LAURENCE FEDER
ASST. DIR., PROGRAM DEVELOP.
INSTITUTE OF GAS TECHNOLOGY
1825 K STREET, NW
SUITE 503
WASHINGTON, DC 20006
202-785-3511

JEROME M FERET
MGR., FUEL CELL TECH. PROGRAMS
WESTINGHOUSE ELECTRIC CORP.
P.O. BOX 10864
PITTSBURGH, PA 15236-0864
412-382-5186

HANS FRIEDERICY
DIR., RESEARCH & TECH.
ALLIED-SIGNAL AEROSPACE CO.
1530 WILSON BLVD.
10TH FLOOR
ARLINGTON, VA 22209
703-276-2095

DAVID GENDERS
MANAGER, R&D
ELECTROSYNTHESIS CO., INC.
P.O. BOX 430
EAST AMHERST, NY 14051
716-684-0513

MOHAMMAD H GHANDEHARI
SENIOR RESEARCH ASSOC.
UNOCAL CORPORATION
376 S. VALENCIA AVE.
BREA, CA 92621
714-577-2230

RICHARD GIBSON
PROGRAM MANAGER
ALLIED-SIGNAL AEROSPACE CO.
2525 W. 190TH STREET
TORRANCE, CA 90509-2960
213-512-3310

JOSE GINER
PRESIDENT
GINER, INC.
14 SPRING ST.
WALTHAM, MA 02254-9147
617-899-7270

DON GLENN
V.P., CORPORATE DEVELOP.
ENERGY RESEARCH CORP.
3 GREAT PASTURE ROAD
DANBURY, CT 06813
203-792-1460

GRETCHEN B GOCKLEY
SENIOR ENGR.
WESTINGHOUSE ELECTRIC CORP.
SCIENCE & TECHNOLOGY CTR.
1310 BEULAH ROAD
PITTSBURGH, PA 15235
412-256-2025

MICHAEL D GODFREY
ENGINEER, R&D
ALLEGHENY POWER SERVICE CORP.
800 CABIN HILL DR.
GREENSBURG, PA 15601
412-838-6499

RICHARD (ROCKY) GOLDSTEIN
PROJECT MANAGER
ELECTRIC POWER RESEARCH INST.
3412 HILLVIEW AVE.
P.O. BOX 10412
PALO ALTO, CA 94303
415-855-2171

JOSEPH W GOLOWSKI
MARKET DEVELOPMENT SPECIALIST
RHONE-POULENC
ONE CORPORATE DR.
P.O. BOX 881
SHELTON, CT 06484
203-925-3558

PAT GRIMES
PROJECT HEAD
EXXON RESEARCH & ENGINEERING
ROUTE 22, EAST
ANNANDALE, NJ 08801
908-730-2420

MANOJ K GUHA
MGR., TECHNICAL ASSESSMENT
AMERICAN ELEC. POWER SERVICE
1 RIVERSIDE PLAZA
P.O. BOX 16631
COLUMBUS, OH 43216-6631
614-223-1285

DAVID E GUSHEE
SR. SPECIALIST ENVIRON. POLICY
LIBRARY OF CONGRESS
CONGRESSIONAL RESEARCH SERVICE
101 INDEPENDENCE AVE. MS LM423
WASHINGTON, DC 20540
202-707-7228

GRAHAM HAGEY
SENIOR SCIENTIST
EA MUELLER
1401 SOUTH EDGEWOOD ST.
BALTIMORE, MD 21227
301-646-4500

NORA HAINES
ENGINEER
WESTINGHOUSE ELECTRIC CORP.
P.O. BOX 10864
PITTSBURGH, PA 15236-0864
412-382-5174

LAWRENCE M HANDLEY
MGR., MCFC PROGRAMS
INTERNATIONAL FUEL CELLS CORP.
P.O. BOX 739
195 GOVERNORS HIGHWAY
SOUTH WINDSOR, CT 06074
203-727-2209

ZIA HAQ
RESEARCH ENGR.
SOUTHERN CO. SERVICES, INC.
P.O. BOX 2625
BIRMINGHAM, AL 35202
205-868-5183

D. P. HARRISON
ALUMNI PROFESSOR
LOUISIANA STATE UNIVERSITY
DEPT. OF CHEMICAL ENGR'G.
BATON ROUGE, LA 70803
504-388-3066

J. B. HEADRICK
PROGRAM MANAGER, R&D
TEXAS UTILITIES ELECTRIC CO.
400 N. OLIVE STREET
LOCK BOX 81
DALLAS, TX 75201
214-812-8412

DONALD P HEITZENRATER
RESEARCH ENGR.
BABCOCK & WILCOX
R&DD, LRC MT. ATHOS ROAD
P.O. BOX 11165
LYNCHBURG, VA 24506
804-522-5972

ALBERT HIMY
ENGINEER
NAVY/WESTINGHOUSE
P.O. BOX 18249
PITTSBURGH, PA 15236
412-382-7883

LEON T HINSON
ENERGY SYSTEMS SPECIALIST
LOUISIANA GAS SERVICE CO.
P.O. BOX 433
HARVEY, LA 70059
504-368-9109

JOHN H HIRSCHENHOFER
PROJECT MANAGER
GILBERT/COMMONWEALTH, INC.
P.O. BOX 1498
READING, PA 19603
215-775-2600

INGO B HOLZHUETER
SR. TECHNOLOGIST
ONTARIO HYDRO
800 KIPLING AVE.
TORONTO, ONTARIO
CANADA, M8Z5S4
416-231-4111

TAKAHIRO HORIUCHI
ASST. MANAGER
OSAKA GAS CO., LTD.
3-2-95 CHIYOZAKI
NISHI-KU
OSAKA 550
JAPAN
06 -584-4567

GORIK HOSSEPIAN
PROJECT ENGINEER
ALLIED-SIGNAL AEROSPACE CO.
2525 W. 190TH STREET
TORRANCE, CA 90509-2960
213-512-1932

MICHAEL HSU
PRESIDENT
ZTEK CORP.
460 TOTTEN POND ROAD
WALTHAM, MA 02154
617-890-5665

WAYNE HUEBNER
PROFESSOR
PENN STATE UNIVERSITY
118 STEIDLE BLDG.
CERAMIC SCIENCE & ENGR'G.
UNIVERSITY PARK, PA 16802
814-863-1206

THOMAS HYNES
U.S. ARMY MATERIALS TECH. LAB
ARSENAL STREET
WATERTOWN, MA 02172
617-923-5463

VINOD JALAN
PRESIDENT
ELECTROCHEM, INC.
400 W. CUMMINGS PARK
WOBURN, MA 01801
617-932-3383

GERALD S JANIK
SENIOR RESEARCH ENGR.
NY STATE ELECTRIC & GAS CORP.
4500 VESTAL PARKWAY EAST
P.O. BOX 3607
BINGHAMTON, NY 13902-3607
607-729-2551

CHRISTINA JENNINGS
CONSULTING MECHANICAL ENGR.
PACIFIC GAS & ELECTRIC CO.
3400 CROW CANYON ROAD
SAN RAMON, CA 94583
415-866-5305

BILL JOHNSON
MECHANICAL ENGR.
NAVAL WEAPONS SUPPORT CENTER
CODE 305D
CRANE, IN 47522
812-854-1593

WALTER H JOHNSON
PROGRAM MANAGER
INTERNATIONAL FUEL CELLS CORP.
P.O. BOX 739
195 GOVERNORS HIGHWAY
SOUTH WINDSOR, CT 06074
203-727-2215

JACK L KELLY
MGR., ENERGY SYSTEMS ENGR'G
WESTINGHOUSE ELECTRIC CORP.
P.O. BOX 10864
PITTSBURGH, PA 15236-0864
412-382-7060

FRED S KEMP
PROGRAM MANAGER
INTERNATIONAL FUEL CELLS CORP.
P.O. BOX 739
SOUTH WINDSOR, CT 06074
203-727-2212

JOHN KENNEDY
CHIEF ENGR.
AIRESEARCH
2525 W. 190TH
TORRANCE, CA 90509
213-512-3304

GENE H KUCERA
RESEARCH CHEMIST
ARGONNE NATIONAL LABORATORY
9700 SOUTH CASS AVE.
ARGONNE, IL 60439
708-972-4038

RANDY KUROSKY
PRODUCTION MANAGER
SEATTLE SPECIALTY CERAMICS
16130 WOODINVILLE REDMOND RD.
NUMBER 7
WOODINVILLE, WA 98072
206-487-1769

ASHOK KUSH
MGR., POWER PLANT DEVELOP.
ENERGY RESEARCH CORP.
3 GREAT PASTURE ROAD
DANBURY, CT 06813
203-792-1460

RENE M LAURENS
MGR., ENGR'G. & MANUFACTURING
M-C POWER CORP.
8040 S. MADISON AVE.
BURR RIDGE, IL 60521
708-986-8040

THOMAS D LAYMAC
TECHNOLOGY ENGR.
DETROIT DIESEL CORP.
13400 WEST OUTER DR.
DETROIT MI 48239-4001
313-592-5958

MAI LEE
ENGINEER
WESTINGHOUSE ELECTRIC CORP.
P.O. BOX 10864
PITTSBURGH, PA 15236-0864
412-382-5138

PAUL A LESSING
TECHNICAL LEADER
IDAHO NATIONAL ENGINEERING LAB
P.O. BOX 1625
IDAHO FALLS, ID 83415-2218
208-526-8776

PETER A LEWIS
MGR., PLANNING & PERFORMANCE
PUBLIC SERVICE ELEC. & GAS CO.
80 PARK PLAZA, T-16A
NEWARK, NJ 07101
201-430-6634

WILLIAM J LUECKEL
V.P., GOVERNMENT PROGRAMS
INTERNATIONAL FUEL CELLS CORP.
P.O. BOX 739
195 GOVERNORS HIGHWAY
SOUTH WINDSOR, CT 06074
203-727-2225

LEONARD G MARIANOWSKI
DIR., ENERGY CONVERSION RES.
INSTITUTE OF GAS TECHNOLOGY
3424 SOUTH STATE STREET
CHICAGO, IL 60616
312-567-3687

DONALD L MARICLE
MGR., MATERIALS ENGINEERING
INTERNATIONAL FUEL CELLS CORP.
195 GOVERNORS HIGHWAY
SOUTH WINDSOR, CT 06074
203-727-2278

HANS C MARU
SENIOR VICE PRES.
ENERGY RESEARCH CORP.
3 GREAT PASTURE ROAD
DANBURY, CT 06813
203-792-1460

N. J. MASKALICK
FELLOW SCIENTIST
WESTINGHOUSE ELECTRIC CORP.
SCIENCE & TECHNOLOGY CTR.
1310 BEULAH ROAD
PITTSBURGH, PA 15235
412-256-2020

G. B. KIRBY MEACHAM
VICE PRESIDENT
MICHAEL A. COBB & CO.
1688 BROOKWOOD DR.
AKRON, OH 44313-5068
216-869-8046

WILLIAM A MESSNER
MGR., FOSSIL GENERATING & RES.
CON EDISON
4 IRVING PLACE
NEW YORK, NY 10003
212-460-2753

DAVID MILLER
CHEMICAL ENGR.
NAVAL WEAPONS SUPPORT CENTER
CODE 305D
CRANE, IN 47522
812-854-1431

ERIC MINFORD
SR. PRINCIPAL RES. CERAMIST
AIR PRODUCTS & CHEMICALS, INC.
7201 HAMILTON BLVD.
ALLENTOWN, PA 18195
215-481-3248

BEEBHAS C MUTSUDDY
PROGRAM MANAGER
INST. OF MATERIALS PROCESSING
MICHIGAN TECHNOLOGICAL UNIV.
HOUGHTON, MI 49931
906-487-2600

KEVIN M MYLES
MGR., ELECTROCHEMICAL TECH.
ARGONNE NATIONAL LABORATORY
9700 S. CASS AVE.
ARGONNE, IL 60439
708-972-4329

JON NEWMAN
VICE PRESIDENT
ENERGY PARTNERS, INC.
1501 NORTHPOINT PARKWAY
SUITE 102
WEST PALM BEACH, FL 33407
407-688-0500

JAMES K O'NEILL
ASST. PROJECT MANAGER
ABB, INC.
1000 PROSPECT HILL ROAD
WINDSOR, CT 06095
203-285-6695

RICHARD OLDENBORG
DEPUTY GROUP LEADER
LOS ALAMOS NATIONAL LABORATORY
P.O. BOX 1663
CLS-4, MS J567
LOS ALAMOS, NM 87545
505-667-2096

BYRON A PALMER
PHYSICIST - TECH. STAFF MEMBER
LOS ALAMOS NATIONAL LABORATORY
P.O. BOX 1663
MS-J567, CLS-4
LOS ALAMOS, NM 87545
505-667-3528

WALTER G PARKER
MGR., APPLICATIONS ENGR'G.
WESTINGHOUSE ELECTRIC CORP.
1310 BEULAH ROAD
PITTSBURGH, PA 15235
412-256-2417

PANDIT G PATIL
MGR., FUEL CELL SYSTEMS R&D
U.S. DEPARTMENT OF ENERGY
ELECTRIC & HYBRID PROPULSION
WASHINGTON, DC 20585
202-586-8055

CHARLES PAX
PROGRAM MANAGER
U.S. DEPARTMENT OF ENERGY
FE-32 GERMANTOWN
WASHINGTON, DC 20545
301-353-2832

A. J. PEREIRA
MGR., PAFC PILOT FACILITY
WESTINGHOUSE ELECTRIC CORP.
P.O. BOX 10864
PITTSBURGH, PA 15236
412-382-7537

A. ED PIGEAUD
MGR., ANALYTICAL LAB
ENERGY RESEARCH CORP.
3 GREAT PASTURE ROAD
DANBURY, CT 06813
203-792-1460

JOHN PLUNKETT
ENGINEER
EG&G WASC, INC.
P.O. BOX 880, MS M02
MORGANTOWN, WV 26507-0880
304-291-4605

FRED J POPE
MGR., MECHANICAL ENGR'G.
UNION ELECTRIC CO.
P.O. BOX 149
ST. LOUIS, MO 63166
314-554-3217

DEAN PRICE
CONSULTANT
GEORGETOWN UNIVERSITY
1315 SCOTT'S RUN ROAD
MCLEAN, VA 22102
703-448-8377

GLYNN RAMSAY
CONSULTANT
ELTEK
7386 HOPKINS WAY
CLARKSVILLE, MD 21029
703-841-7223

DANIEL M RASTLER
PROJECT MANAGER
ELECTRIC POWER RESEARCH INST.
3412 HILLVIEW AVE.
P.O. BOX 10412
PALO ALTO, CA 94303
415-855-2521

C. TOM RATCLIFFE
MGR., MATERIALS RESEARCH
UNOCAL CORPORATION
376 SOUTH VALENCIA AVE.
P.O. BOX 76
BREA, CA 92621
714-528-7201

EMERSON R RAY
MANAGER, AGENCY PROGRAMS
WESTINGHOUSE ELECTRIC CORP.
SCIENCE & TECHNOLOGY CTR.
1310 BEULAH ROAD
PITTSBURGH, PA 15235
412-256-2125

MICHAEL E REED
STUDENT
OAK RIDGE ASSOCIATED UNIV.
P.O. BOX 880, MS E01
MORGANTOWN, WV 26507-0880
304-291-4674

CARL A REISER
PROJECT ENGINEER
INTERNATIONAL FUEL CELLS CORP.
195 GOVERNORS HIGHWAY
P.O. BOX 739
SOUTH WINDSOR, CT 06074
203-727-2285

ROBERT J REMICK
ASSISTANT DIRECTOR
INSTITUTE OF GAS TECHNOLOGY
3424 SOUTH STATE ST.
CHICAGO, IL 60616-3896
312-567-5731

KENNETH J RICHARDS
PRESIDENT-TECHNOLOGY DIV.
KERR-MCGEE CORP.
P.O. BOX 25861
OKLAHOMA CITY, OK 73132
405-270-4002

BOB RIORDAN
PRESIDENT
FUEL CELL ENGR'G. CORP.
3 GREAT PASTURE ROAD
DANBURY, CT 06813
203-792-1460

ROBERT ROSENFELD
PROGRAM MANAGER
DARPA
3701 N. FAIRFAX DR.
ARLINGTON, VA 22203-1714
703-614-3580

JOHN RUBY
ENGINEER
BECHTEL GROUP
50 BEALE ST.
SAN FRANCISCO, CA 94105-1895
415-718-1410

J. M. RUSSELL
SUPERVISING ENGR.
HOUSTON LIGHTING & POWER CO.
12301 KURLAND DR.
HOUSTON, TX 77034
713-481-7897

ANTHONY F SAMMELLS
PRESIDENT
ELTRON RESEARCH, INC.
4260 WESTBROOK DR.
AURORA, IL 60504
708-898-1583

GLENN W SCHEFFLER
PROJECT MANAGER
INTERNATIONAL FUEL CELLS CORP.
P.O. BOX 739
195 GOVERNORS HIGHWAY
SOUTH WINDSOR, CT 06074
203-727-2259

FRANK C SCHORA
PRESIDENT
M-C POWER CORP.
8040 S. MADISON AVE.
BURR RIDGE, IL 60521
708-986-8040

RUSSELL SCHUSSLER
SUPERVISOR OF SYSTEM PLANNING
ALABAMA ELEC. COOPERATIVE, INC
P.O. BOX 550
ANDALUSIA, AL 36420
205-222-2571

GARLAND E SCOTT
PRESIDENT
RSI ASSOCIATES, INC.
226 W. FOOTHILL BLVD.
SUITE D-1
CLAREMONT, CA 91711
714-626-4120

JOHN A SHELNUTT
MEMBER OF TECHNICAL STAFF
SANDIA NATIONAL LABORATORIES
DIVISION 6211
ALBUQUERQUE, NM 87185
505-844-8856

SUBHASH C SINGHAL
MGR., FUEL CELL TECH.
WESTINGHOUSE ELECTRIC CORP.
SCIENCE & TECHNOLOGY CENTER
1310 BEULAH ROAD
PITTSBURGH, PA 15235-5098
412-256-1208

MICHAEL W SNOW
PROJECT MANAGER
ABB, INC.
1000 PROSPECT HILL ROAD
WINDSOR, CT 06095
203-285-6688

S. SRINIVASAN
DEPUTY DIRECTOR
TEXAS A&M UNIVERSITY
P.O. BOX 3578
COLLEGE STATION, TX 77843-3577
409-845-0624

WILLIAM A SUMMERS
PROJECT MANAGER
WESTINGHOUSE ELECTRIC CORP.
P.O. BOX 10864
PITTSBURGH, PA 15236-0864
412-382-5161

S. SWATHIRAJAN
SECTION MANAGER
GENERAL MOTORS RESEARCH LABS
PHYSICAL CHEMISTRY DEPT.
RCEL, 30500 MOUND ROAD
WARREN, MI 48090-9055
313-986-0702

PAUL F SWENSON
DIR., RESEARCH & DEVELOP.
CONSOLIDATED NATURAL GAS
CNG TOWER
625 LIBERTY AVE.
PITTSBURGH, PA 15222-3199
412-227-1321

KENJI TANAKA
ENGINEER
NGK - LOCKE, INC.
2525 INSULATOR DR.
BALTIMORE, MD 21230
301-347-1995

W. PETER TEAGAN
VICE PRESIDENT
ARTHUR D. LITTLE, INC.
20 ACORN PARK
CAMBRIDGE, MA 02140
617-864-5770

MICHAEL R THARP
PLANNING ANALYST
BABCOCK & WILCOX
1562 BEESON ST.
ALLIANCE, OH 44601
216-829-7822

VICTOR M TRACY
PRINCIPAL ENGINEER
PACIFICORP ELECTRIC OPERATIONS
1407 WEST NORTH TEMPLE
SALT LAKE CITY, UT 84140
801-220-2188

DONALD TRYK
SR. RESEARCH ASSOCIATE
CASE WESTERN RESERVE UNIV.
CHEMISTRY DEPARTMENT
MILLIS SCIENCE CENTER
CLEVELAND, OH 44106-7078
216-368-3736

NIELS R UDENGAARD
MGR., PROCESS ENGR'G.
HALDOR TOPSOE, INC.
P.O. BOX 58767
HOUSTON, TX 77258-8767
713-480-2600

LAWRENCE E VAN BIBBER
MARKETING MANAGER
WESTINGHOUSE ELECTRIC CORP.
BOX 10864
PITTSBURGH, PA 15236
412-382-5158

STEPHEN E VEYO
MGR., COMMERICAL PROJECTS
WESTINGHOUSE ELECTRIC CORP.
1310 BEULAH RD.
PITTSBURGH, PA 15235
412-256-1901

RICHARD F VON HOLLEN
MGR., FUEL CELL SYSTEMS ENGR'G
ABB, INC.
1000 PROSPECT HILL ROAD
WINDSOR, CT 06095
203-285-5628

DAVID G VUTETAKIS
SR. RESEARCH SCIENTIST
BATTELLE
505 KING AVENUE
COLUMBUS, OH 43201
614-424-5389

LARRY WATKINS
PROJECT MANAGER
SOUTH COAST AIR QUALITY
9150 FLAIR DR.
EL MONTE, CA 91731
818-572-6308

HARVEY WEN
ENGR'G. SPECIALIST
BECHTEL CORP.
9801 WASHINGTONIAN BLVD.
GAITHERSBURG, MD 20878-5356
301-417-5453

GERALD WHEELER
LEAD PROGRAM MANAGER
U.S. DEPARTMENT OF ENERGY
19901 GERMANTOWN RD.
FE-231
GERMANTOWN, MD 20585
301-353-3511

MICHAEL P WHELAN
MGR., COGENERATION RESEARCH
GAS RESEARCH INSTITUTE
8600 WEST BRYN MAWR AVE.
CHICAGO, IL 60631
312-399-8339

DANE WILSON
STAFF MEMBER
OAK RIDGE NATIONAL LABORATORY
P.O. BOX 2008
OAK RIDGE, TN 37831-6156
615-576-4810

LARRY WITTRUP
SENIOR ENGR.
SACRAMENTO MUNICIPAL UTILITY
P.O. BOX 15830
6201 S. STREET (95817)
SACRAMENTO, CA 95852-1830
916-732-6222

RICHARD R WOODS
MGR., BUSINESS MARKETING
ABB, INC.
1000 PROSPECT HILL ROAD
CEP-9351-A
WINDSOR, CT 06095
203-285-5612

JOHN D WRIGHT
PRINCIPAL ENGR.
TDA RESEARCH
12421 W. 49TH AVE.
WHEAT RIDGE, CO 80033
303-422-7918

MAYNARD WRIGHT
ADVISORY ENGR.
WESTINGHOUSE ELECTRIC CORP.
P.O. BOX 10864
PITTSBURGH, PA 15236
412-382-5188

THOMAS E WROBLEWSKI
ENGINEER III
WISCONSIN ELECTRIC POWER CO.
231 W. MICHIGAN ST. - P279
MILWAUKEE, WI 53201
414-221-2536

JOHN YAMANIS
GROUP MANAGER
ALLIED-SIGNAL, INC.
P.O. BOX 1021
MORRISTOWN, NJ 07962-1021
201-455-5052

C. Y. YUH
MGR., MATERIALS DEVELOP.
ENERGY RESEARCH CORP.
3 GREAT PASTURE ROAD
DANBURY, CT 06813
203-792-1460

FRED ZERKEL
VICE PRESIDENT
INSTITUTE OF GAS TECHNOLOGY
1825 K ST., N.W.
SUITE 503
WASHINGTON, DC
202-785-3511

MARTIN A ZGRAGGEN
MGR., MATERIALS ENGR'G.
ONAN CORPORATION
1400 - 73RD AVE., N.E.
MINNEAPOLIS, MN 55432
612-574-5347

★U.S. GOVERNMENT PRINTING OFFICE: 1991 - 548-193/41301

END

DATE FILMED

12/31/91